Ultrashort lasers to increase efficiency in solar energy harvesting via intermediate states

2014 High Power Laser Ablation Symposium
Santa Fe, NM 23 April 2014

Ultrashort lasers to increase efficiency in solar energy harvesting via intermediate states

2014 High Power Laser Ablation S osium
Santa Fe, NM 23 April 2014

Renee Sher

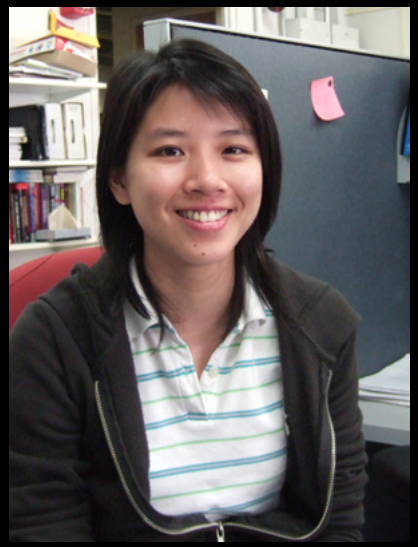

Yu-Ting Lin

Kasey Philips

Ben Franta

eric_mazur

and also....

Hemi Gandhi
Alexander Raymond
Marc Winkler
Eric Diebold
Haifei Albert Zhang
Dr. Brian Tull
Dr. Jim Carey (SiOnyx)
Prof. Tsing-Hua Her (UNC Charlotte)
Dr. Shrenik Deliwala
Dr. Richard Finlay
Dr. Michael Sheehy
Dr. Claudia Wu
Dr. Rebecca Younkin
Prof. Catherine Crouch (Swarthmore)
Prof. Mengyan Shen (Lowell U)
Prof. Li Zhao (Fudan U)

Prof. Alan Aspuru-Guzik
Prof. Michael Aziz
Prof. Michael Brenner
Prof. Cynthia Friend
Prof. Howard Stone

Dr. Martin Pralle (SiOnyx)
and everyone else at SiOnyx…

Prof. Tonio Buonassisi (MIT)
Prof. Silvija Gradecak (MIT)
Prof. Jeff Grossman (MIT)
Dr. Bonna Newman (MIT)
Joe Sullivan (MIT)
Matthew Smith (MIT)

Prof. Augustinus Asenbaum (Vienna)

Dr. François Génin (LLNL)
Mark Wall (LLNL)

Dr. Richard Farrell (RMD)
Dr. Arieh Karger (RMD)
Dr. Richard Meyers (RMD)

Dr. Pat Maloney (NVSED)

Dr. Jeffrey Warrander (ARDEC)

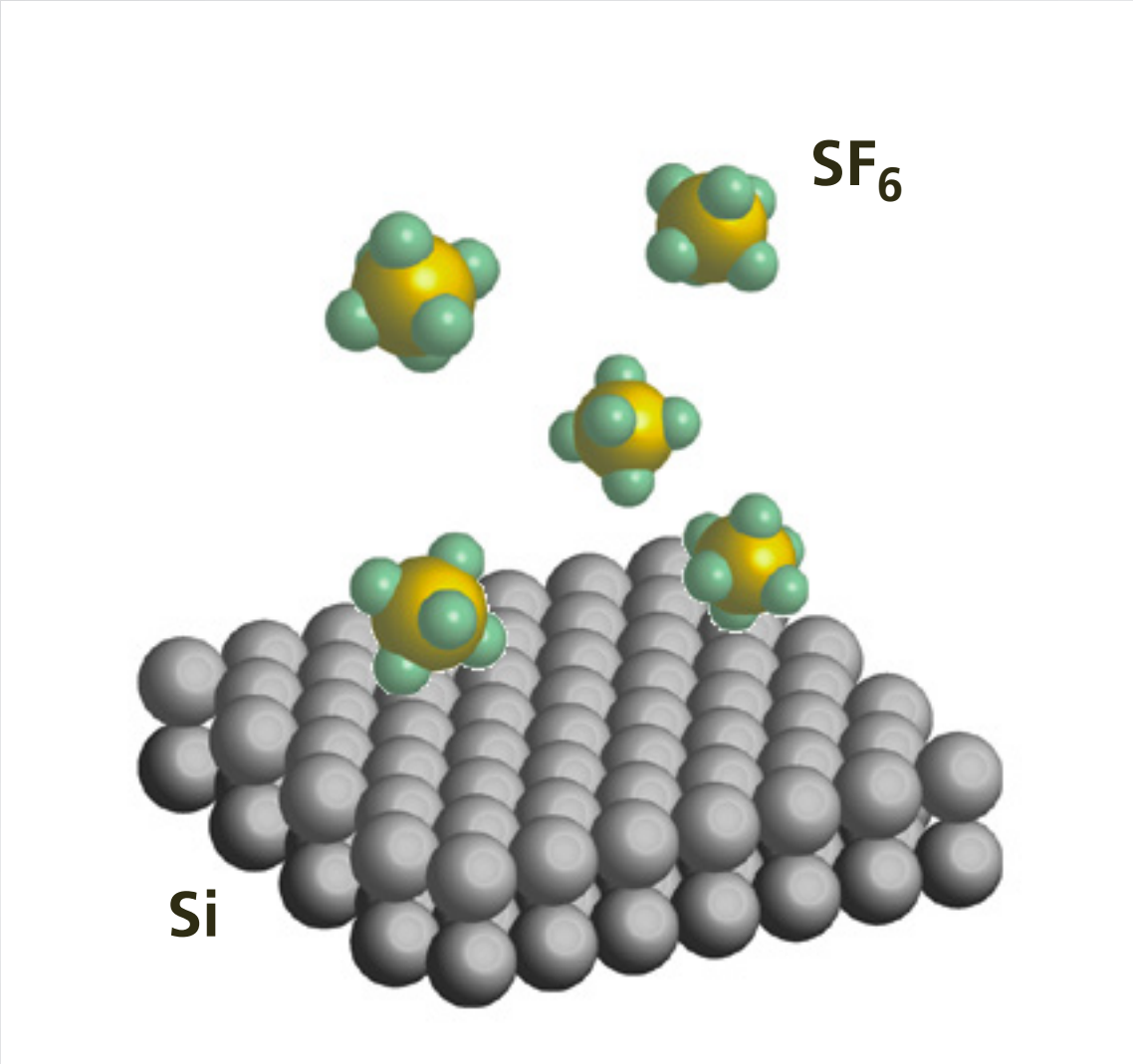

irradiate with 100-fs 10 kJ/m^2 pulses

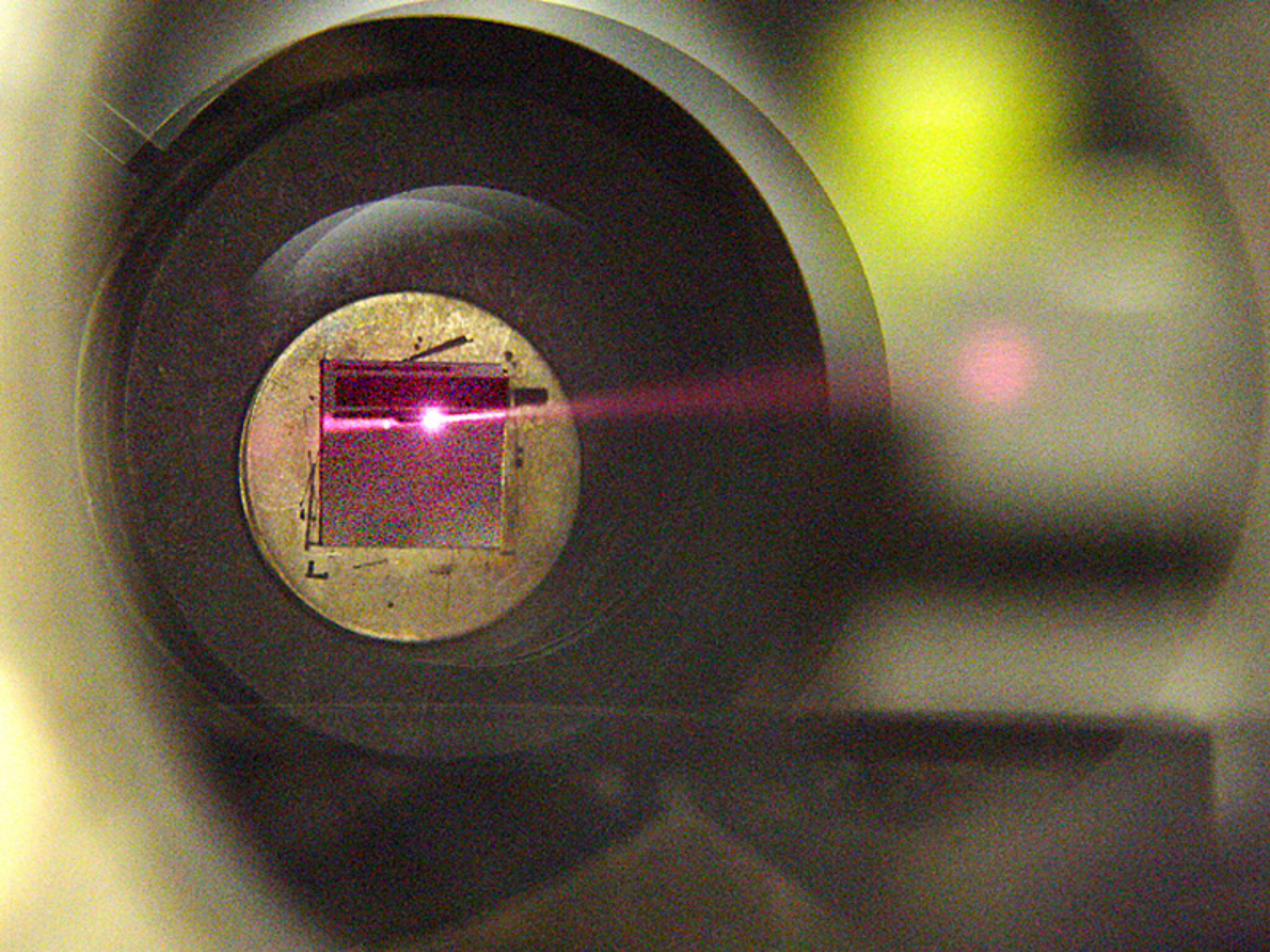

“black silicon”

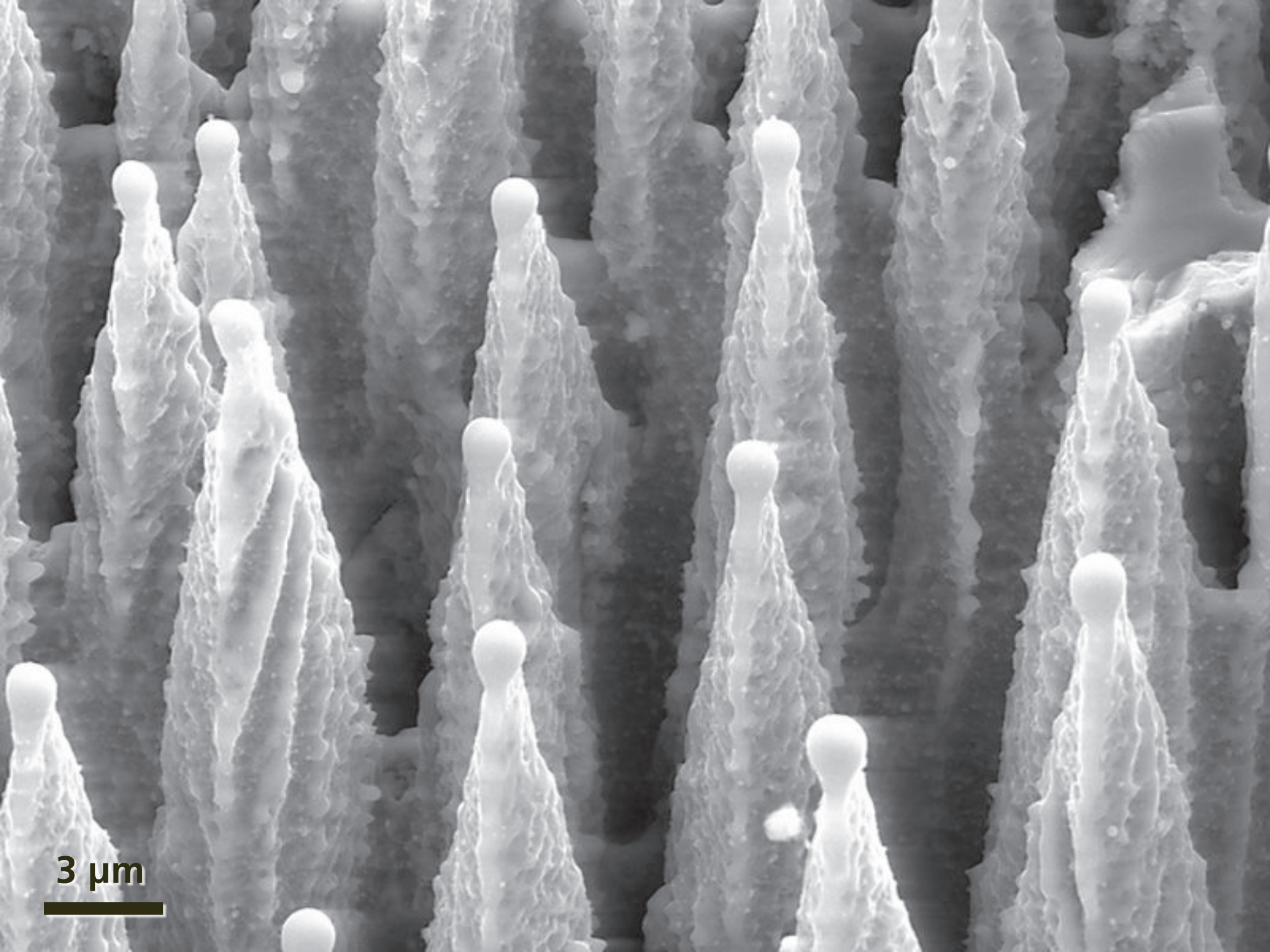
3 µm

absorptance (1 – R_{int} – T_{int})

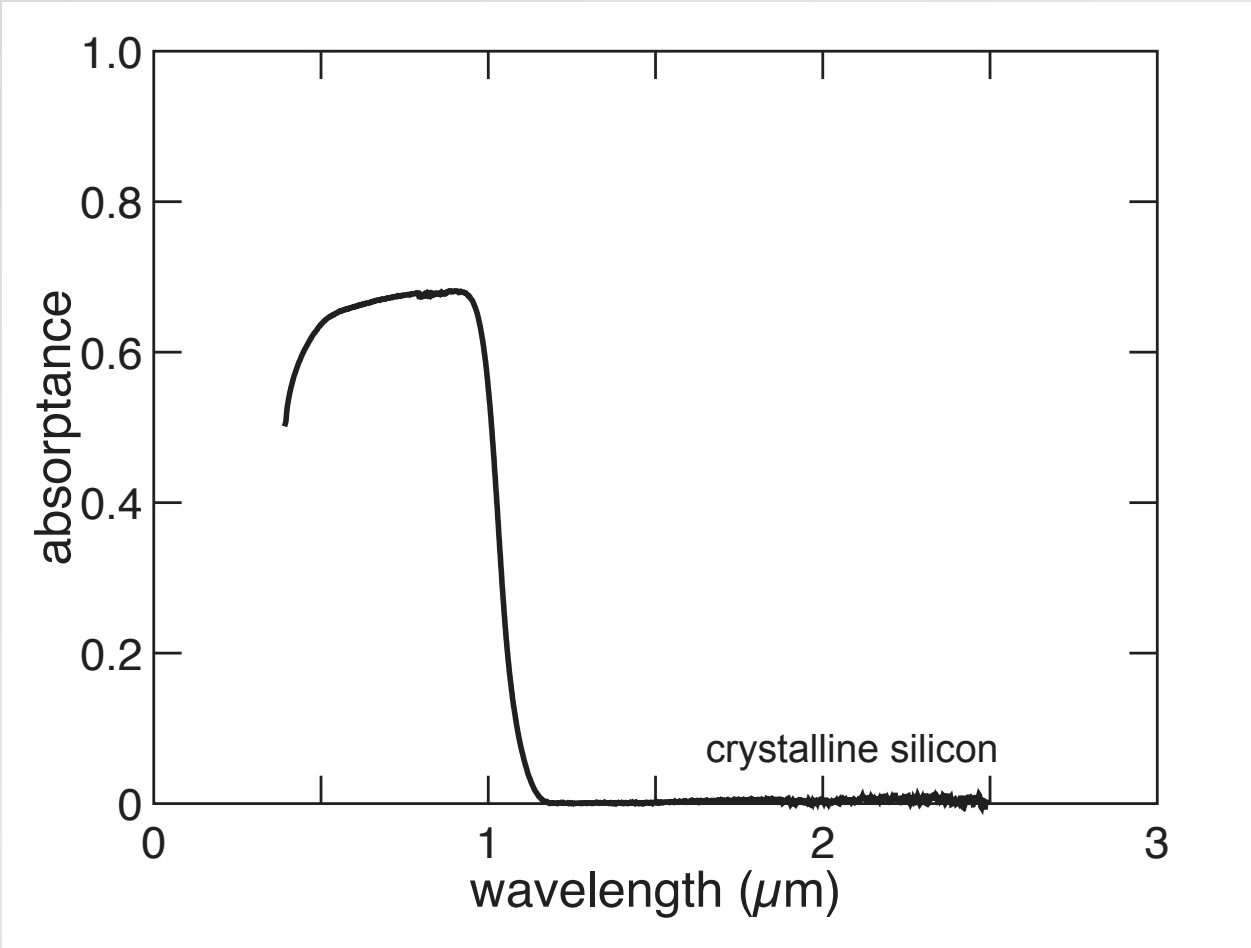

absorptance ($1 - R_{int} - T_{int}$)

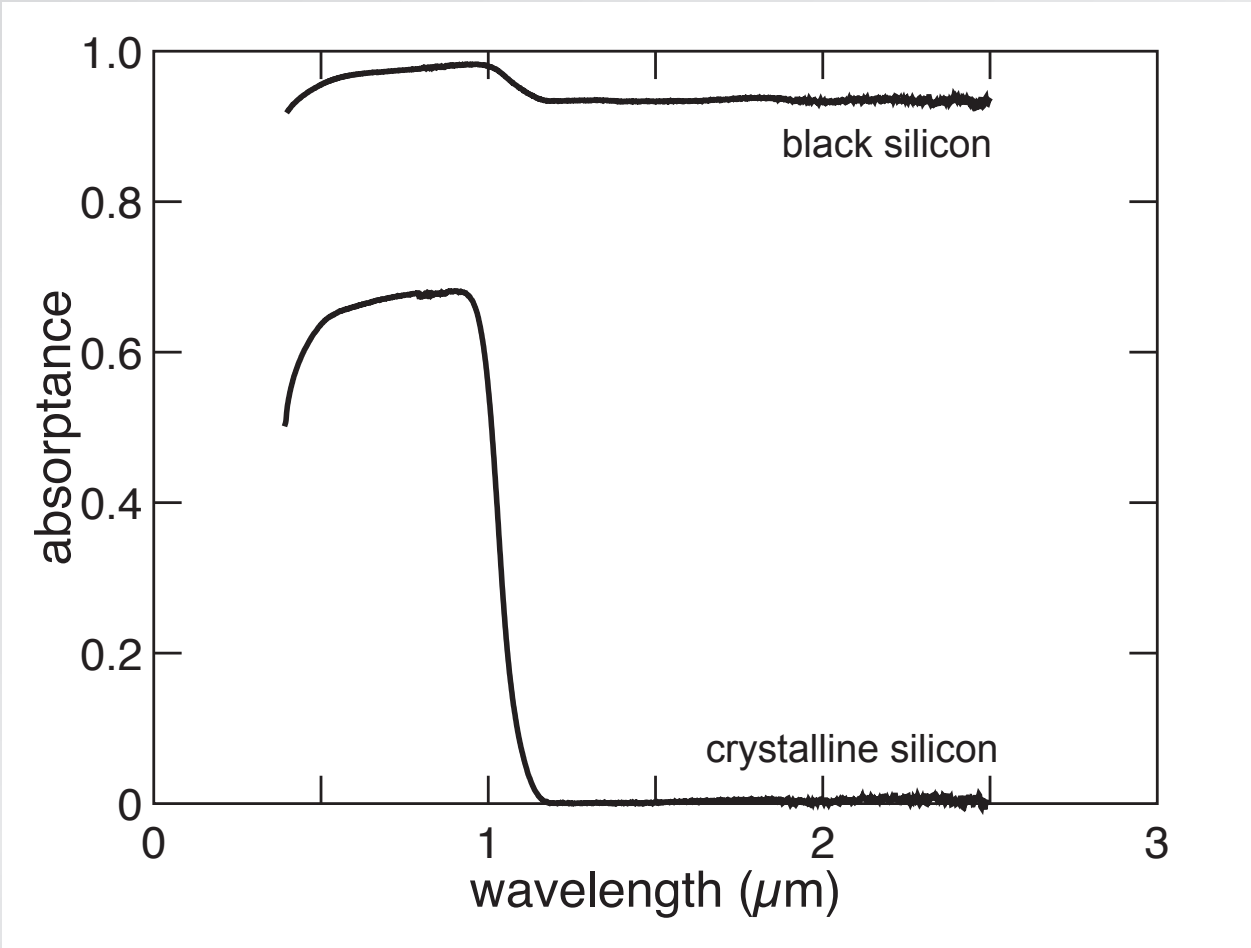

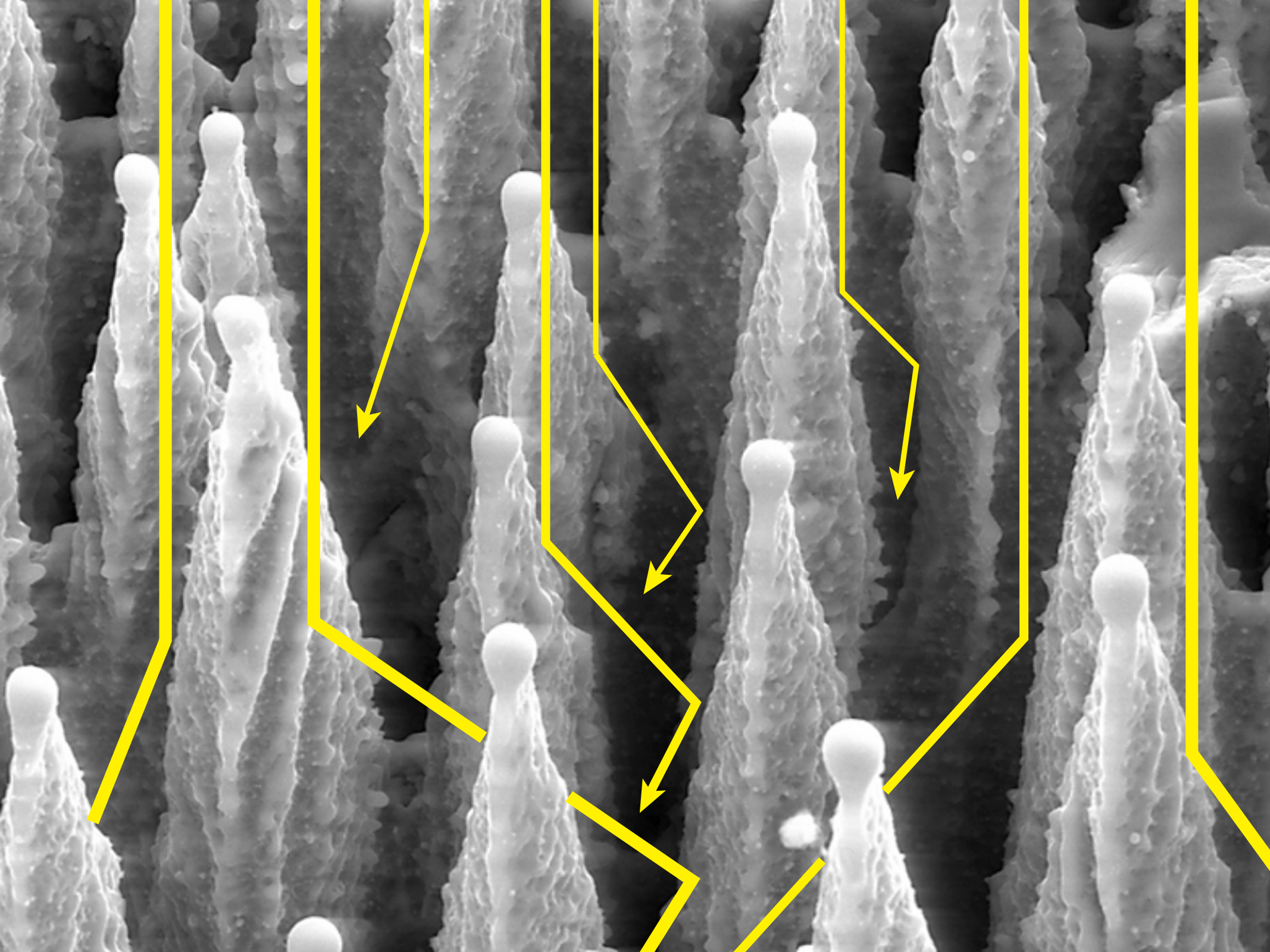

absorptance ($1 - R_{int} - T_{int}$)

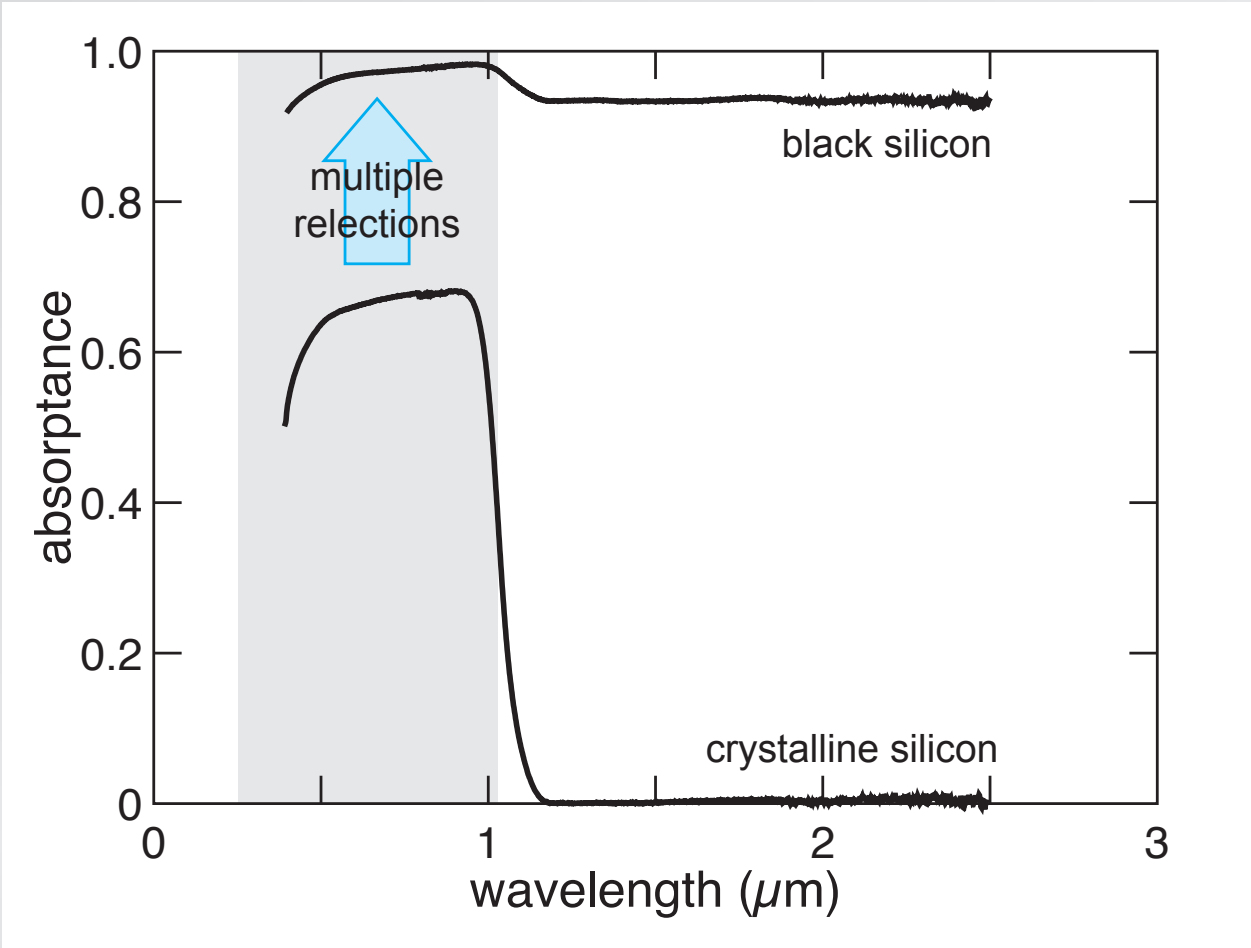

absorptance ($1 - R_{int} - T_{int}$)

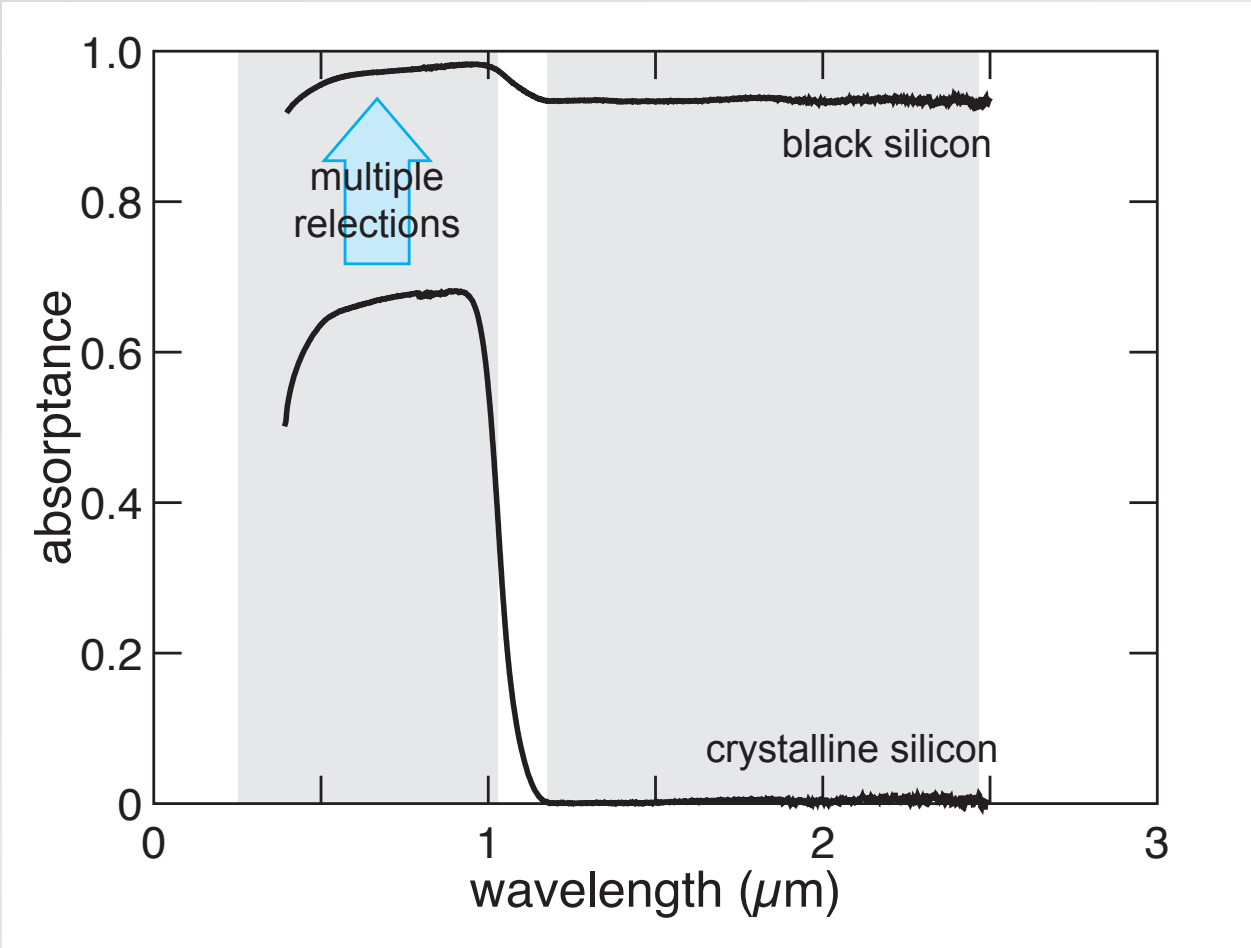

absorptance ($1 - R_{int} - T_{int}$)

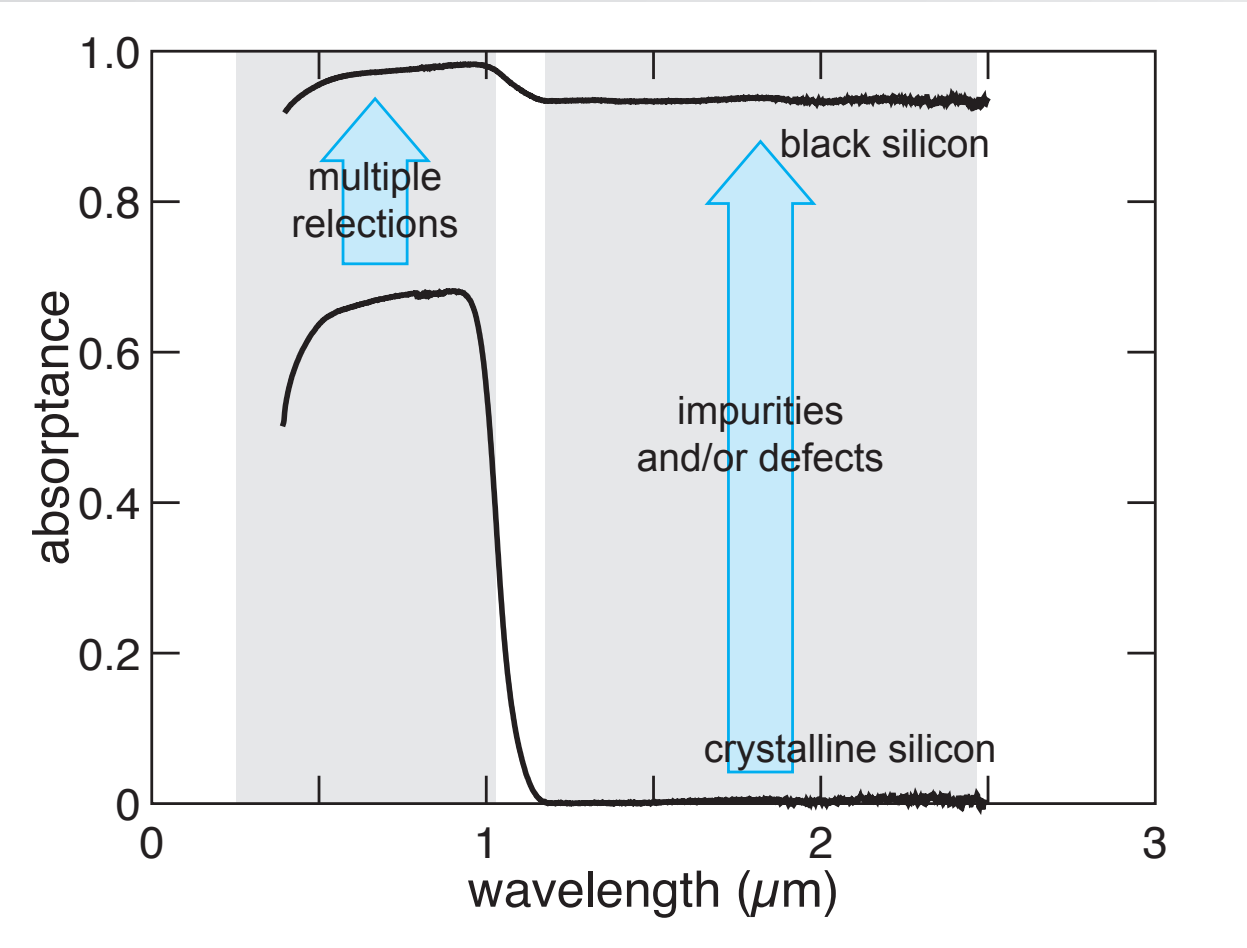

laser treatment causes:

- surface structuring
- inclusion of dopants

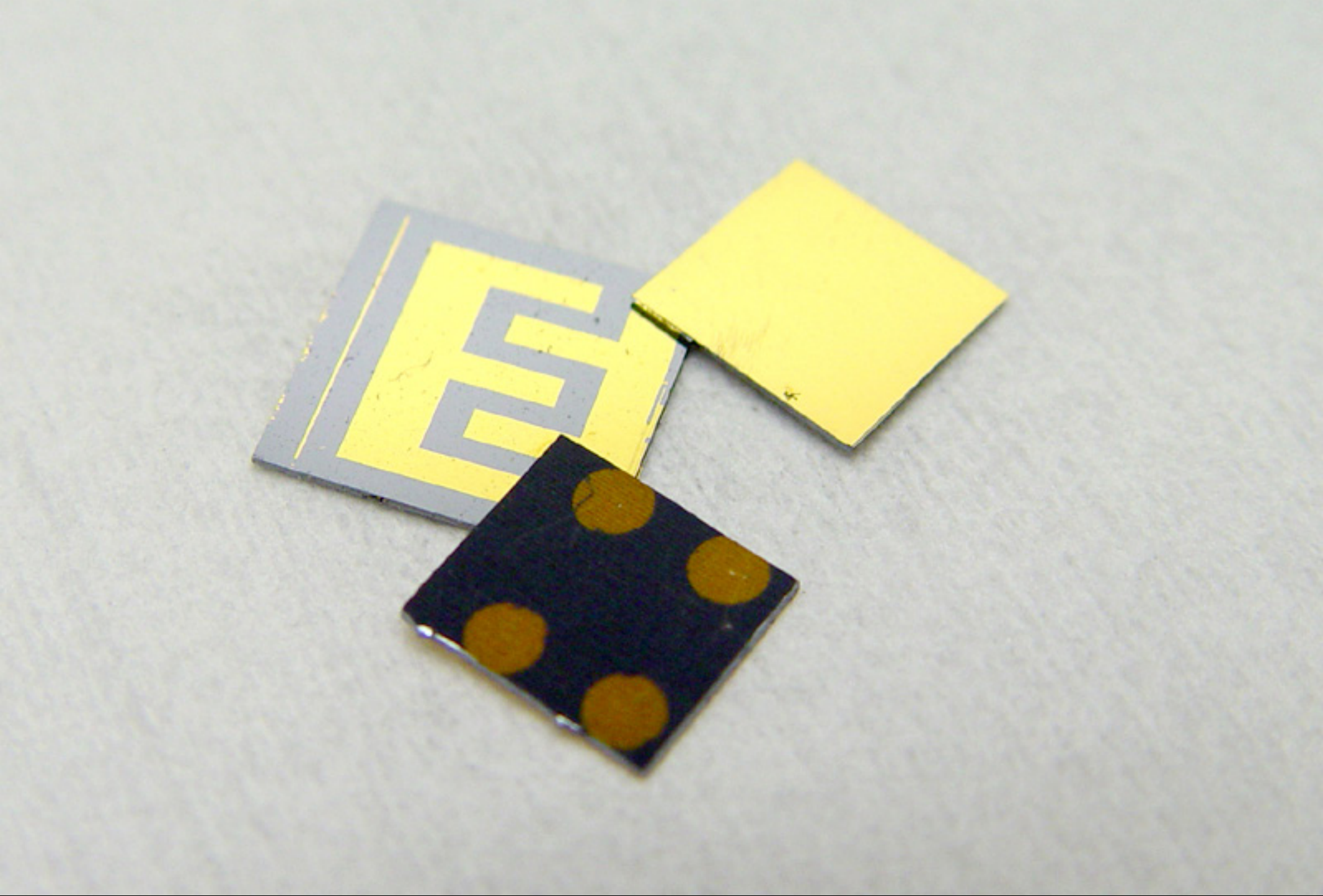

1 properties

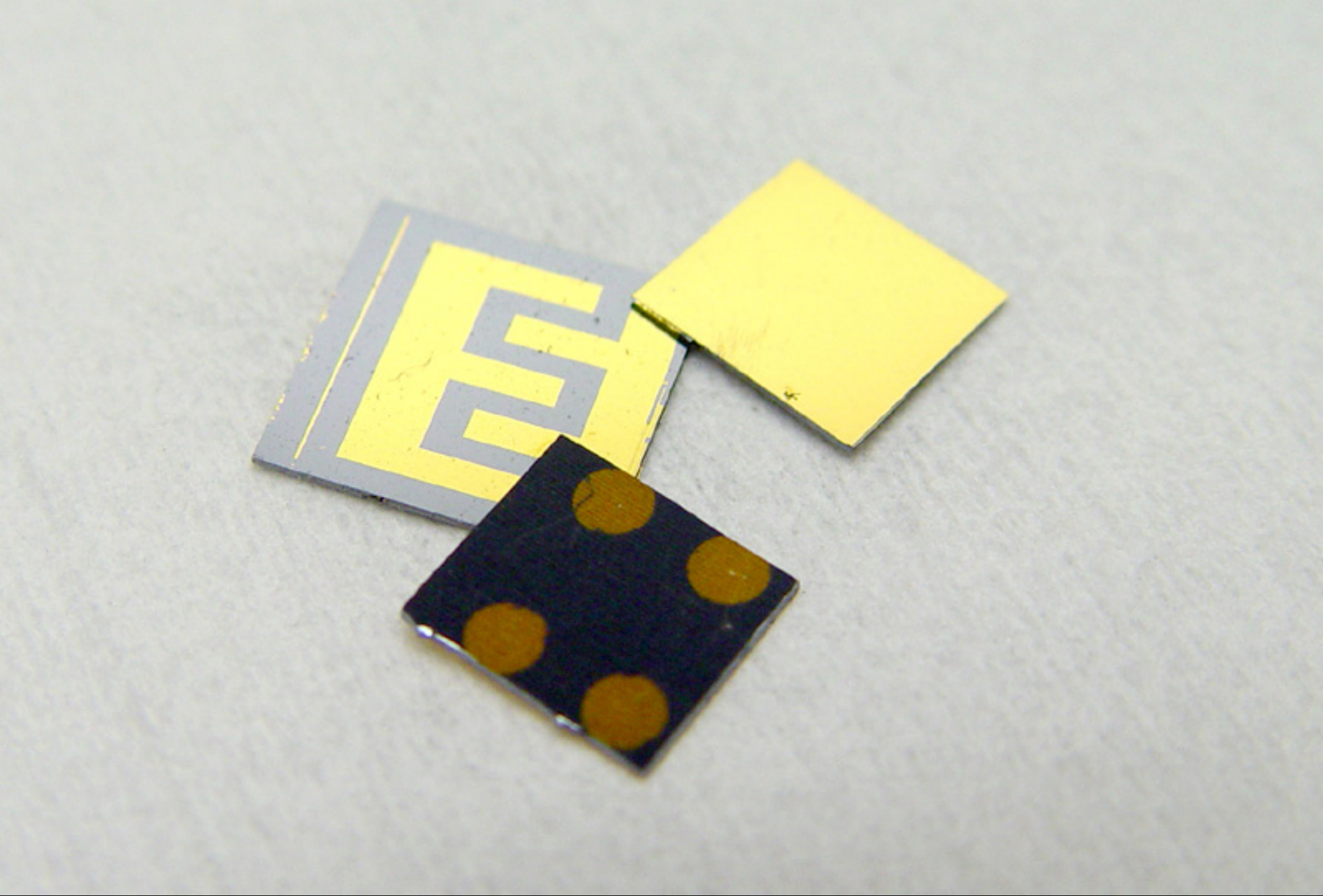

1 properties 2 intermediate band

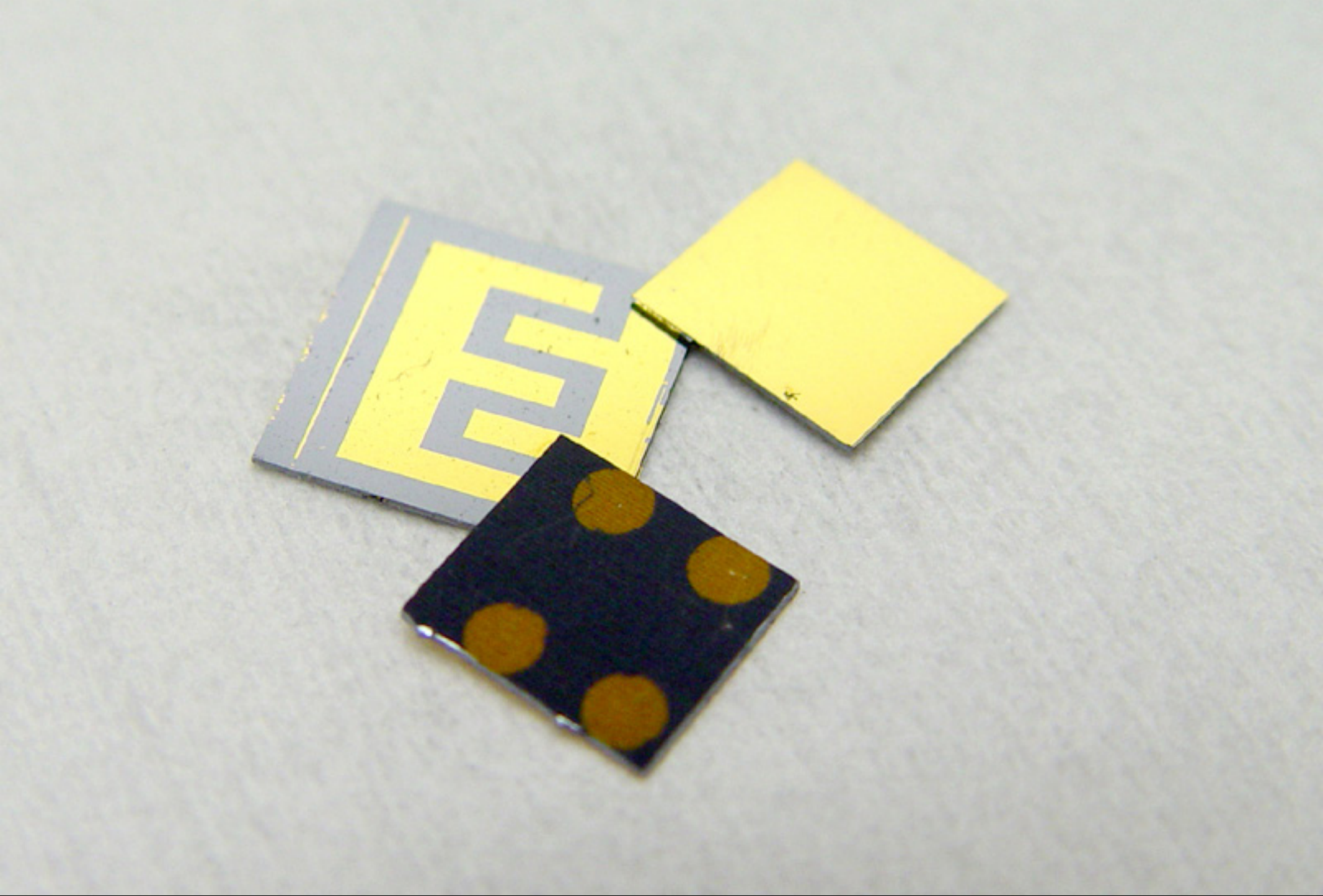

1 properties 2 intermediate band 3 devices

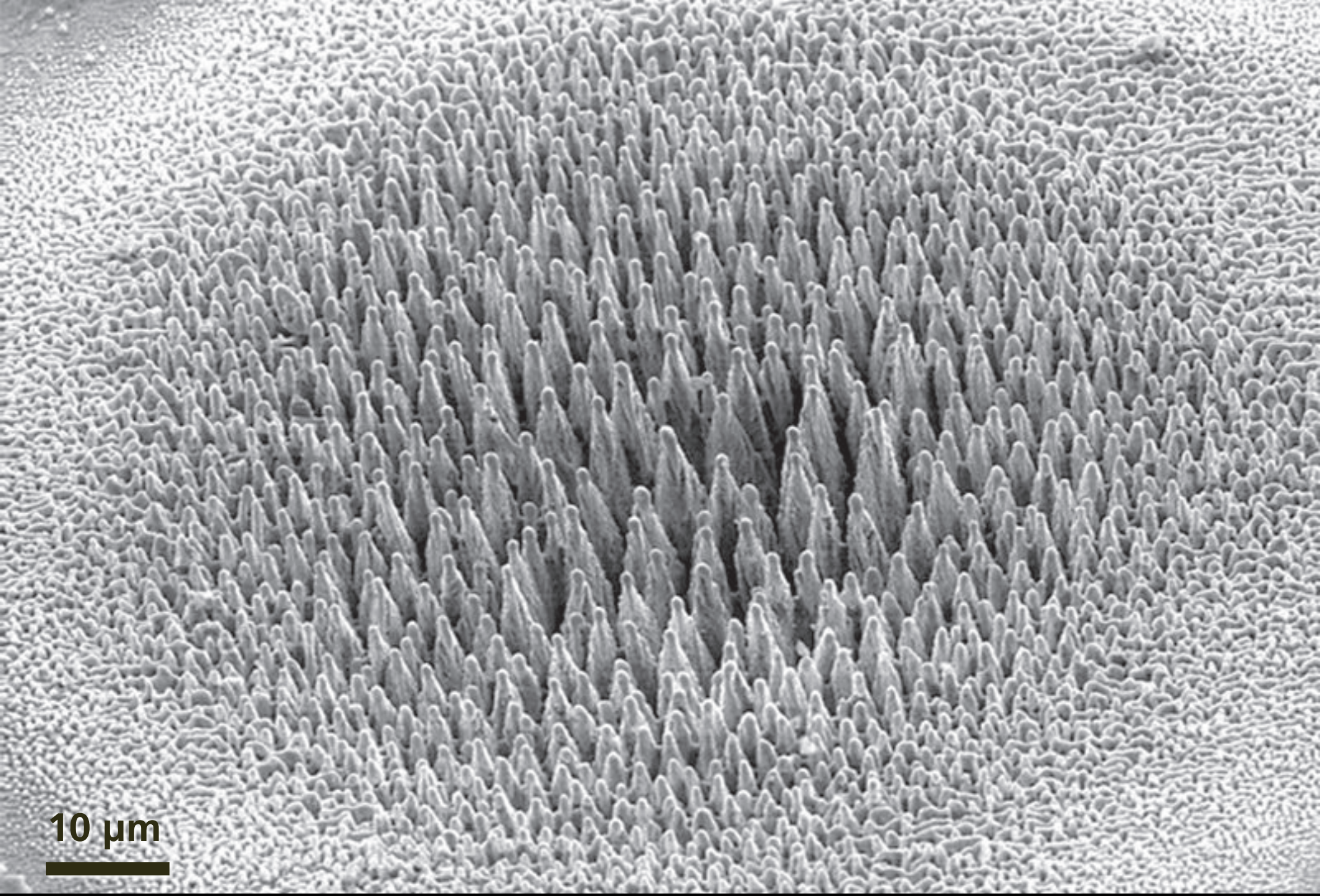

1 properties

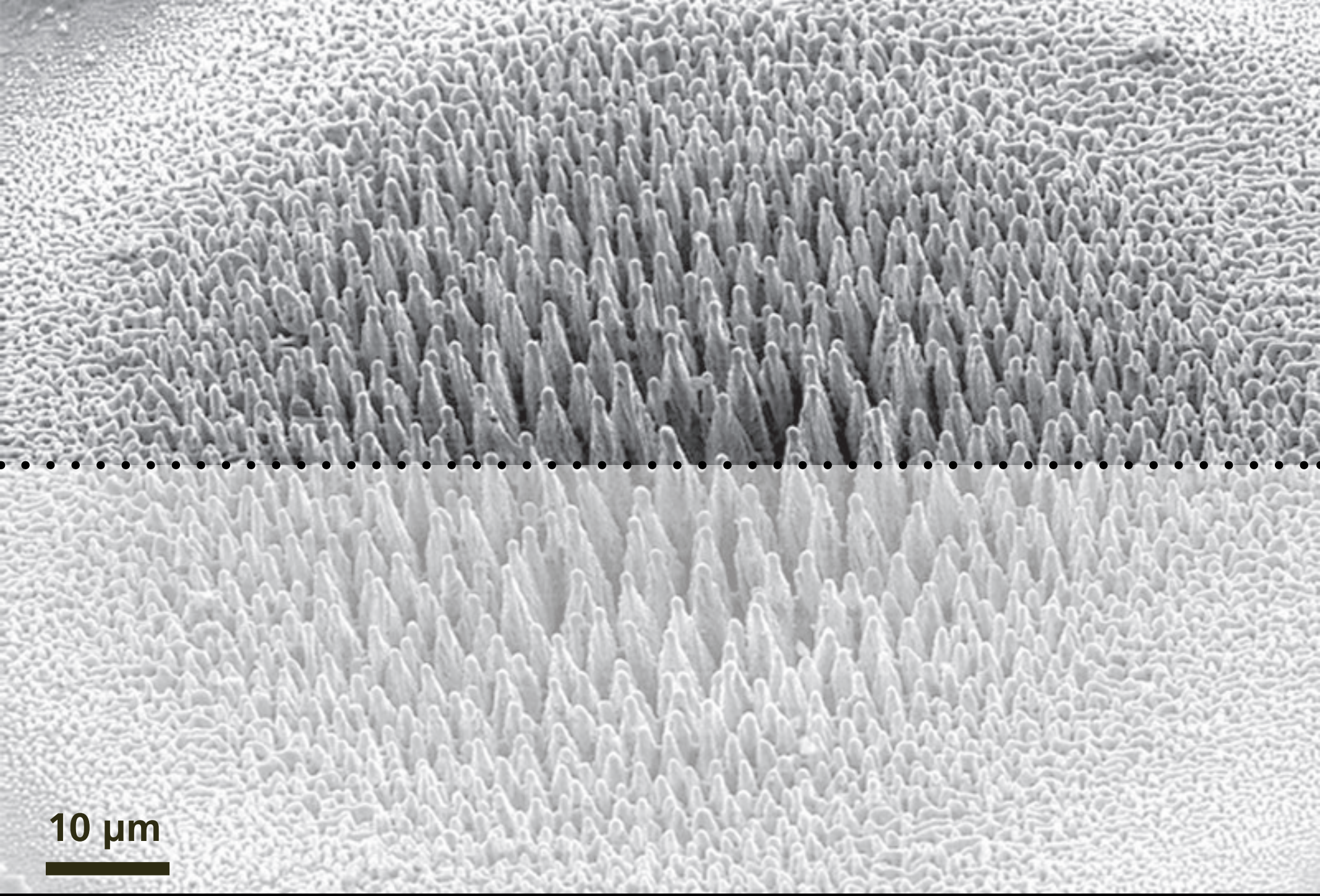

1 properties

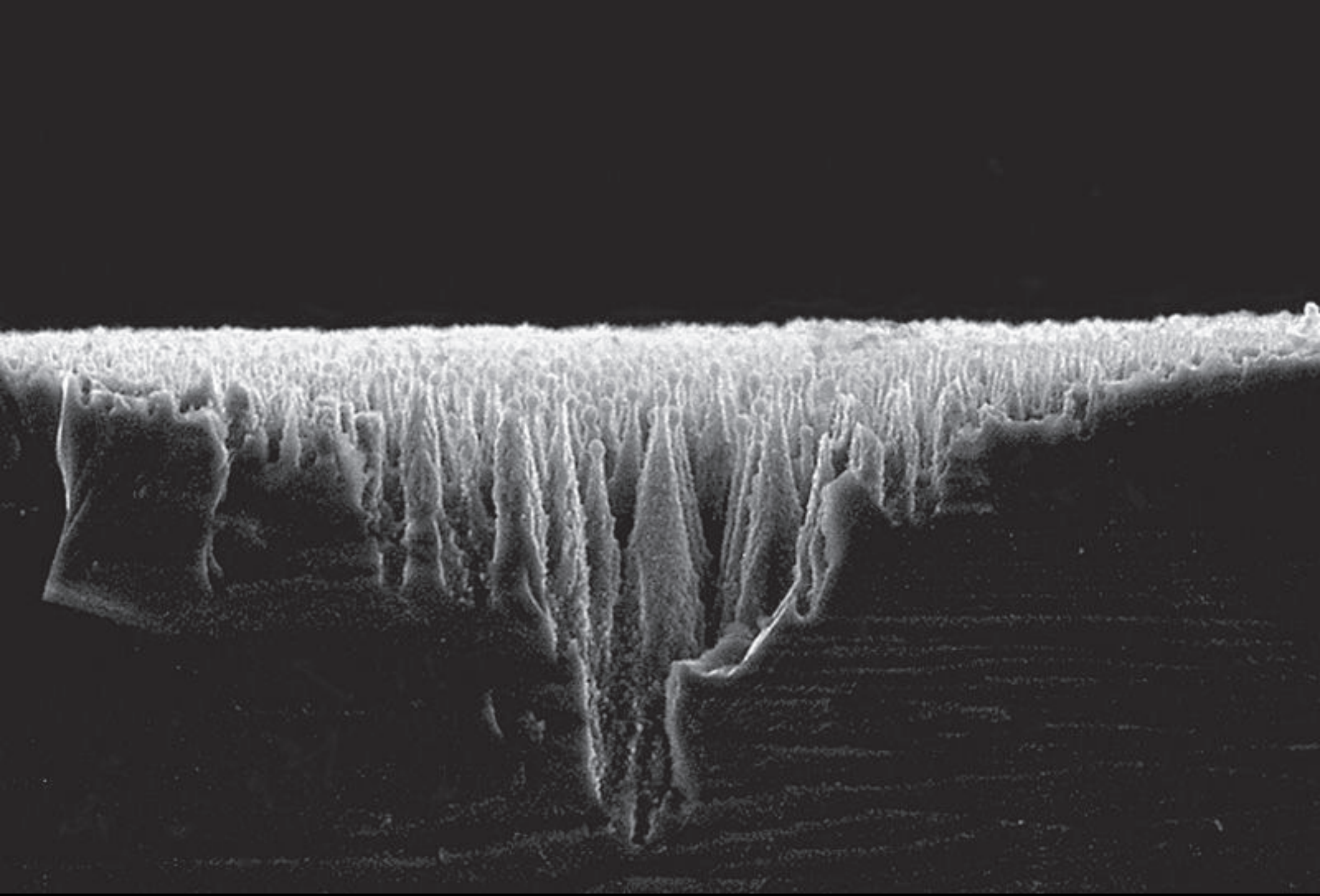

1 properties

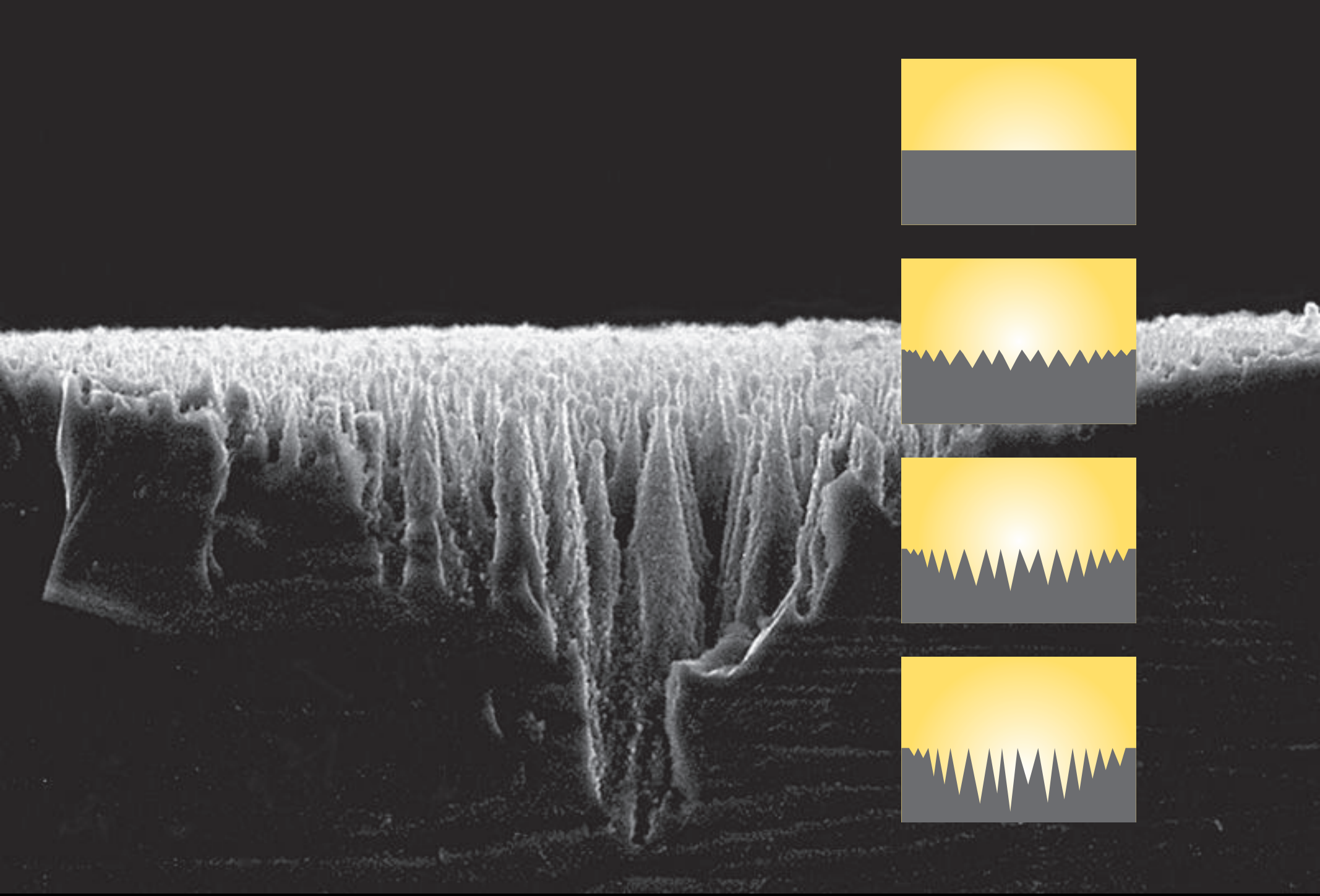

1 properties

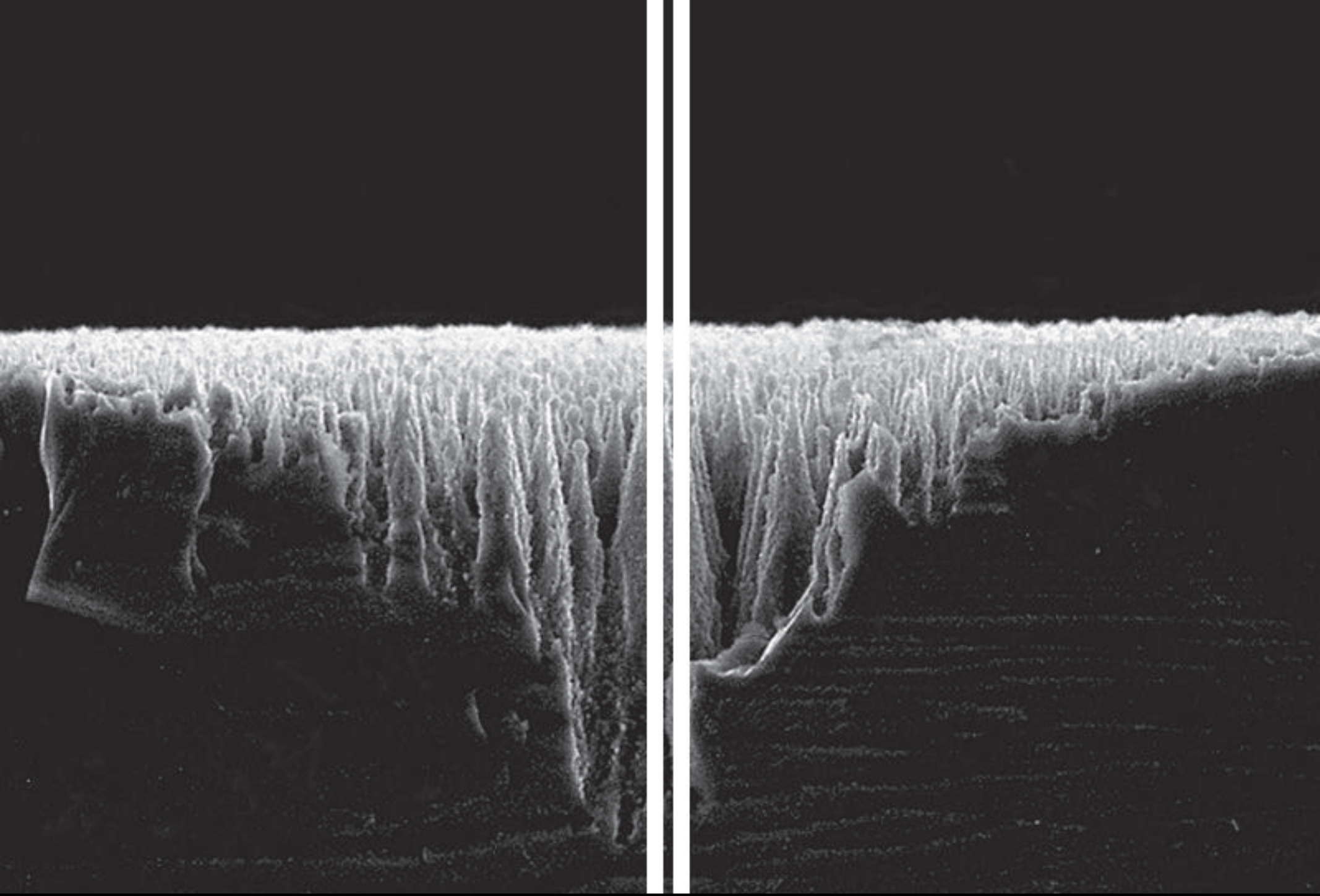

1 properties

cross-sectional
Transmission Electron
Microscopy

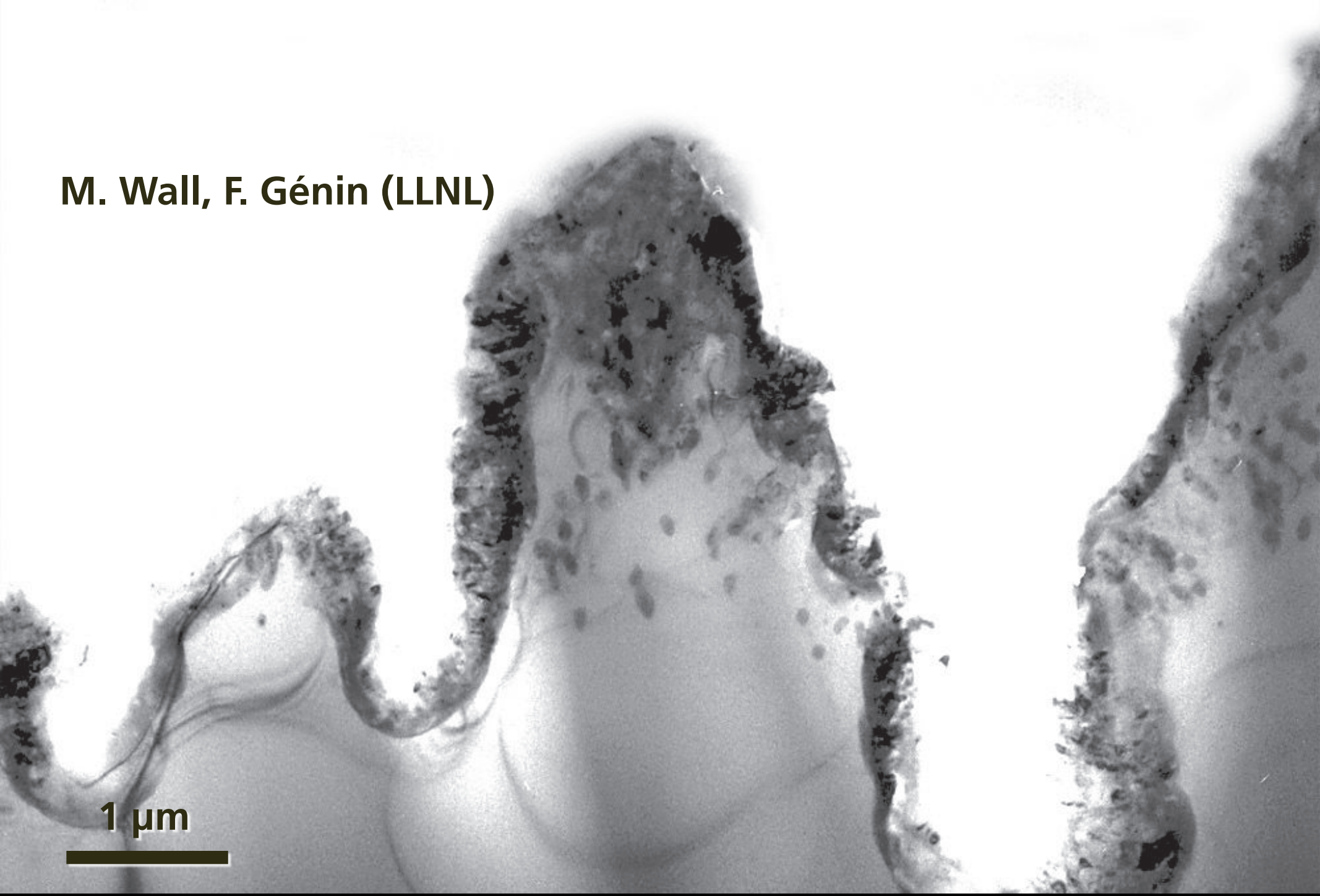

1 properties

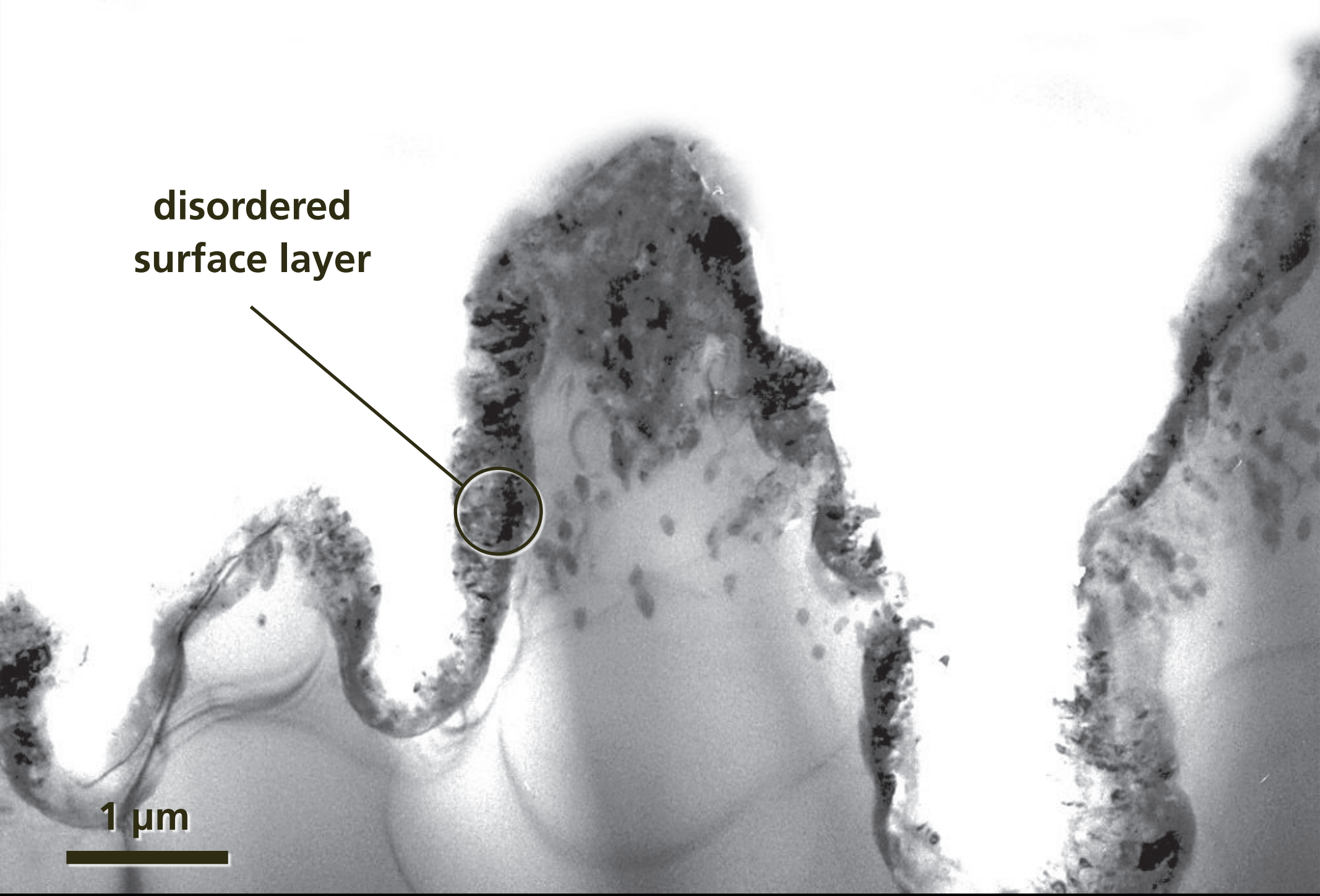
disordered
surface layer
1 µm

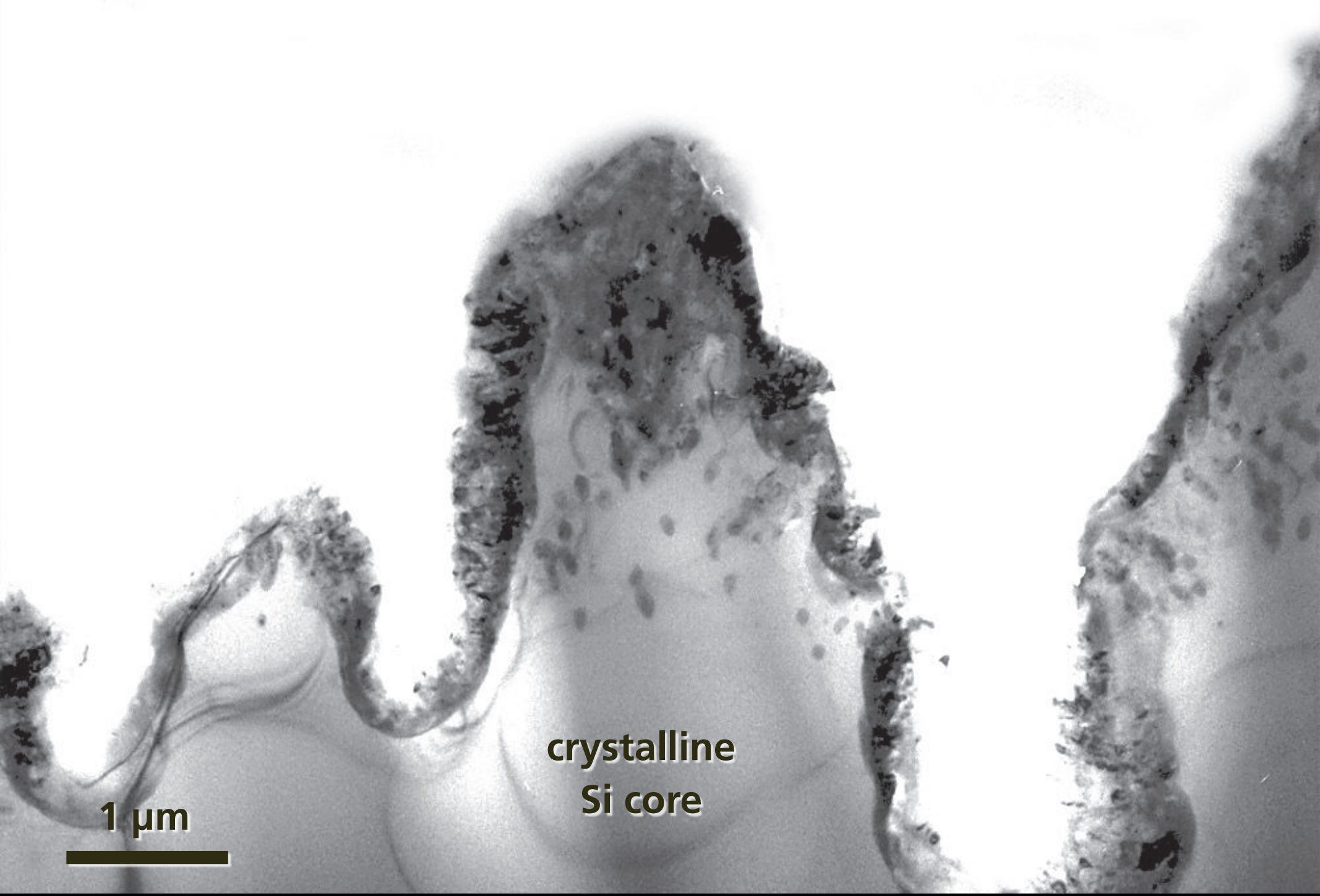

1 properties

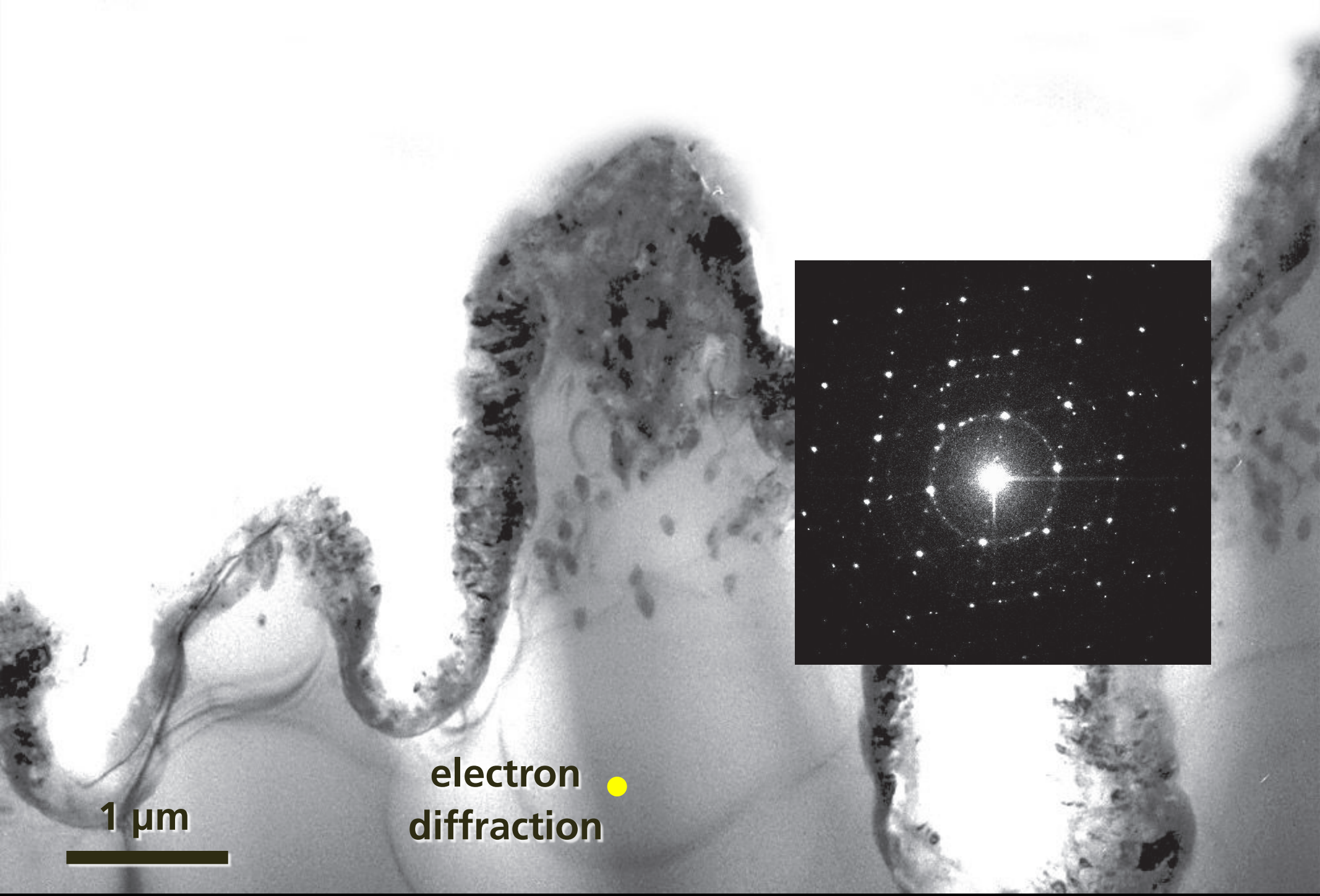
1 µm
electron
diffraction

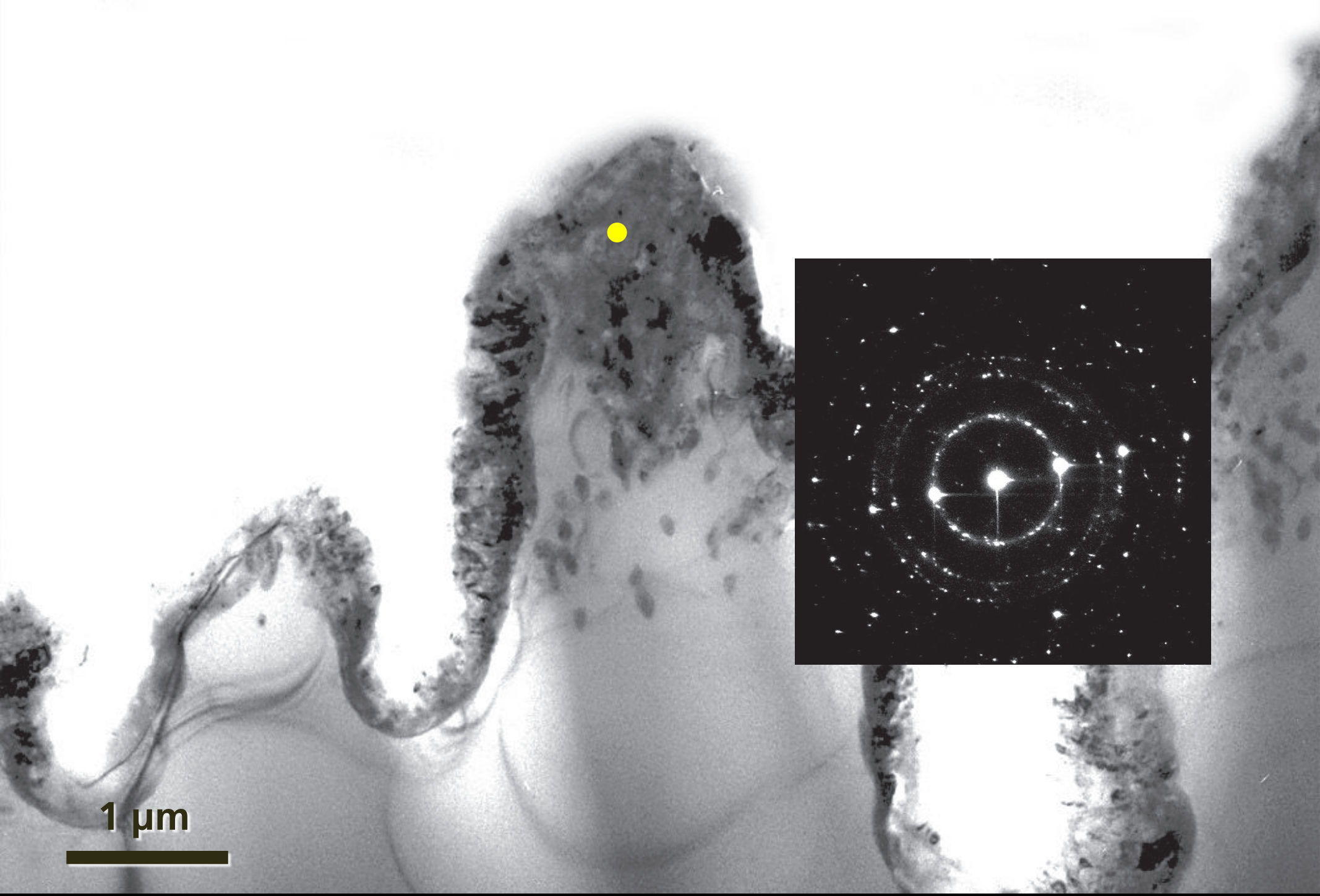

1 properties

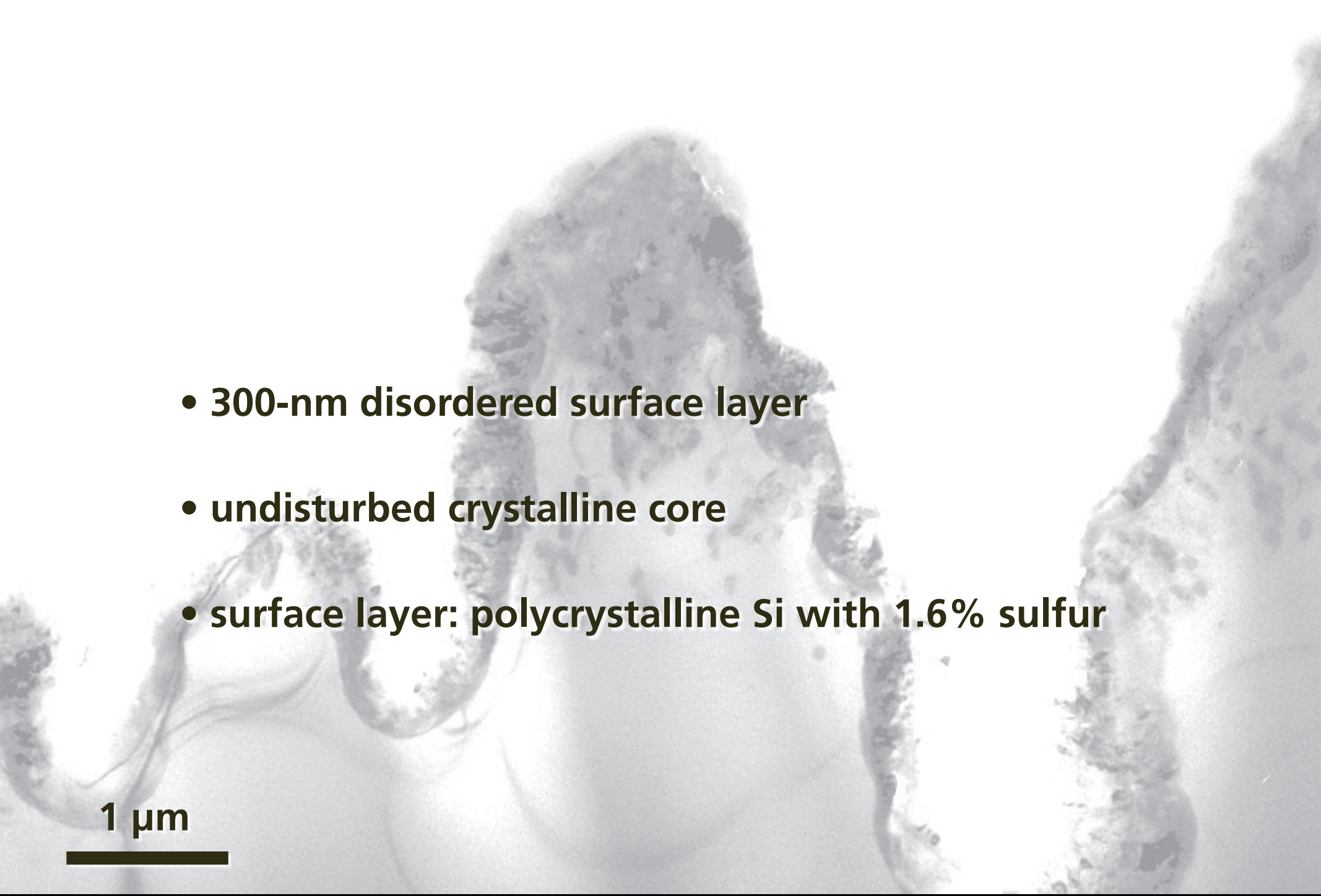
• 300-nm disordered surface layer
• undisturbed crystalline core
• surface layer: polycrystalline Si with 1.6% sulfur
1 µm

two processes: melting and ablation

relevant time scales

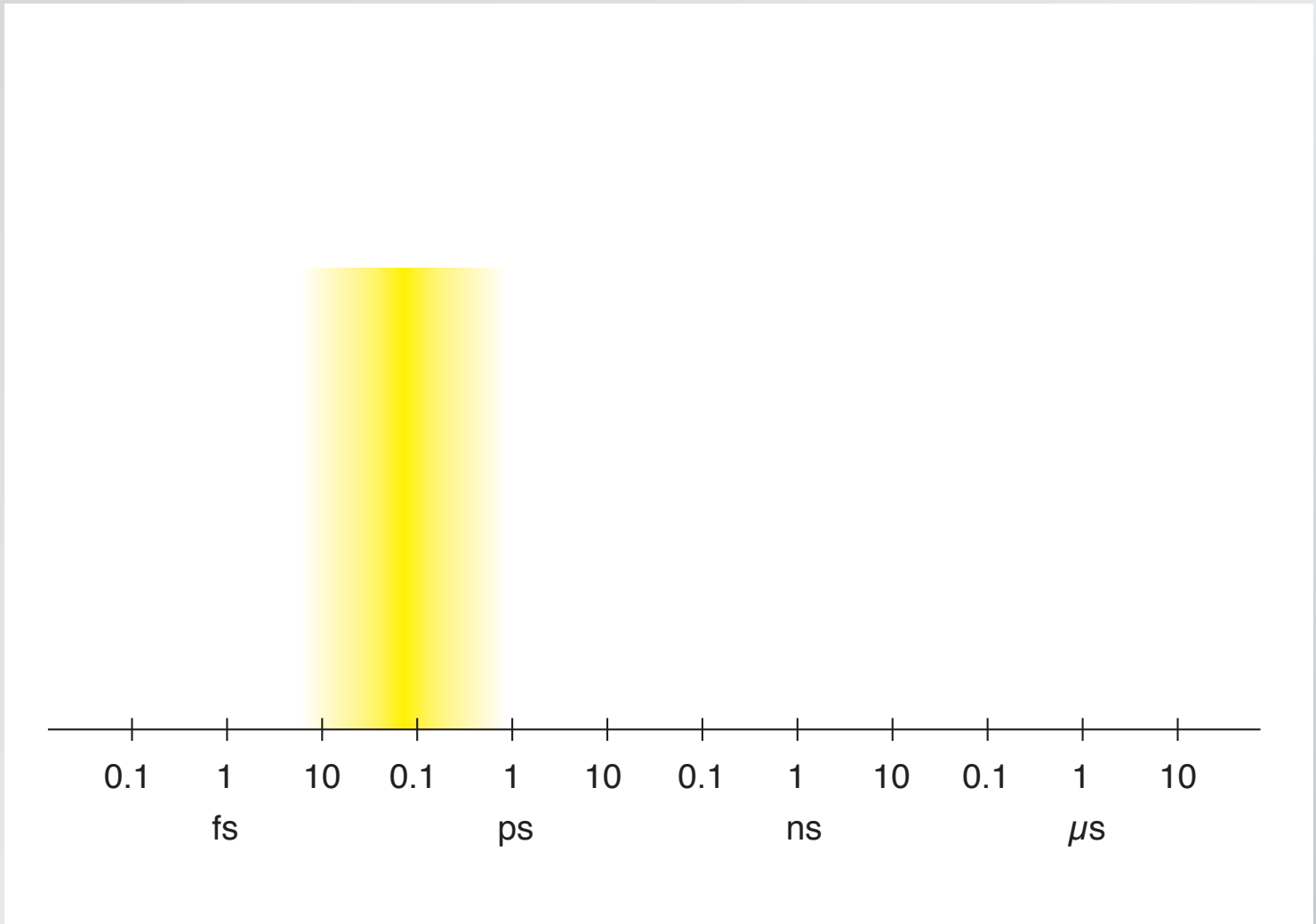

relevant time scales

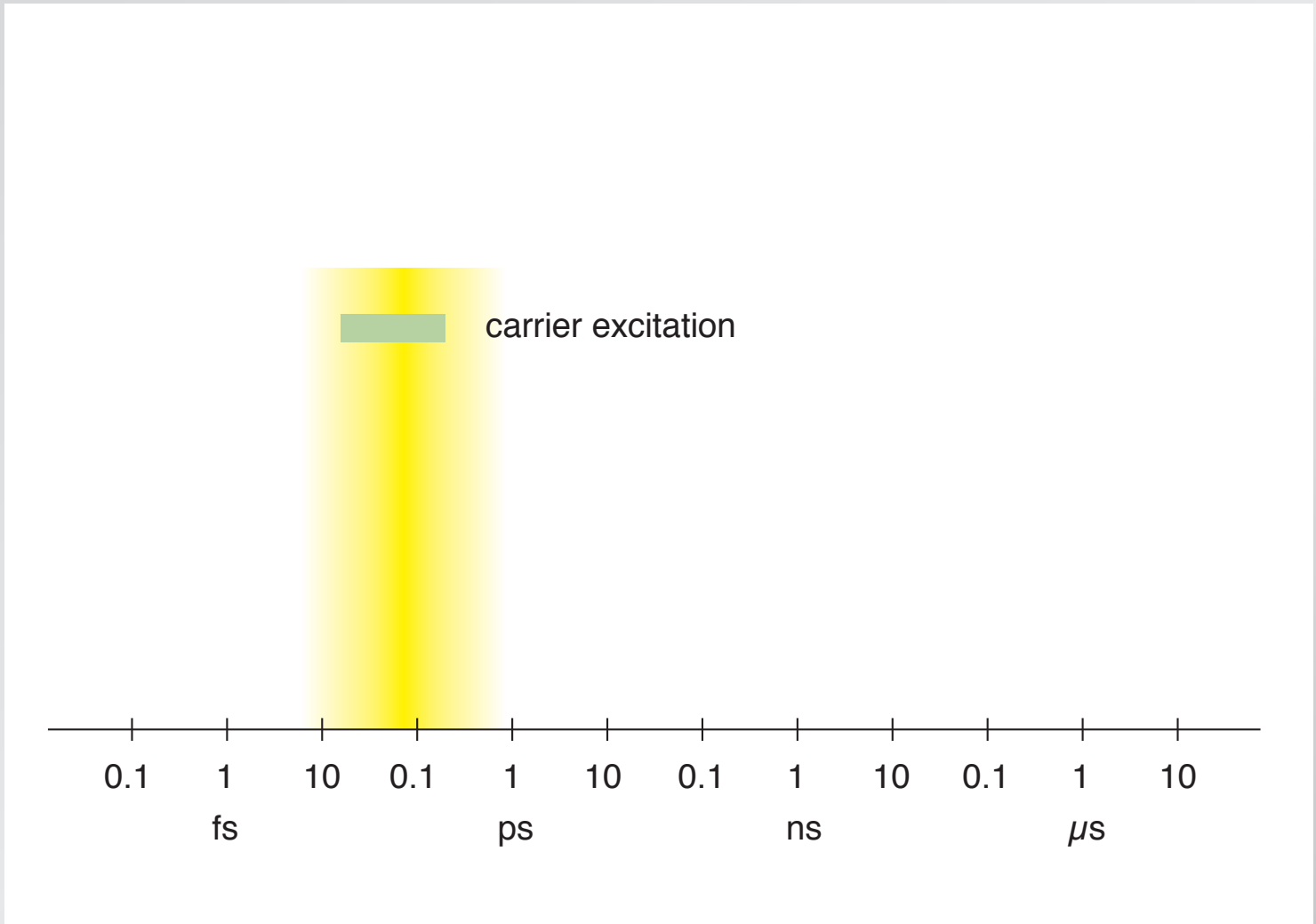

relevant time scales

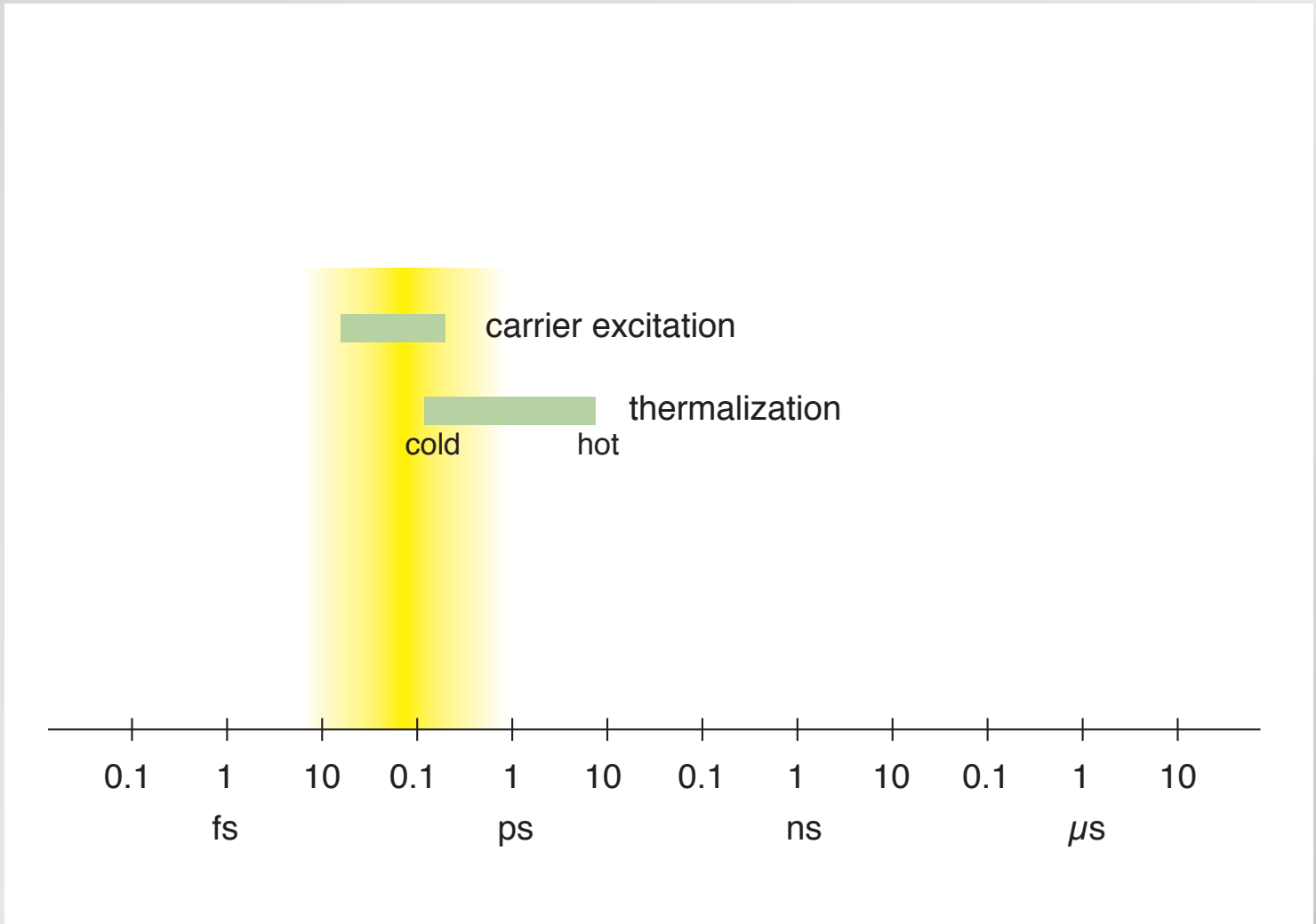

relevant time scales

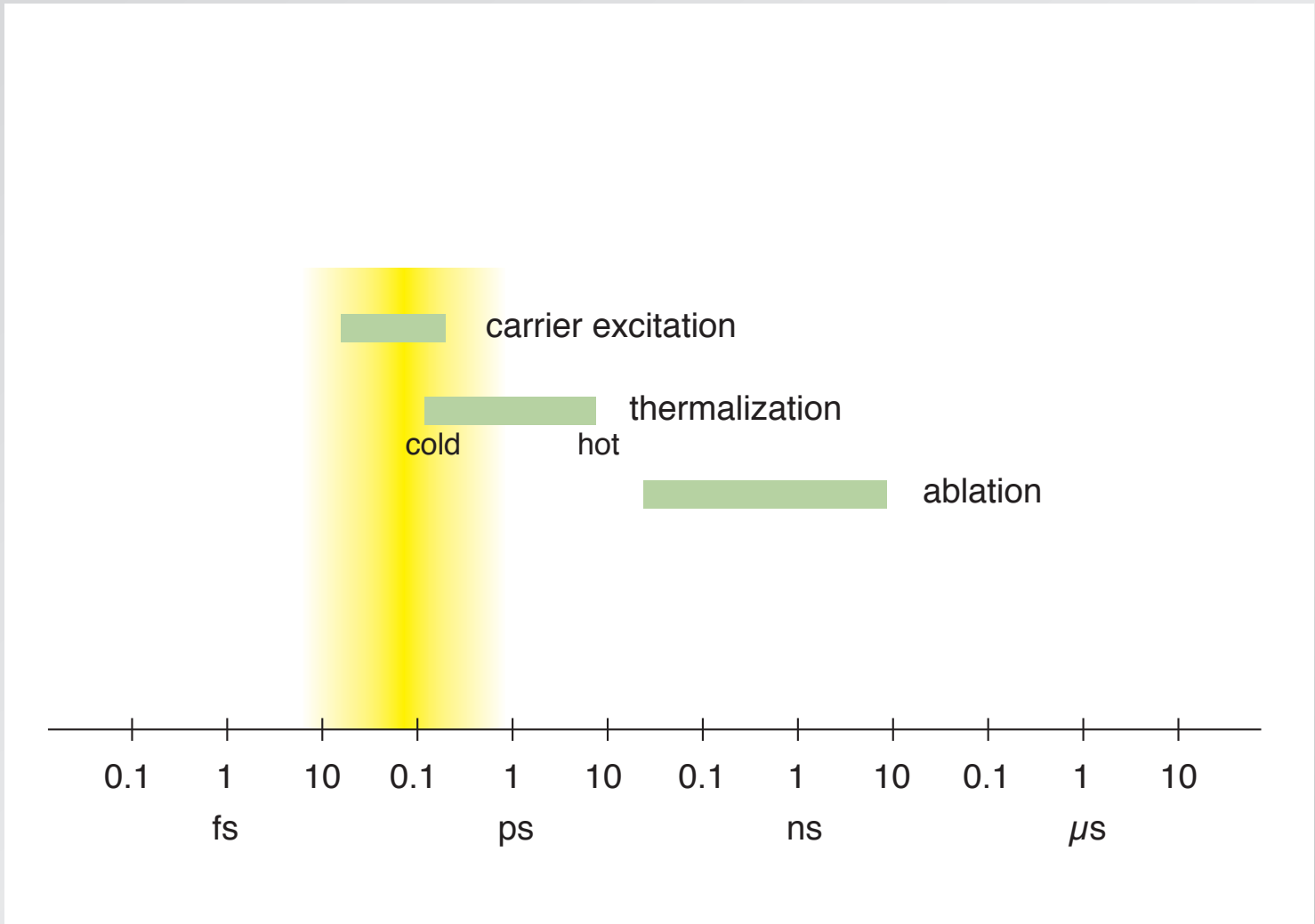

relevant time scales

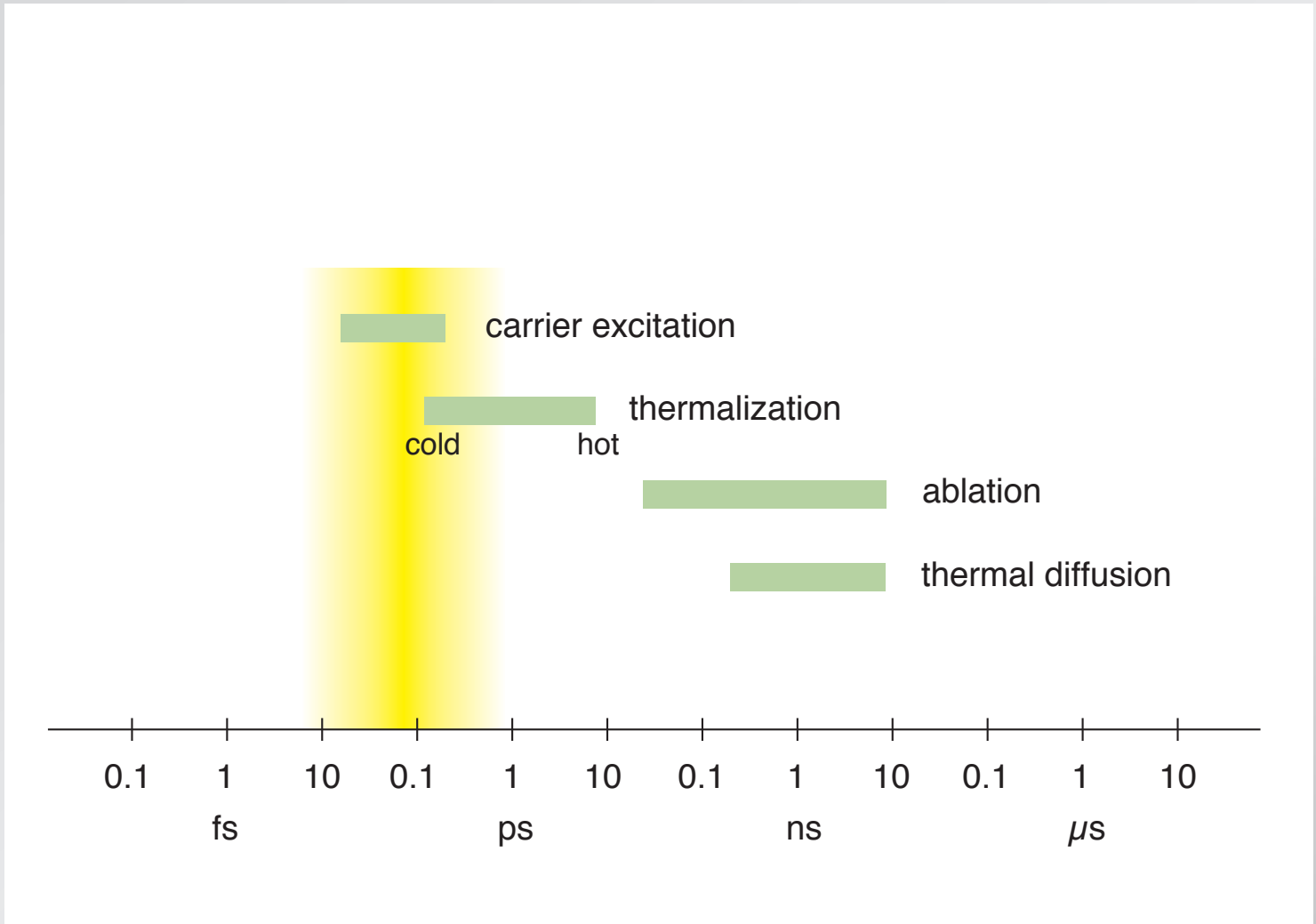

relevant time scales

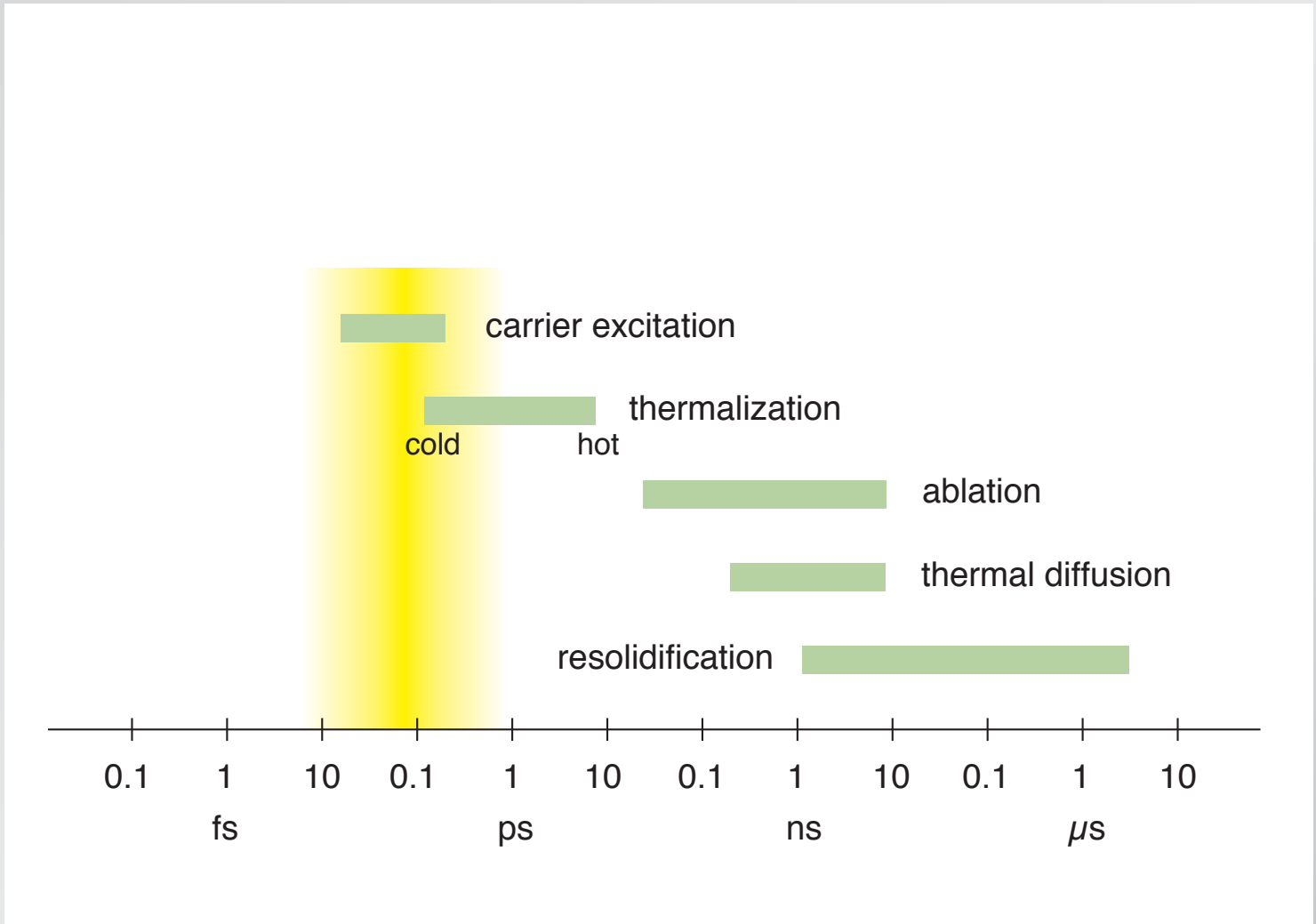

relevant time scales

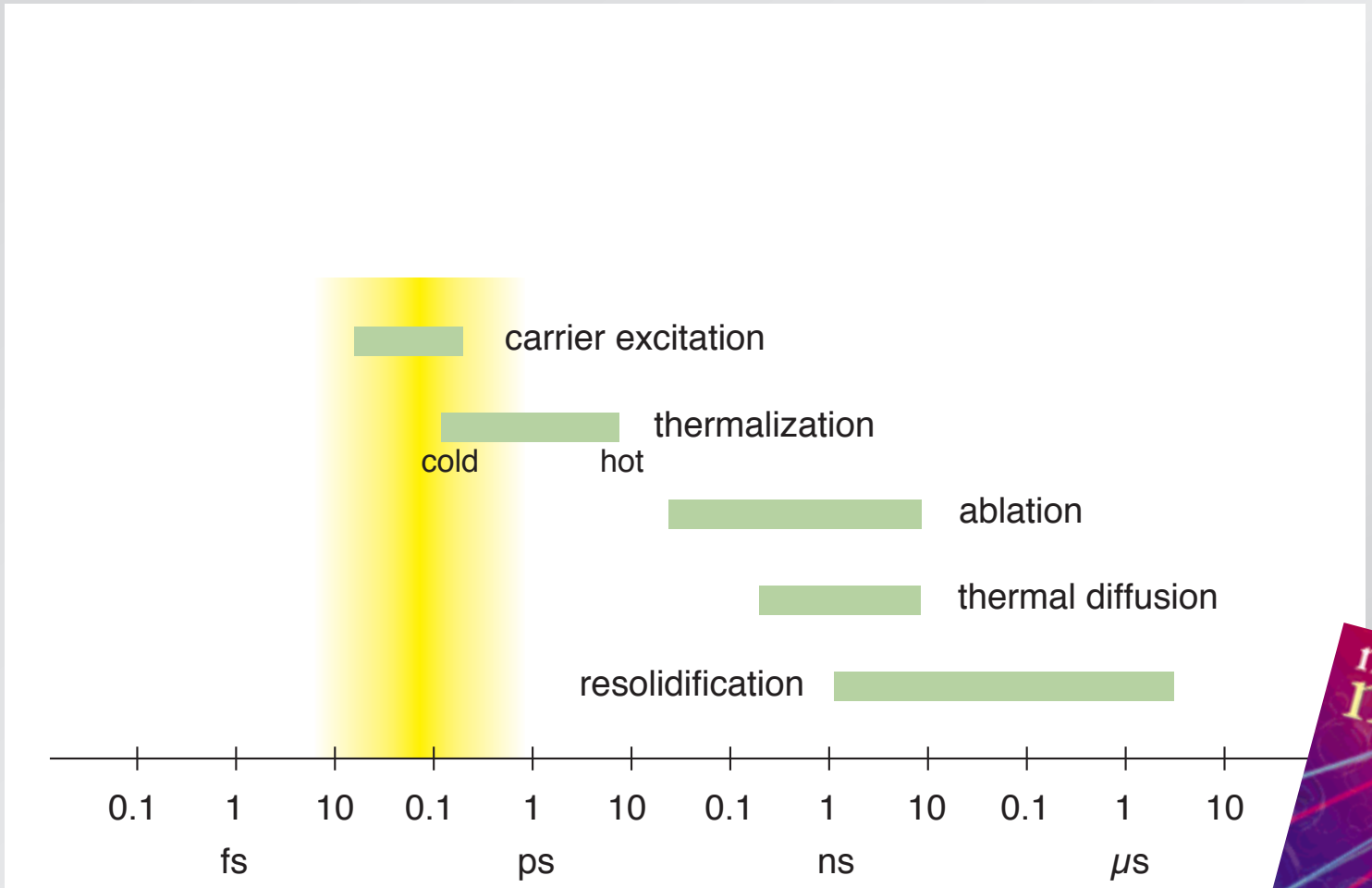

Nature Materials **1**, 217 (2002)

relevant time scales

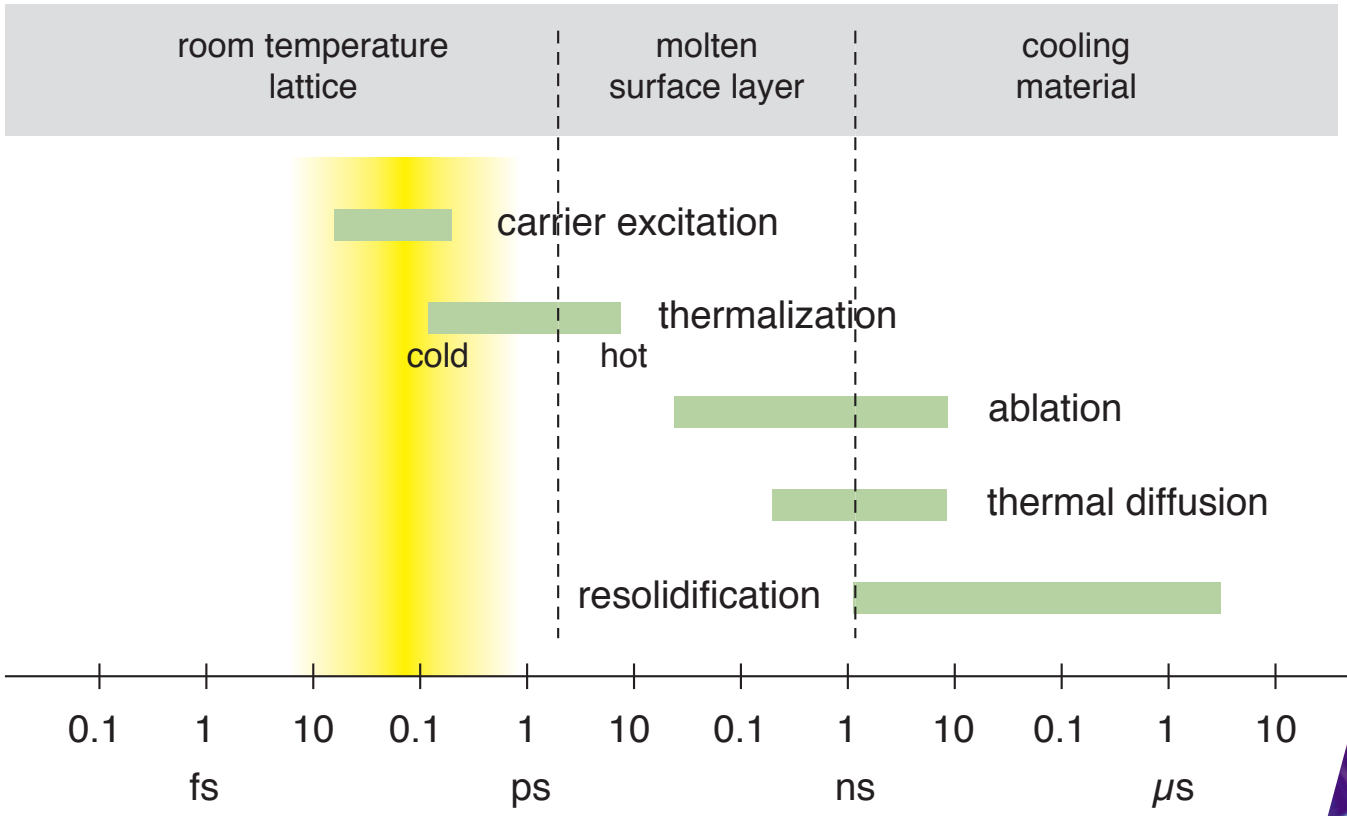

Nature Materials **1**, 217 (2002)

relevant time scales

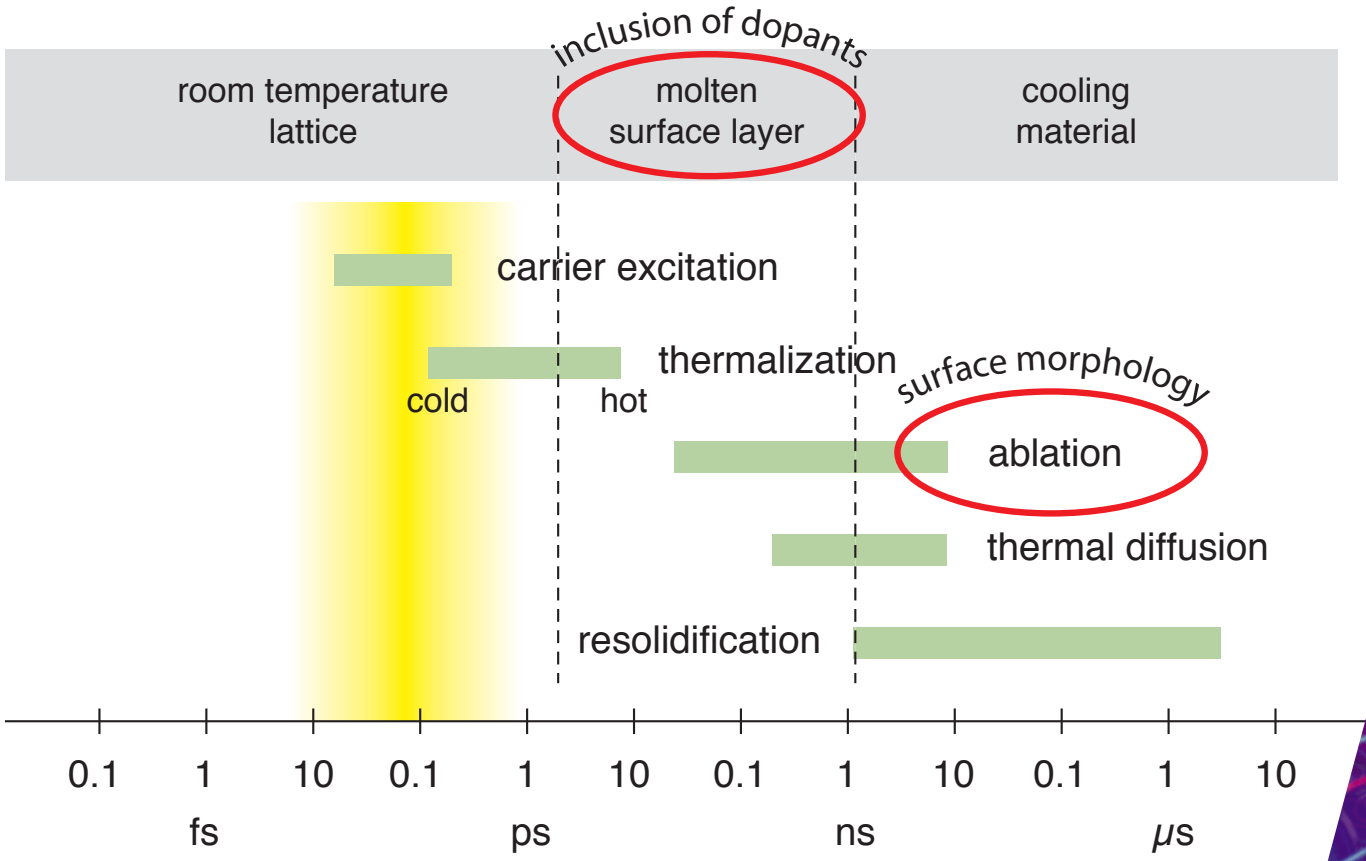

Nature Materials **1**, 217 (2002)

different thresholds:

melting: 1.5 kJ/m^2

ablation: 3.1 kJ/m^2

decouple ablation from melting

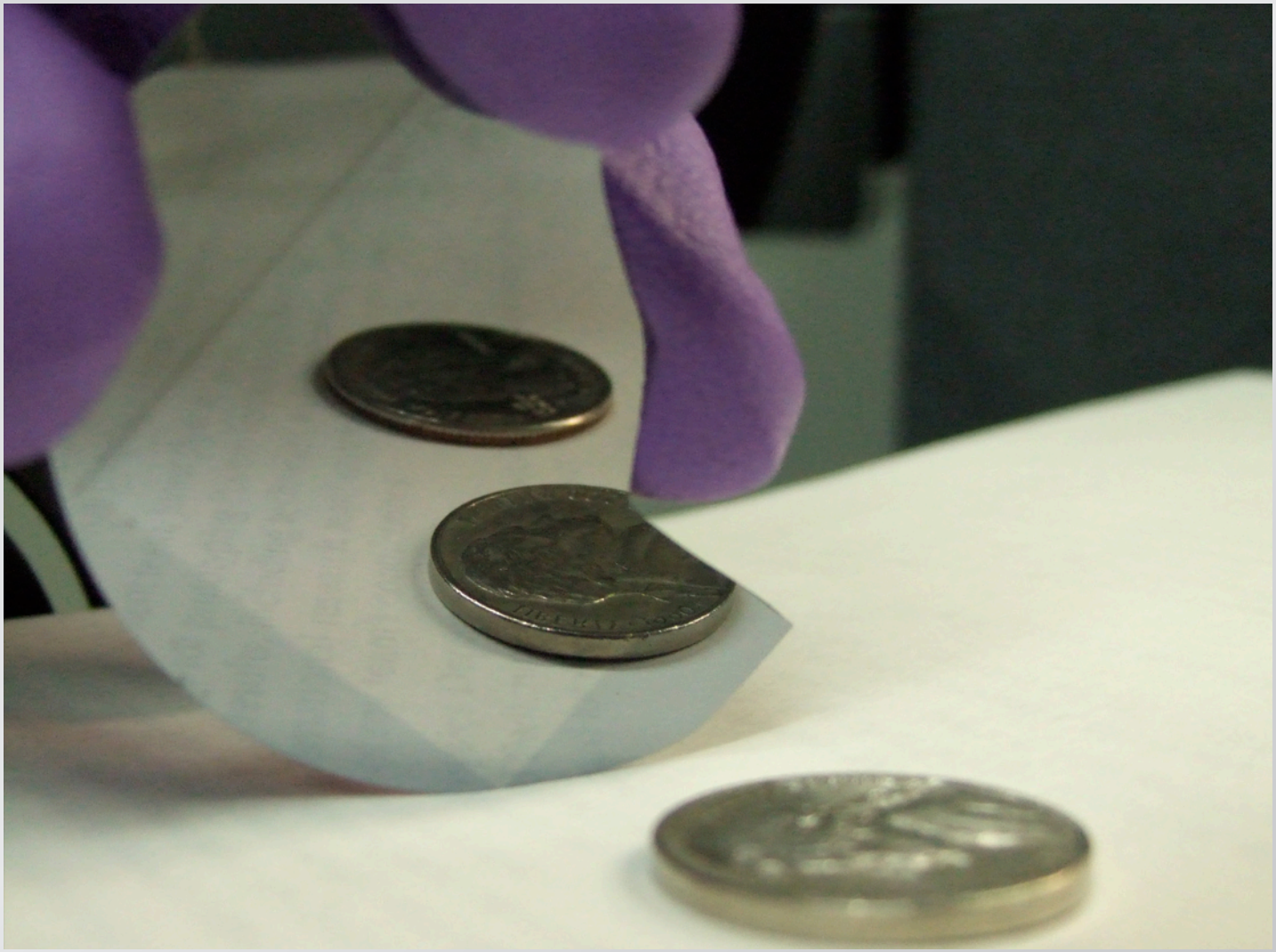

decouple ablation from melting

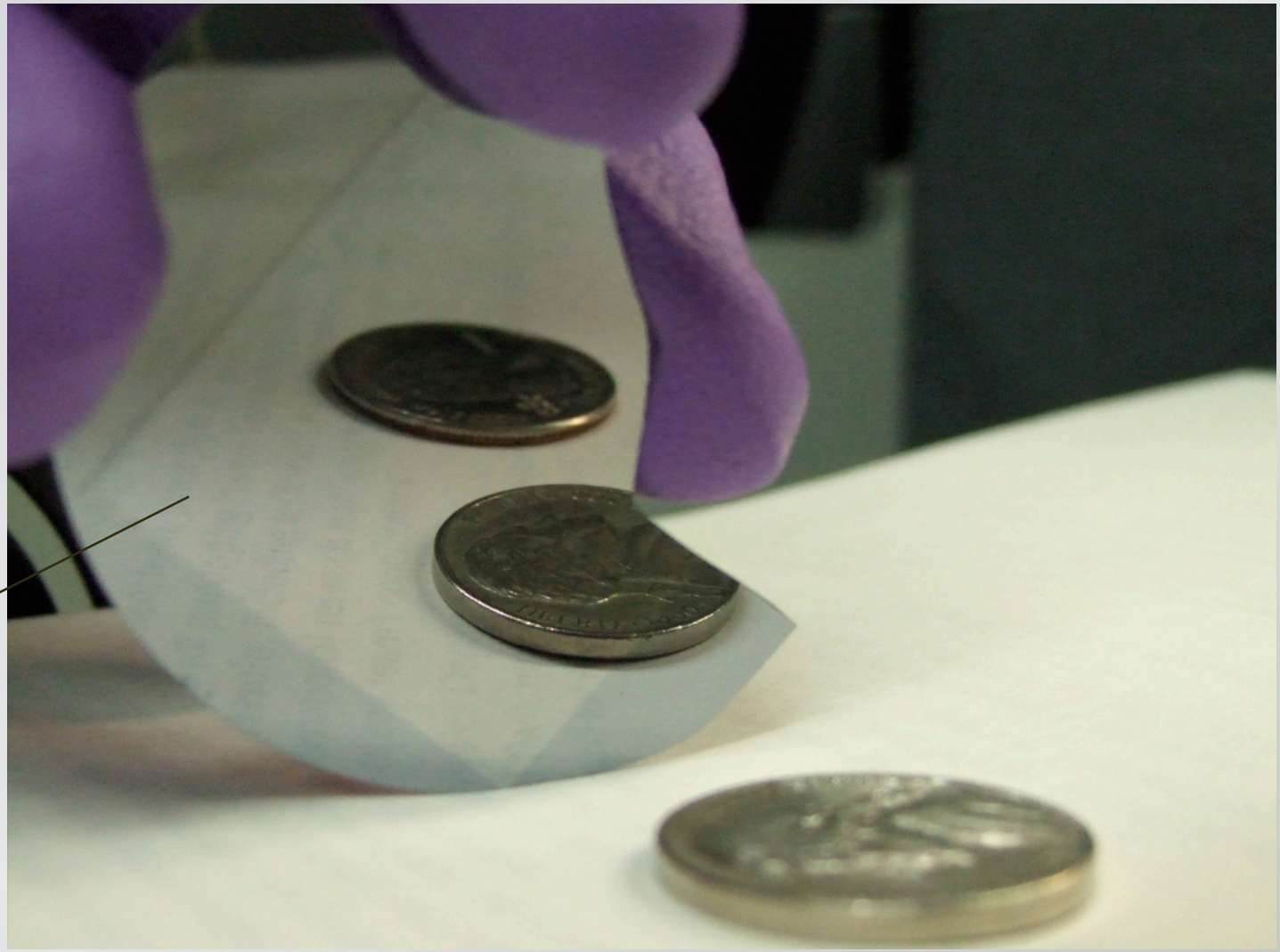

decouple ablation from melting

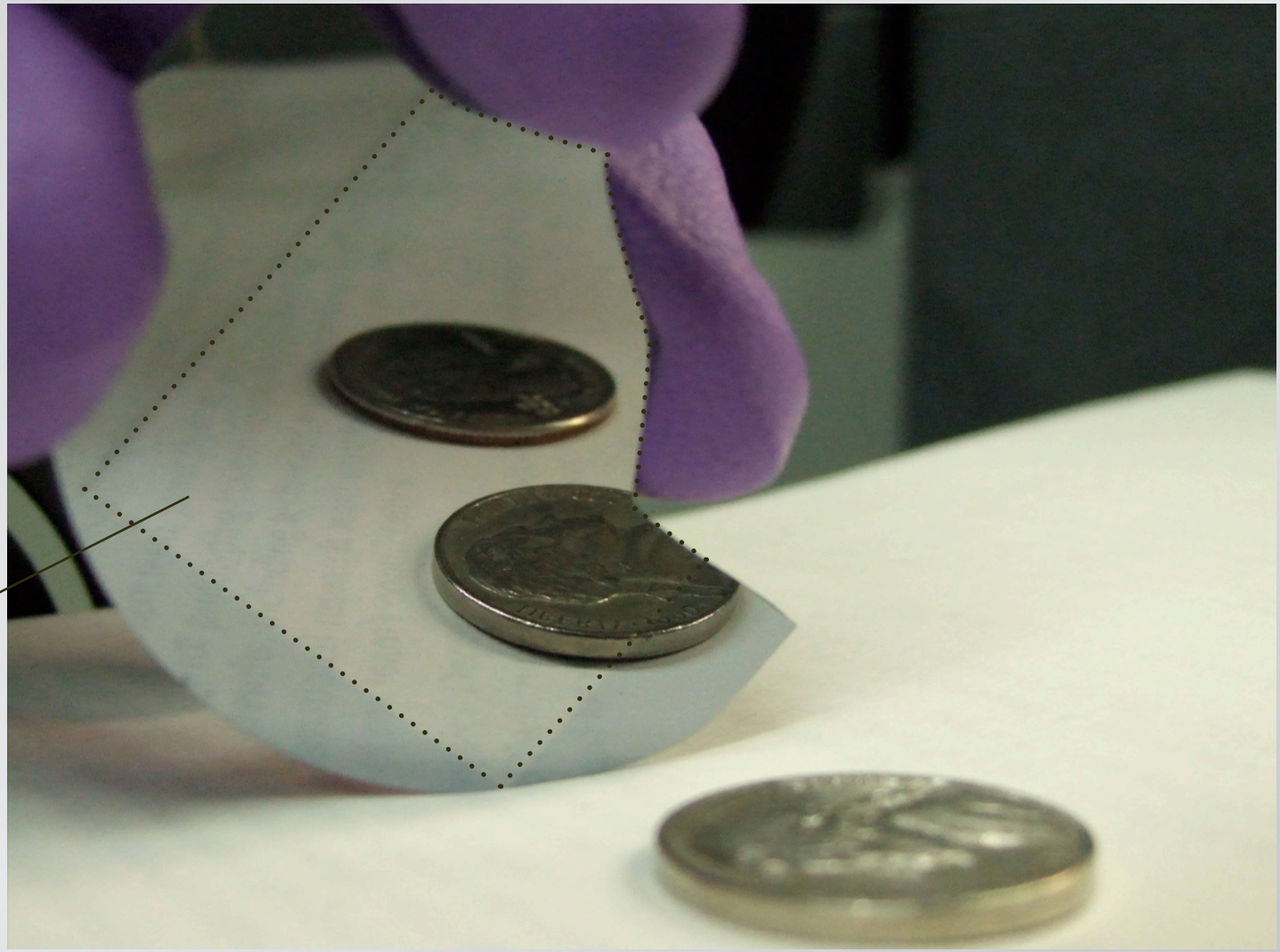

decouple ablation from melting

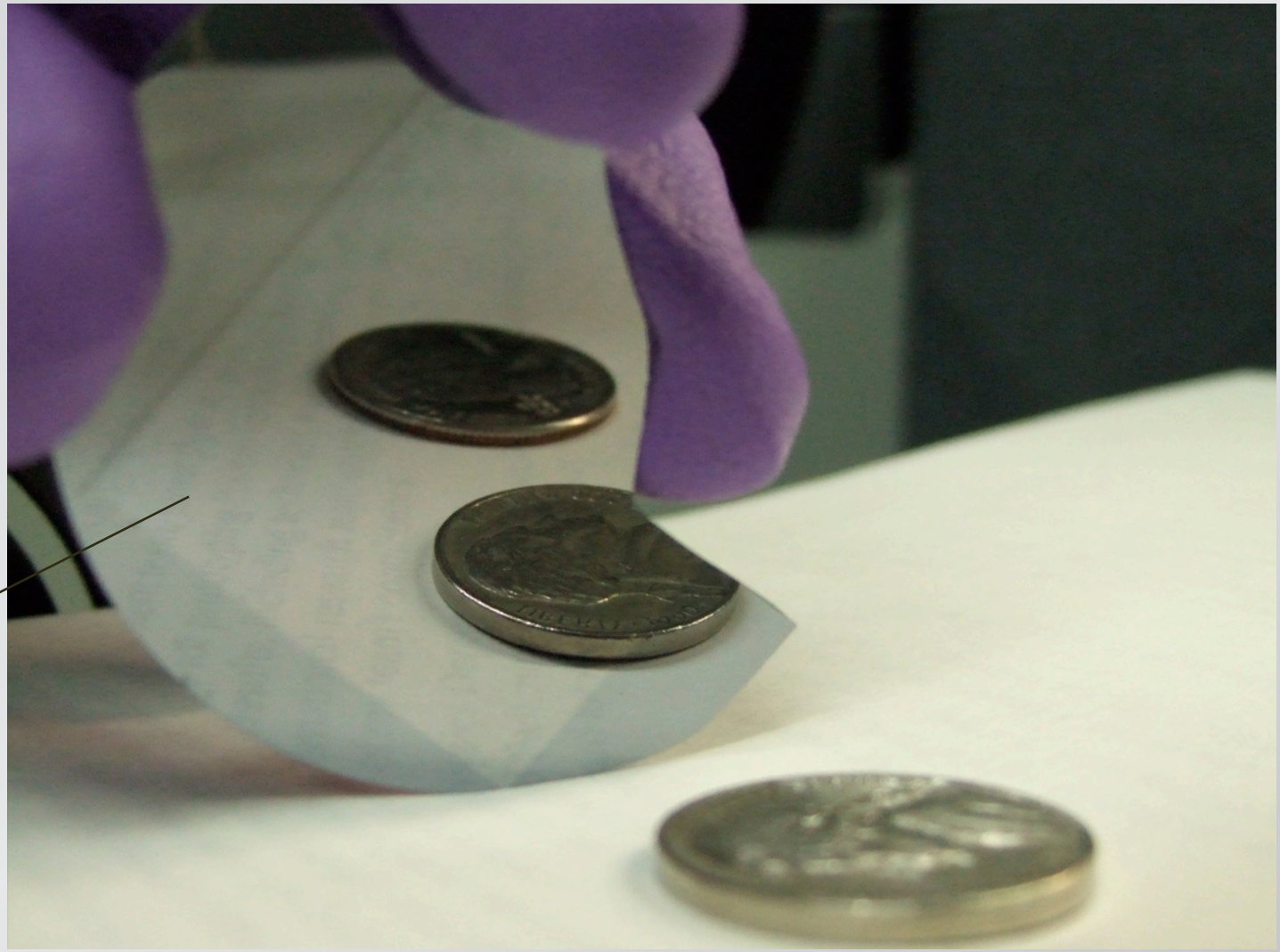

decouple ablation from melting

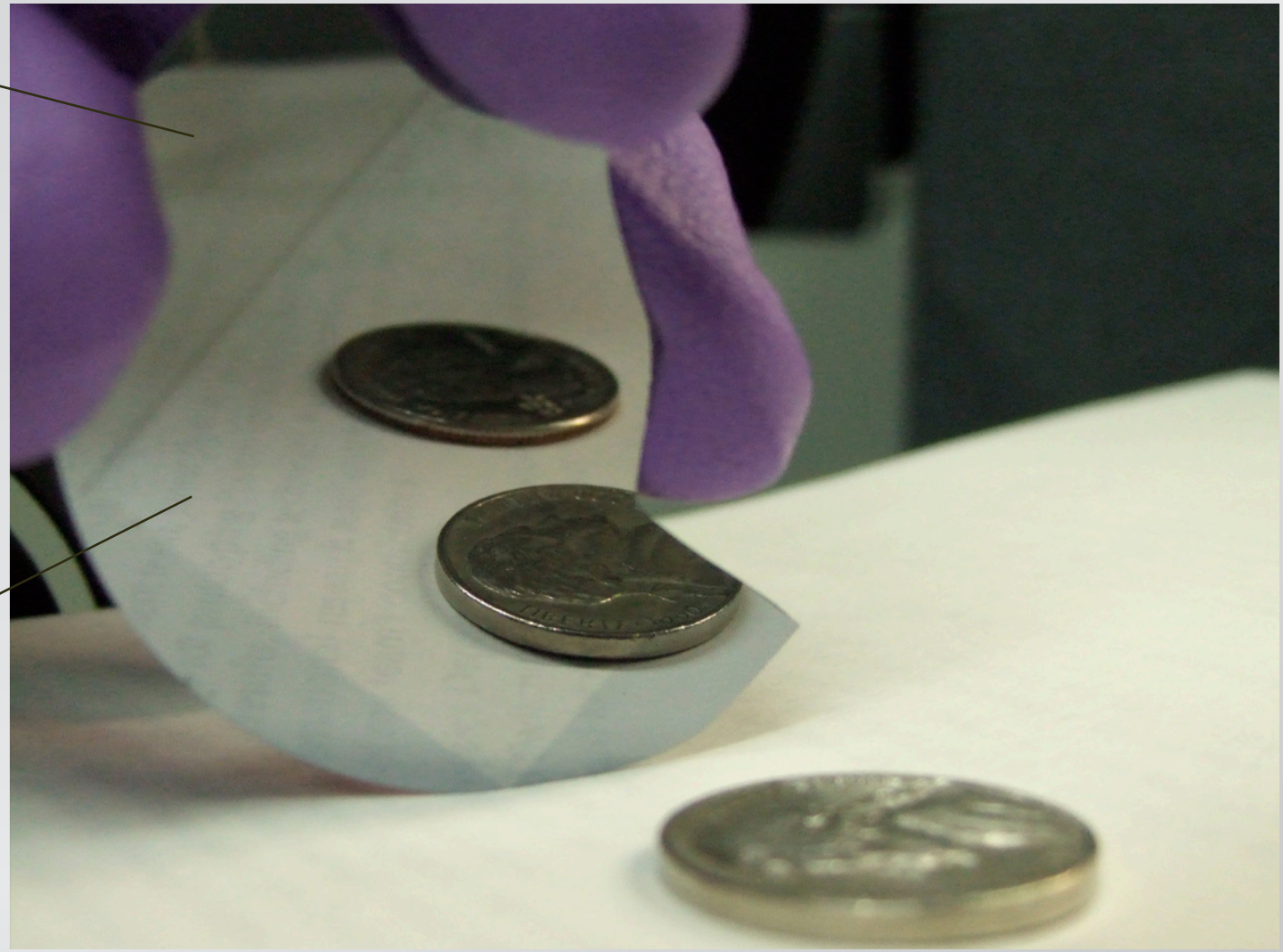

decouple ablation from melting

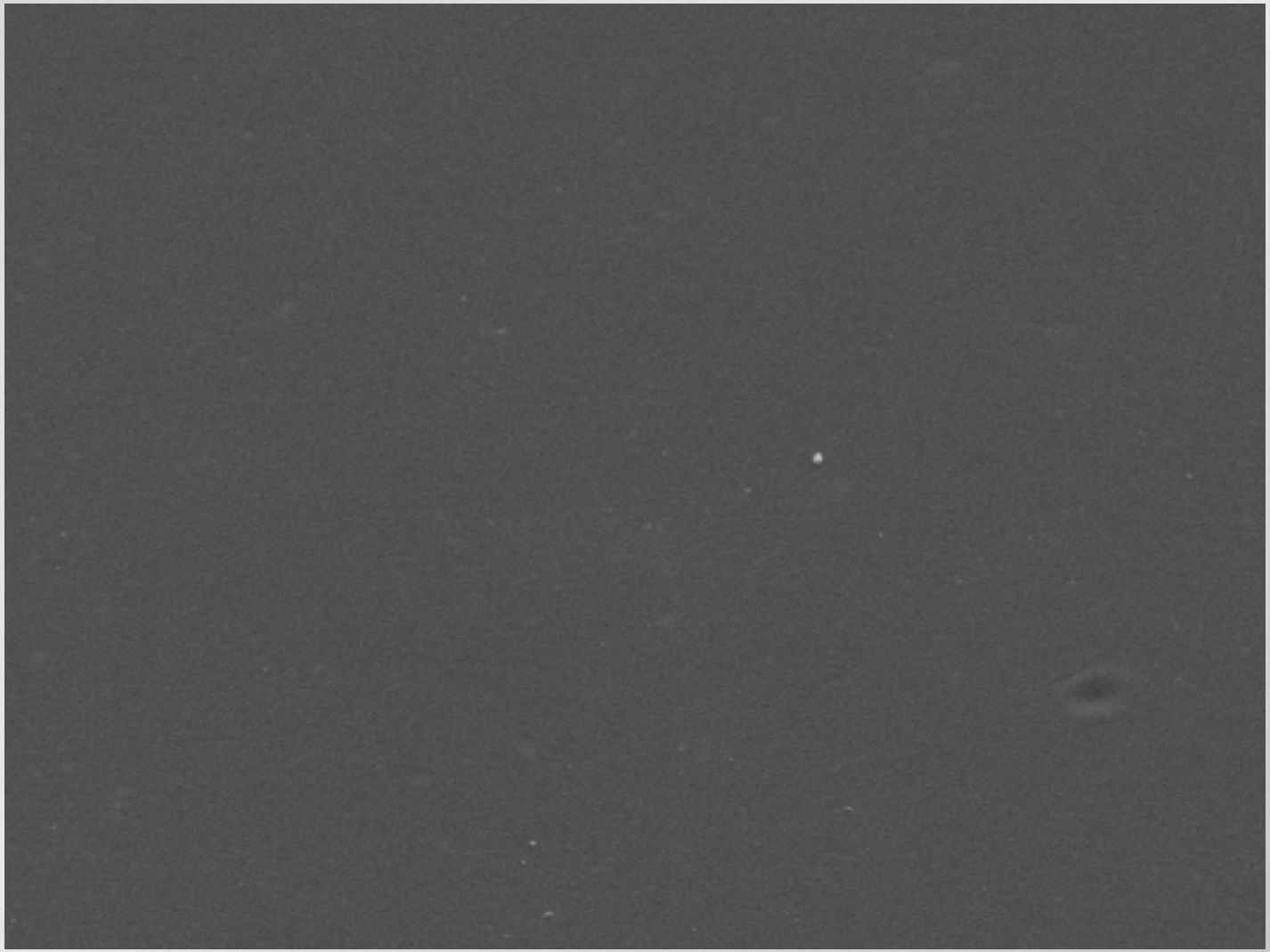

decouple ablation from melting

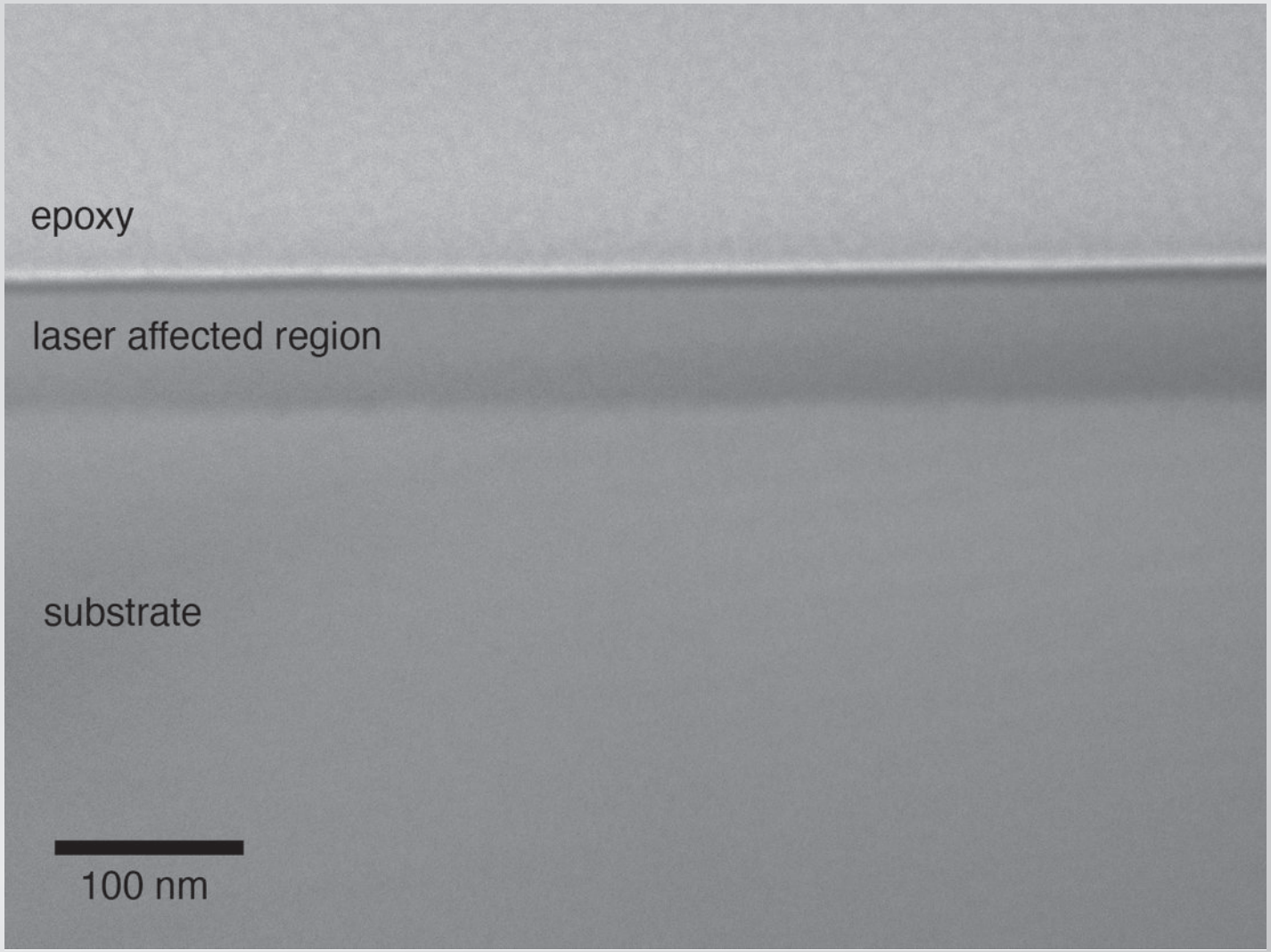

decouple ablation from melting

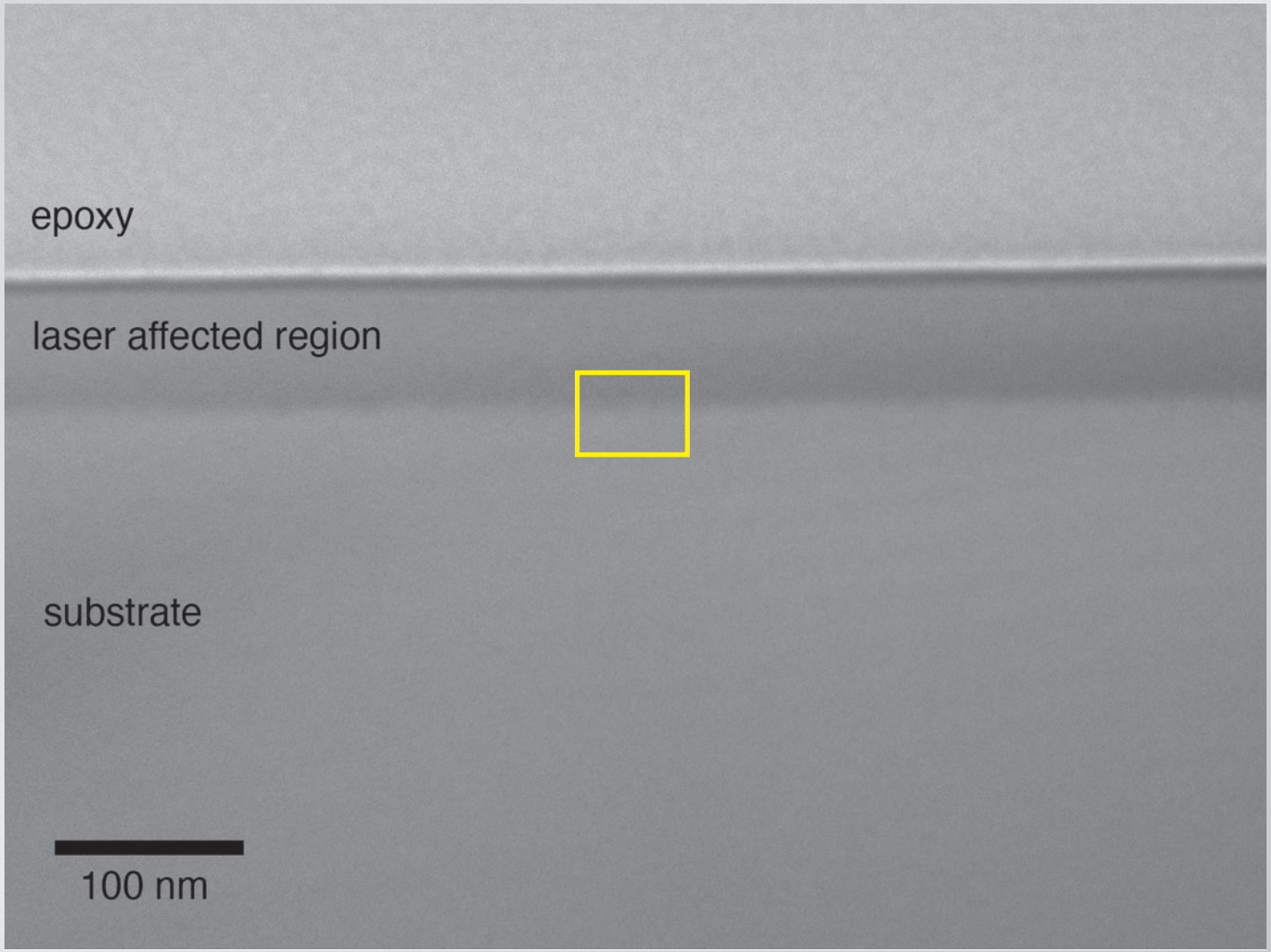

decouple ablation from melting

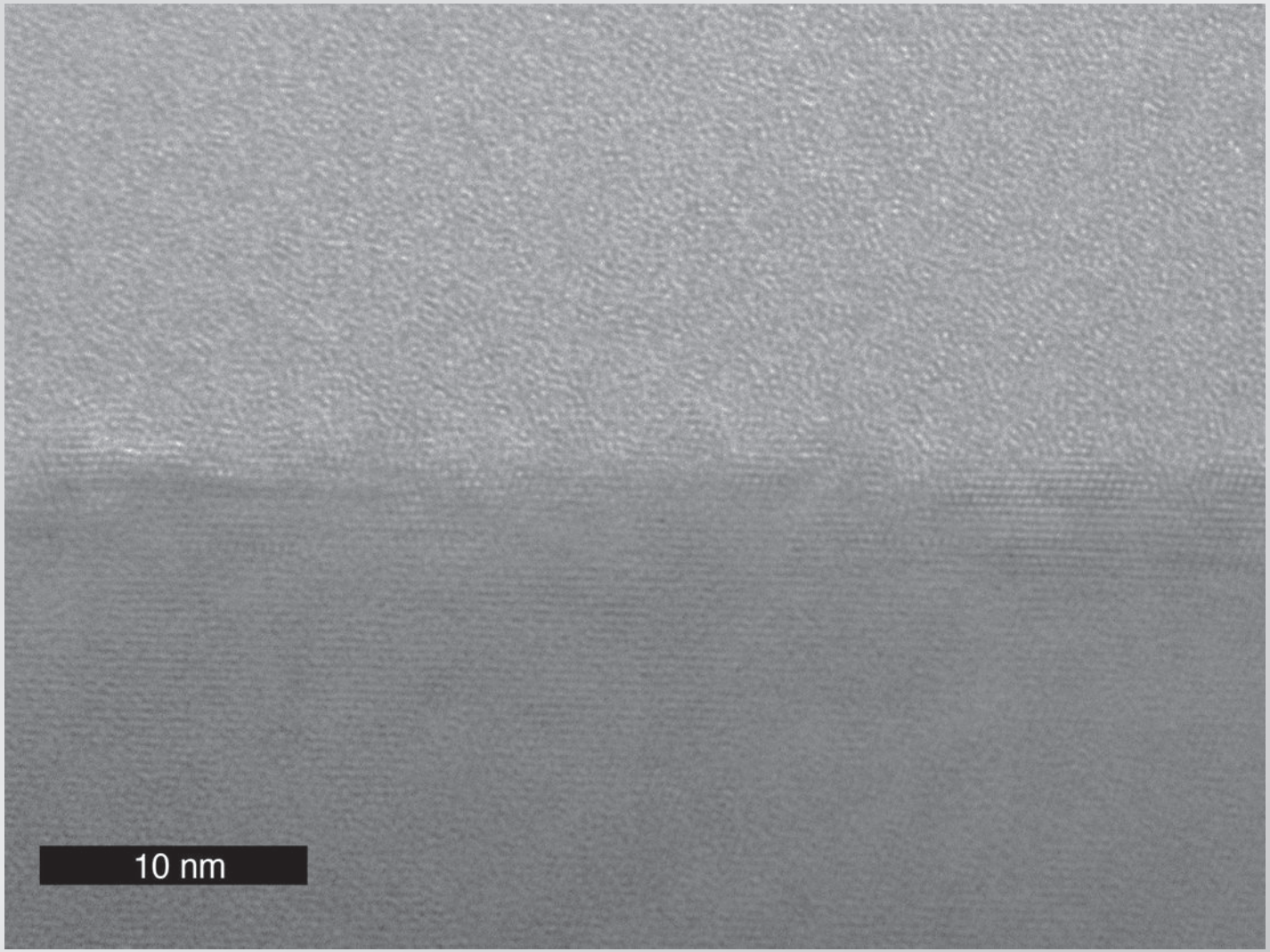

decouple ablation from melting

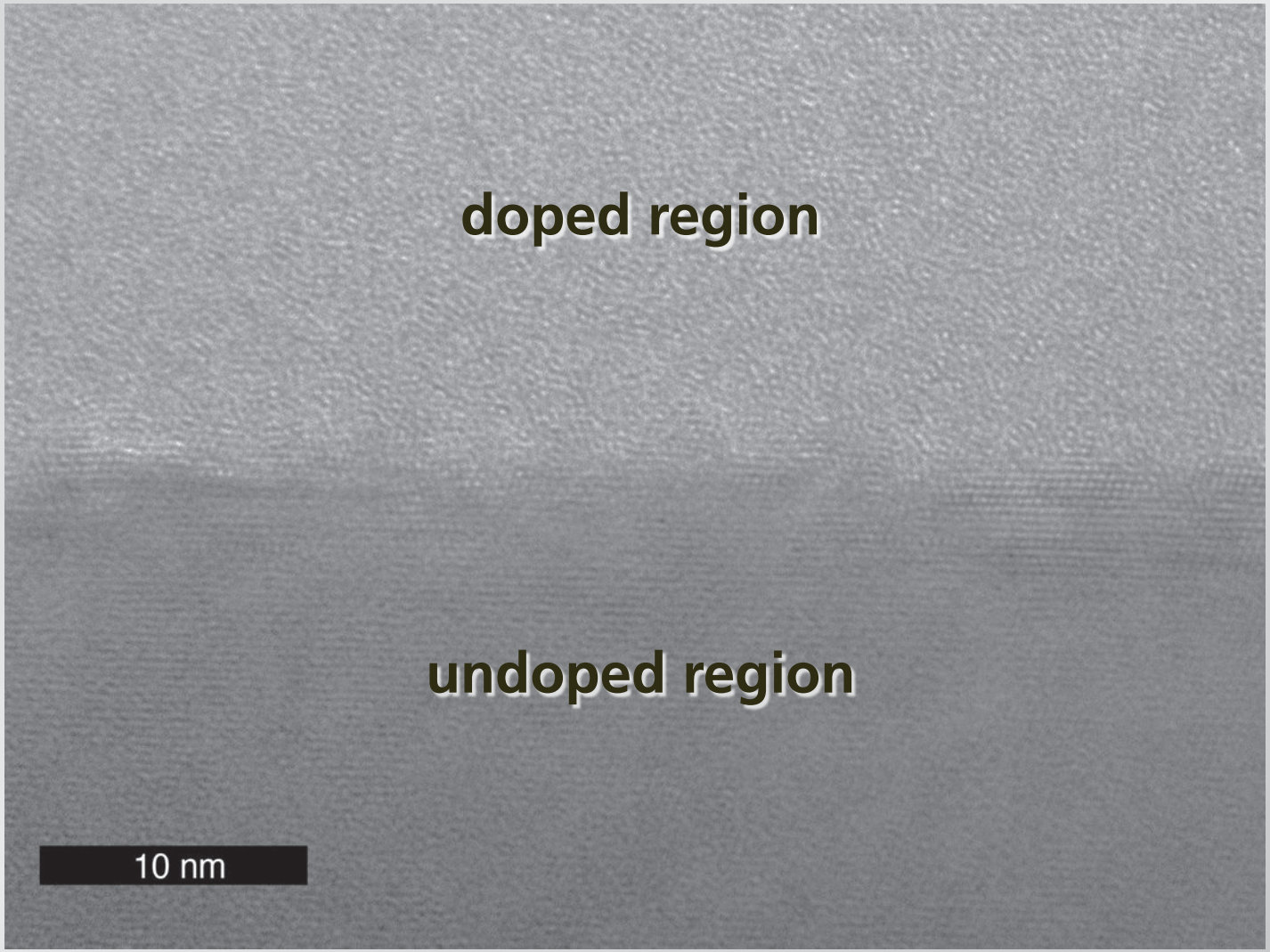

secondary ion mass spectrometry

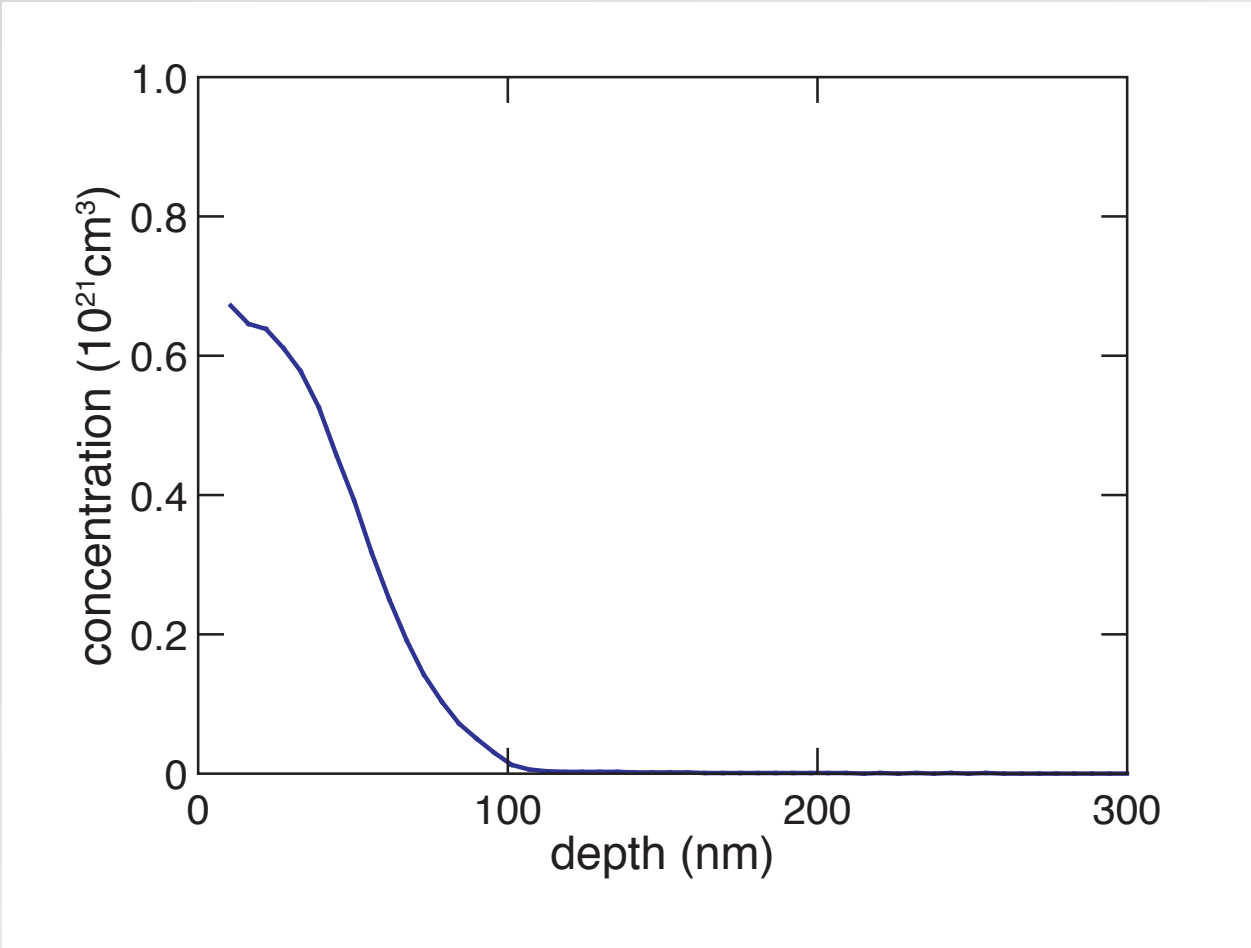

Things to keep in mind

- near unit absorption extending into IR
- surface structure due to ablation
- hyperdoping due to rapid melting and resolidification
- can decouple both processes

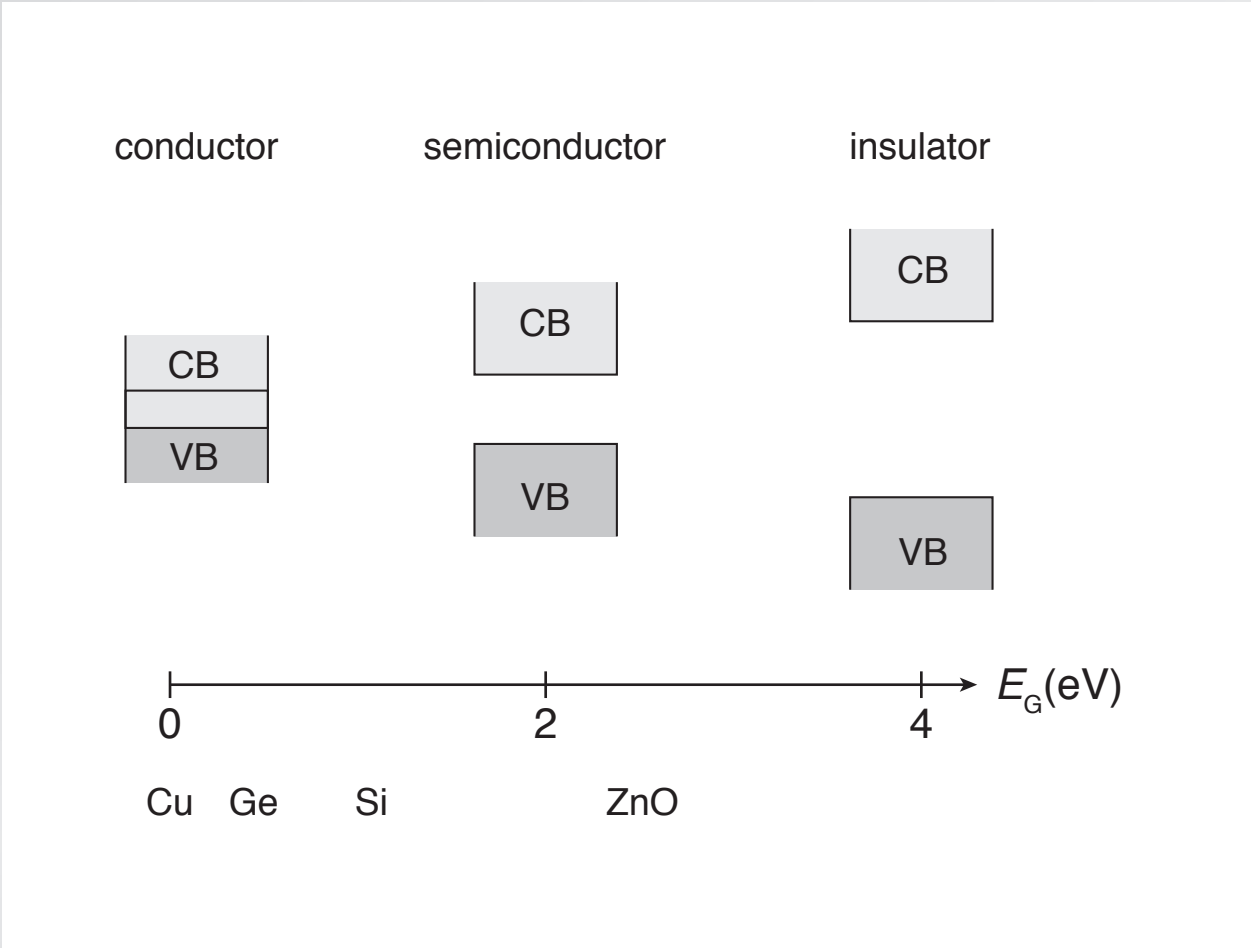

1 properties

2 intermediate band

gap determines optical and electronic properties

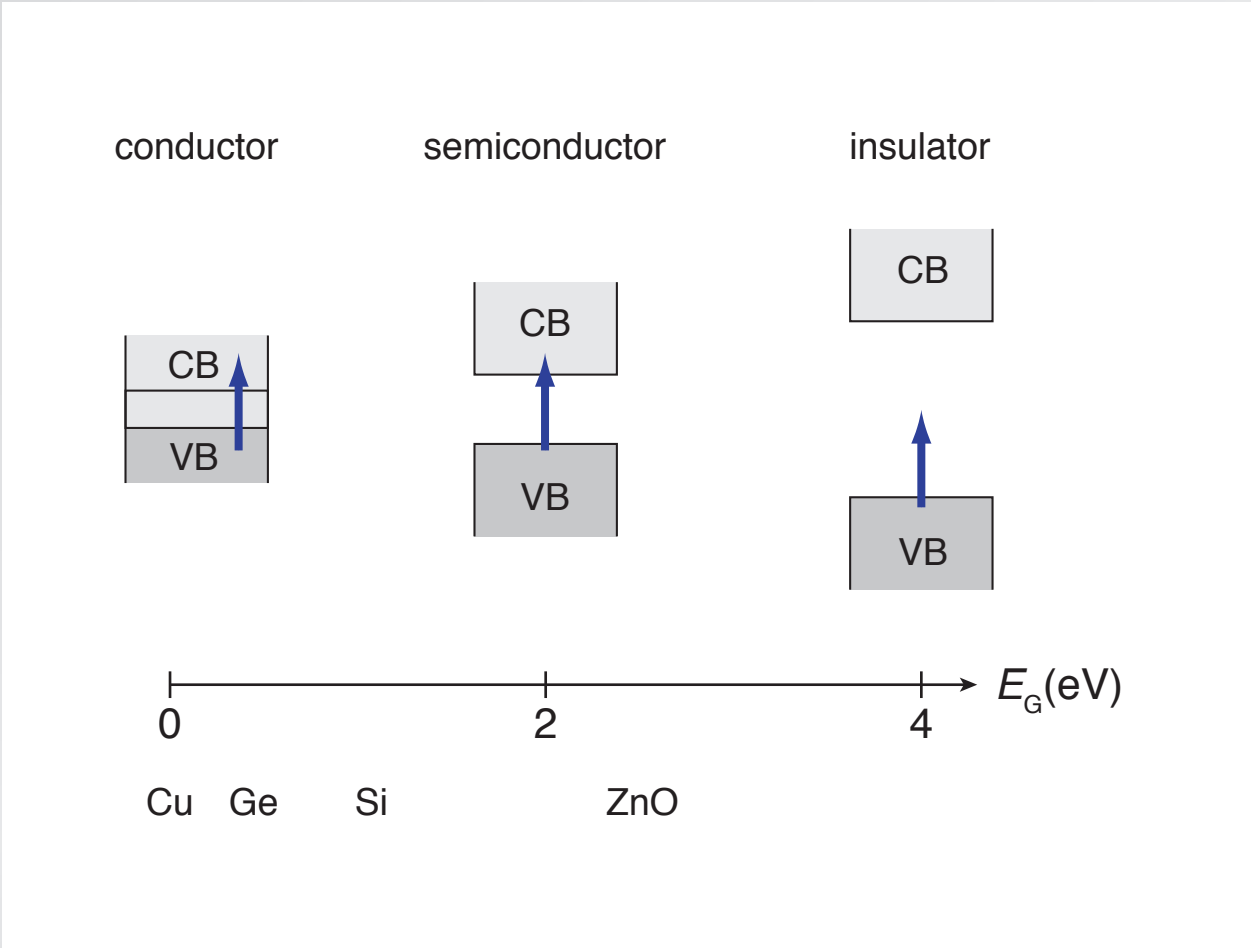

shallow-level dopants control electronic properties

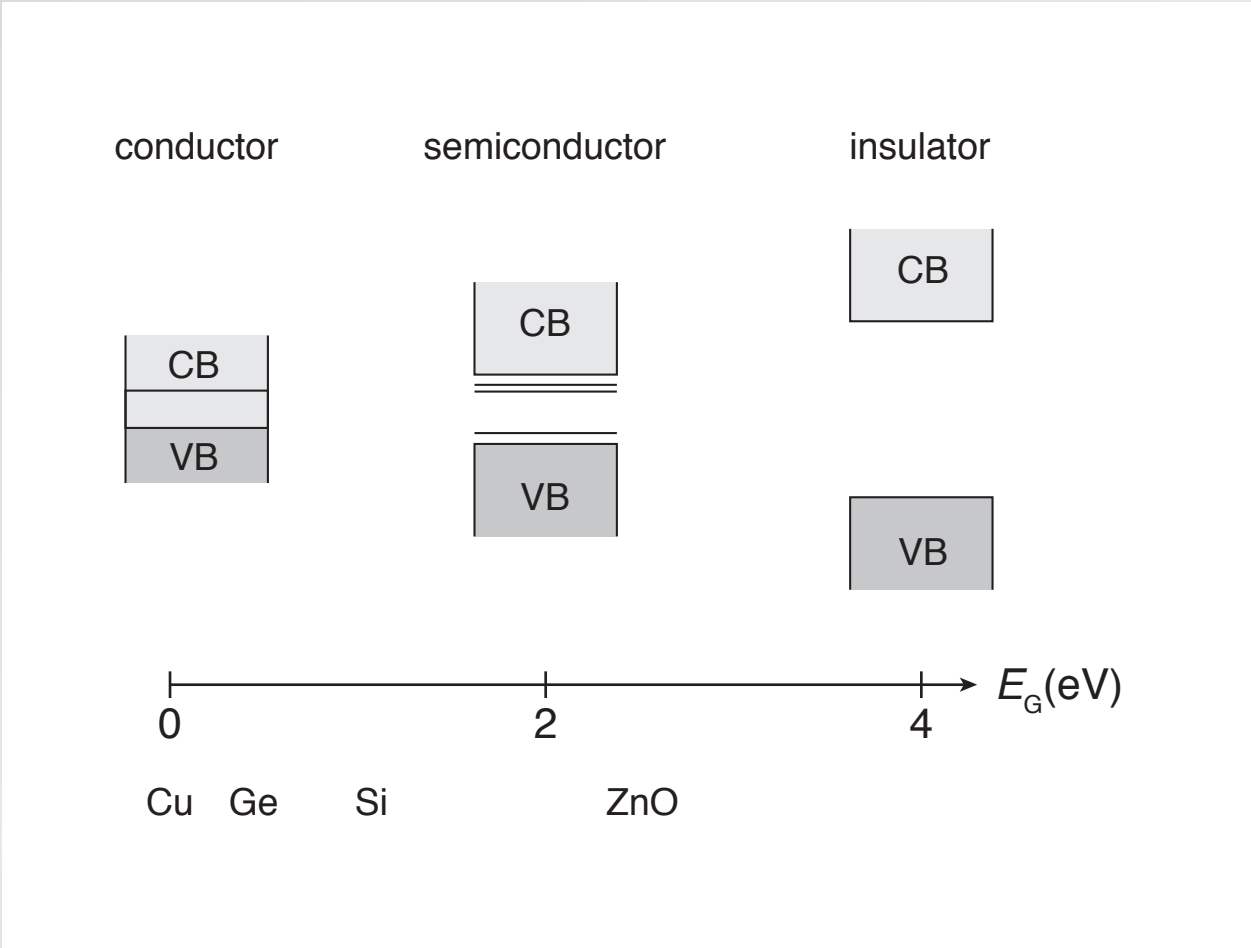

1 properties

2 intermediate band

deep-level dopants typically avoided

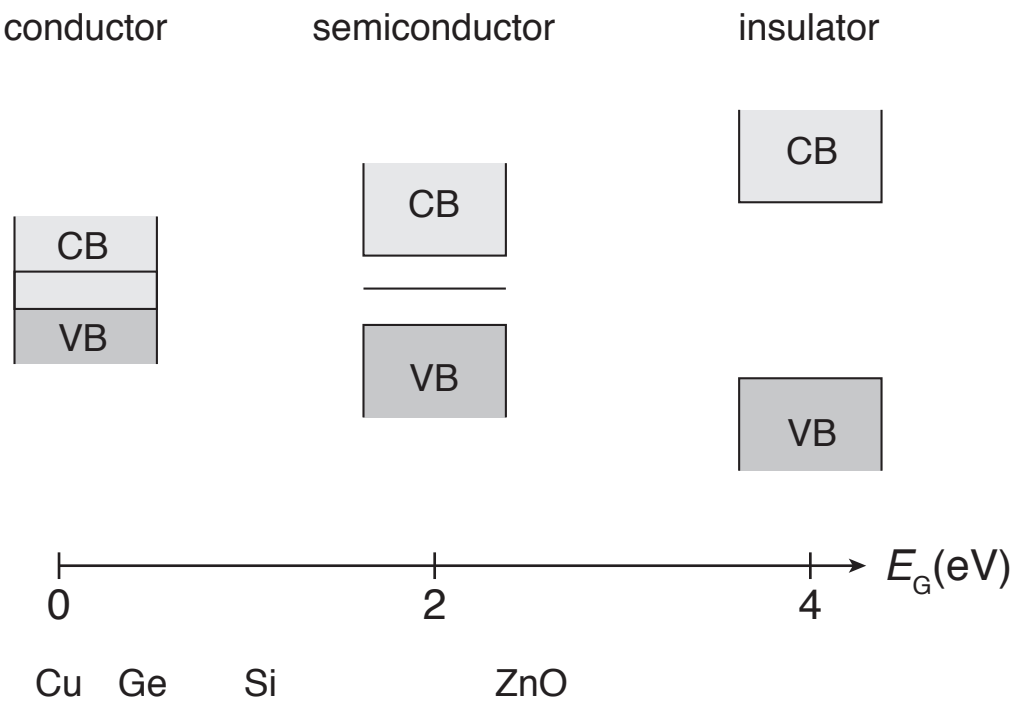

1 part in 10^6 sulfur introduces donor states in gap

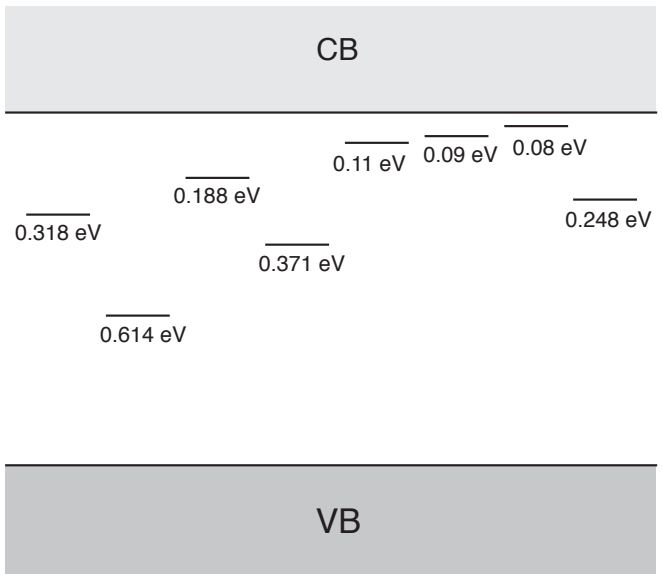

Janzén *et al.*, Phys. Rev. B 29, 1907 (1984)

1 part in 10^6 sulfur introduces donor states in gap

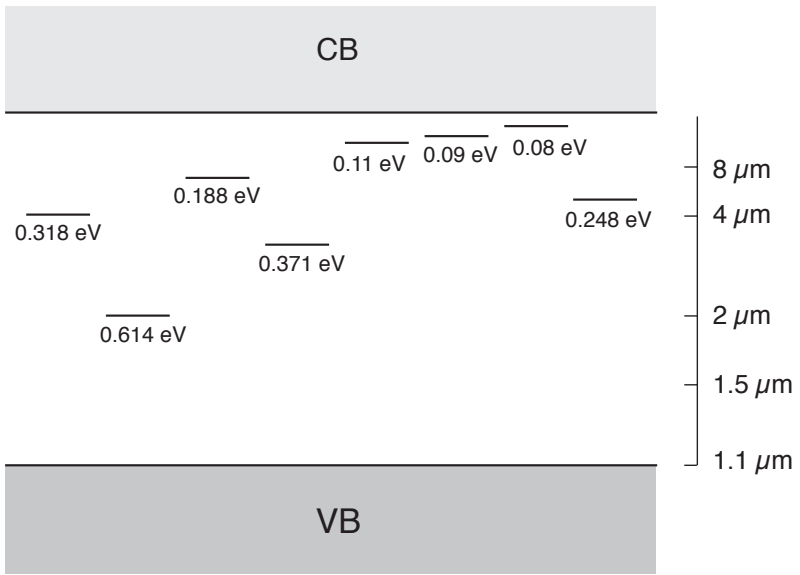

Janzén *et al.*, Phys. Rev. B 29, 1907 (1984)

1 part in 10^6 sulfur introduces donor states in gap

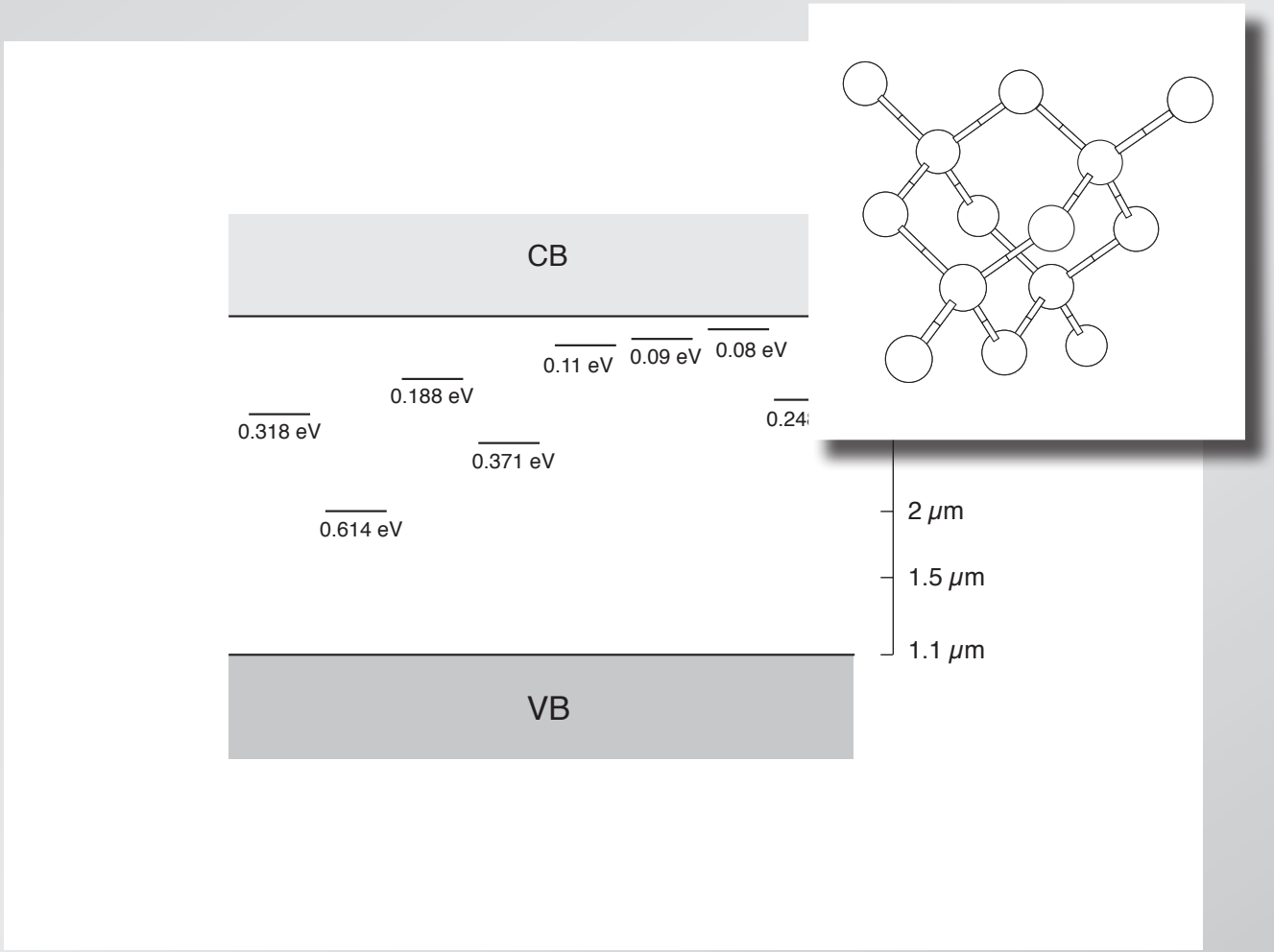

Janzén *et al.*, Phys. Rev. B 29, 1907 (1984)

1 part in 10^6 sulfur introduces donor states in gap

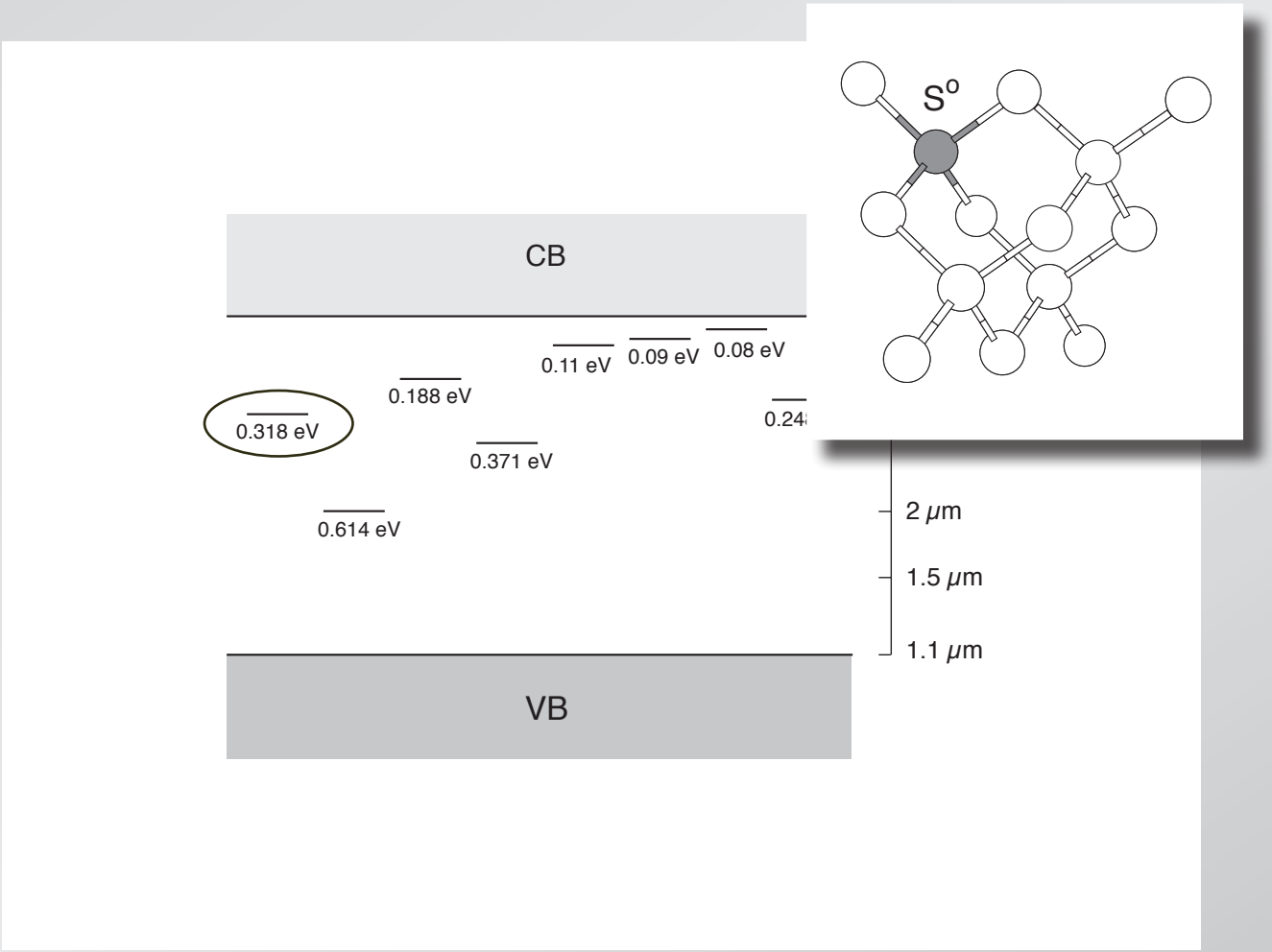

Janzén *et al.*, Phys. Rev. B 29, 1907 (1984)

1 part in 10^6 sulfur introduces donor states in gap

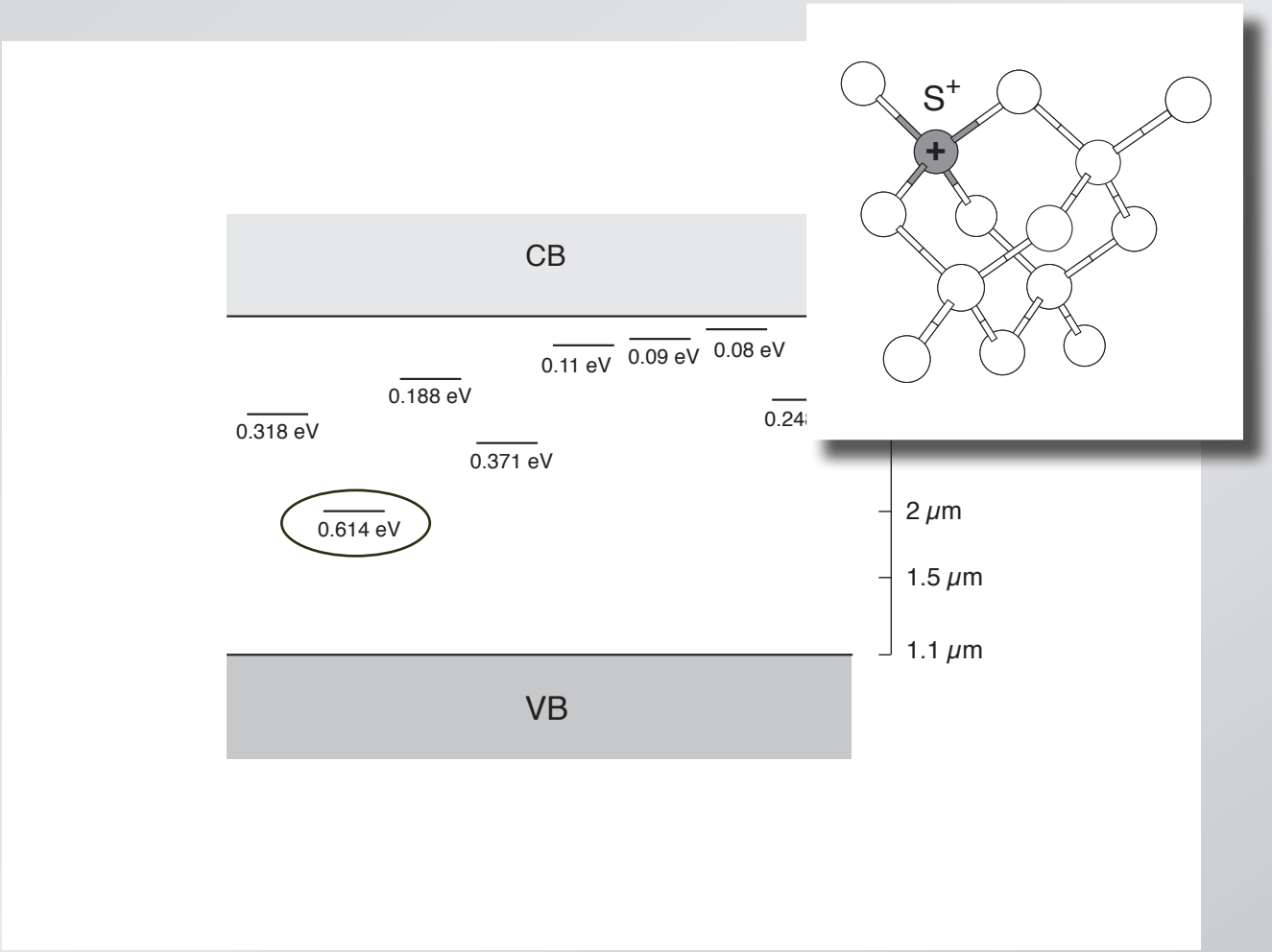

Janzén *et al.*, Phys. Rev. B 29, 1907 (1984)

1 part in 10^6 sulfur introduces donor states in gap

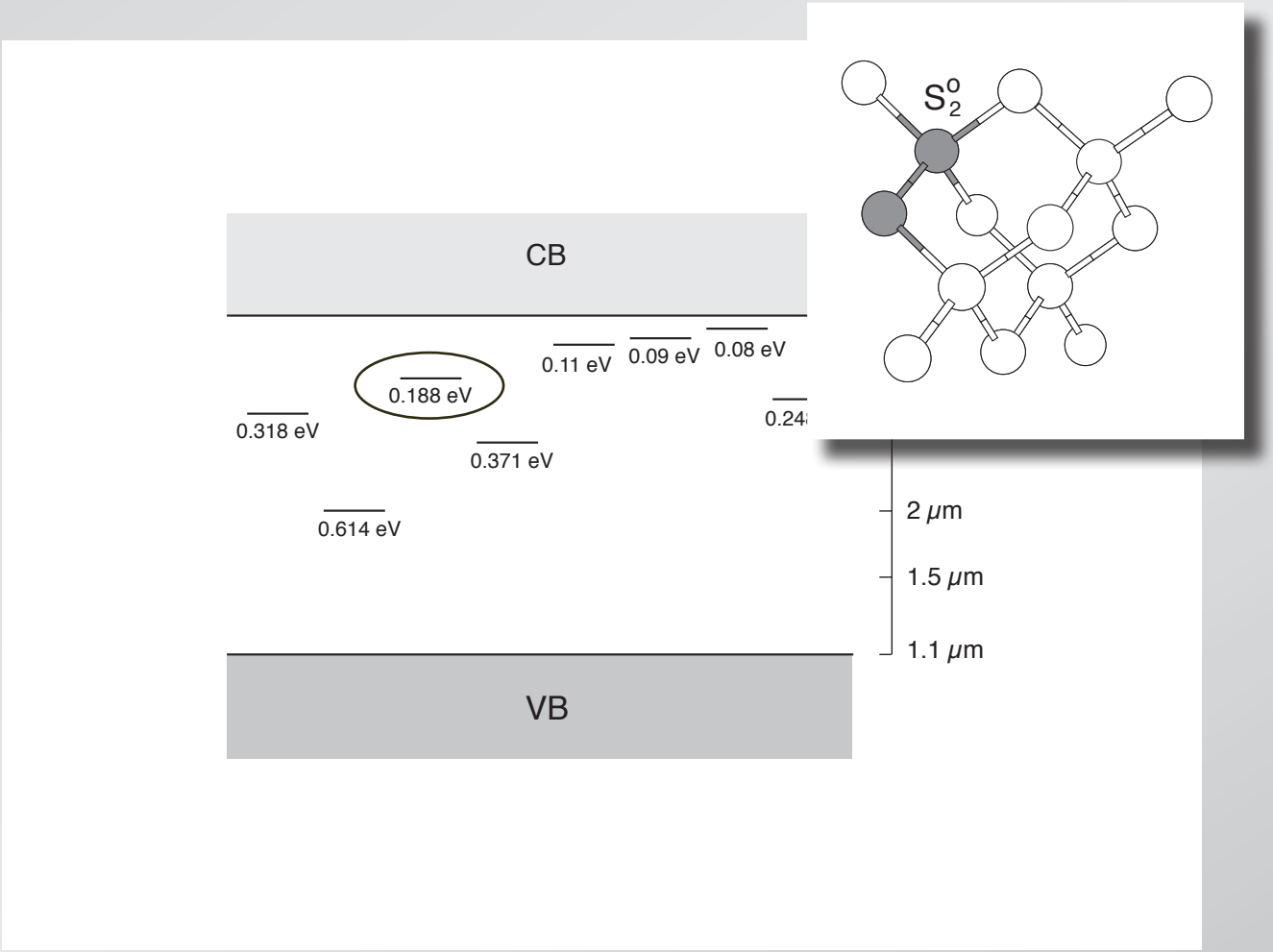

Janzén *et al.*, Phys. Rev. B 29, 1907 (1984)

1 part in 10^6 sulfur introduces donor states in gap

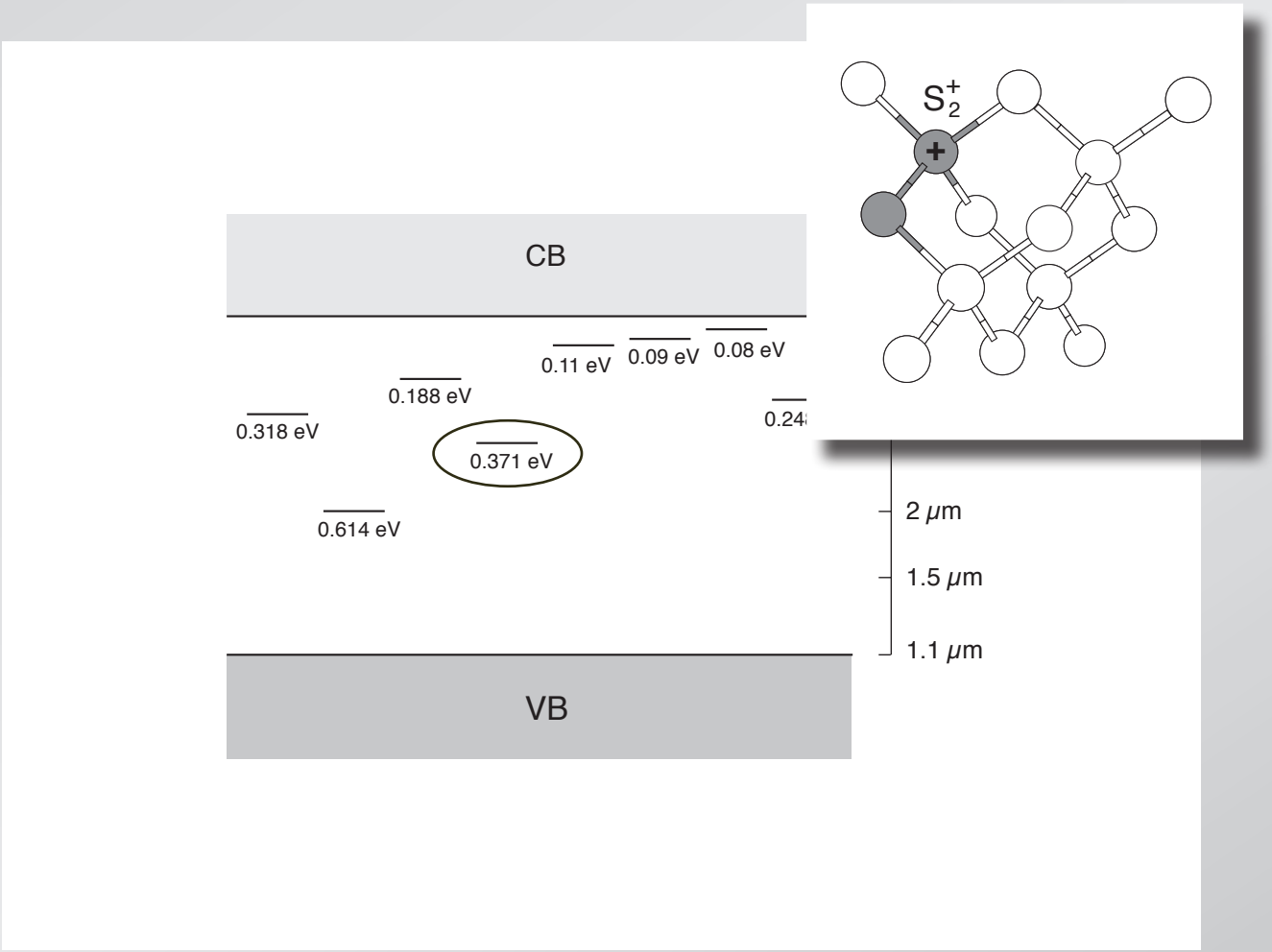

Janzén *et al.*, Phys. Rev. B 29, 1907 (1984)

1 part in 10^6 sulfur introduces donor states in gap

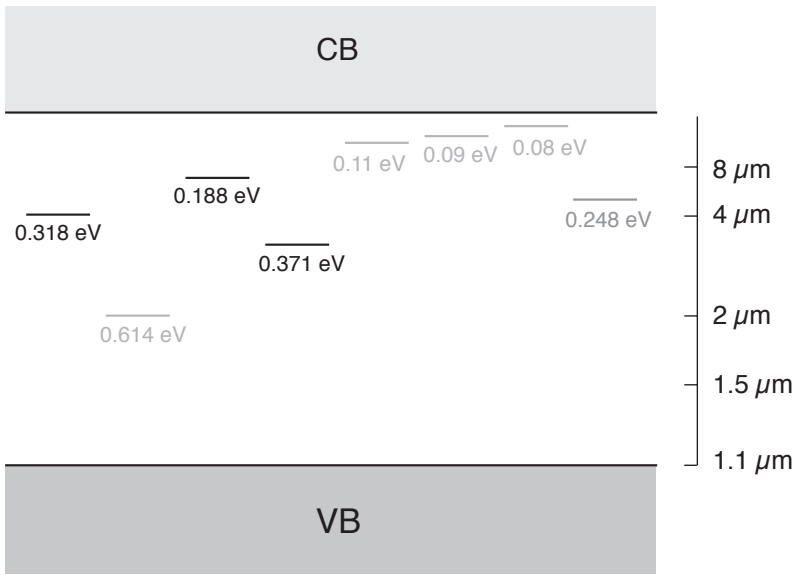

Janzén *et al.*, Phys. Rev. B 29, 1907 (1984)

at high concentration states broaden into band

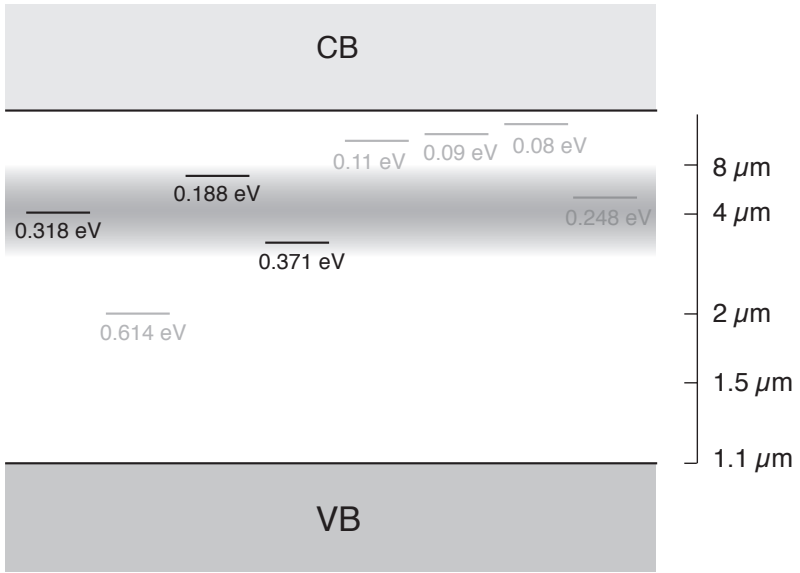

1 properties

2 intermediate band

10^{-6} sulfur doping

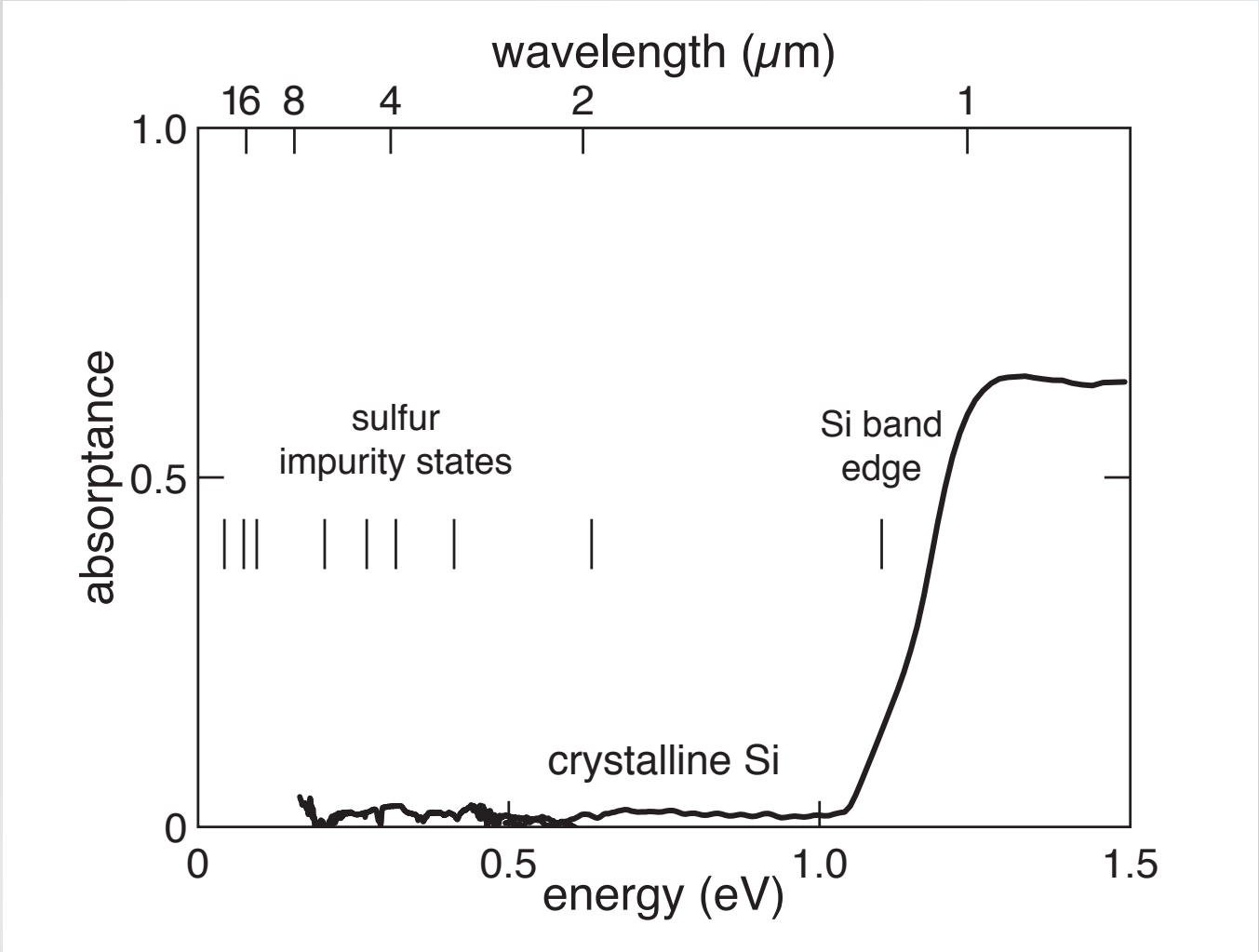

laser-doped S:Si

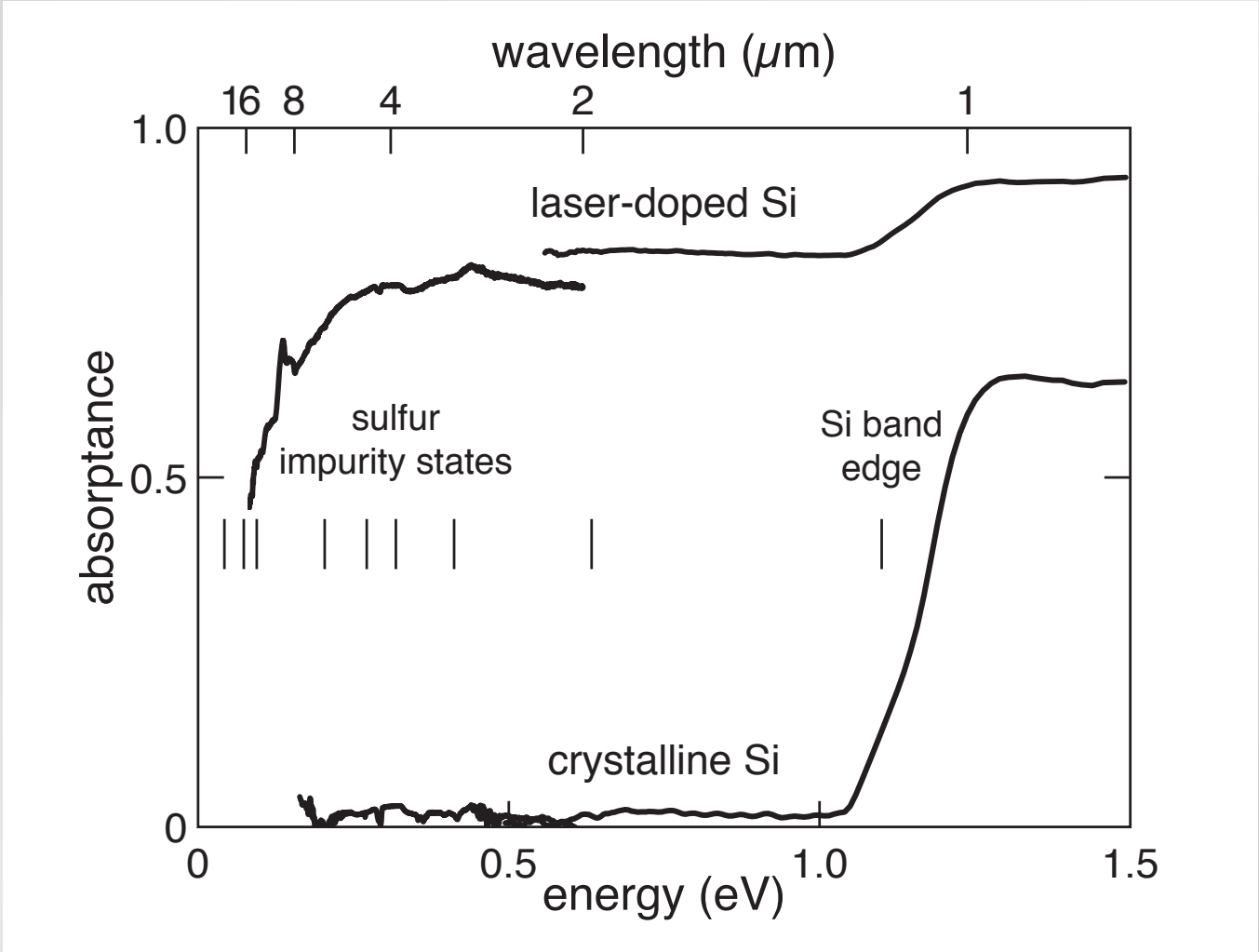

1 properties 2 intermediate band

laser-doped S:Si

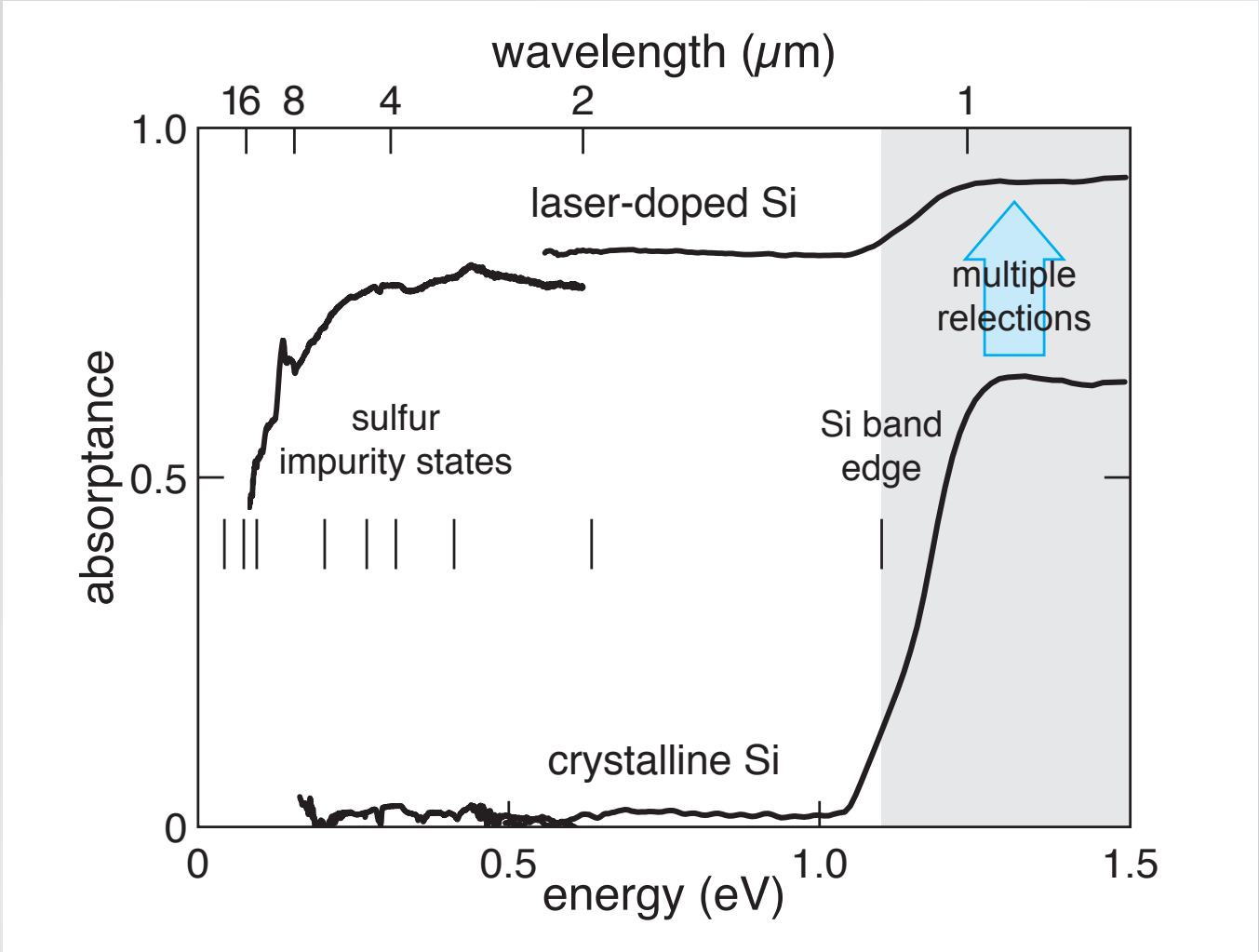

1 properties 2 intermediate band

laser-doped S:Si

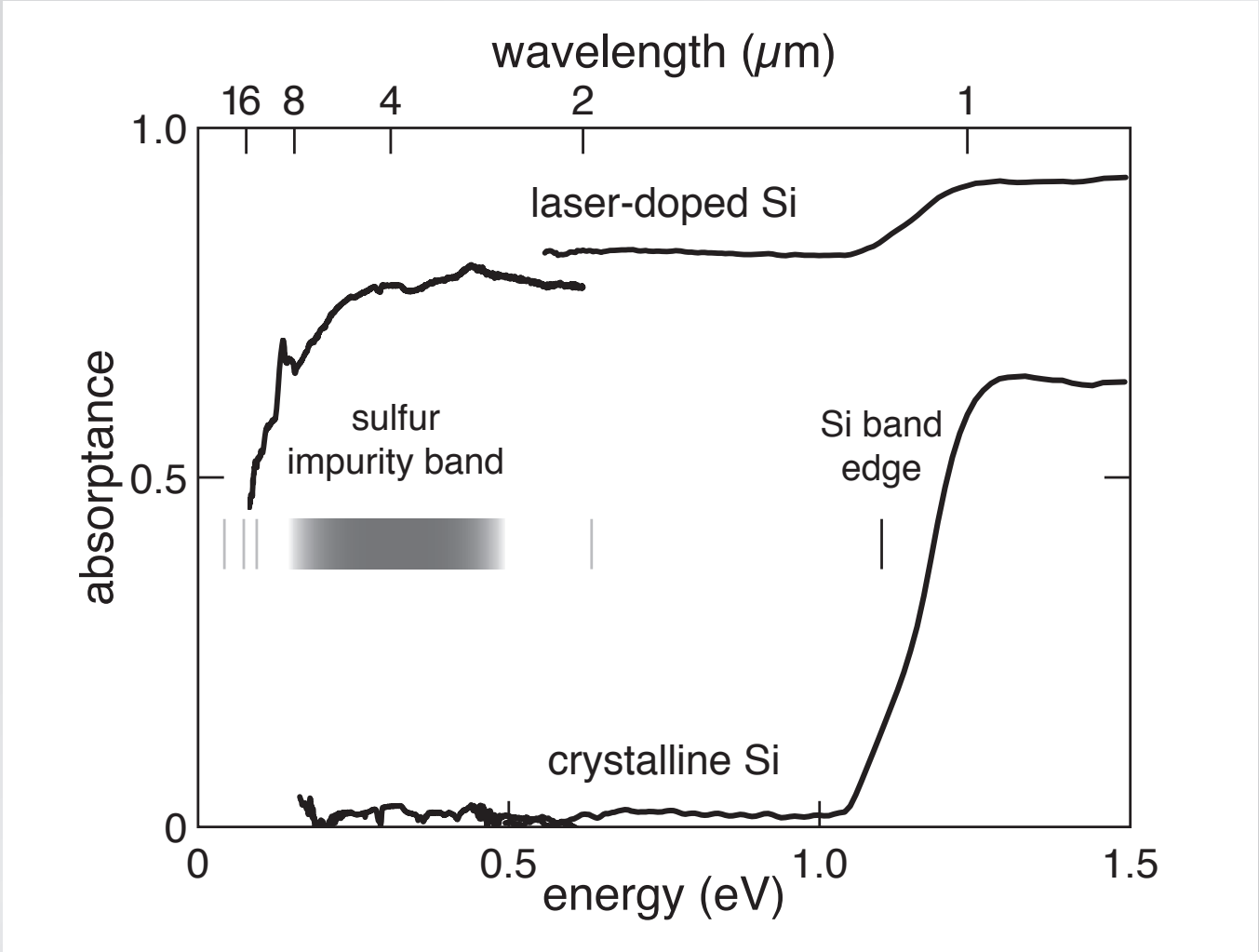

isolate surface layer for Hall measurements

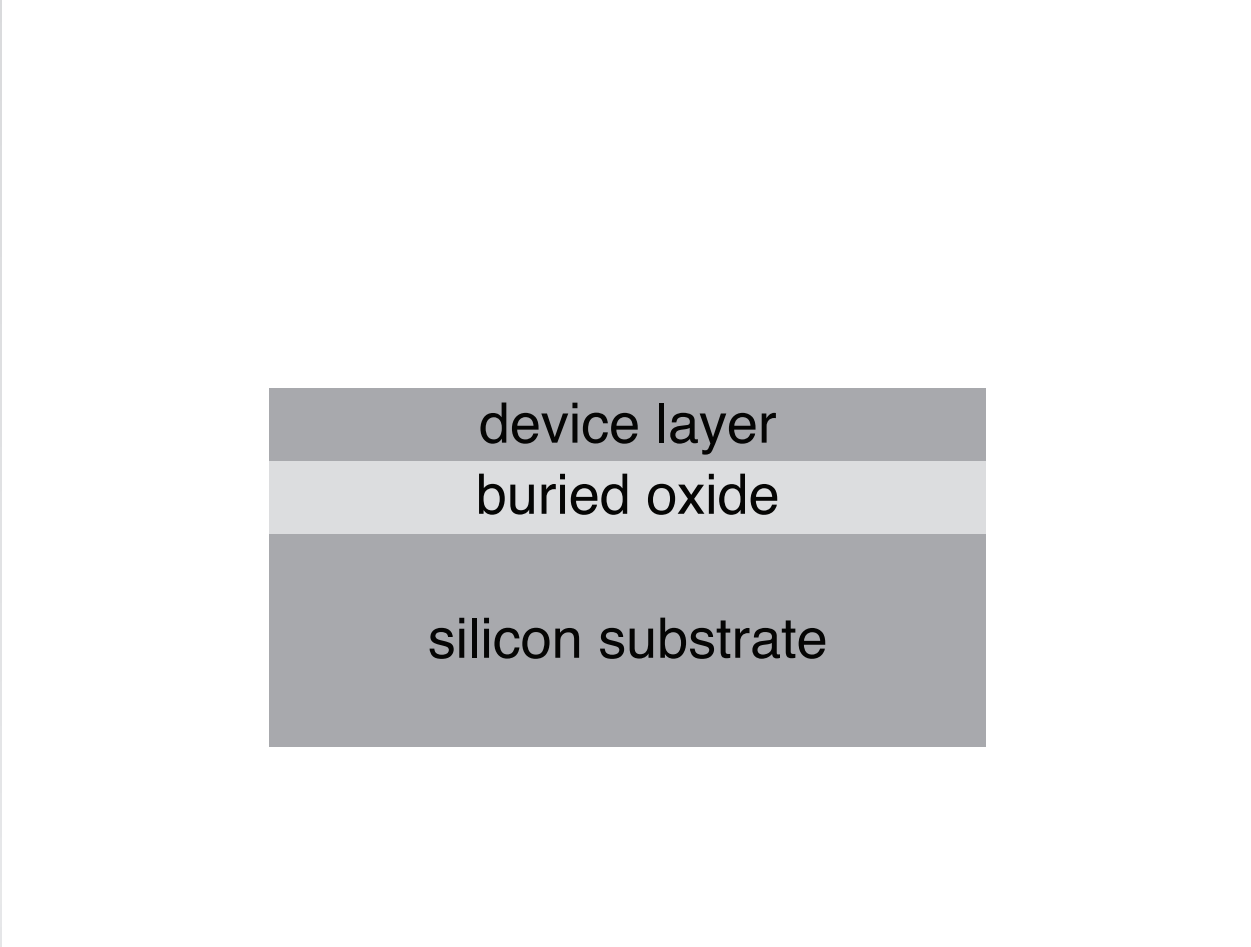

isolate surface layer for Hall measurements

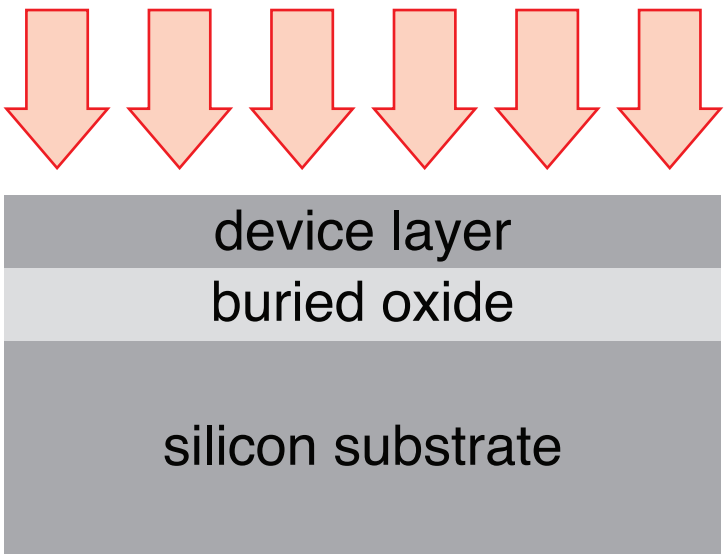

isolate surface layer for Hall measurements

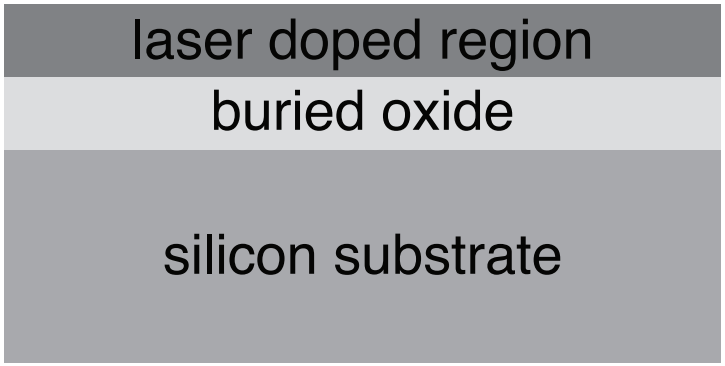

isolate surface layer for Hall measurements

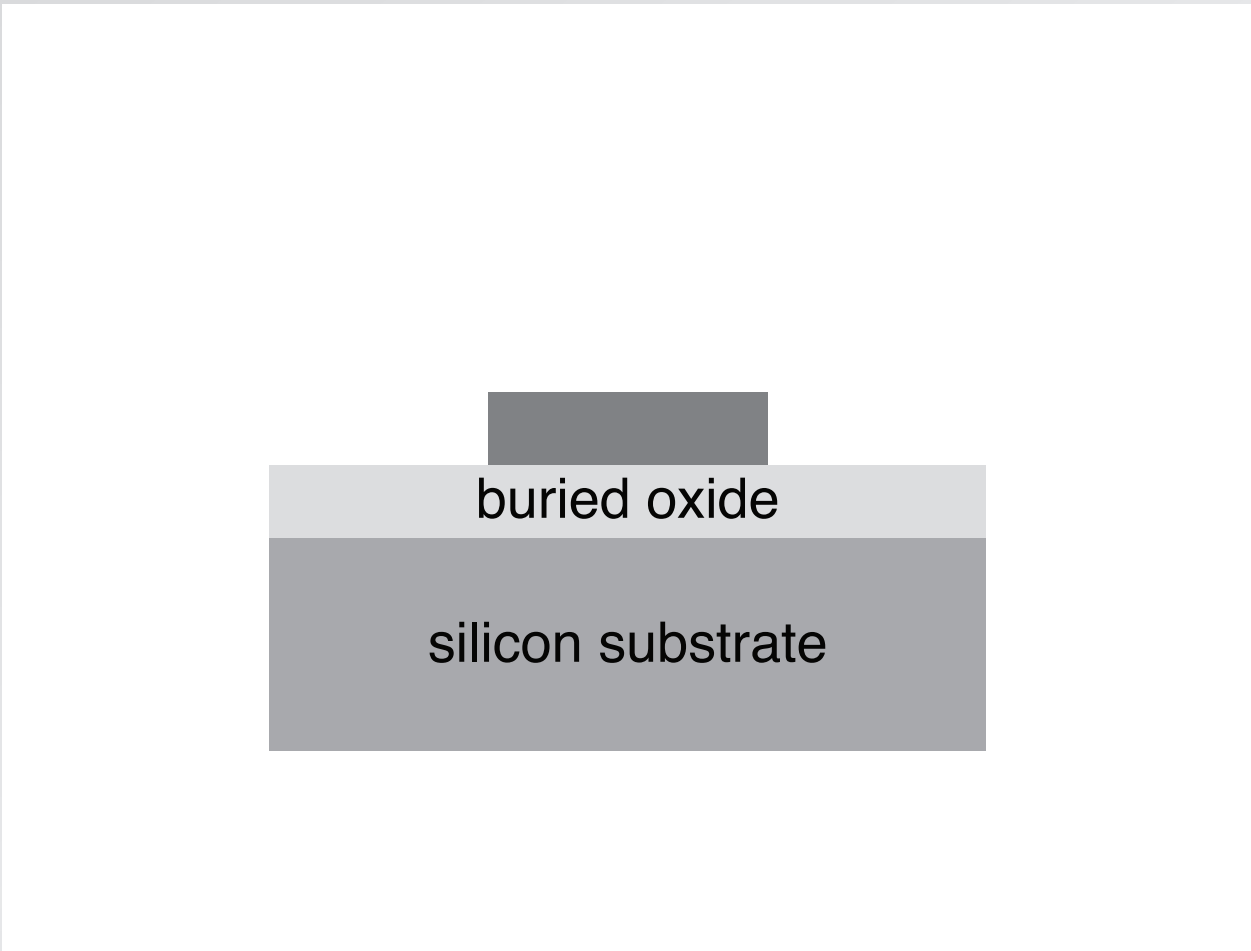

isolate surface layer for Hall measurements

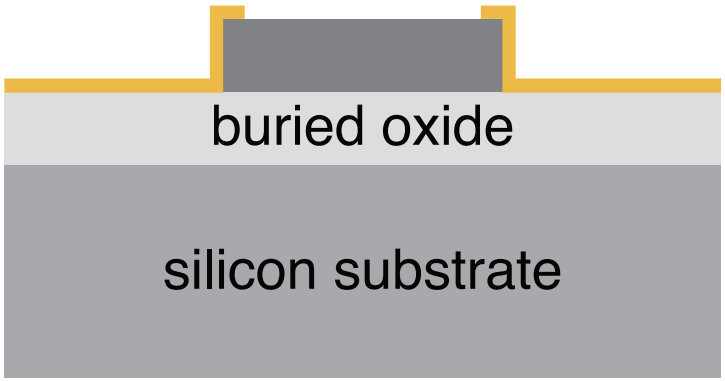

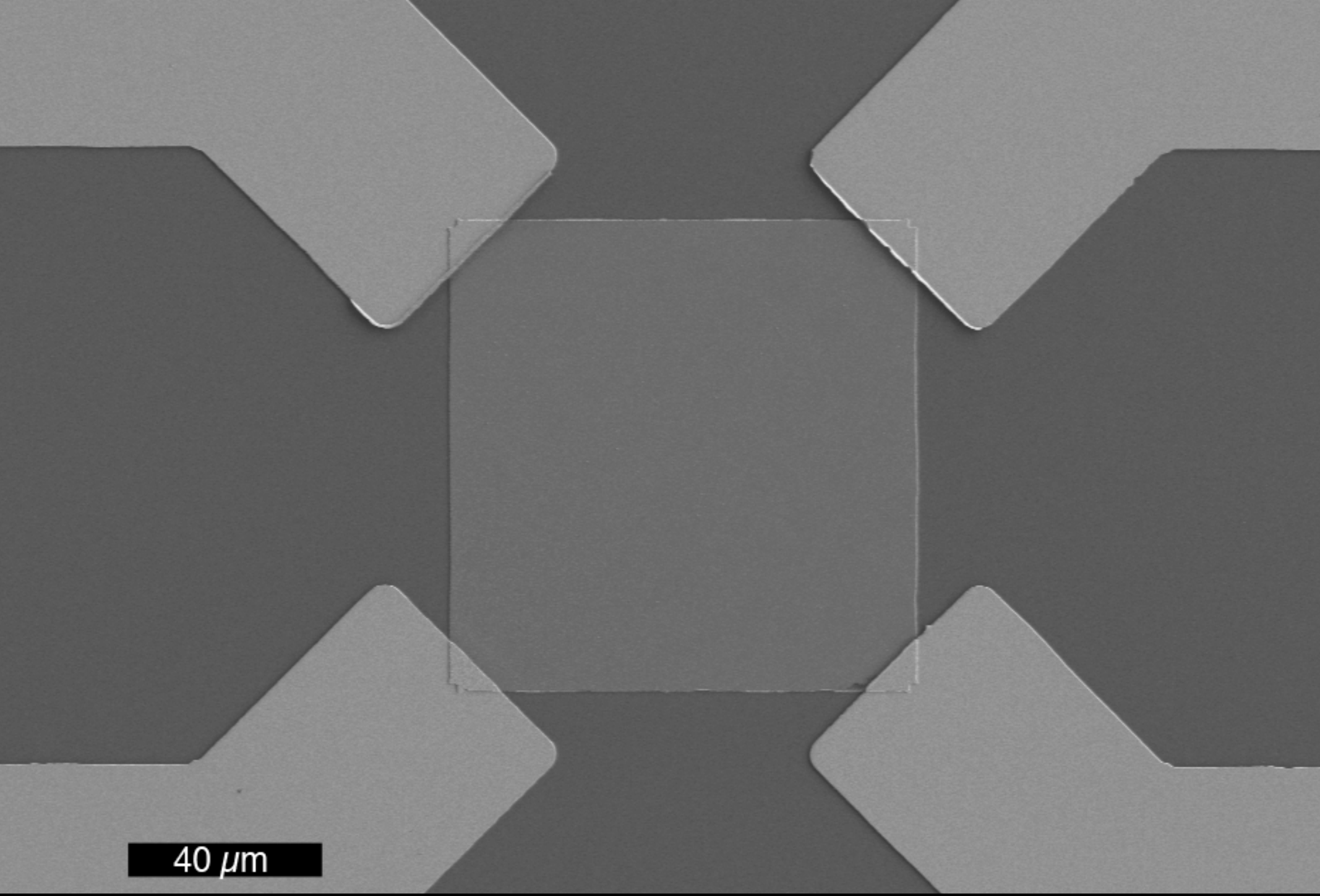

1 properties

2 intermediate band

Hall measurements

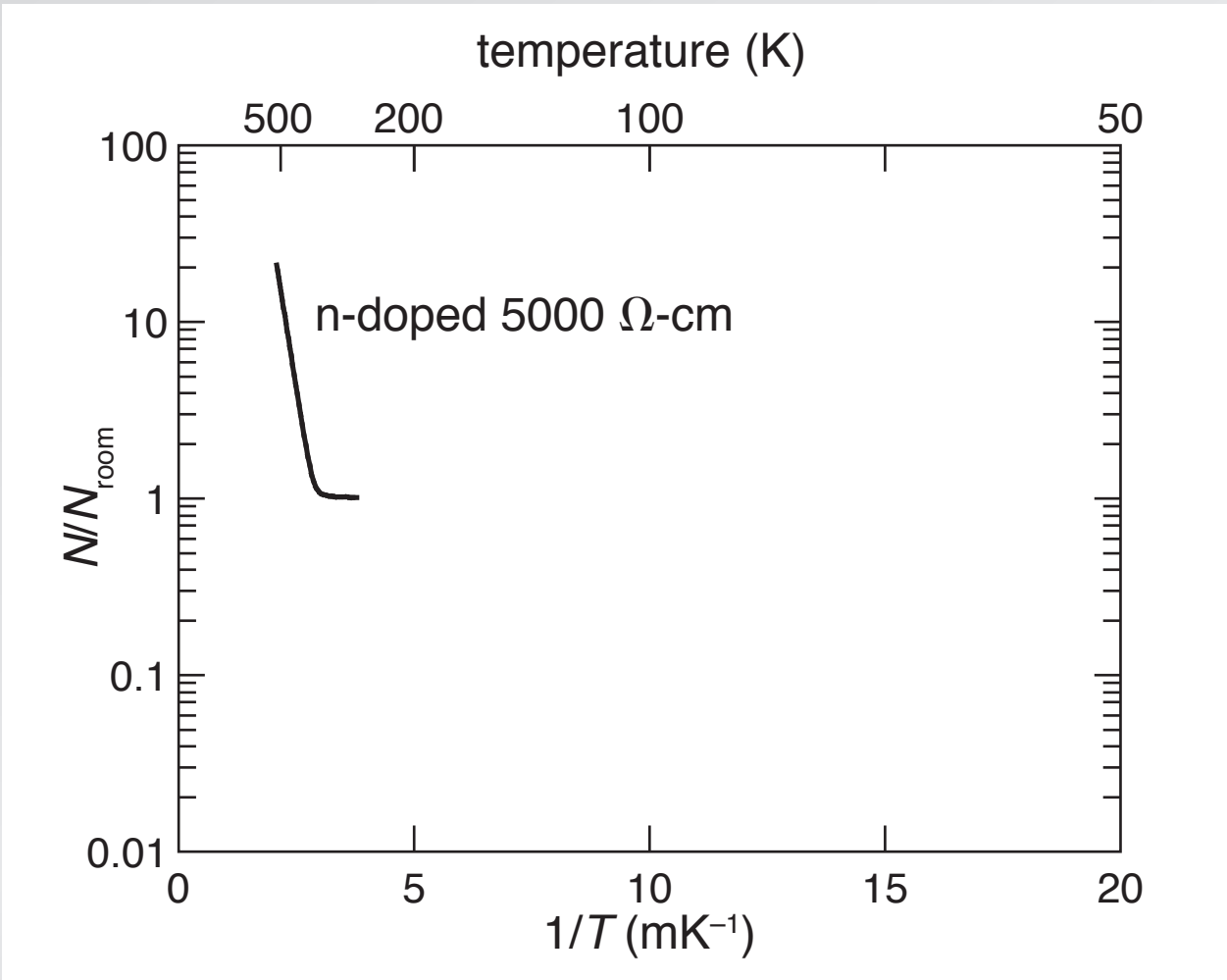

Hall measurements

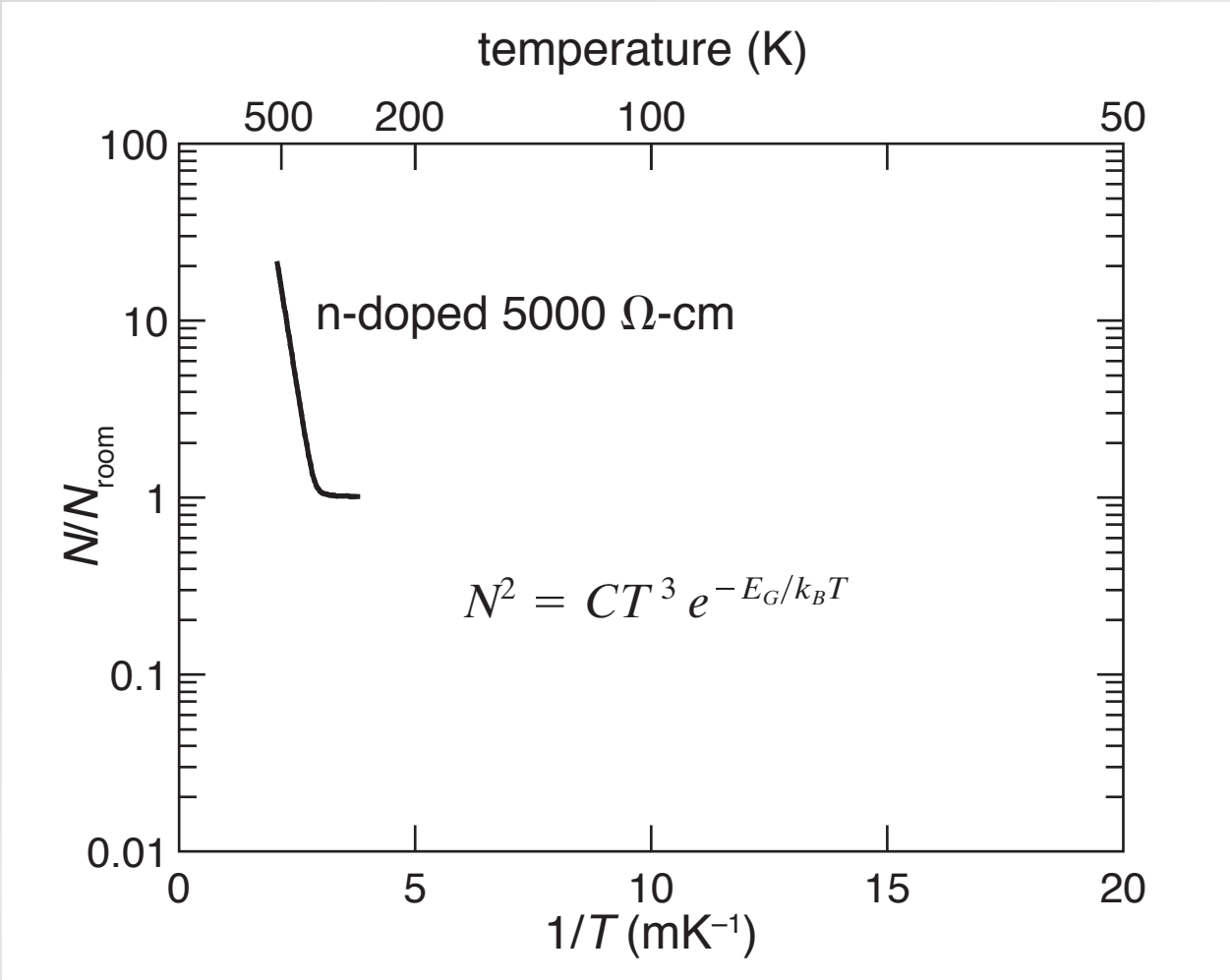

Hall measurements

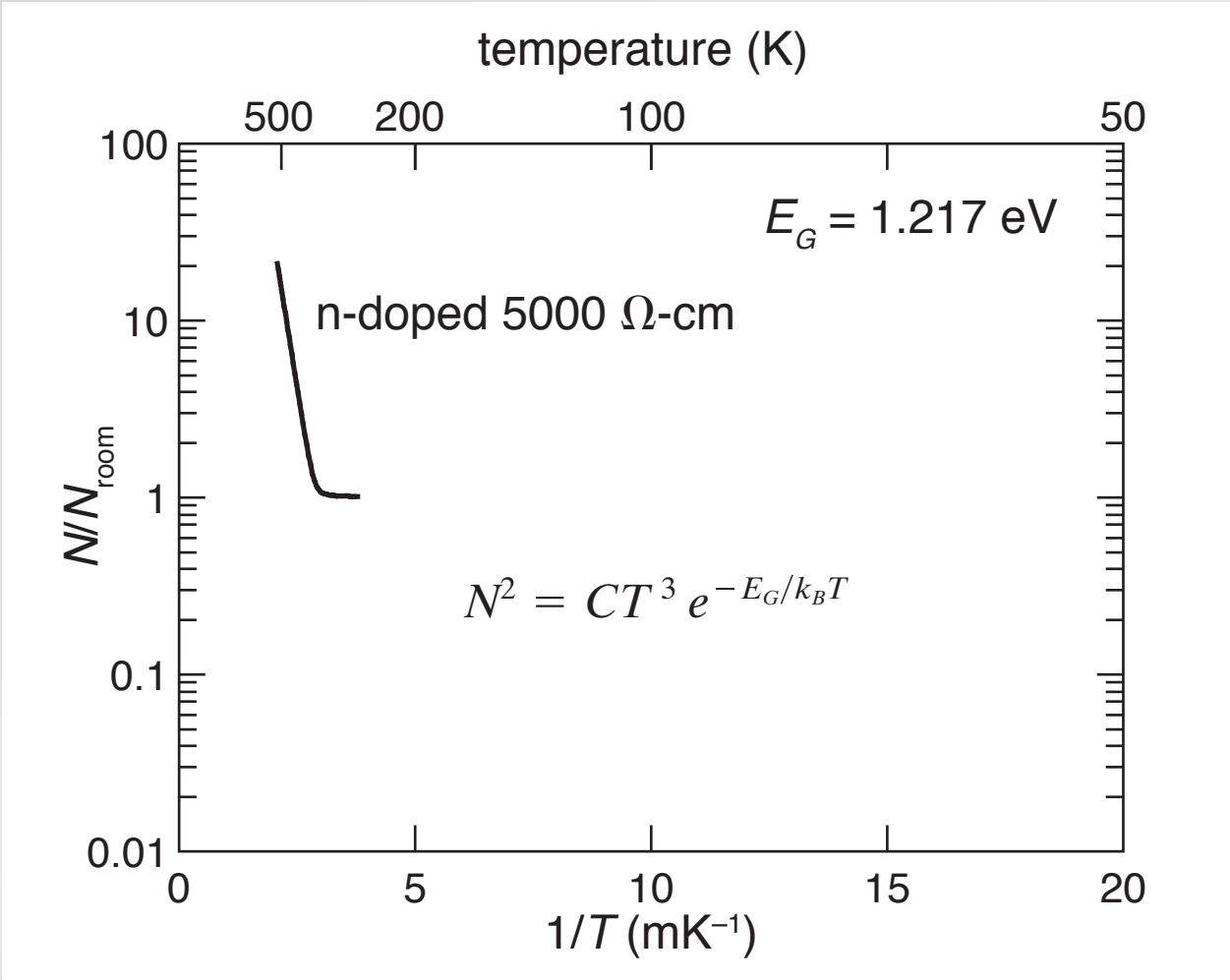

Hall measurements

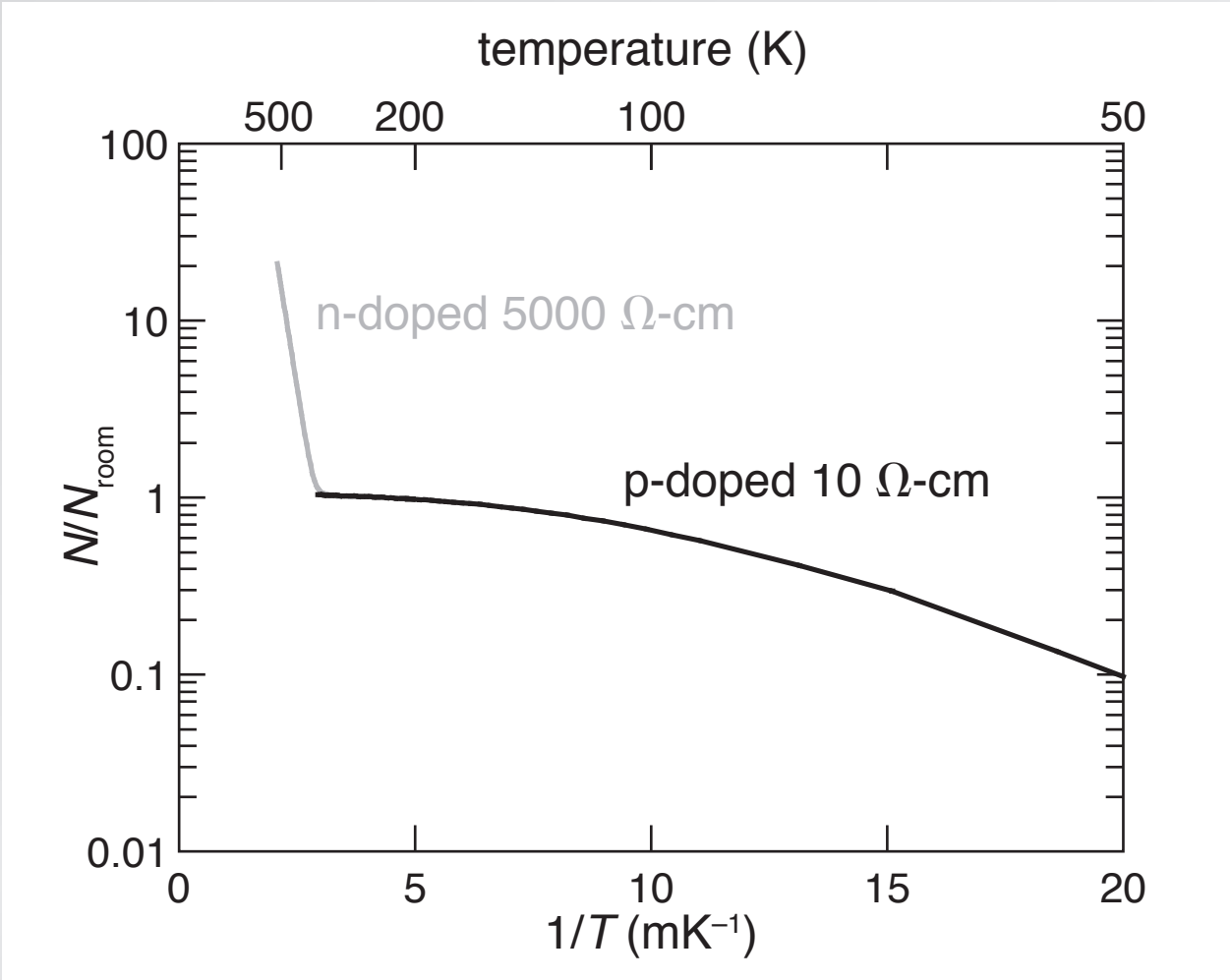

Hall measurements

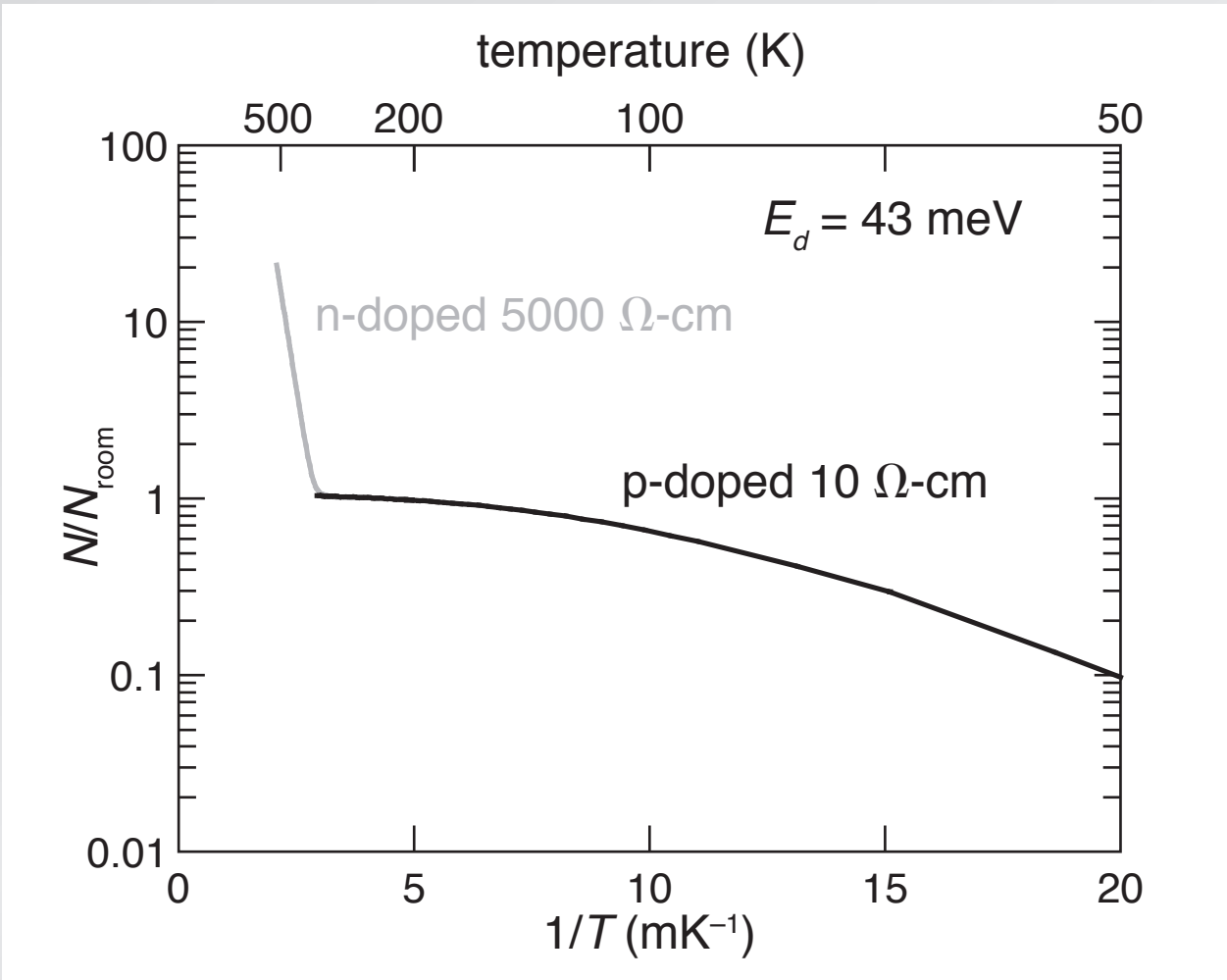

Hall measurements

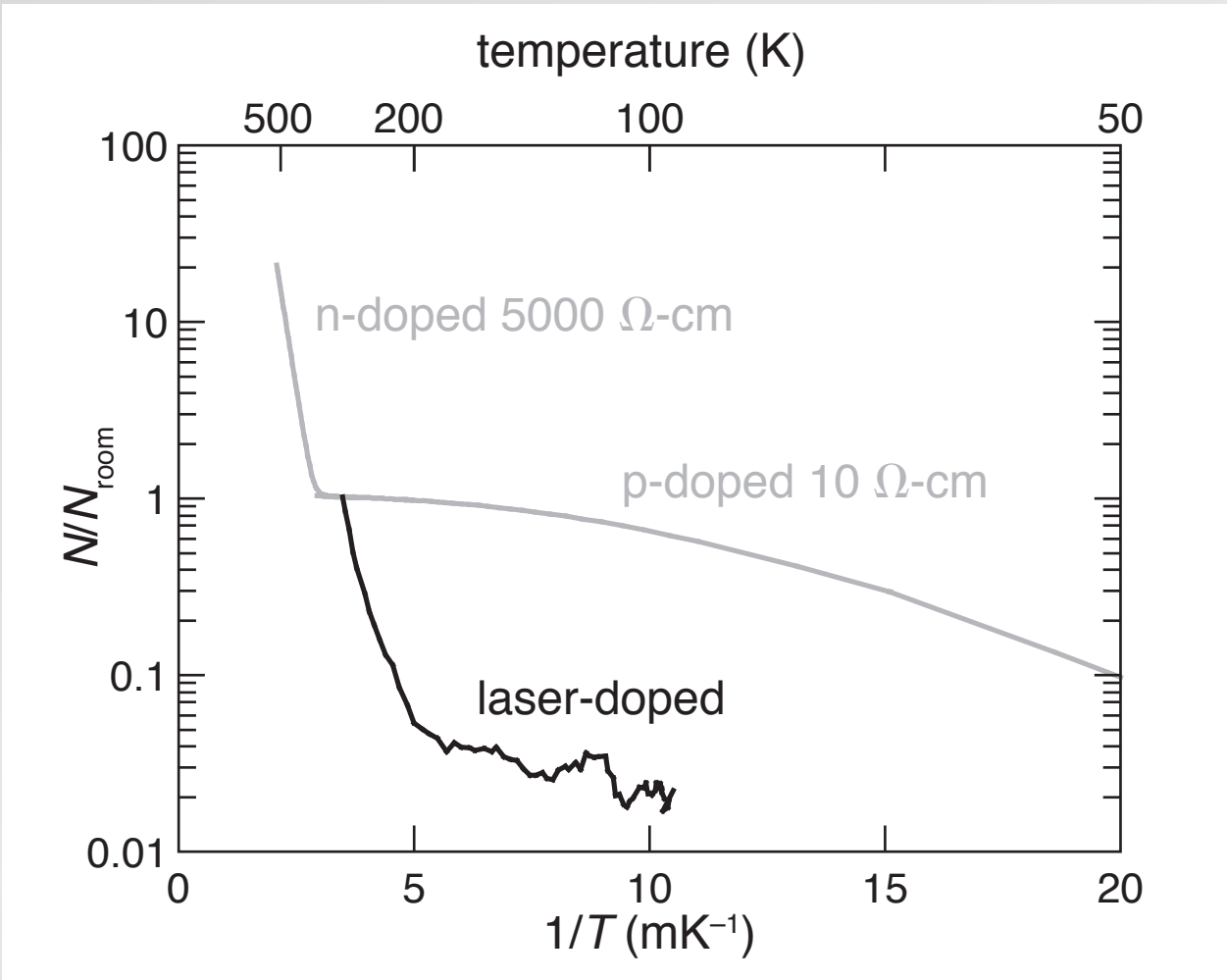

Hall measurements

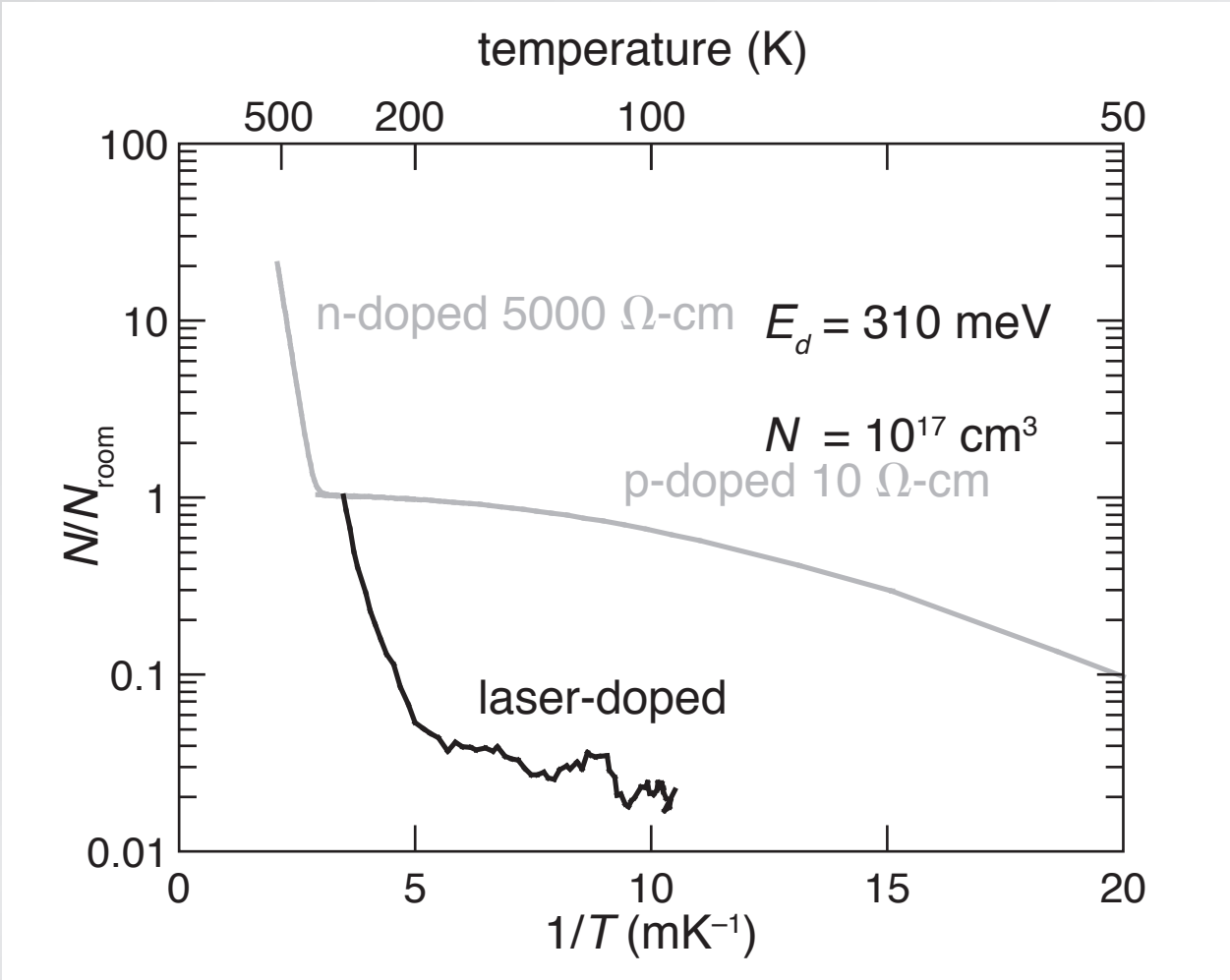

Hall measurements

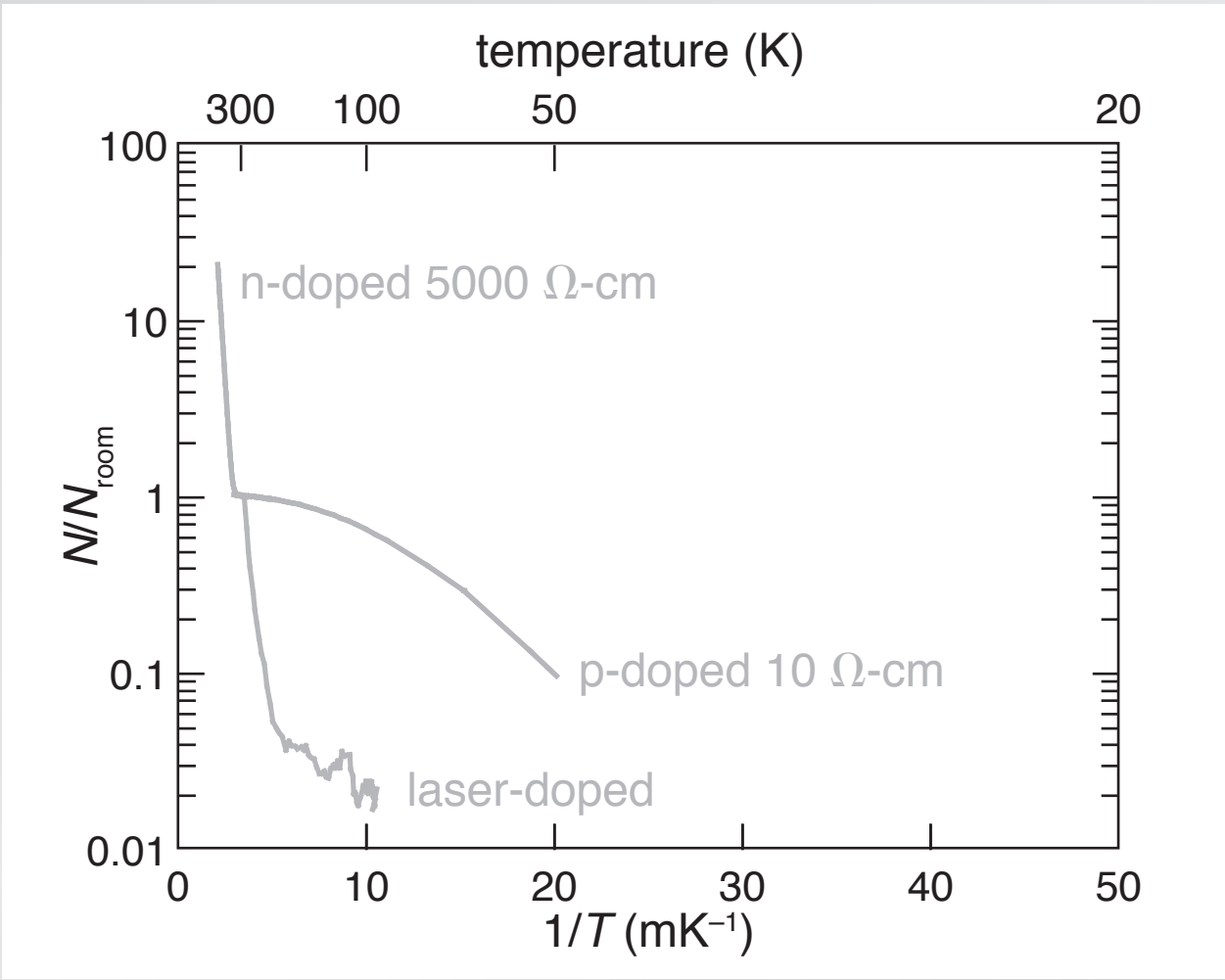

Hall measurements

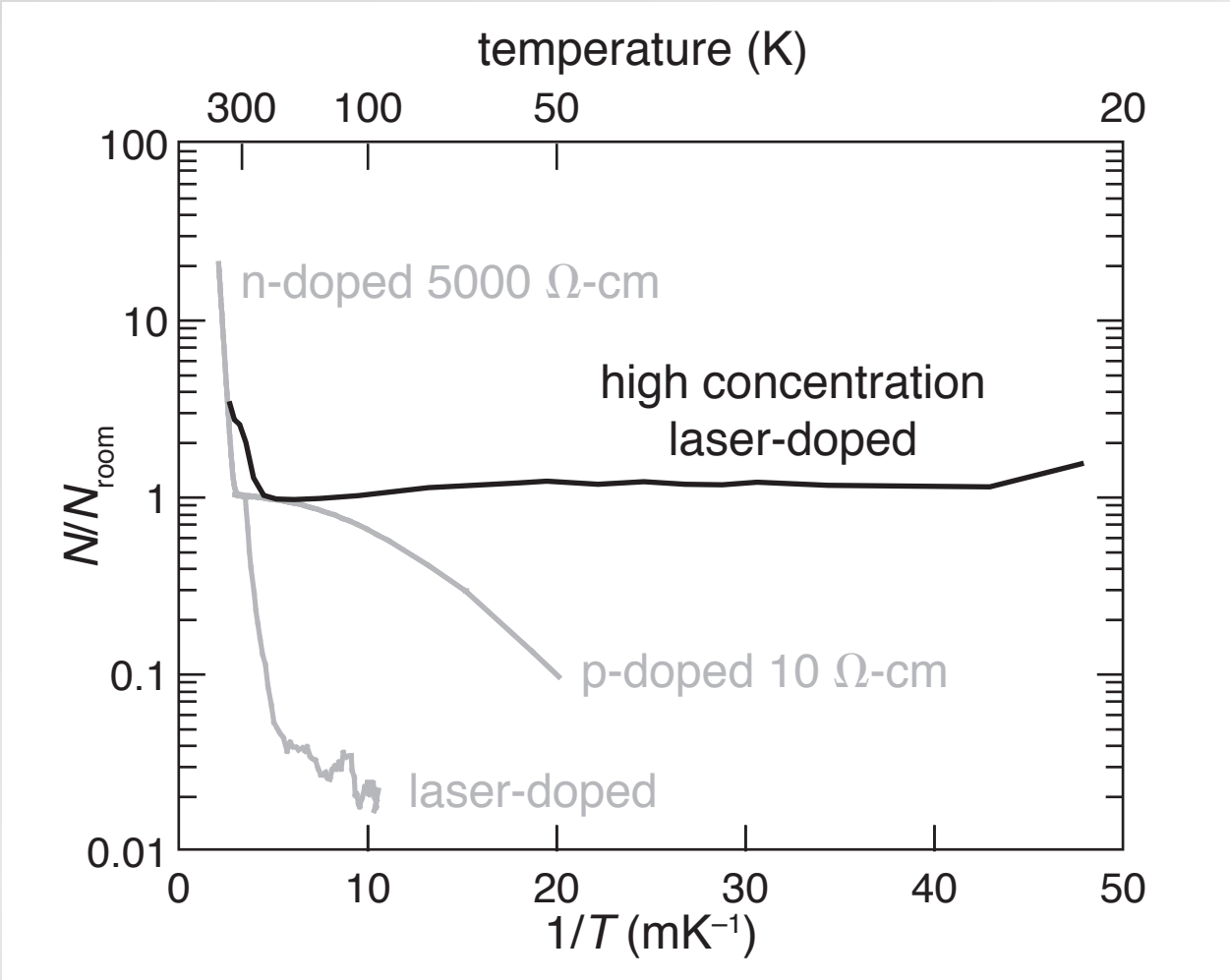

majority carrier mobility

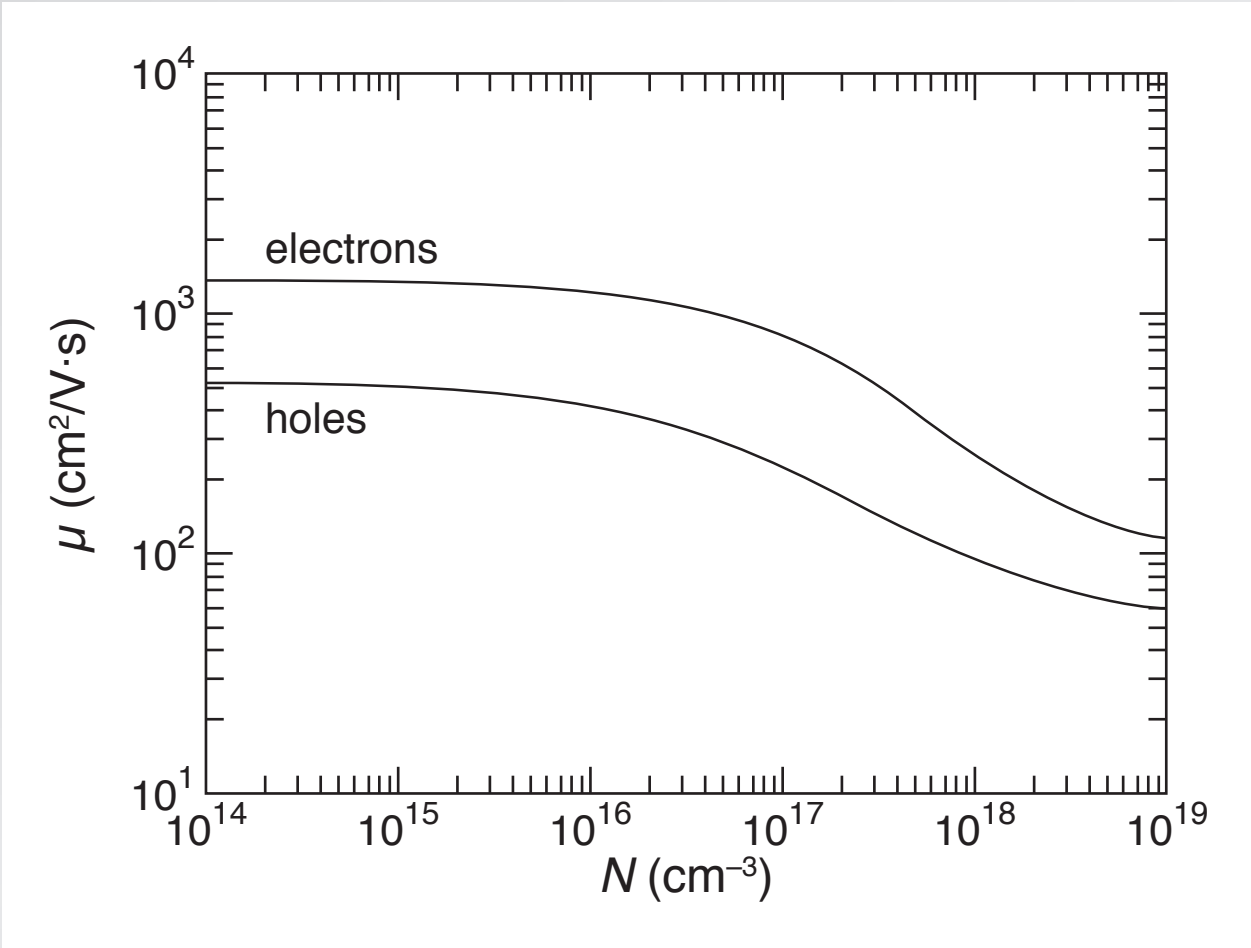

Caughey *et al.*, Proc. IEEE 55, 2192 (1967)

majority carrier mobility

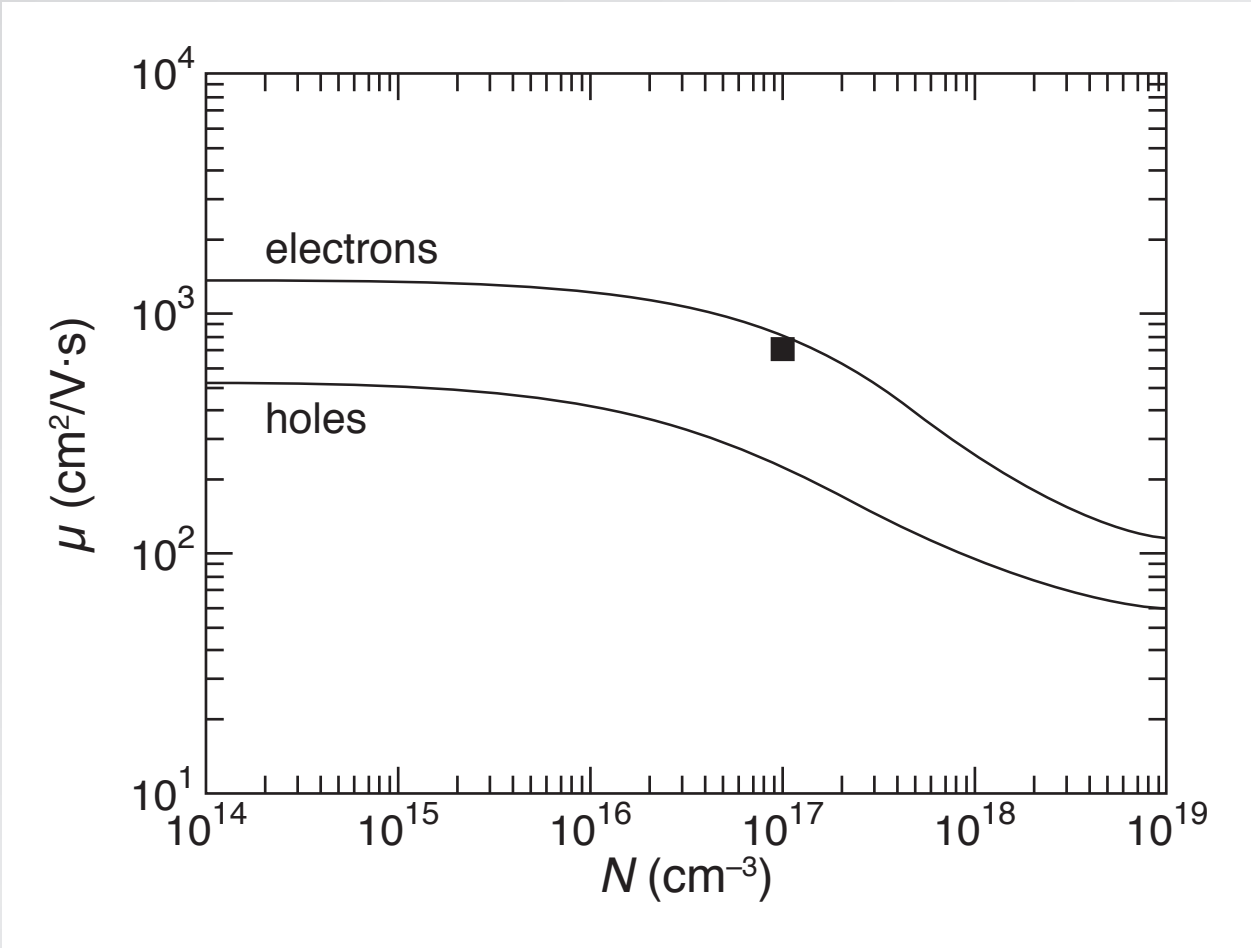

Caughey *et al.*, Proc. IEEE 55, 2192 (1967)

impurity (donor) band centered at 310 meV

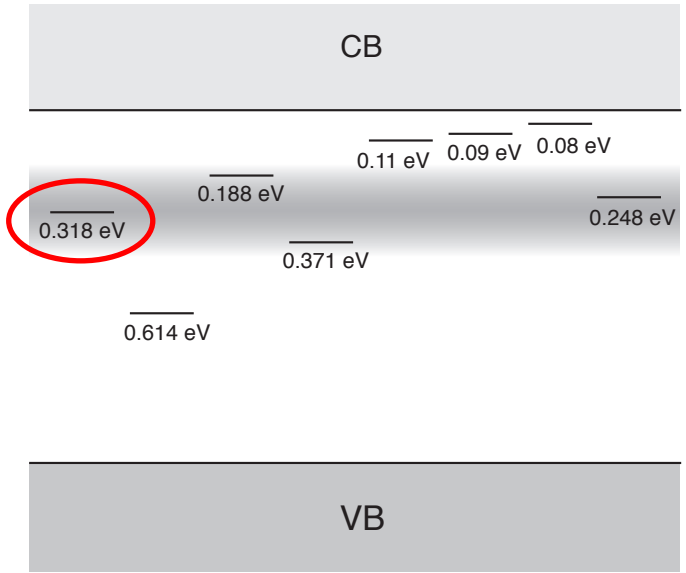

Insulator-to-Metal Transition in Selenium-Hyperdoped Silicon: Observation and Origin

Elif Ertekin,[1,*] Mark T. Winkler,[2,†] Daniel Recht,[3] Aurore J. Said,[3] Michael J. Aziz,[3] Tonio Buonassisi,[2] and Jeffrey C. Grossman[1,2,‡]

[1]*Department of Materials Science and Engineering, Massachusetts Institute of Technology, Cambridge Massachusetts 02139, USA*
[2]*Department of Mechanical Engineering, Massachusetts Institute of Technology, Cambridge Massachusetts 02139, USA*
[3]*Harvard School of Engineering and Applied Sciences, Cambridge Massachusetts 02138, USA*

(Received 14 October 2011; published 11 January 2012)

Hyperdoping has emerged as a promising method for designing semiconductors with unique optical and electronic properties, although such properties currently lack a clear microscopic explanation. Combining computational and experimental evidence, we probe the origin of sub–band-gap optical absorption and metallicity in Se-hyperdoped Si. We show that sub–band-gap absorption arises from direct defect–to–conduction-band transitions rather than free carrier absorption. Density functional theory predicts the Se-induced insulator-to-metal transition arises from merging of defect and conduction bands, at a concentration in excellent agreement with experiment. Quantum Monte Carlo calculations confirm the critical concentration, demonstrate that correlation is important to describing the transition accurately, and suggest that it is a classic impurity-driven Mott transition.

DOI: 10.1103/PhysRevLett.108.026401 PACS numbers: 71.30.+h, 61.72.sd, 73.61.Cw, 78.20.Bh

Of all the experimentally measurable physical properties of materials, electronic conductivity exhibits the largest variation, spanning a factor of 10^{31} from the best metals to the strongest insulators [1]. Over the last century, the puzzle of why some materials are conductors and others insulators, and the mechanisms underlying the transformation from one to the other, have been carefully scrutinized; yet even after such a vast body of research over such a long period, the subject remains the object of controversy. In 1956, Mott introduced a model for the insulator-to-metal transition (IMT) in doped semiconductors, in which long-ranged electron correlations are the driving force [2]. Hyperdoping (doping beyond the solubility limit) creates a new materials playground to explore defect-mediated IMTs in semiconductors. In this Letter, we identify a defect-induced IMT in silicon hyperdoped with selenium to concentrations exceeding 10^{20} cm^{-3} (compared to the equilibrium solubility limit [3] of about 10^{16} cm^{-3}) and we detailed nature of the transition with both tation. We find that the IMT is tion and most resembles ditionally, we lds

silicon appears to justify such interest. While isolated S and Se dopants are well-established deep double donors in silicon [3,14], the enhanced optical properties of hyperdoped silicon (in which these chalcogenic impurities are present at much higher concentrations) are not yet well understood. Further, unlike the prototypical system of phosphorus-doped silicon for which the IMT has been extensively studied and characterized [15,16], there are very few studies of an IMT resulting from deep defects such as chalcogens [17].

We prepared Se-doped silicon (Se:Si) samples using ion implantation followed by nanosecond pulsed-laser melting (PLM) and rapid resolidification. The PLM process enables chalcogen doping with concentrations exceeding 1% atomic; such samples exhibit unexplained optical properties including broad, featureless absorption of photons with energy lower than the band gap of silicon [9]. Silicon substrates (boron doped, $\rho \approx 25\ \Omega\,\mathrm{cm}$) were ion implanted with Se to nominal doses of 3×10^{15} and 1×10^{16} cm^2 using an ion beam energy of 176 keV. The implanted samples were exposed to four laser pulses (fluences of 1.7, 1.7, 1.7 and 1.8 J cm^{-2}). This fluence regimen results in a slightly shallower dopant profile, and higher Se concentration, than reported previously [18]. The crystalline, extends approximately 350 nm electrically isolated from the ction formed between as measured

1 properties 2 intermediate band

DFT calculations

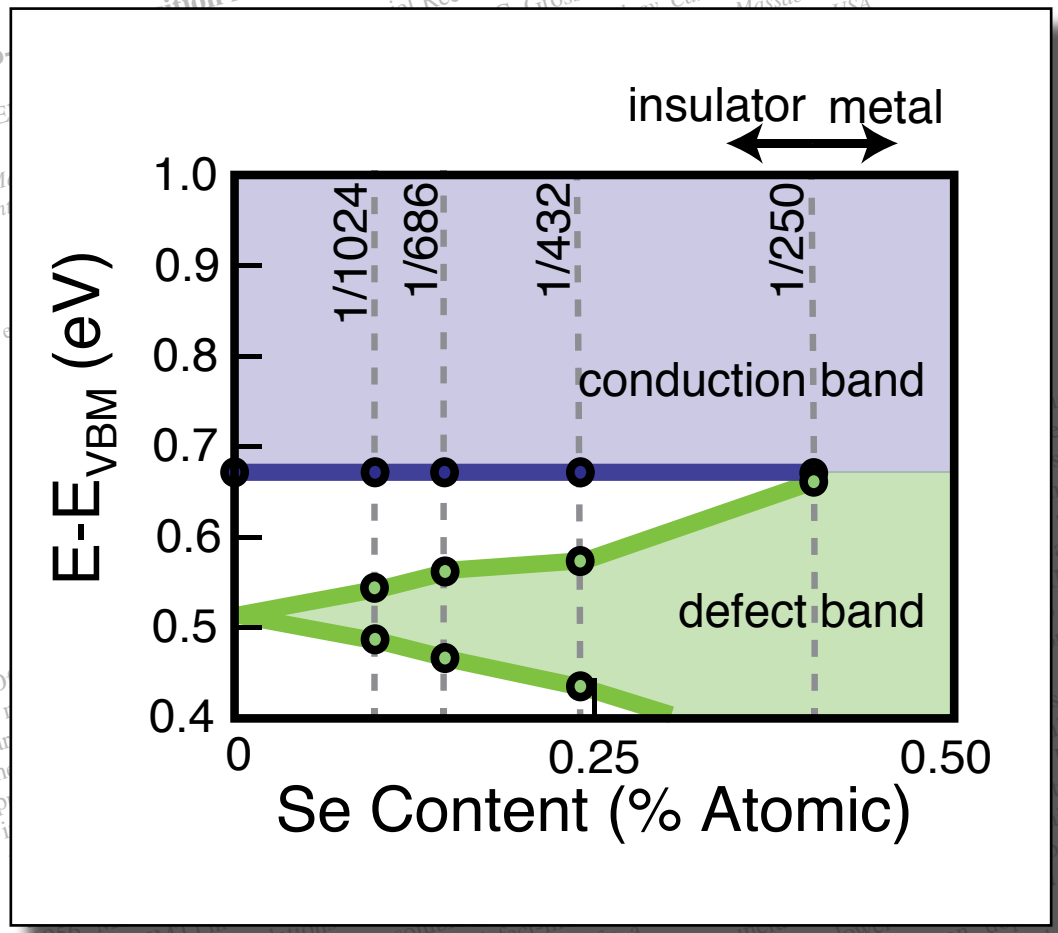

Ertekin *et al.*, Phys. Rev. Lett. 108, 026401 (2012)

1 properties

2 intermediate band

JOURNAL OF APPLIED PHYSICS **113**, 213501 (2013)

Emergence of very broad infrared absorption band by hyperdoping of silicon with chalcogens

Ikurou Umezu,[1] Jeffrey M. Warrender,[2] Supakit Charnvanichborikarn,[3] Atsushi Kohno,[4] James S. Williams,[3] Malek Tabbal,[5] Dimitris G. Papazoglou,[6,7] Xi-Cheng Zhang,[8,a)] and Michael J. Aziz[9]

[1]*Department of Physics, Konan University, Kobe 658-8501, Japan*
[2]*U.S. Army ARDEC–Benét Laboratories, Watervliet, New York 12189, USA*
[3]*Research School of Physics and Engineering, The Australian National University, Canberra, ACT 0200, Australia*
[4]*Department of Applied Physics, Fukuoka University, Fukuoka 814-0180, Japan*
[5]*Department of Physics, American University of Beirut, Beirut 1107 2020, Lebanon*
[6]*Institute of Electronic Structure and Laser, Foundation for Research and Technology Hellas, P.O. Box 1527, 71110 Heraklion, Greece*
[7]*Materials Science and Technology Department, University of Crete, P.O. Box 2208, 71003 Heraklion, Greece*
[8]*Department of Physics, Applied Physics and Astronomy, Rensselaer Polytechnic Institute, Troy, New York 12180, USA*
[9]*Harvard School of Engineering and Applied Sciences, Cambridge, Massachusetts 02138, USA*

(Received 9 September 2012; accepted 29 April 2013; published online 3 June 2013)

We report the near through mid-infrared (MIR) optical absorption spectra, over the range 0.05–1.3 eV, of monocrystalline silicon layers hyperdoped with chalcogen atoms synthesized by ion implantation followed by pulsed laser melting. A broad mid-infrared optical absorption band emerges, peaking near 0.5 eV for sulfur and selenium and 0.3 eV for tellurium hyperdoped samples. Its strength and width increase with impurity concentration. Its strength decreases markedly with subsequent thermal annealing. The emergence of a broad MIR absorption band is consistent with the formation of an impurity band from isolated deep donor levels as the concentration of chalcogen atoms in metastable local configurations increases. © 2013 *AIP Publishing LLC*.

[http://dx.doi.org/10.1063/1.4804935]

I. INTRODUCTION

Silicon hyperdoped with chalcogens can be synthesized by pulsed laser irradiation in a sulfur-bearing atmosphere,[1,2] ion implantation followed by pulsed laser melting,[3,4] or pulsed laser mixing.[5] This material has attracted interest because of its sub band gap absorption and has been studied as a candidate for infrared (IR) photodetectors[6–8] and efficient solar cells.[9–11] In addition, observations of carrier lifetime recovery for sufficiently high concentrations of titanium has aroused similar interest in this material.[12,13] erdoping has been shown to cause an has been proposed to form an [4,10,14–16] However, bandgap

II. EXPERIMENT

Double side polished p type (001) Si wafers, resistivity of 5–25 Ω cm, were ion implanted at room temperature with either 95 keV $^{32}S^-$, 176 keV $^{80}Se^+$, or 245 keV $^{130}Te^+$ to doses of 1×10^{16} ions/cm^2. The dose of $^{32}S^-$ was varied from 3×10^{14} to 1×10^{16} ions/cm^2 and pre-amorphized by 85 keV Si^- to doses of 3×10^{15} ions/cm^2. Pulsed laser melting was performed using a XeCl excimer laser beam (308 nm, 25 ns FWHM, 50 ns total duration). Each sample received three laser shots at 1.7 J/cm^2 followed by a fourth laser shot at 1.8 J/cm^2. Time-resolved reflectivity of a 488 nm Ar^+ ion laser was used to measure the melt duration. The laser fluence was calibrated by comparing the melt duration with numerical solutions to the one-dimensional heat [18] The details of the sample preparation method chalcogen atoms observed by secondary are reported elsewhere.[3] For edure is the same amples,

1 properties 2 intermediate band

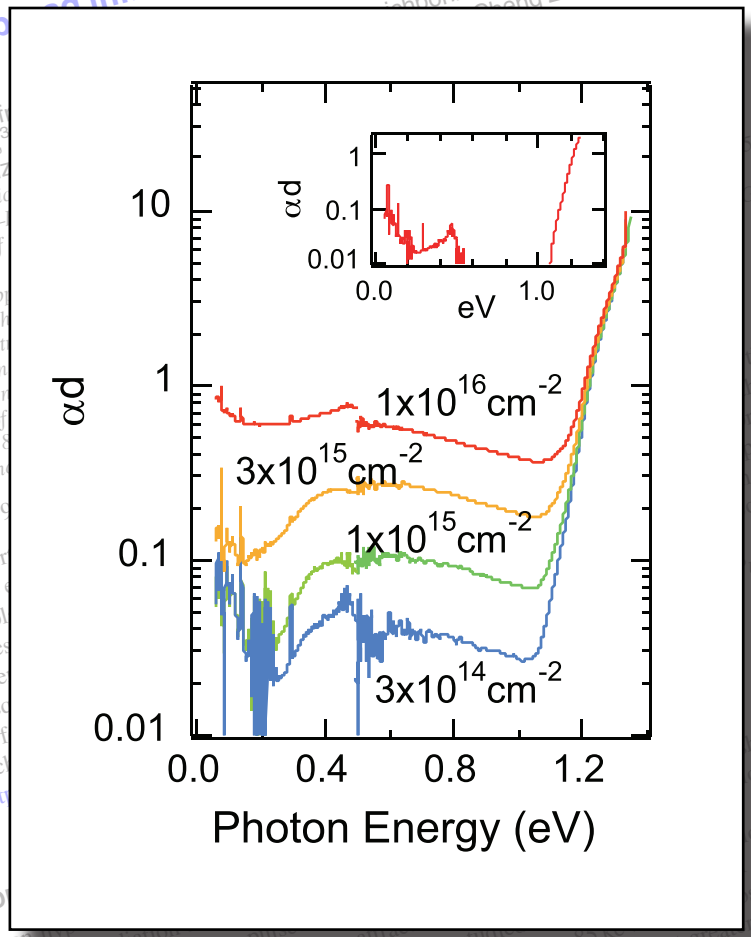

Umezu *et al.*, J. Appl. Phys. 113, 213501 (2013)

1 properties

2 intermediate band

Understanding the Viability of Impurity-Band Photovoltaics: A Case Study of S-doped Si

by

Joseph Timothy Sullivan

Submitted to the Department of Mechanical Engineering
on May 18, 2013, in partial fulfillment of the
requirements for the degree of
Doctor of Philosophy

Abstract

This thesis explores the electronic structure, optical properties, and carrier lifetimes in silicon that is doped with sulfur beyond the equilibrium solid solubility limit, with a focus on applications as an absorber layer for an impurity-band photovoltaic device. The concept of an impurity-band material envisions the creation of a band of electronic states by incorporating high concentrations of deep-level dopants, which enable the generation of free carriers using photons with energy less than that of the band gap of the host semiconductor. The investigations reported in this thesis provide a framework for the appropriate selection of impurity-band candidate materials. The thesis is divided into three primary sections, one for each of three experimental techniques, respectively.

First, the electronic band structure is studied using synchrotron-based x-ray emission spectroscopy. These spectra provide the first insights into how the electronic structure changes as the sulfur concentration is increased across the metal-insulator transition, and how the electronic structure is linked to the anomalously high sub-band gap absorption. A discrete change in local electronic structure is seen that corresponds to the macroscopic change in electronic behavior. Additionally, a direct correlation is seen between sulfur-induced states and the sub-band gap absorption.

the optical properties are studied using Fourier transform infrared spec-

of the complex index of refraction is performed using numerical

transmission and reflection measurements. Analysis of

position of the sulfur-induced states within

ifferent sulfur concentrations and

tal-insulator transition,

ction band,

1 properties

2 intermediate band

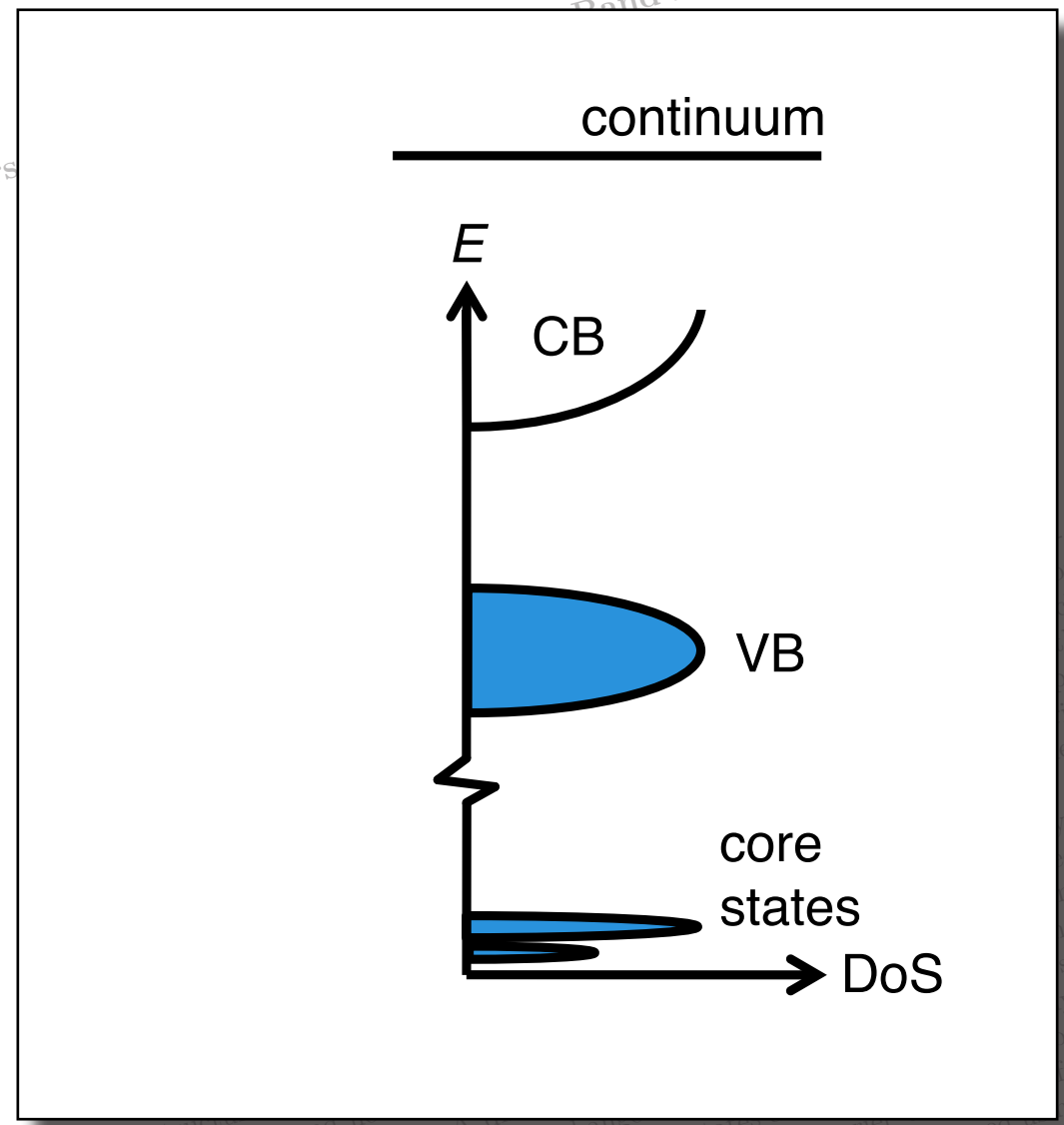

J. Sullivan, Ph.D. Thesis, MIT (2013)

1 properties

2 intermediate band

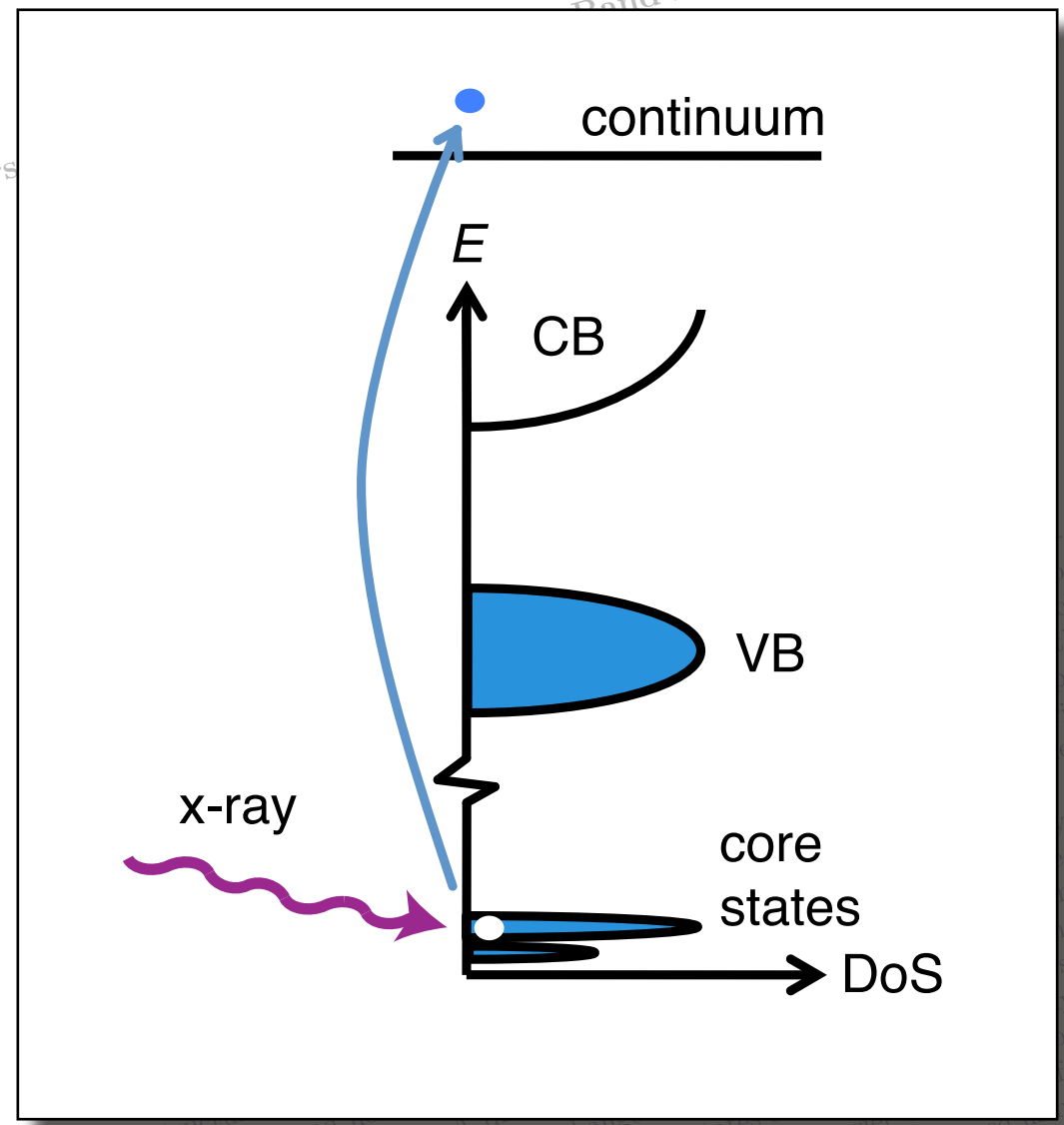

J. Sullivan, Ph.D. Thesis, MIT (2013)

1 properties

2 intermediate band

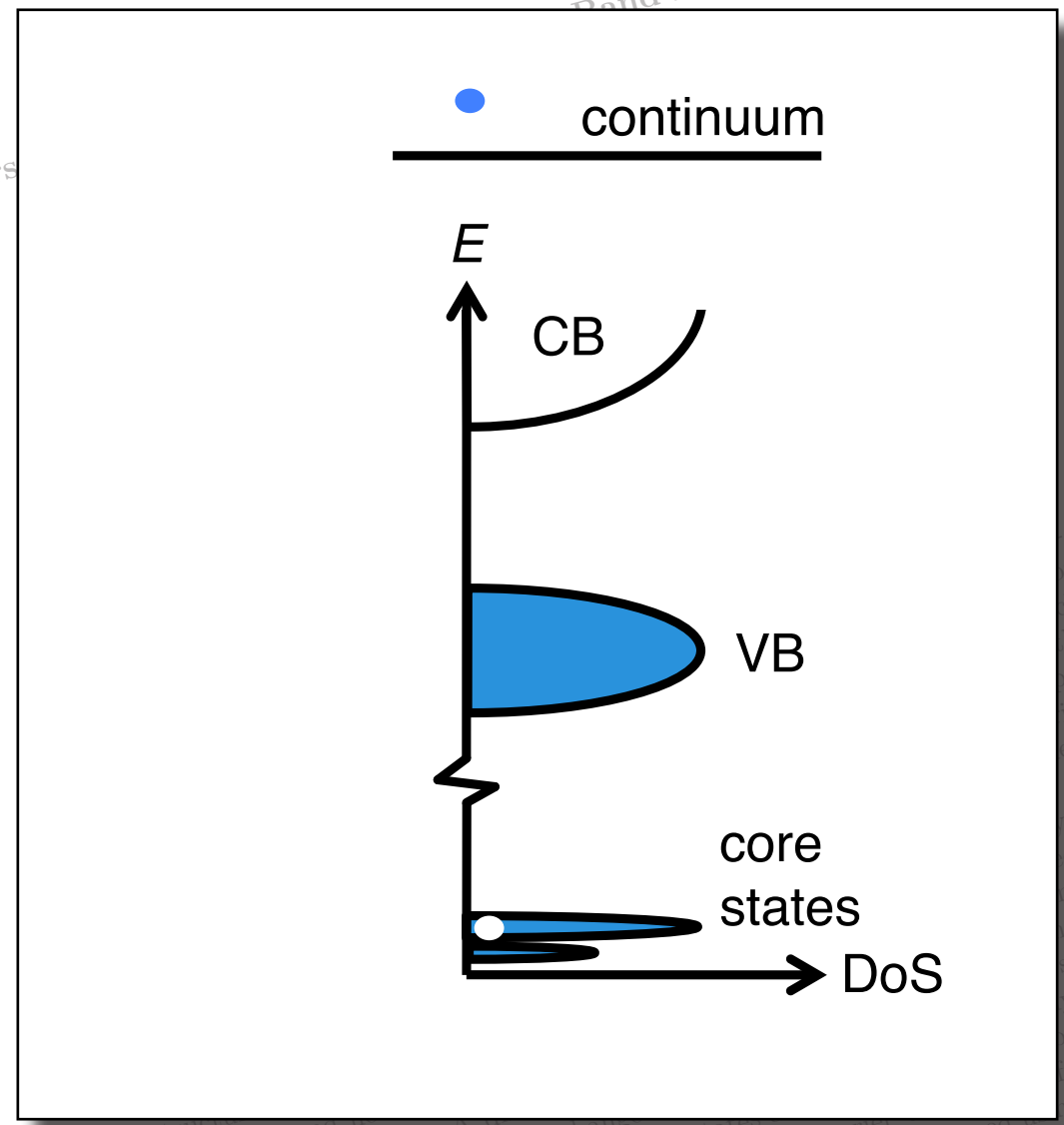

J. Sullivan, Ph.D. Thesis, MIT (2013)

1 properties 2 intermediate band

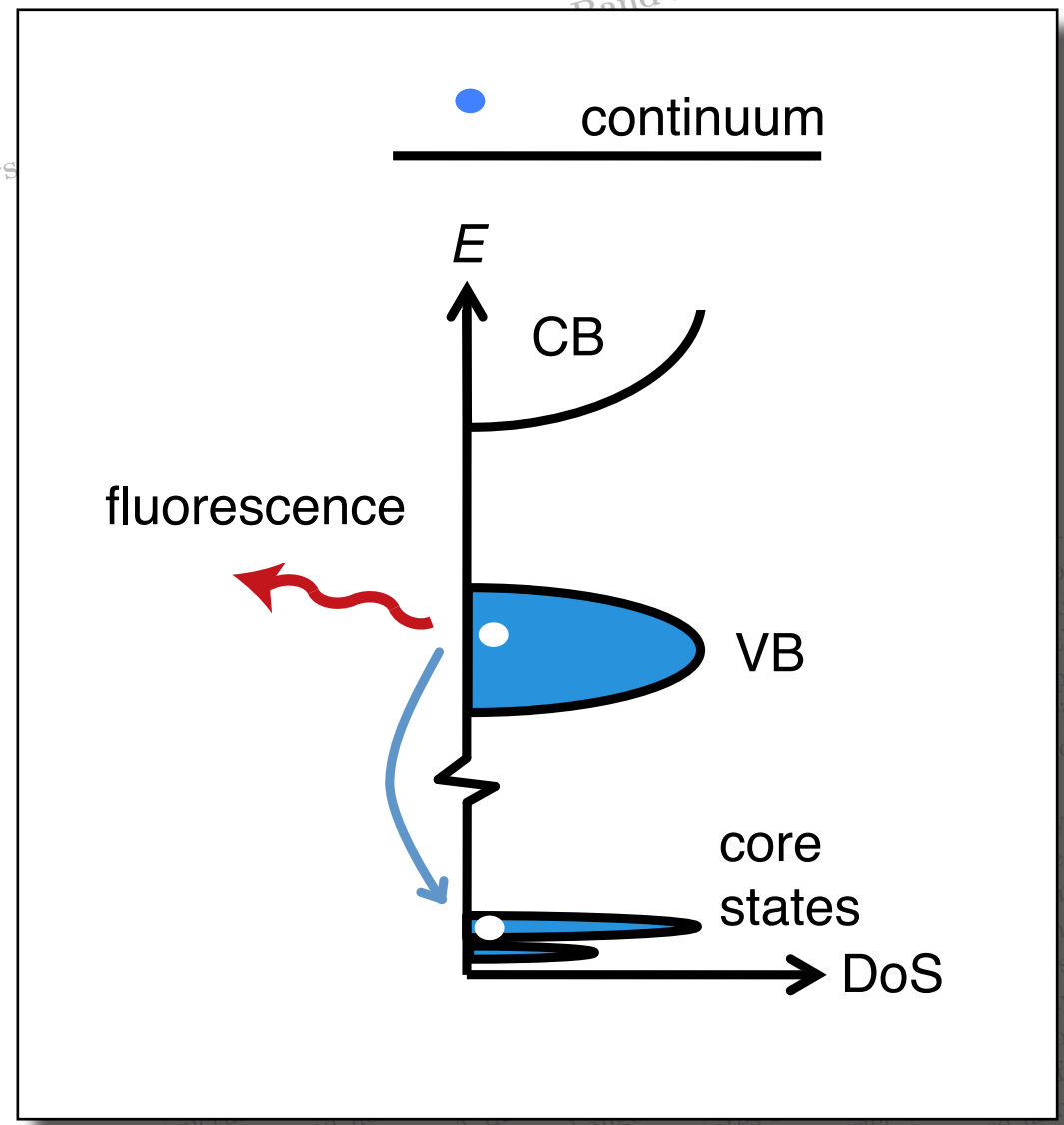

J. Sullivan, Ph.D. Thesis, MIT (2013)

1 properties

2 intermediate band

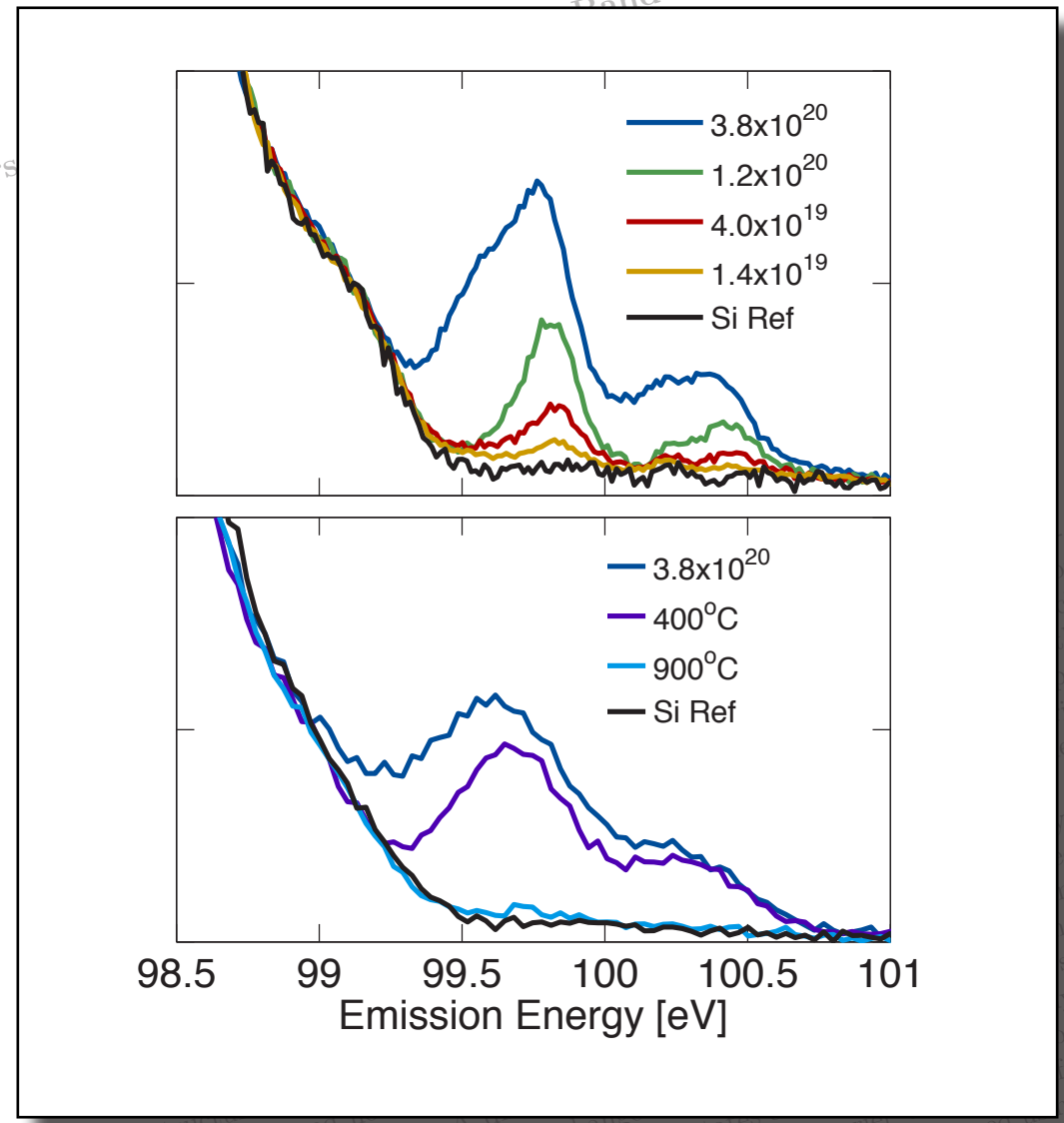

J. Sullivan, Ph.D. Thesis, MIT (2013)

1 properties **2** intermediate band

Things to keep in mind

- IR absorption rolls off around 8 μm
- consistent evidence of intermediate band formation
- IB forms at 0.1% at. doping, broadens at higher doping
- IB merges with CB at 0.4% at. yielding metallic behavior

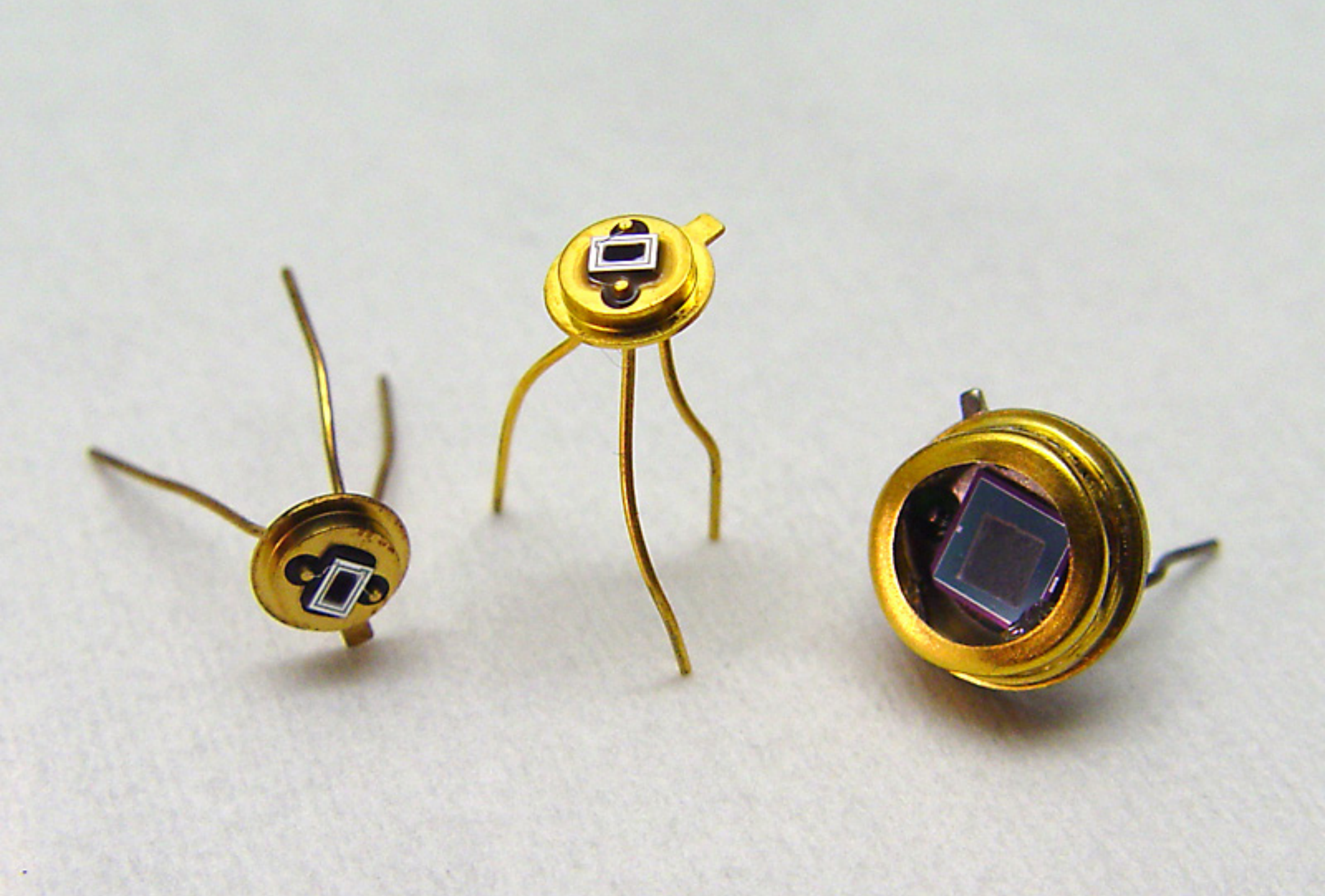

1 properties 2 intermediate band 3 devices

should have shallow junction below surface

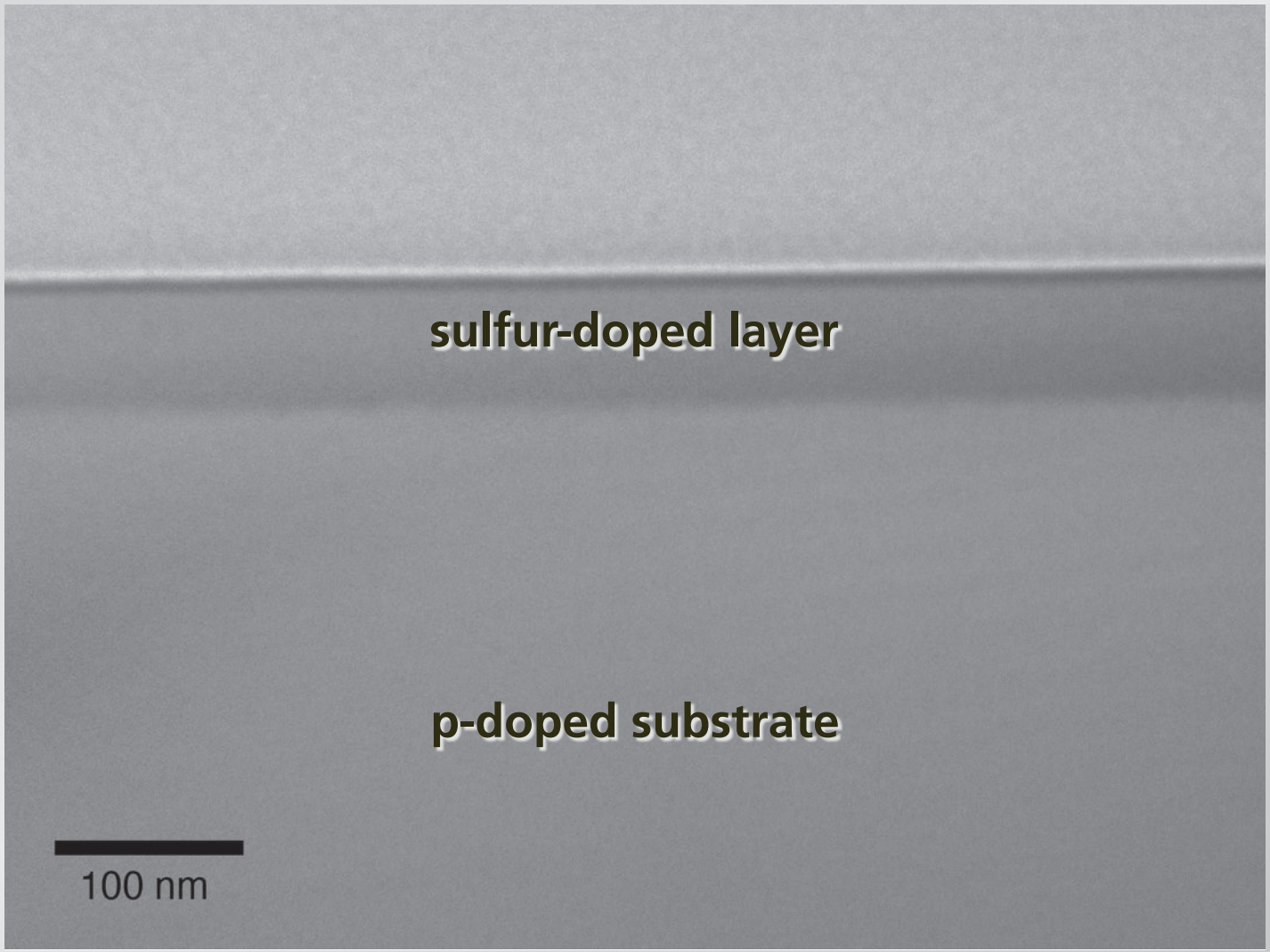

excellent rectification (after annealing)

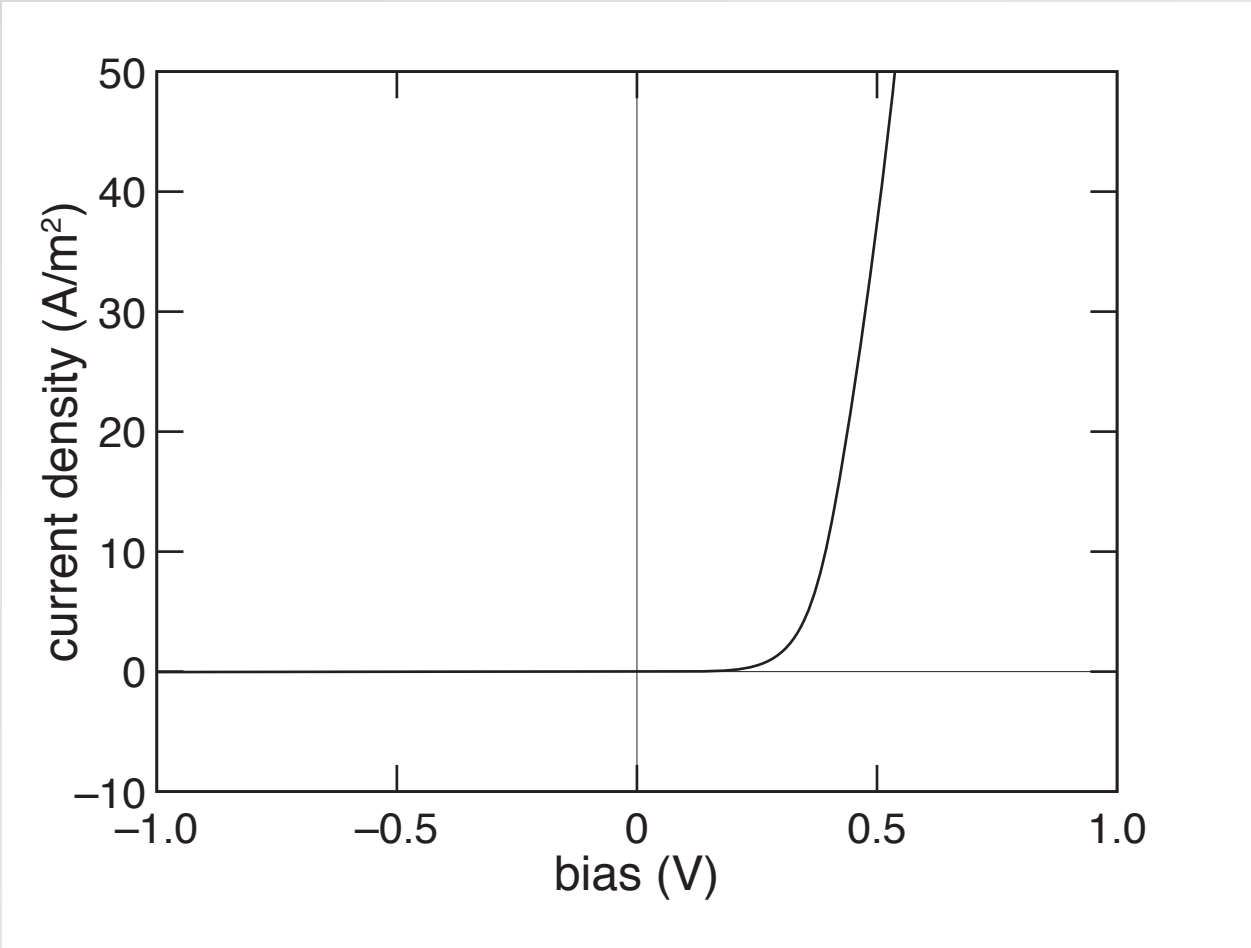

responsivity

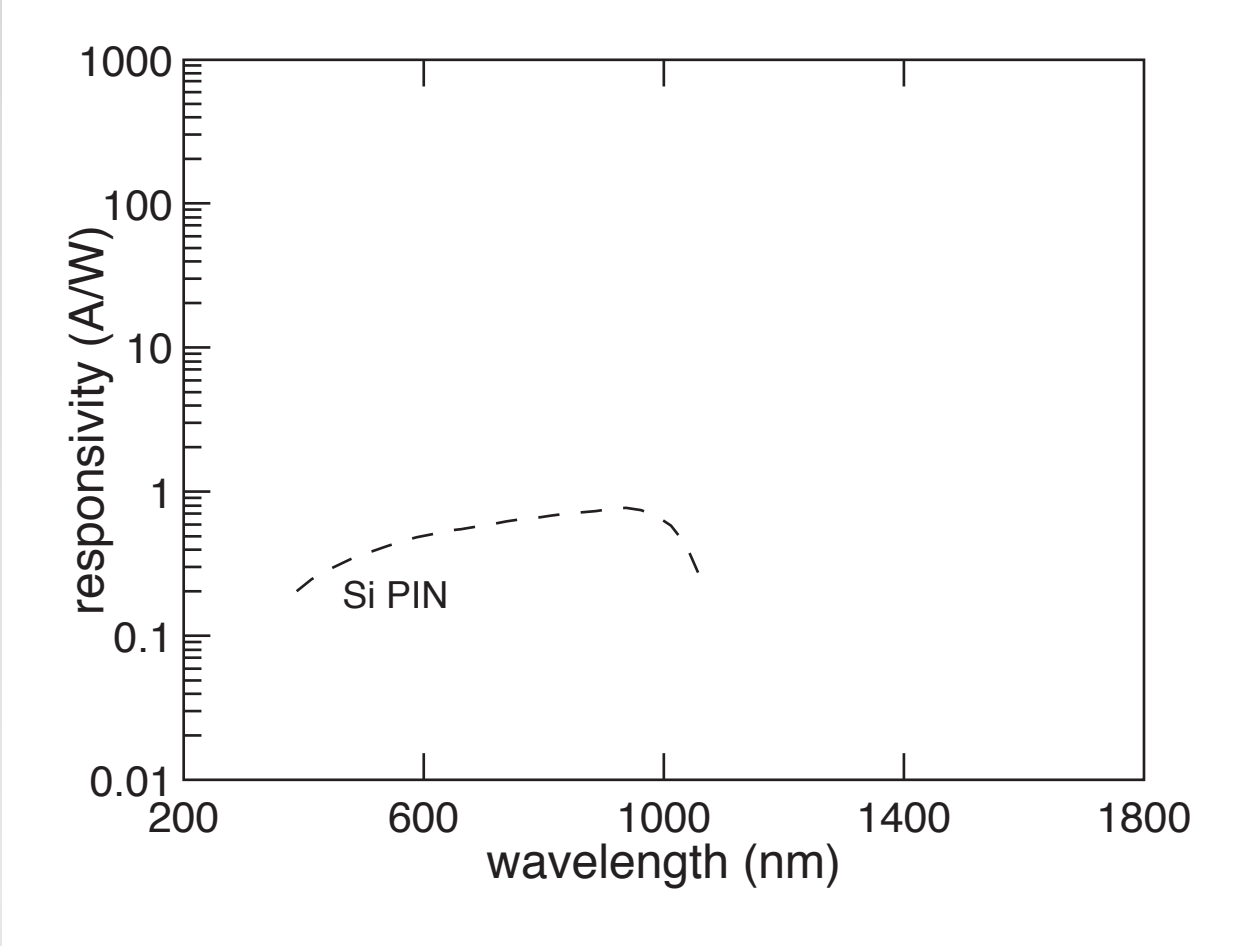

responsivity

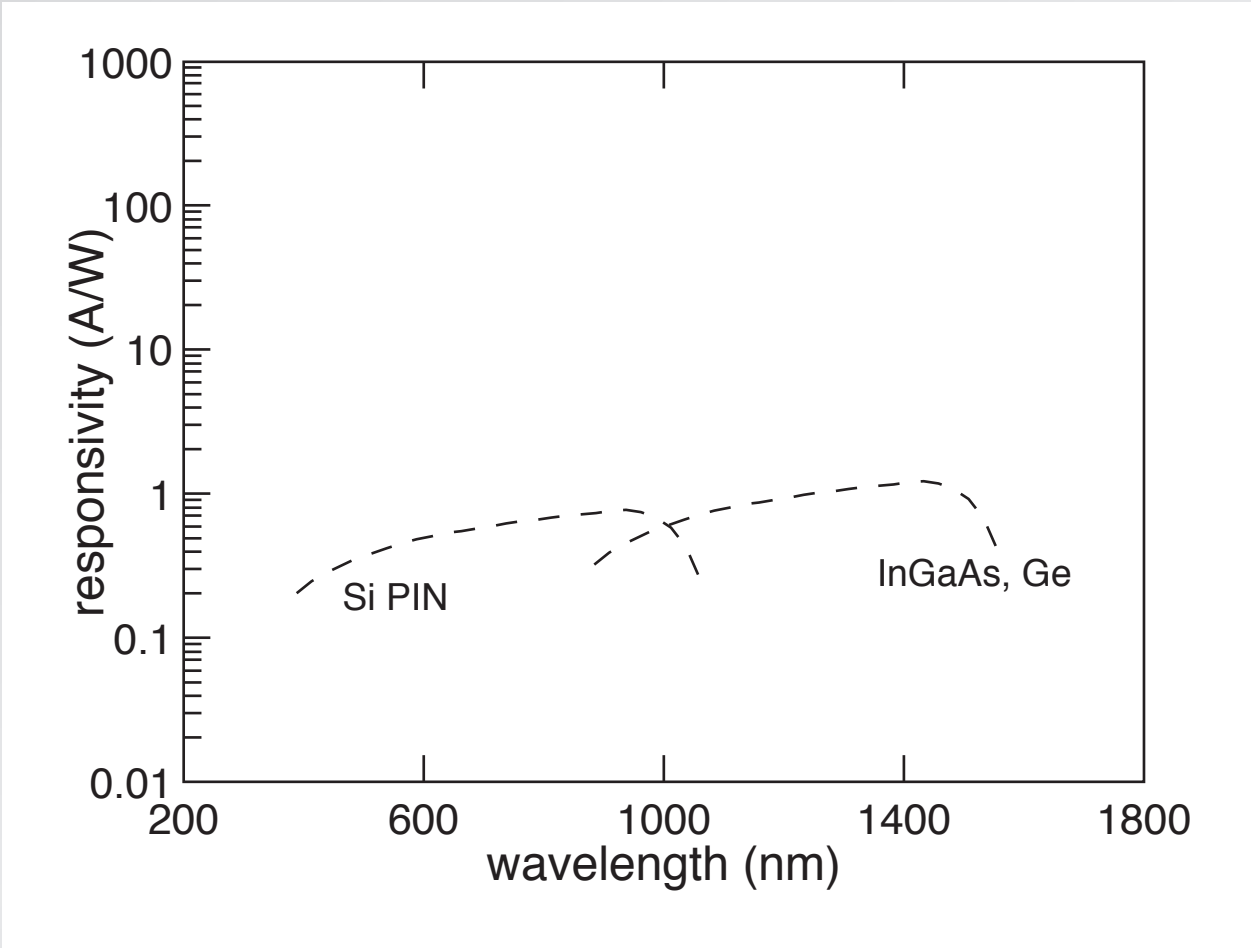

responsivity

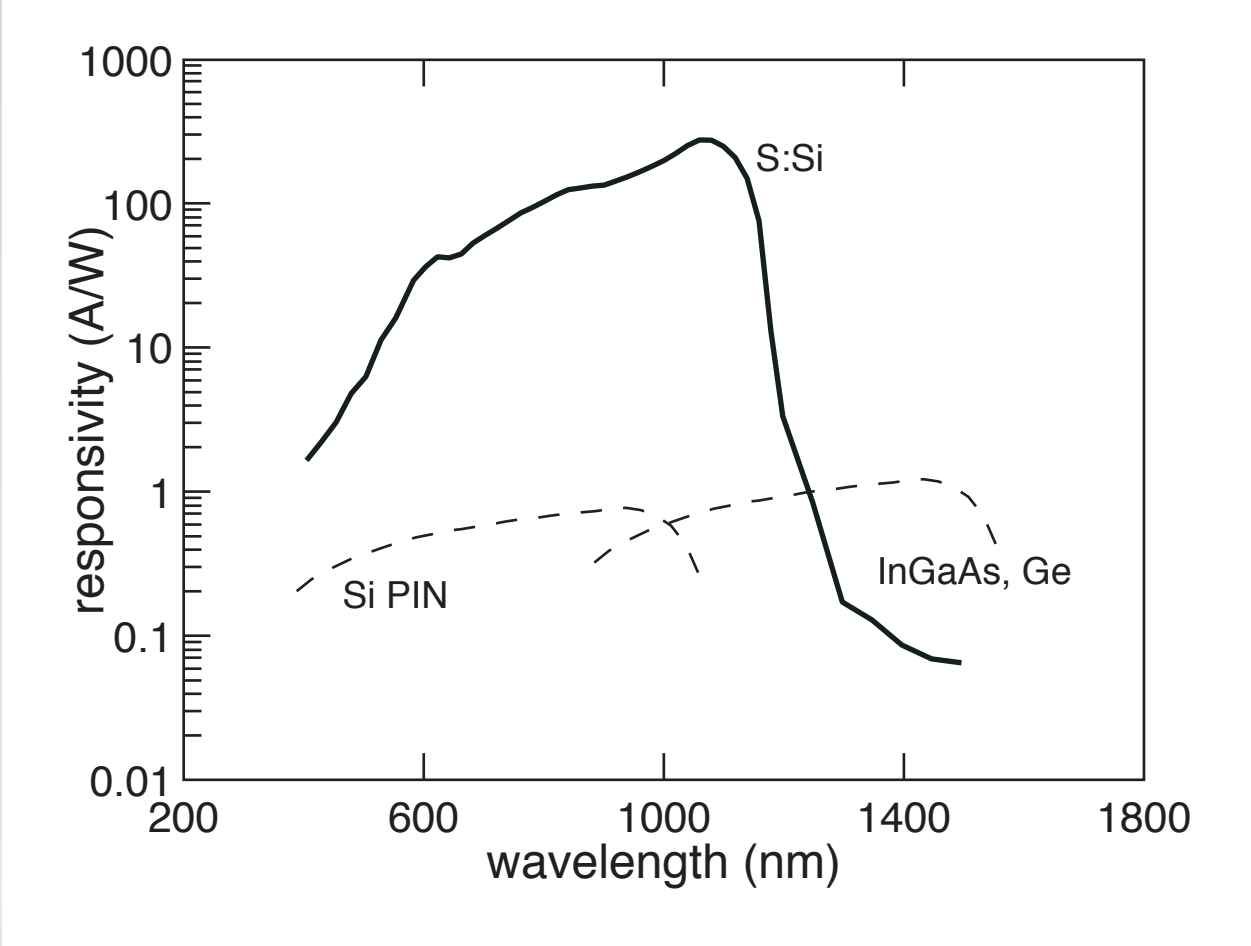

responsivity

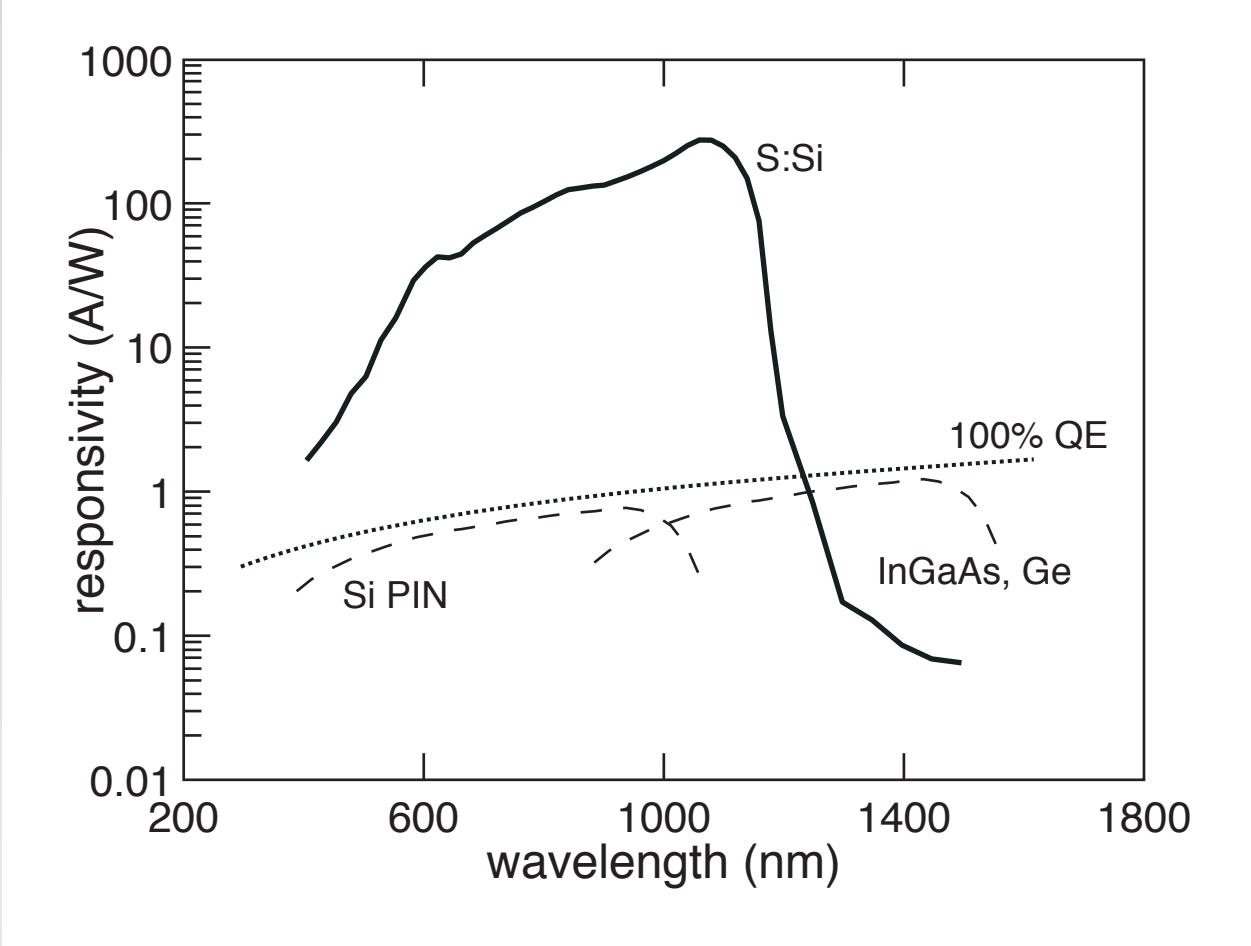

responsivity

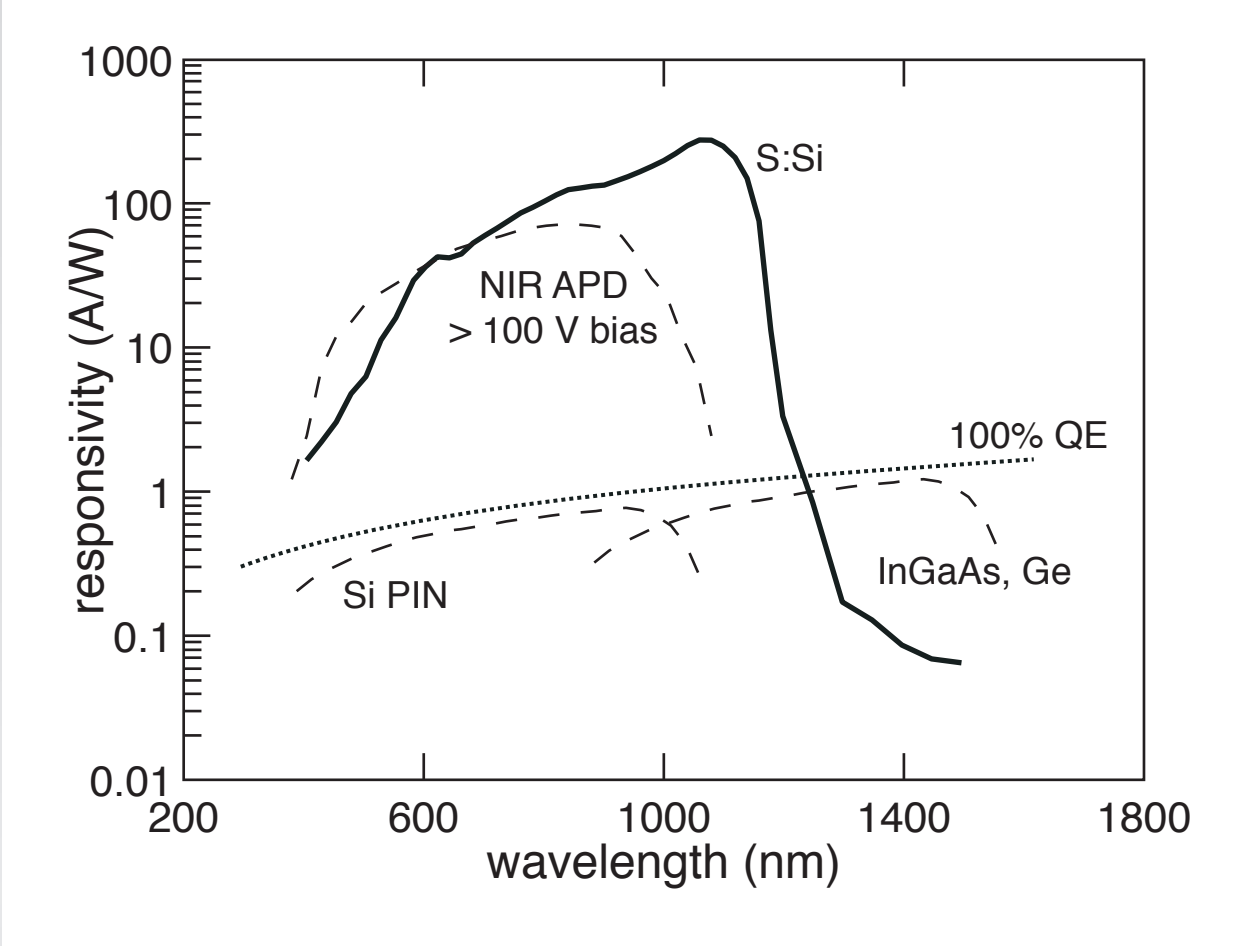

- enhanced sensitivity
- extended IR response

near-IR is next wave in imaging!

1 properties 2 intermediate band 3 devices

1 properties 2 intermediate band 3 devices

1 properties 2 intermediate band 3 devices

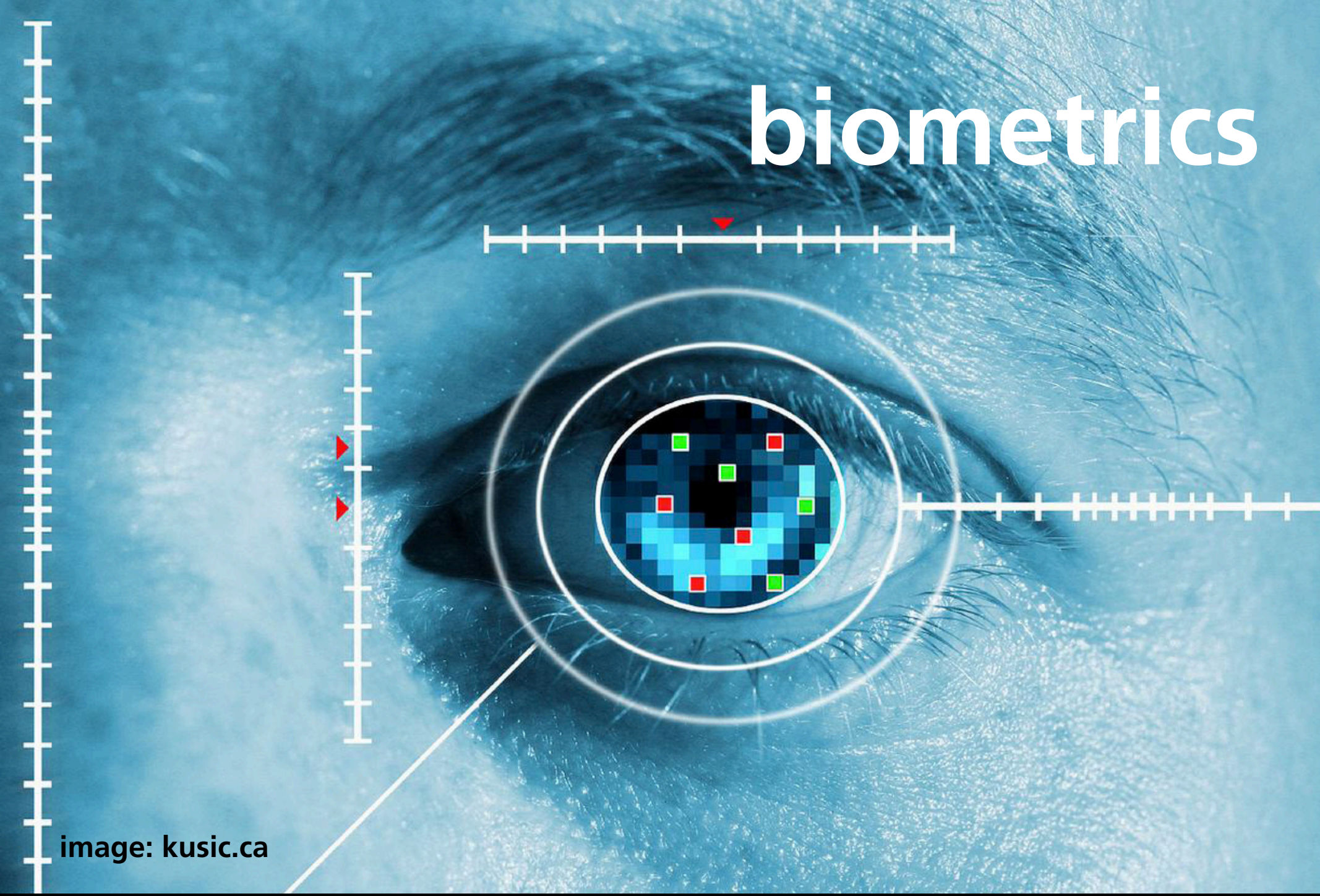

1 properties 2 intermediate band 3 devices

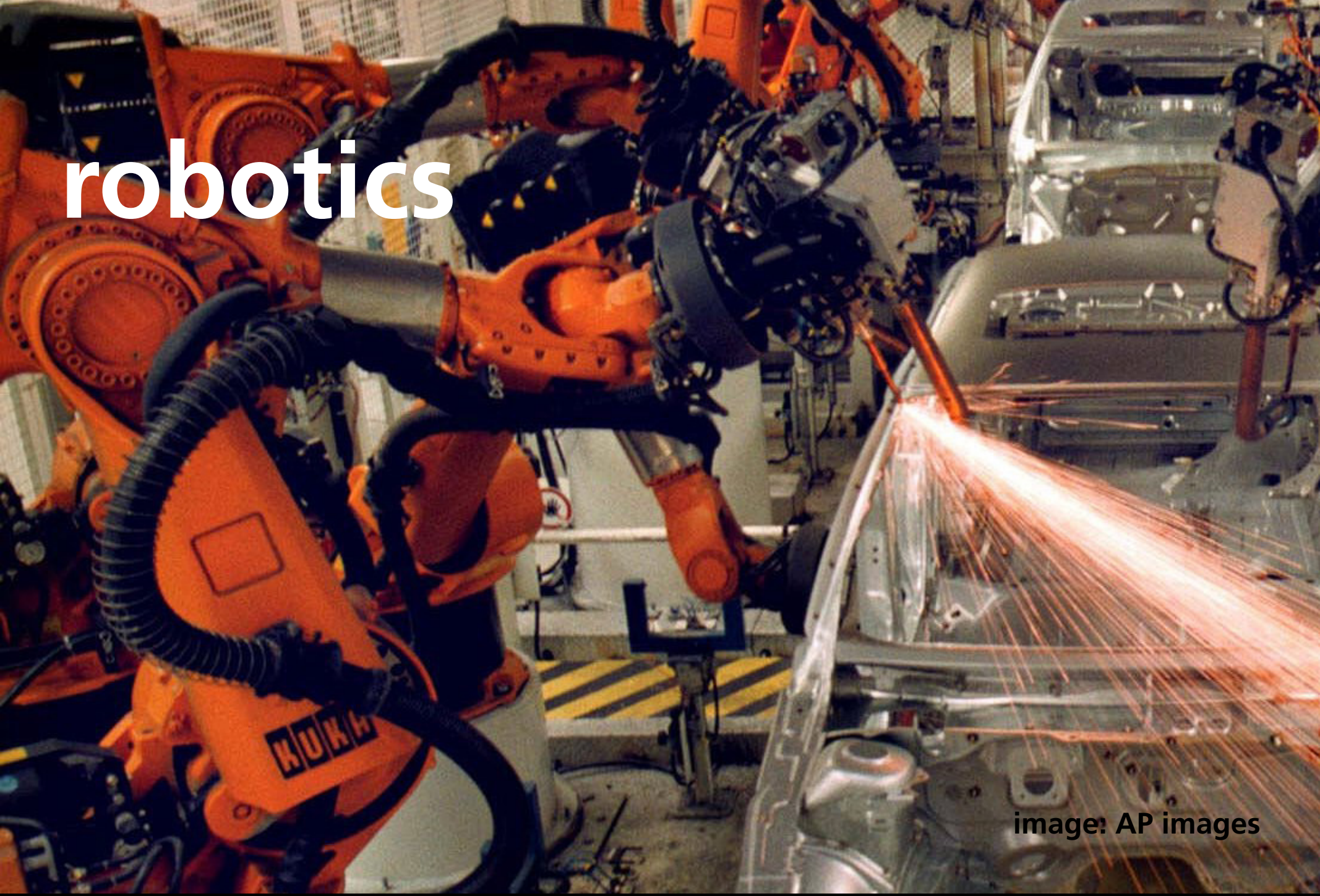

1 properties 2 intermediate band 3 devices

1 properties 2 intermediate band 3 devices

Combine state-of-the-art low-noise CMOS image

sensor design with enhanced quantum efficiency

US Patents: US 8,058,615; US 7,928,355; US 7,968,834

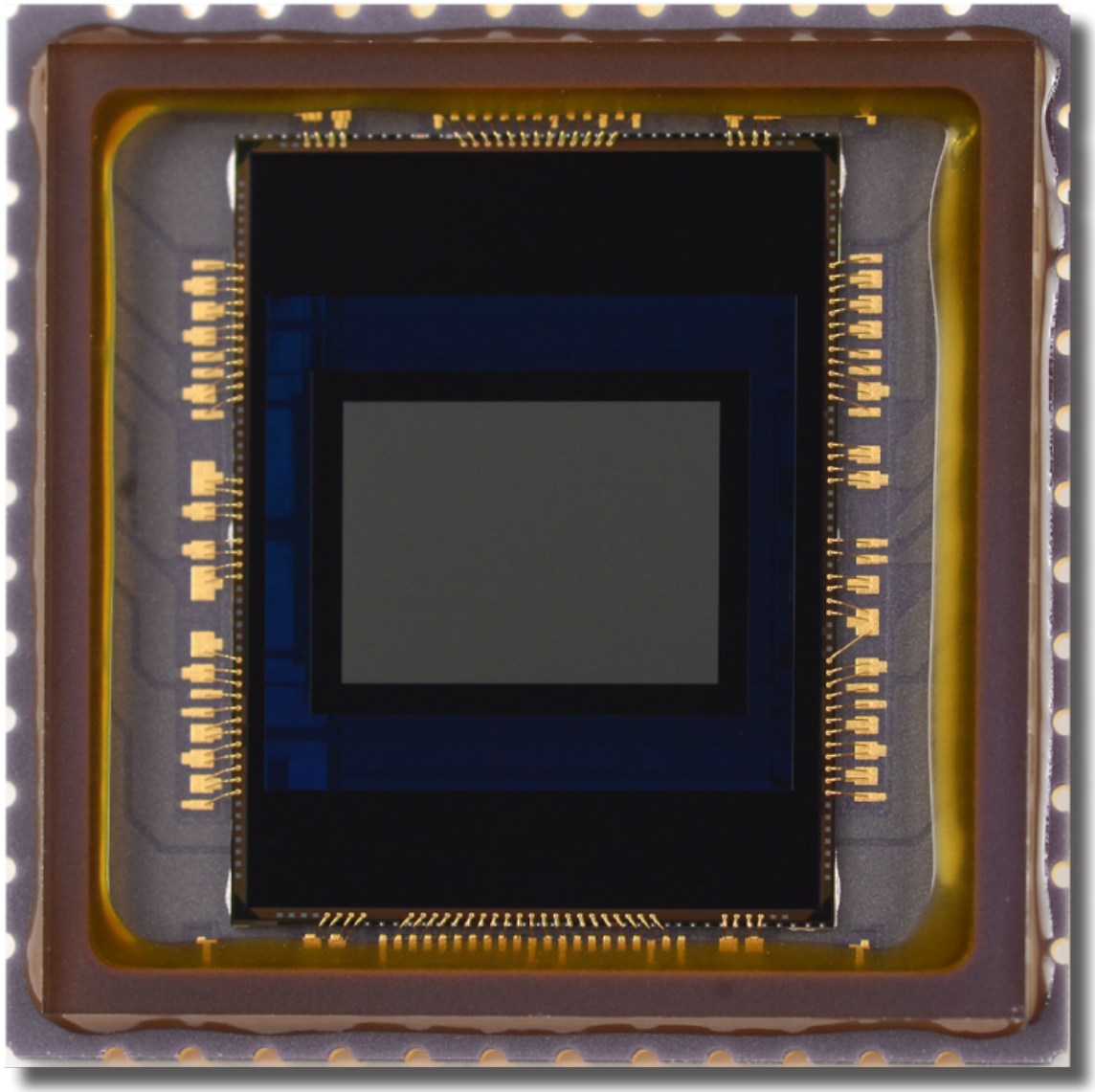

US Patents: US 8,058,615; US 7,928,355; US 7,968,834

SiOnyx

1 properties 2 intermediate band 3 devices

Resolution	pixel (μm)	noise (*e*/pix)	I_{dark} (*e*/pix/s)	*P* (mW)
872 x 654	5.6	2.1	24	300
1280 x 720	5.6	2.1	24	360
1280 x 1024	10	2.6	83	400

8” CIS process flow

4T pixel architecture

SiOnyx

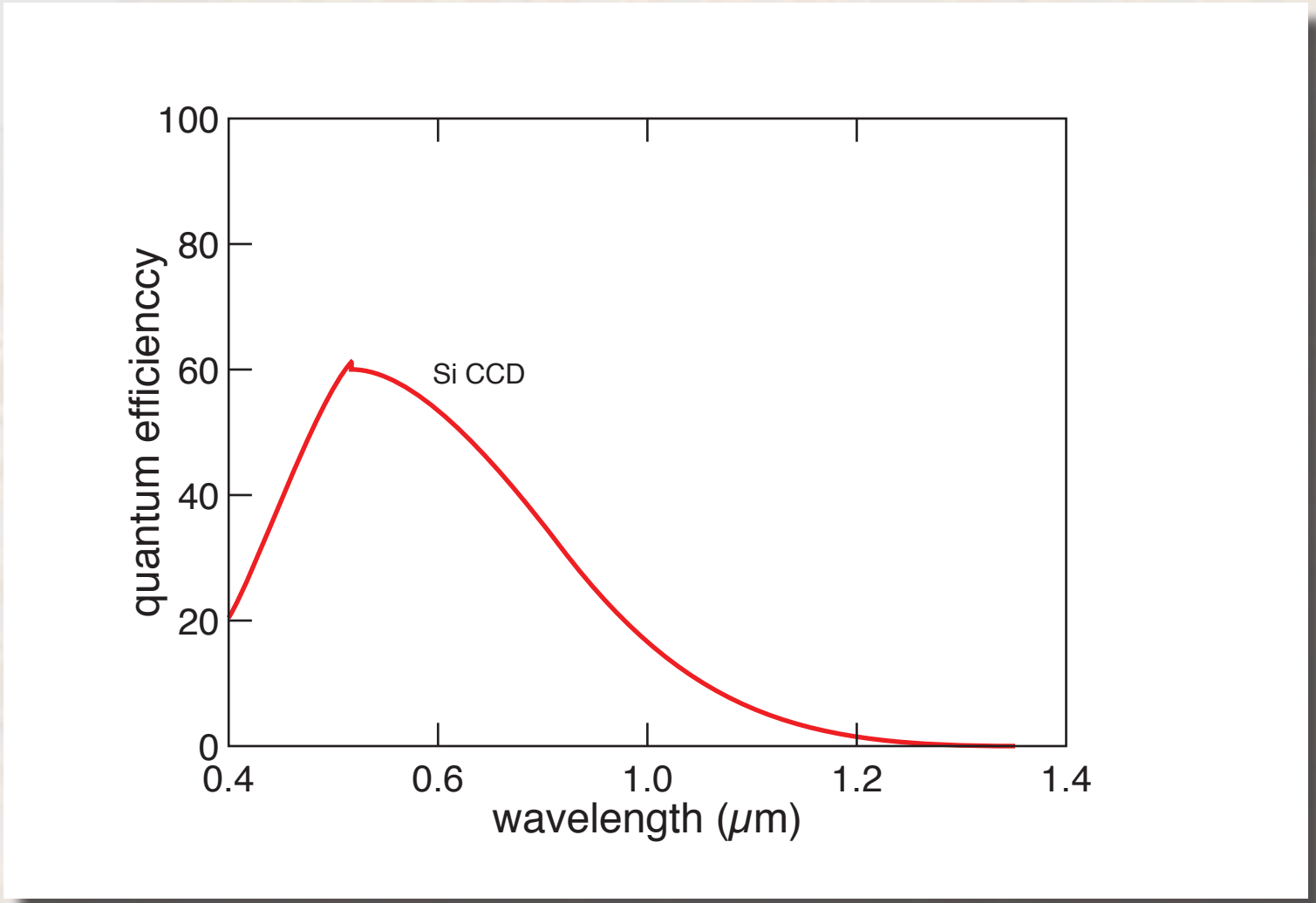
100
80
60
40
20
0
quantum efficienccy
Si CCD
0.4
0.6
1.0
1.2
1.4
wavelength (μm)

SiOnyx

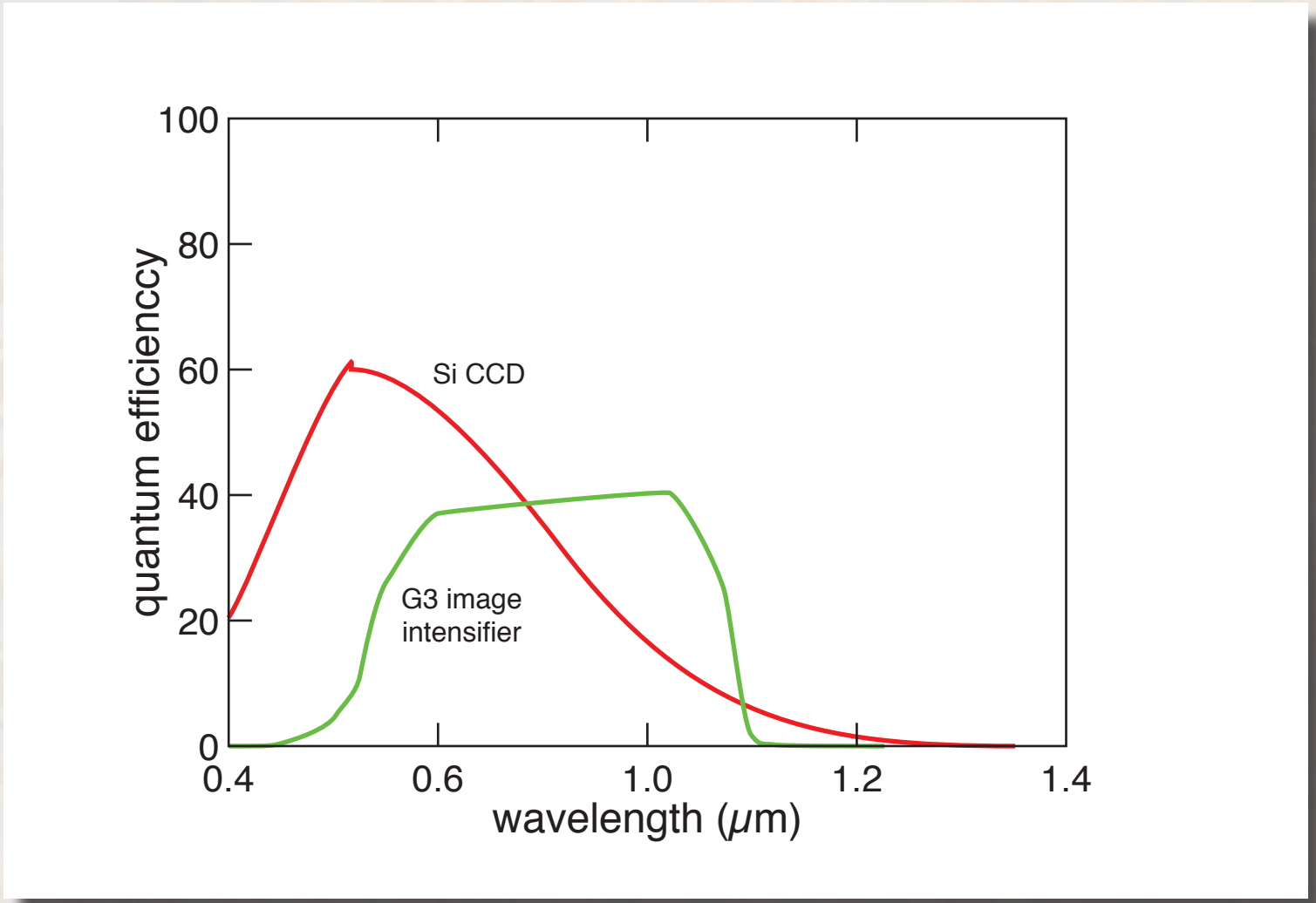
100
80
60
40
20
0
quantum efficienccy
Si CCD
G3 image
intensifier
0.4
0.6
1.0
1.2
1.4
wavelength (μm)

SiOnyx

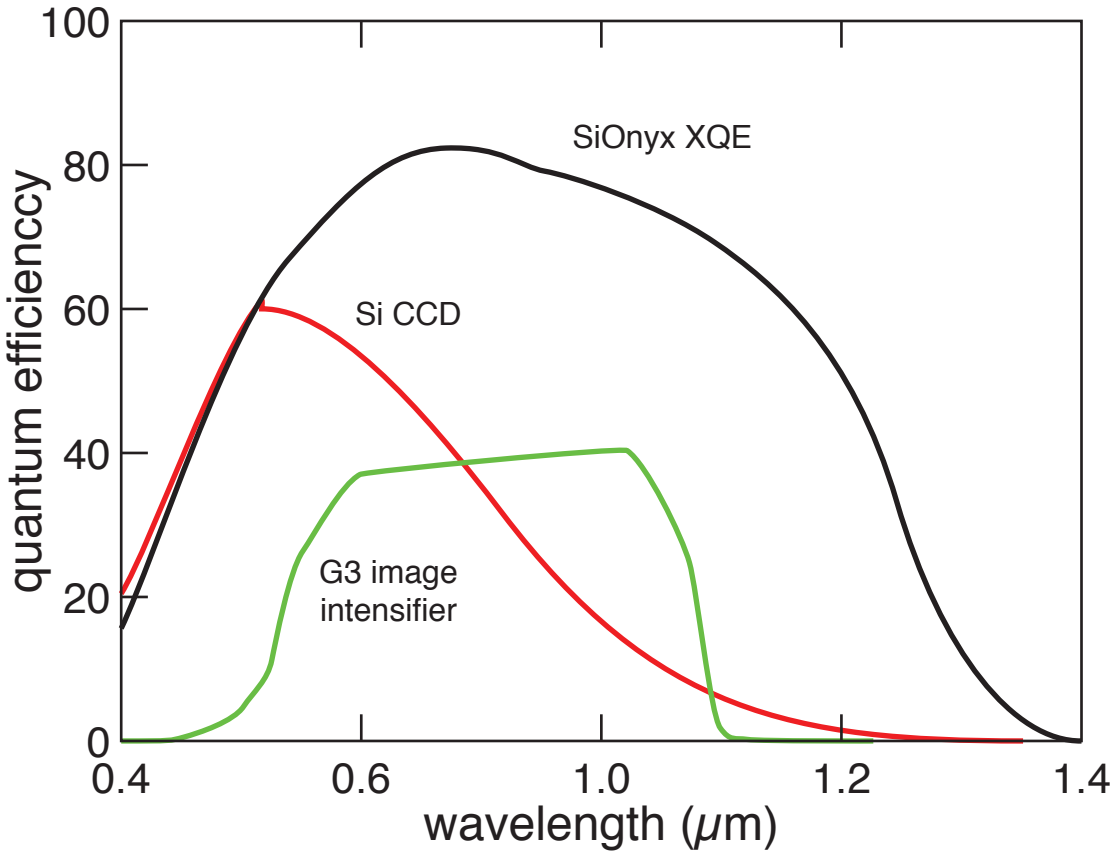
100
80
60
40
20
0
quantum efficienccy
SiOnyx XQE
Si CCD
G3 image
intensifier
0.4
0.6
1.0
1.2
1.4
wavelength (μm)

SiOnyx

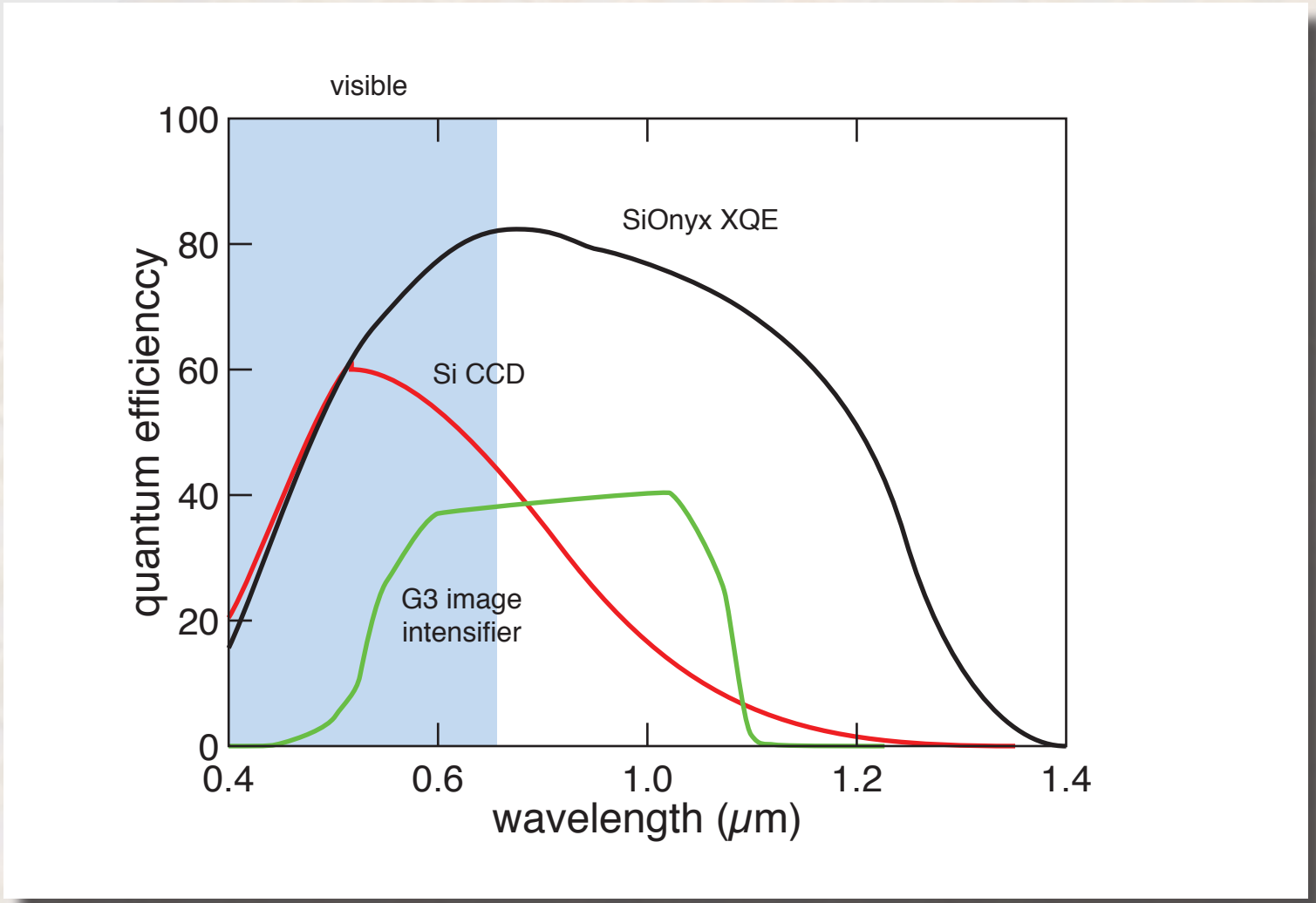
visible
100
80
60
40
20
0
quantum efficienccy
SiOnyx XQE
Si CCD
G3 image
intensifier
0.4
0.6
1.0
1.2
1.4
wavelength (μm)

SiOnyx

no compromises in visible

Sony color CCD

SiOnyx

no compromises in visible

Sony color CCD

SiOnyx XQE sensor

SiOnyx

1 properties 2 intermediate band 3 devices

90+ dB dynamic range

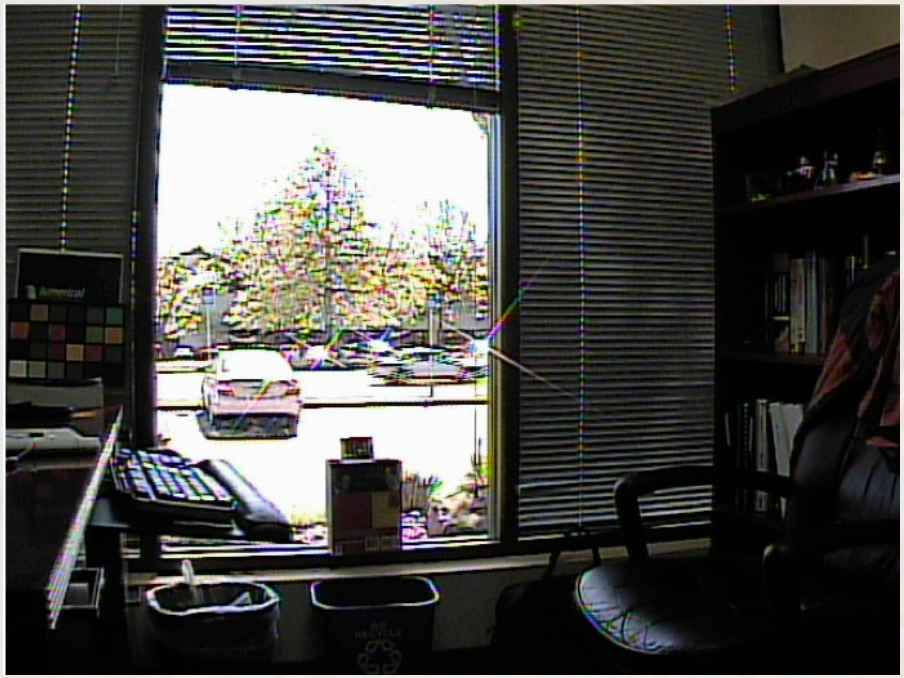

Sony color CCD

SiOnyx

90+ dB dynamic range

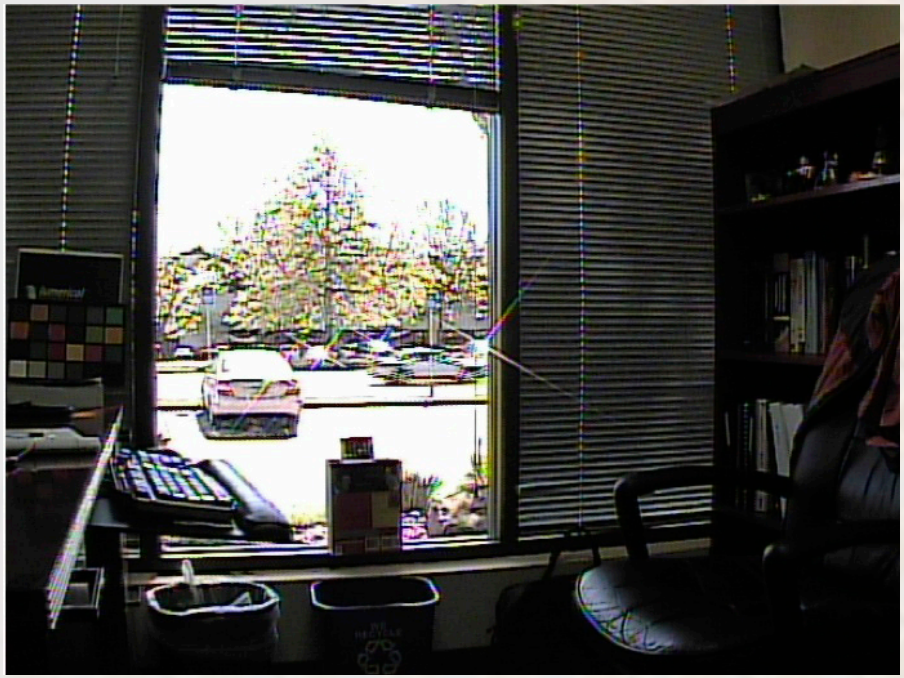

Sony color CCD

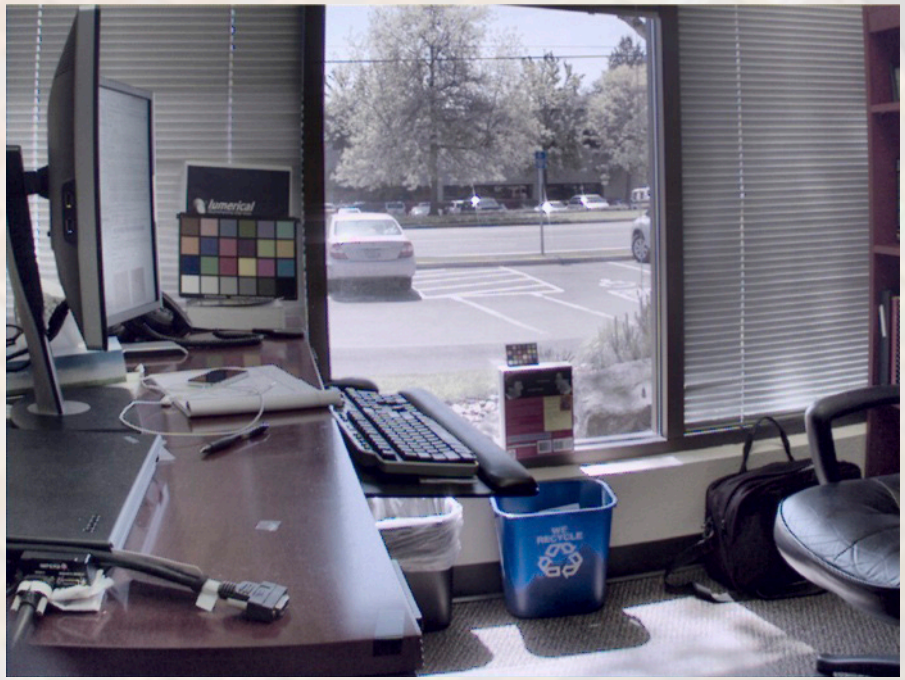

SiOnyx X1 sensor

SiOnyx

0.9 mlux irradiance from 2850 K source

SiOnyx (50 mm, F1.4, 30 fps)

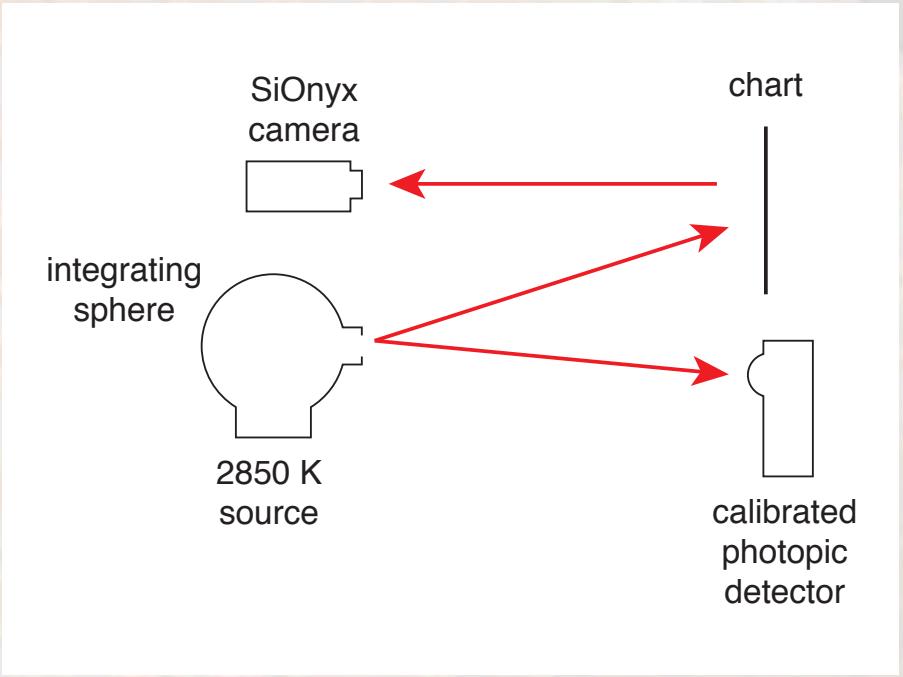

SiOnyx

1 properties 2 intermediate band 3 devices

0.9 mlux irradiance from 2850 K source

SiOnyx (50 mm, F1.4, 60 fps)

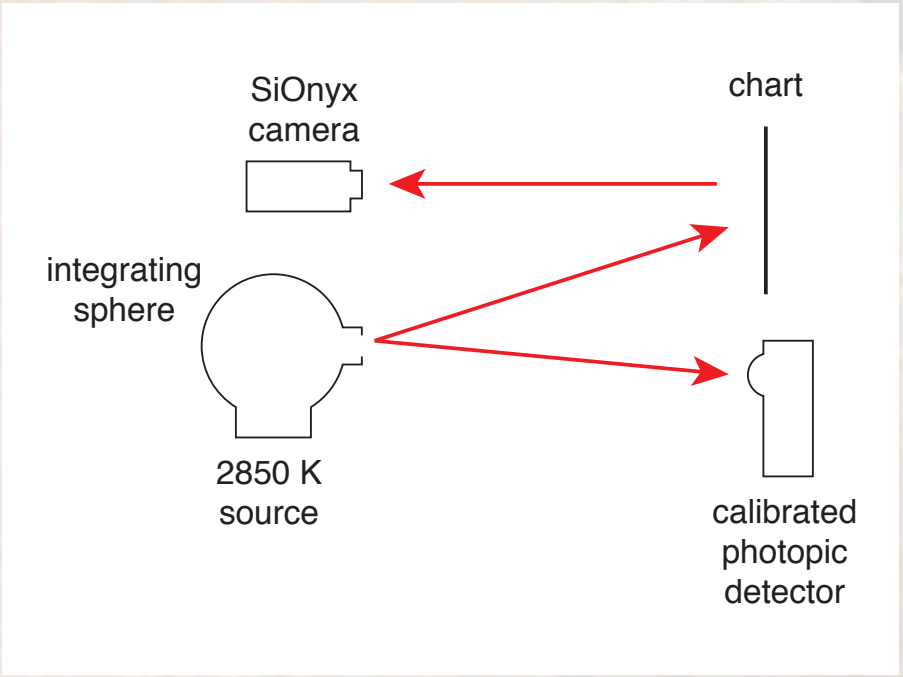

SiOnyx

1 properties 2 intermediate band 3 devices

0.9 mlux irradiance from 2850 K source

SiOnyx (50 mm, F1.4, 60 fps)

CCD (8 mm, F1.4, 60 fps)

SiOnyx

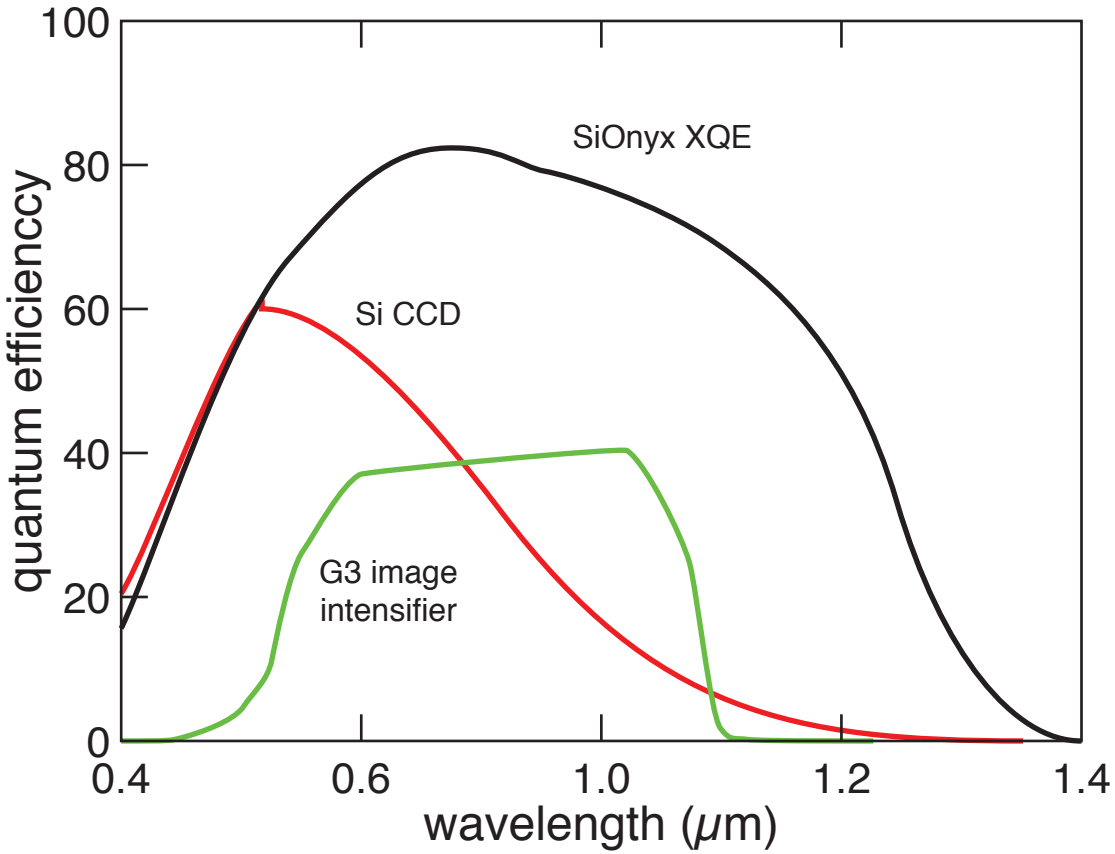
100
80
60
40
20
0
quantum efficienccy
SiOnyx XQE
Si CCD
G3 image
intensifier
0.4
0.6
1.0
1.2
1.4
wavelength (μm)

SiOnyx

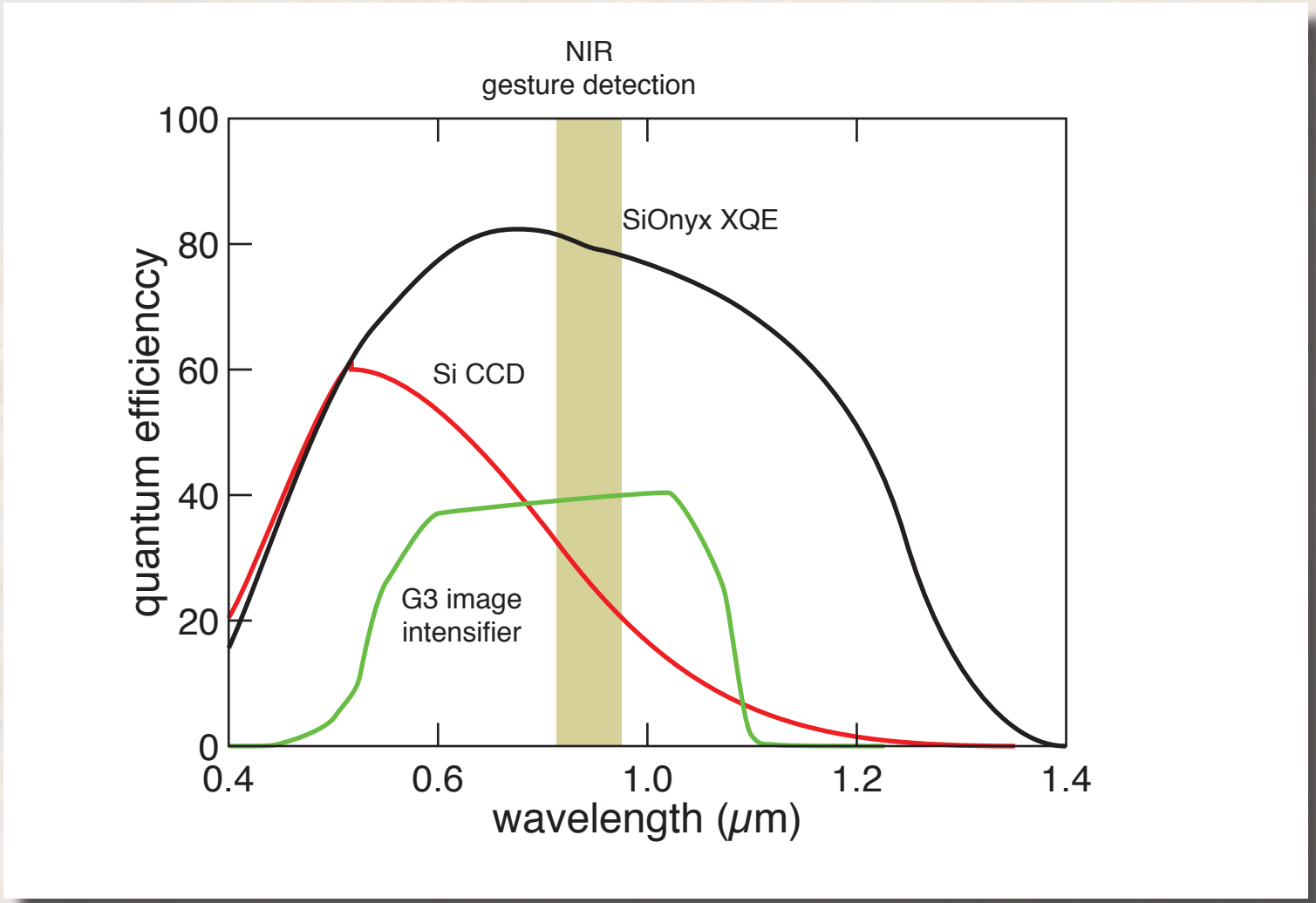

SiOnyx

1 properties 2 intermediate band 3 devices

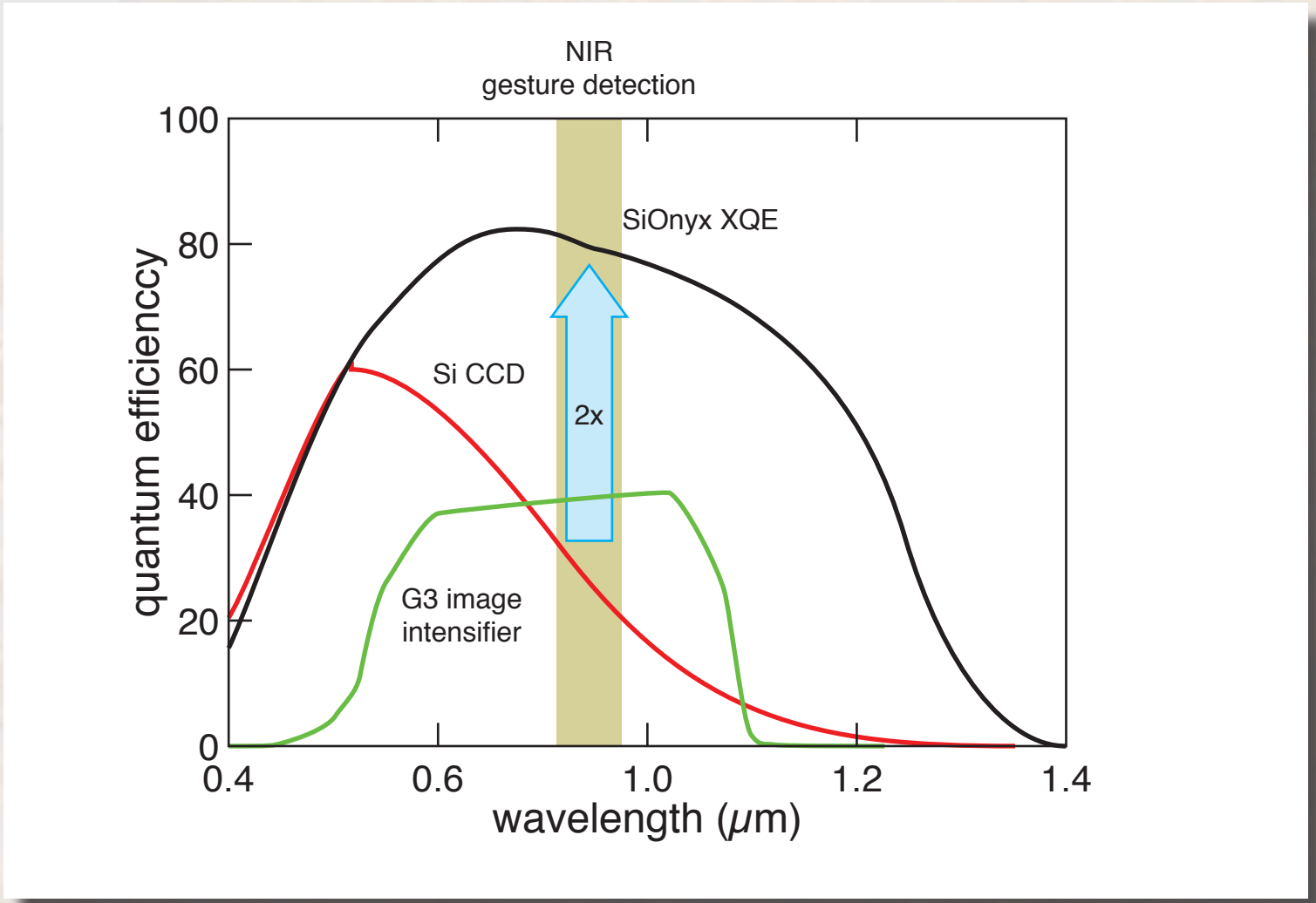

SiOnyx

1 properties 2 intermediate band 3 devices

3D imaging for gesture user interface (850 nm)

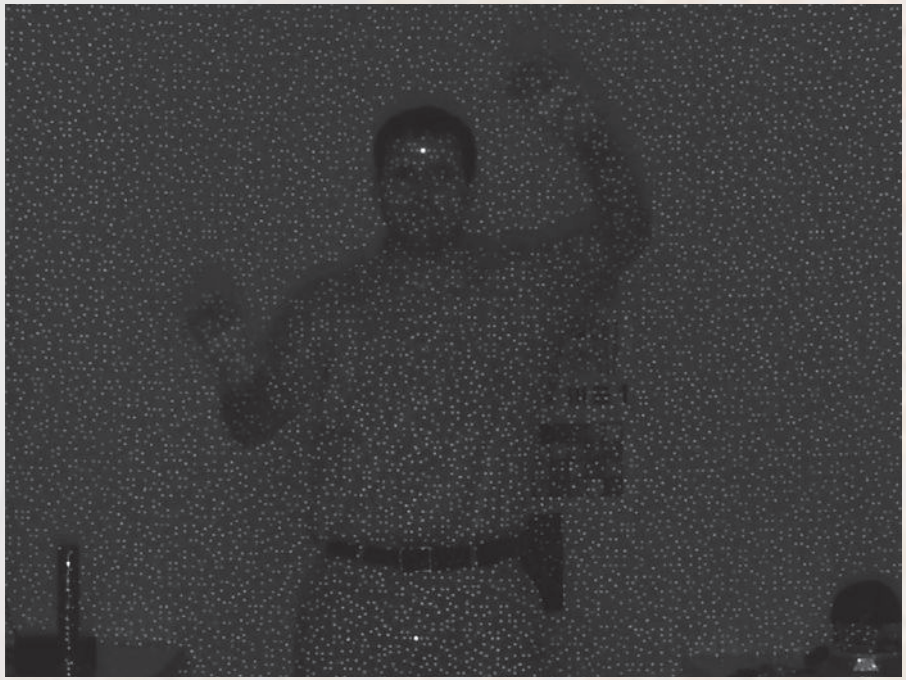

SiOnyx XQE

standard CCD

SiOnyx

1 properties 2 intermediate band 3 devices

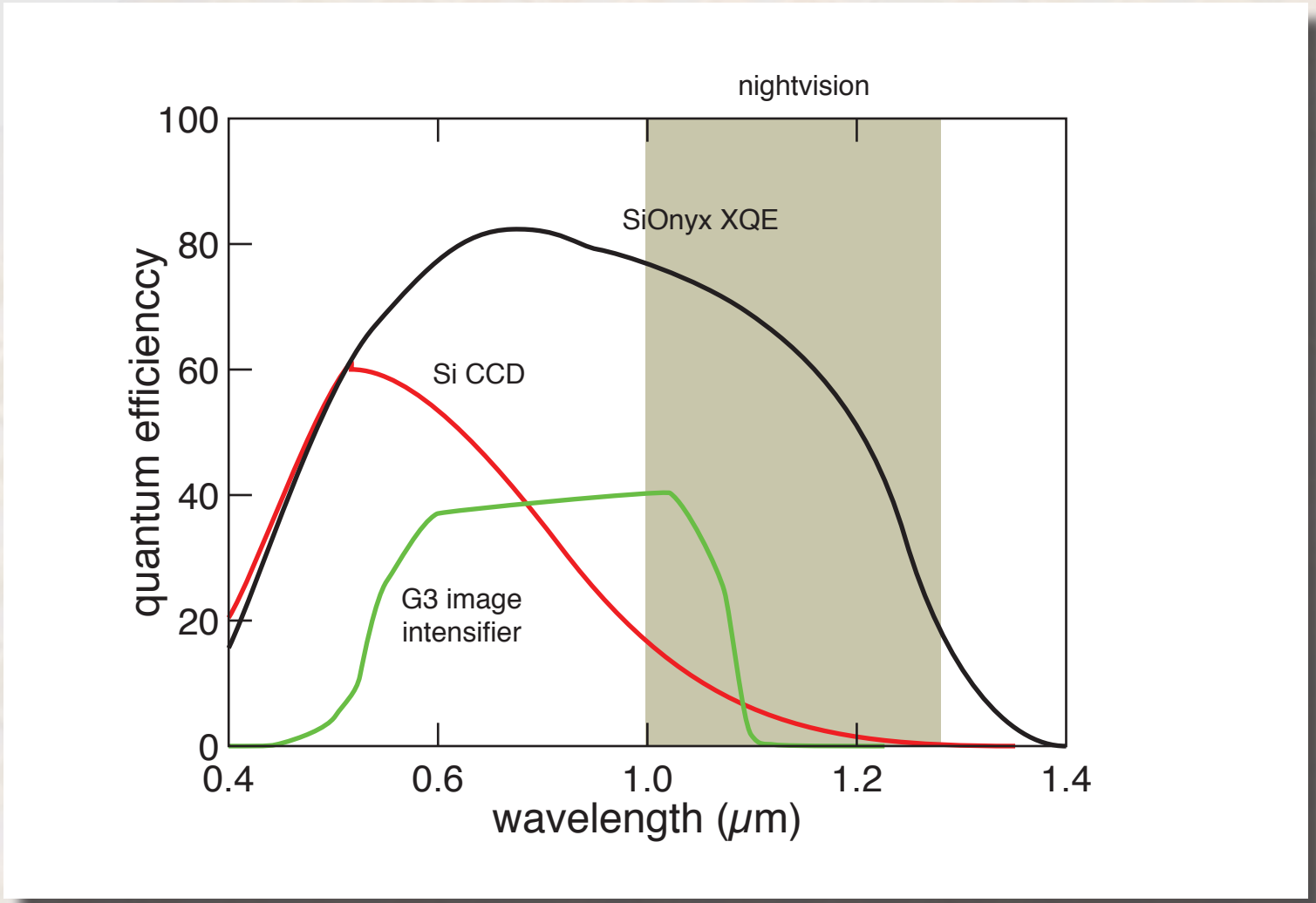
nightvision
100
80
60
40
20
0
quantum efficienccy
SiOnyx XQE
Si CCD
G3 image
intensifier
0.4
0.6
1.0
1.2
1.4
wavelength (μm)

SiOnyx

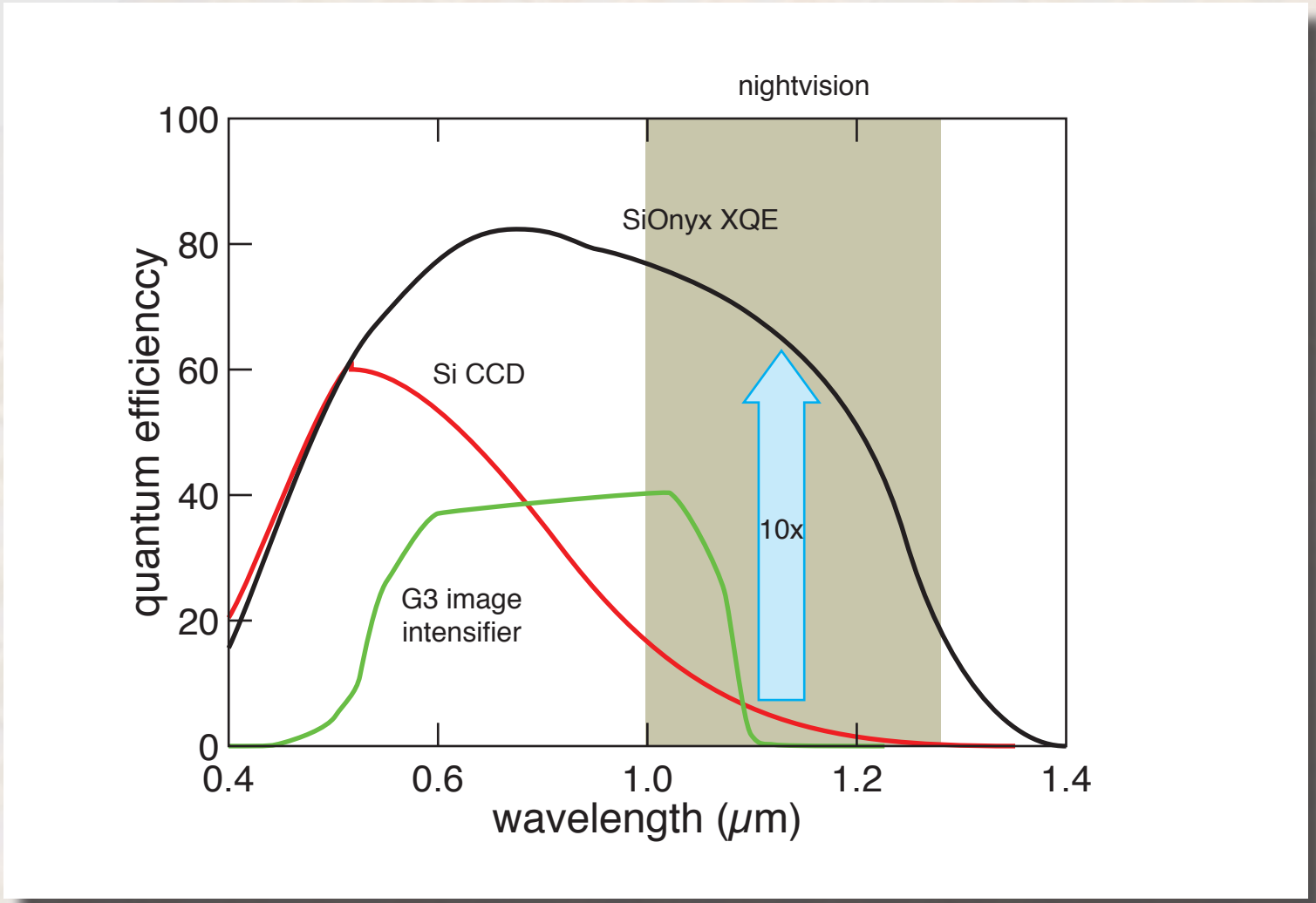
nightvision
100
80
60
40
20
0
quantum efficienccy
SiOnyx XQE
Si CCD
10x
G3 image
intensifier
0.4
0.6
1.0
1.2
1.4
wavelength (μm)

SiOnyx

dark room 1050 illumination

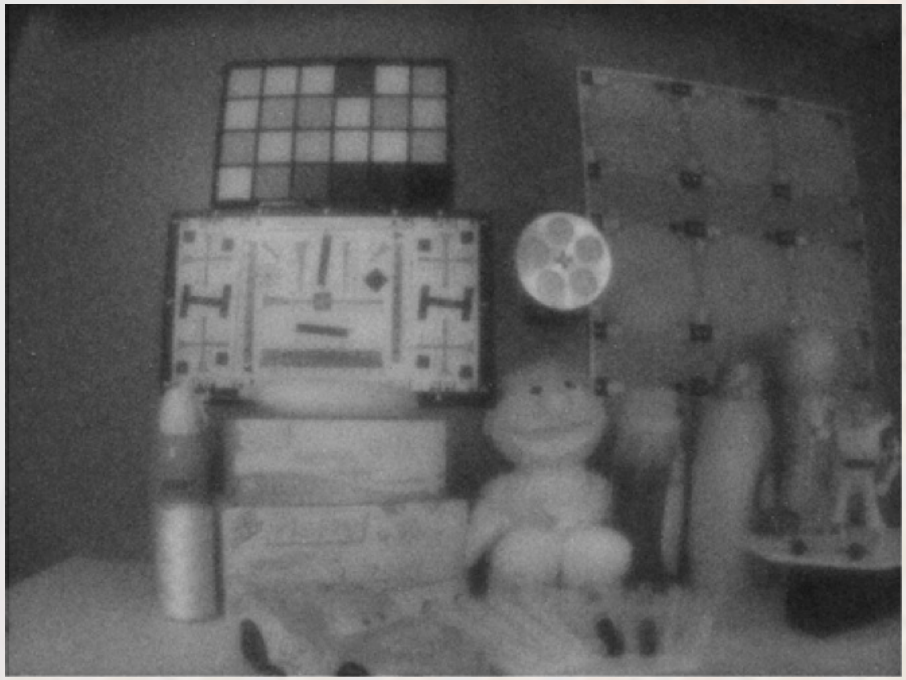

SiOnyx (F1.4, 33 ms, 24x)

SiOnyx

dark room 1050 illumination

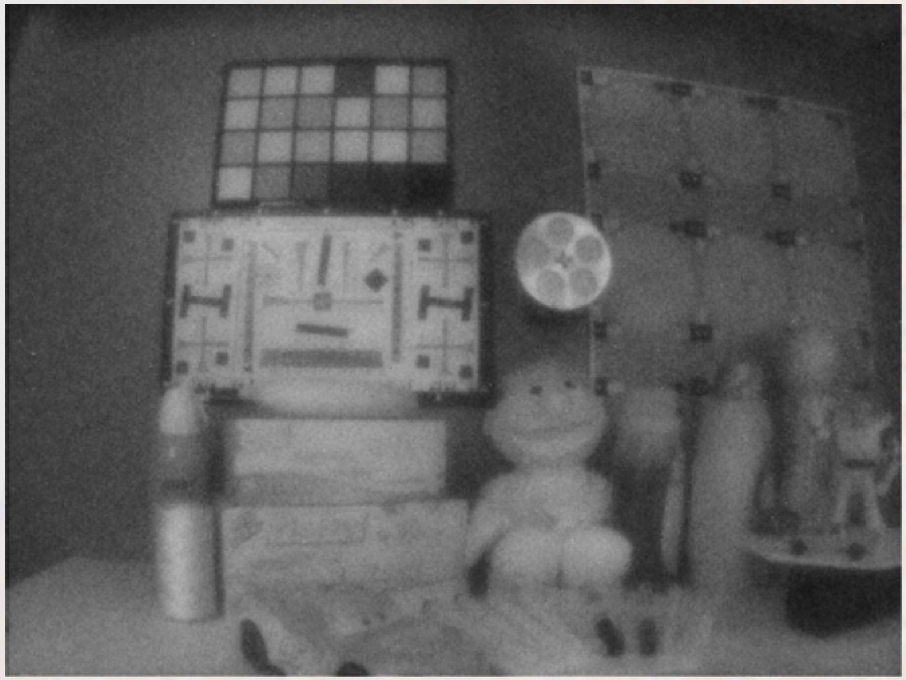

SiOnyx (F1.4, 33 ms, 24x)

reference (F1.4, 33 ms, 24x)

SiOnyx

dark room 1050 illumination

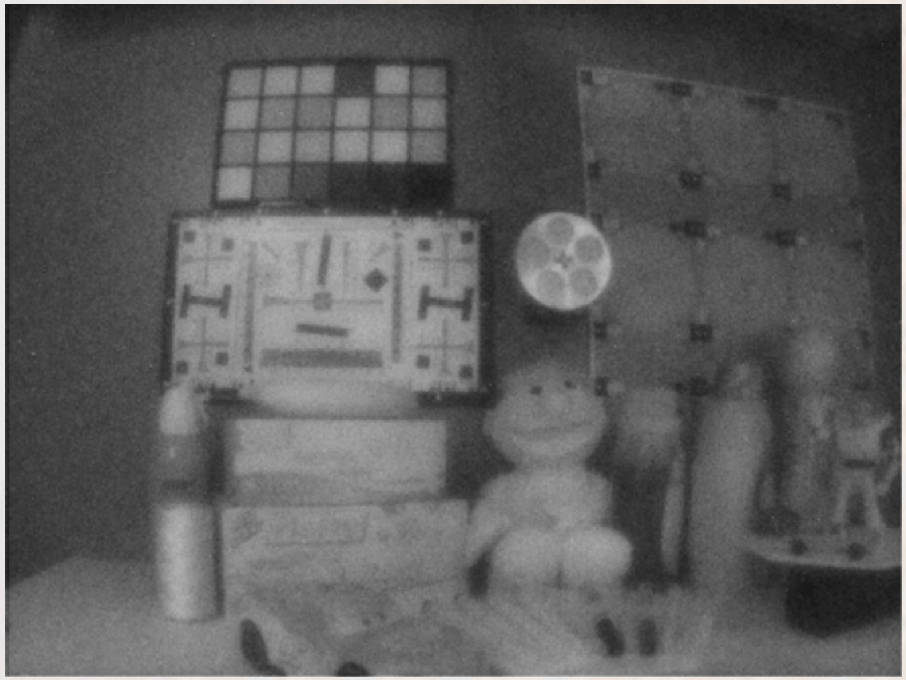

SiOnyx (F1.4, 33 ms, 24x)

reference (F1.4, 33 ms, 24x)

no image processing

SiOnyx

dark room 1050 illumination

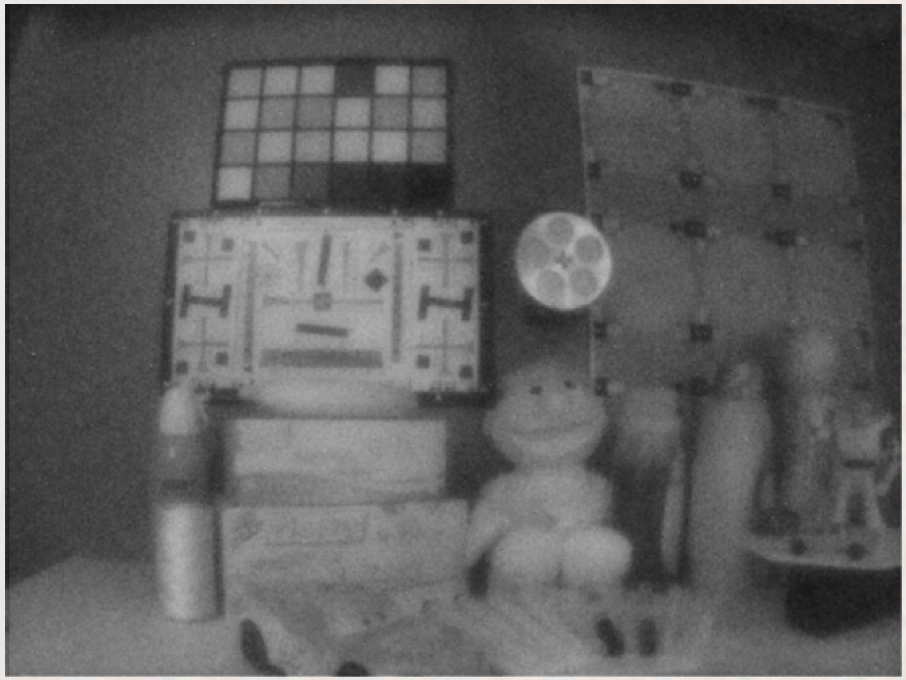

SiOnyx (F1.4, 33 ms, 24x)

reference (F1.4, 33 ms, 24x)
2x DIGITAL GAIN ADDED

no image processing

SiOnyx

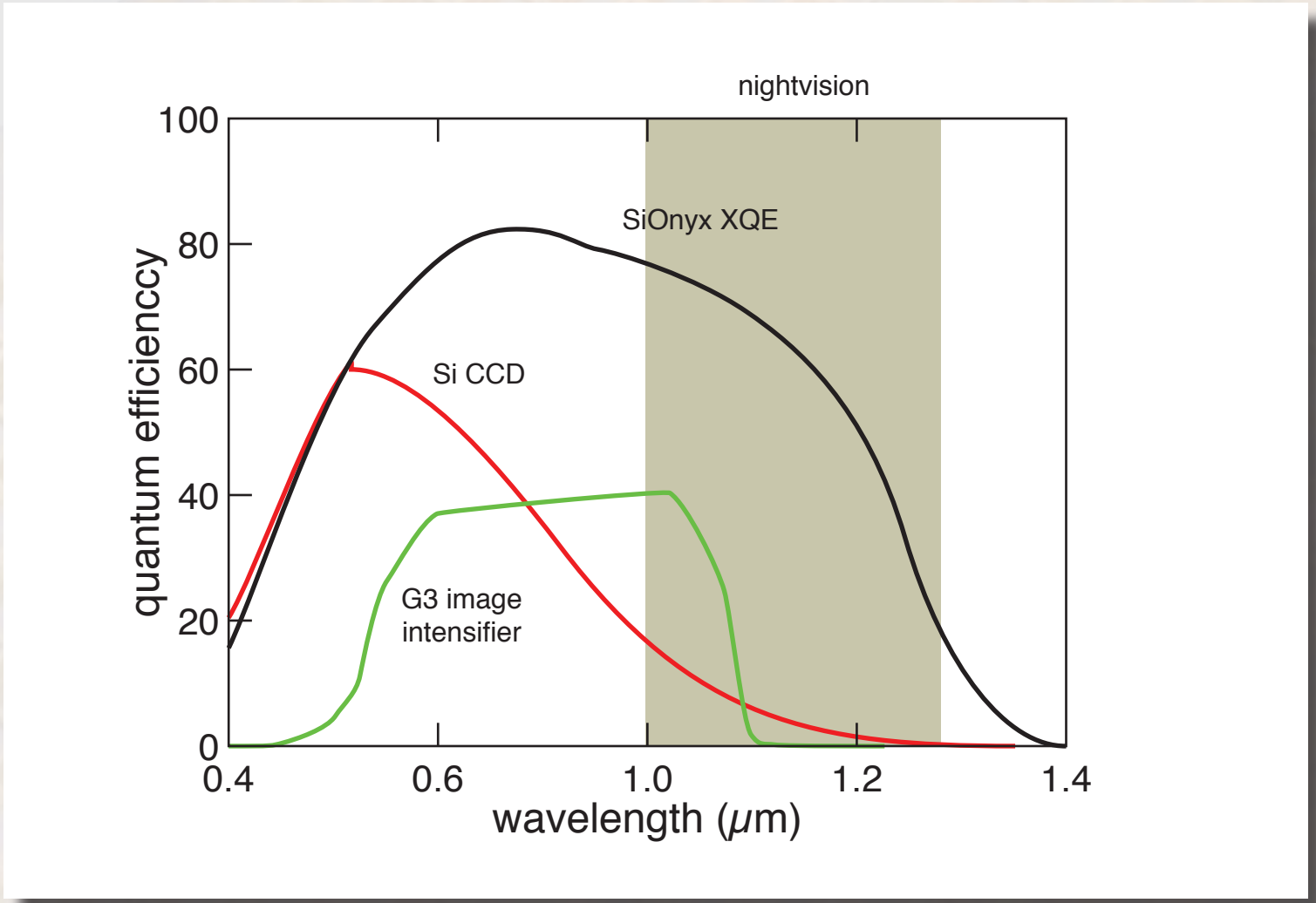
nightvision
100
80
60
40
20
0
quantum efficienccy
SiOnyx XQE
Si CCD
G3 image
intensifier
0.4
0.6
1.0
1.2
1.4
wavelength (μm)

SiOnyx

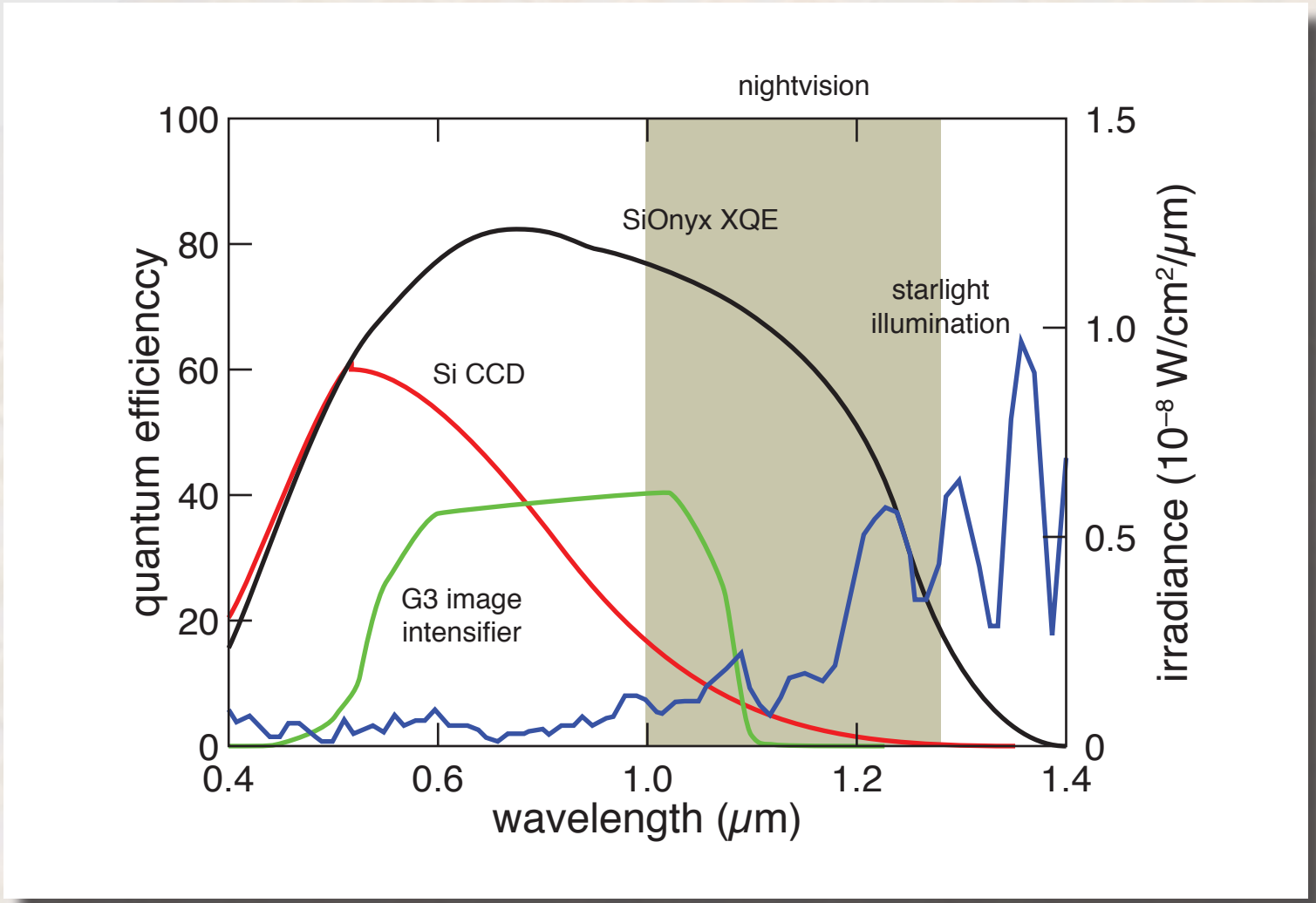
nightvision
100
80
60
40
20
0
quantum efficiency
1.5
1.0
0.5
0
irradiance (10^{-8} W/cm^2/μm)
SiOnyx XQE
starlight
illumination
Si CCD
G3 image
intensifier
0.4
0.6
1.0
1.2
1.4
wavelength (μm)

SiOnyx

starlight illumination

SiOnyx
25 mm
F1.4
30 fps

clear, moonless night (laser targeting spot: 30 µJ at 100 m)

SiOnyx

solar spectrum

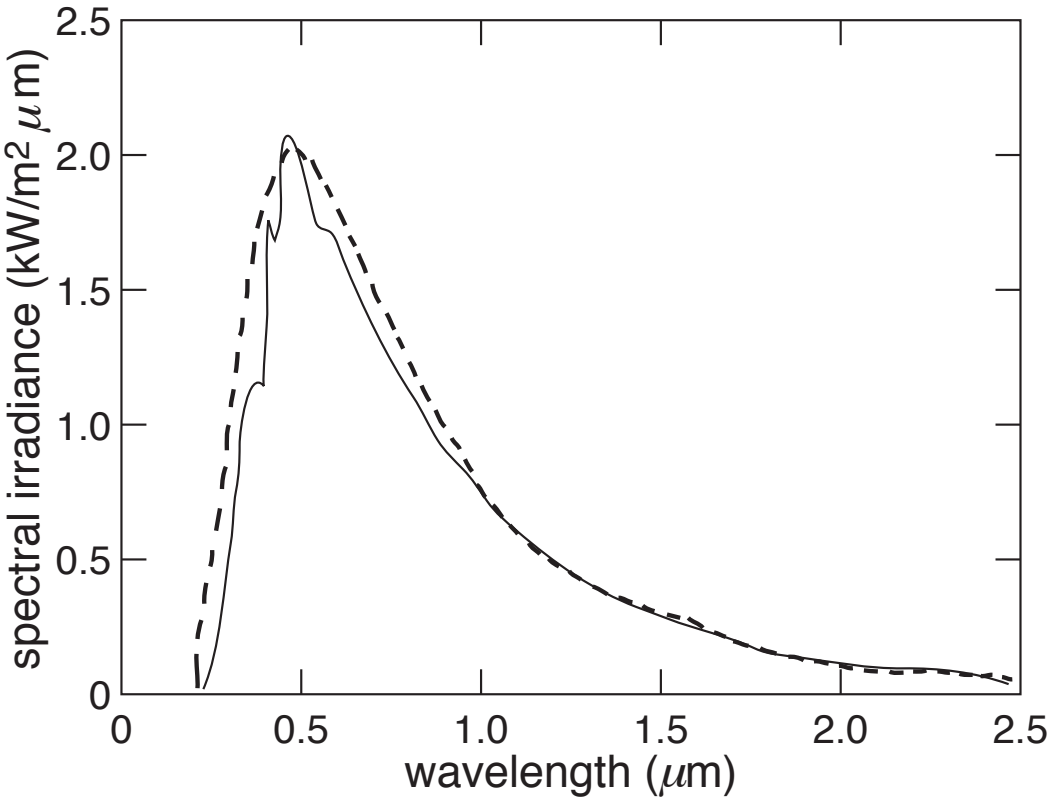

solar spectrum

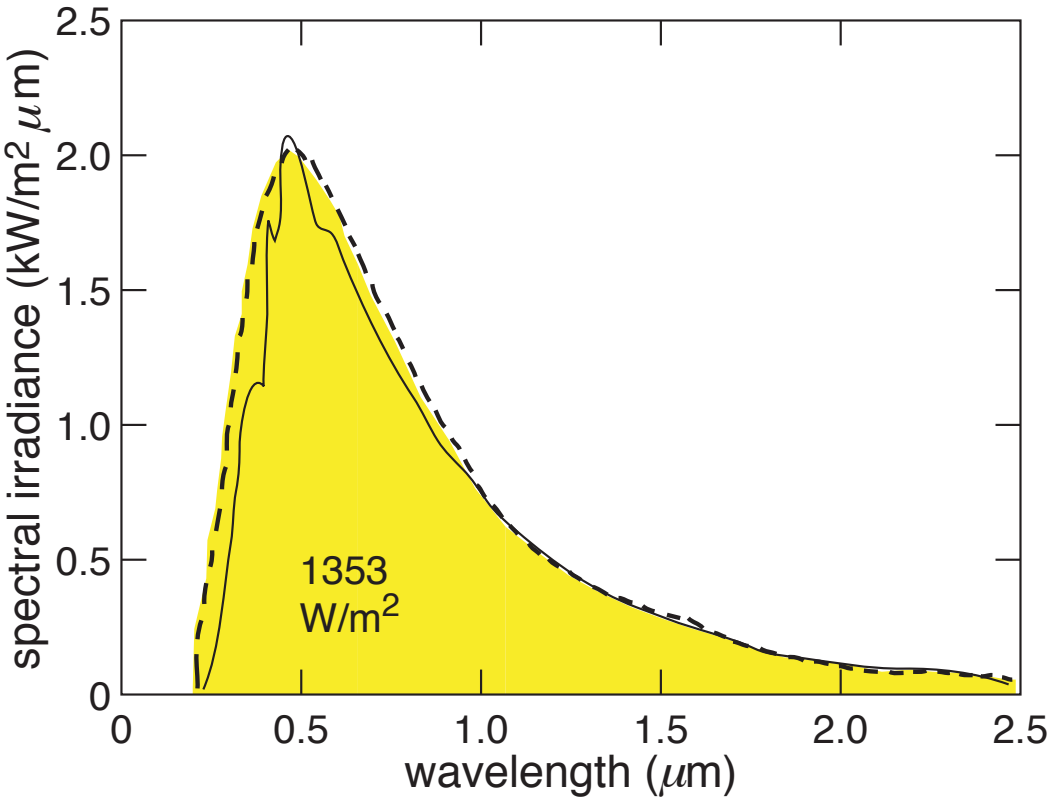

crystalline silicon: transparent to 23% of solar radiation

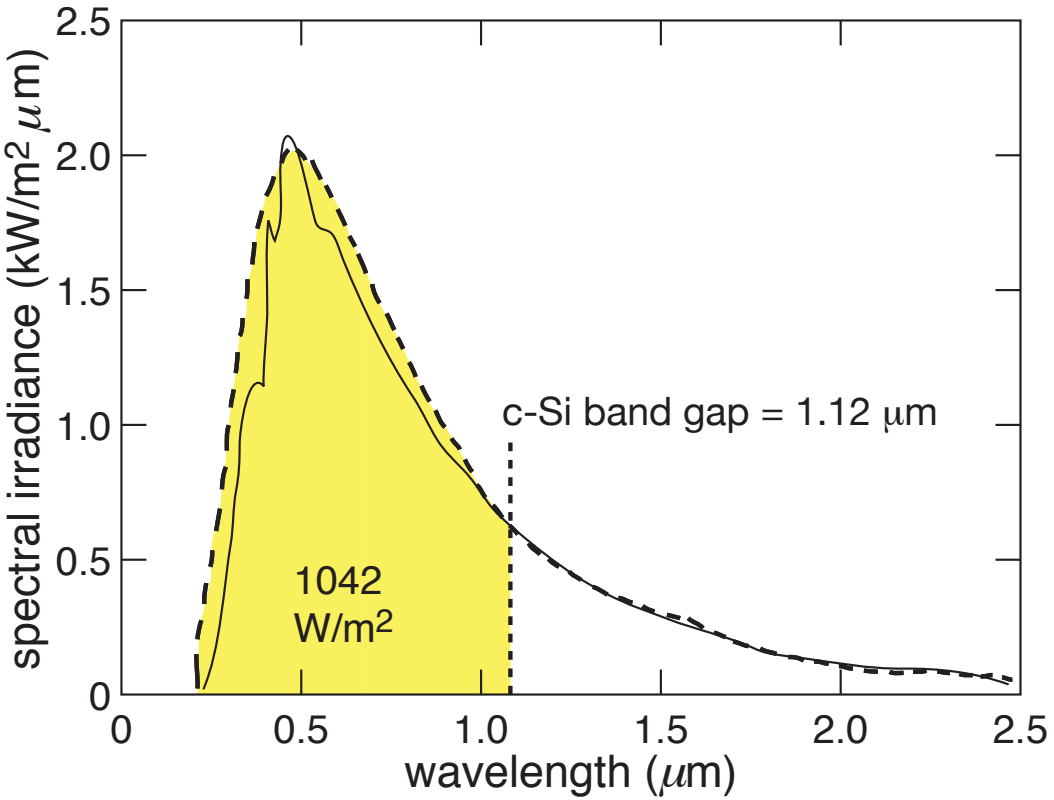

amorphous silicon: transparent to 53% of solar radiation

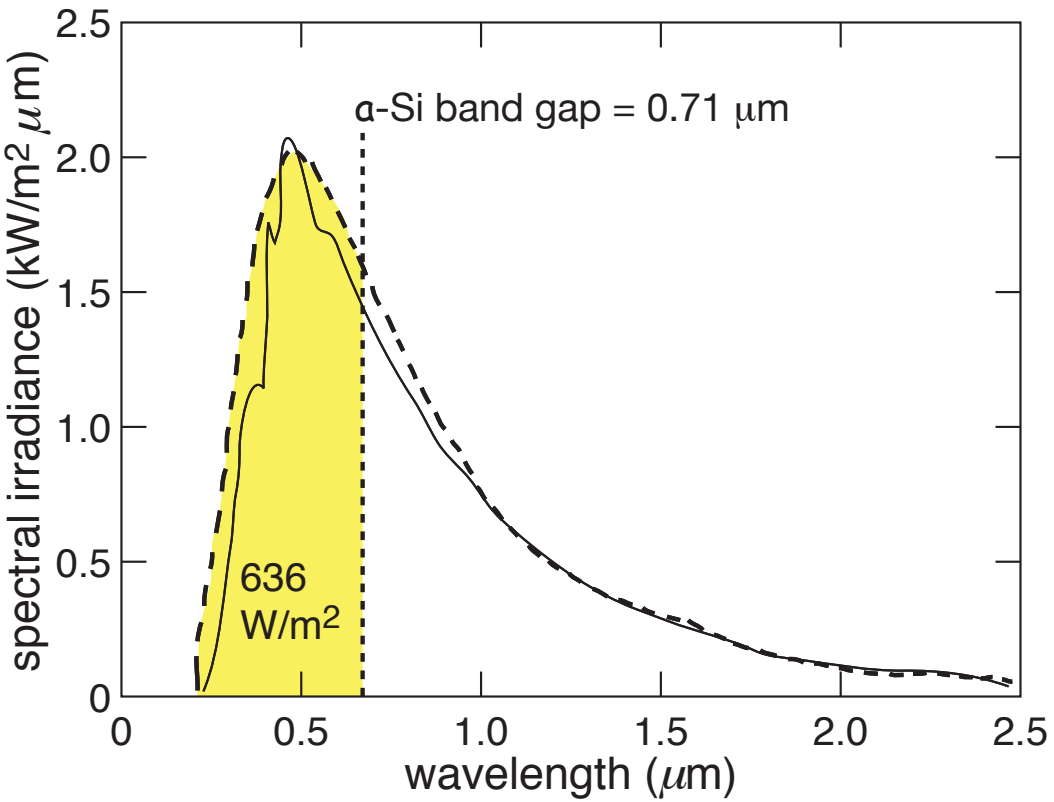

black silicon: potential to recover transmitted energy

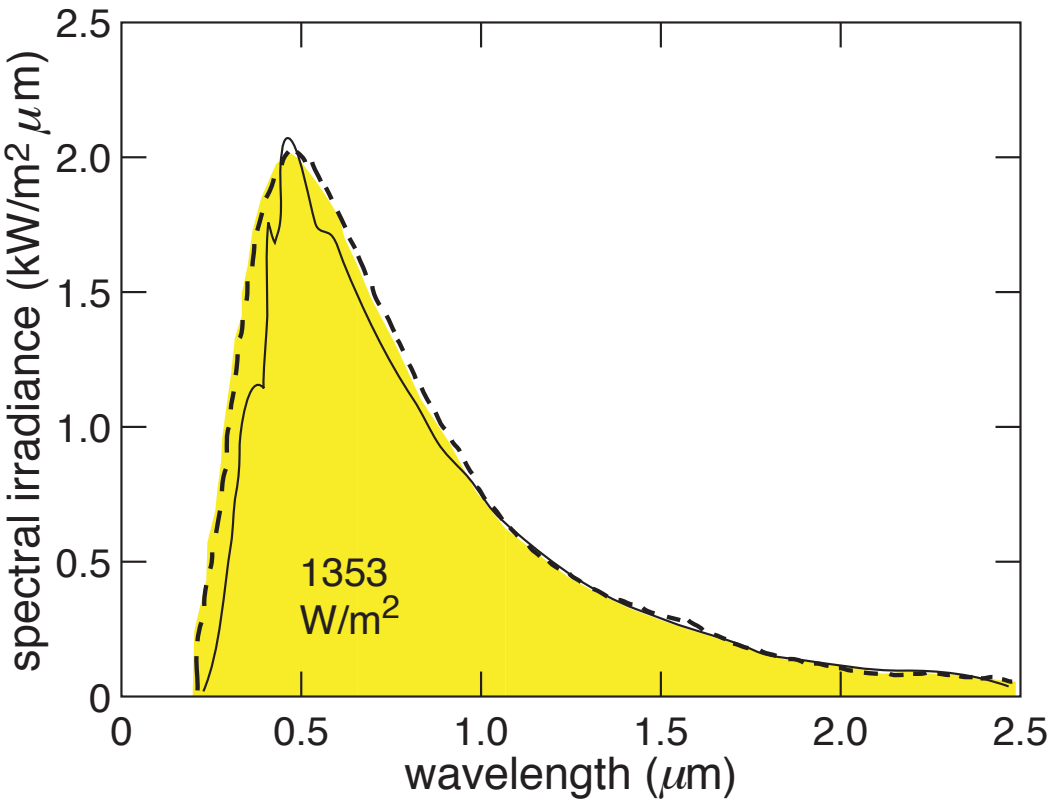

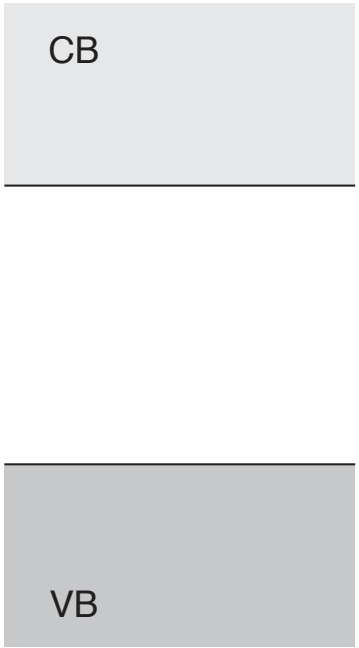
CB
VB

photon with gap energy

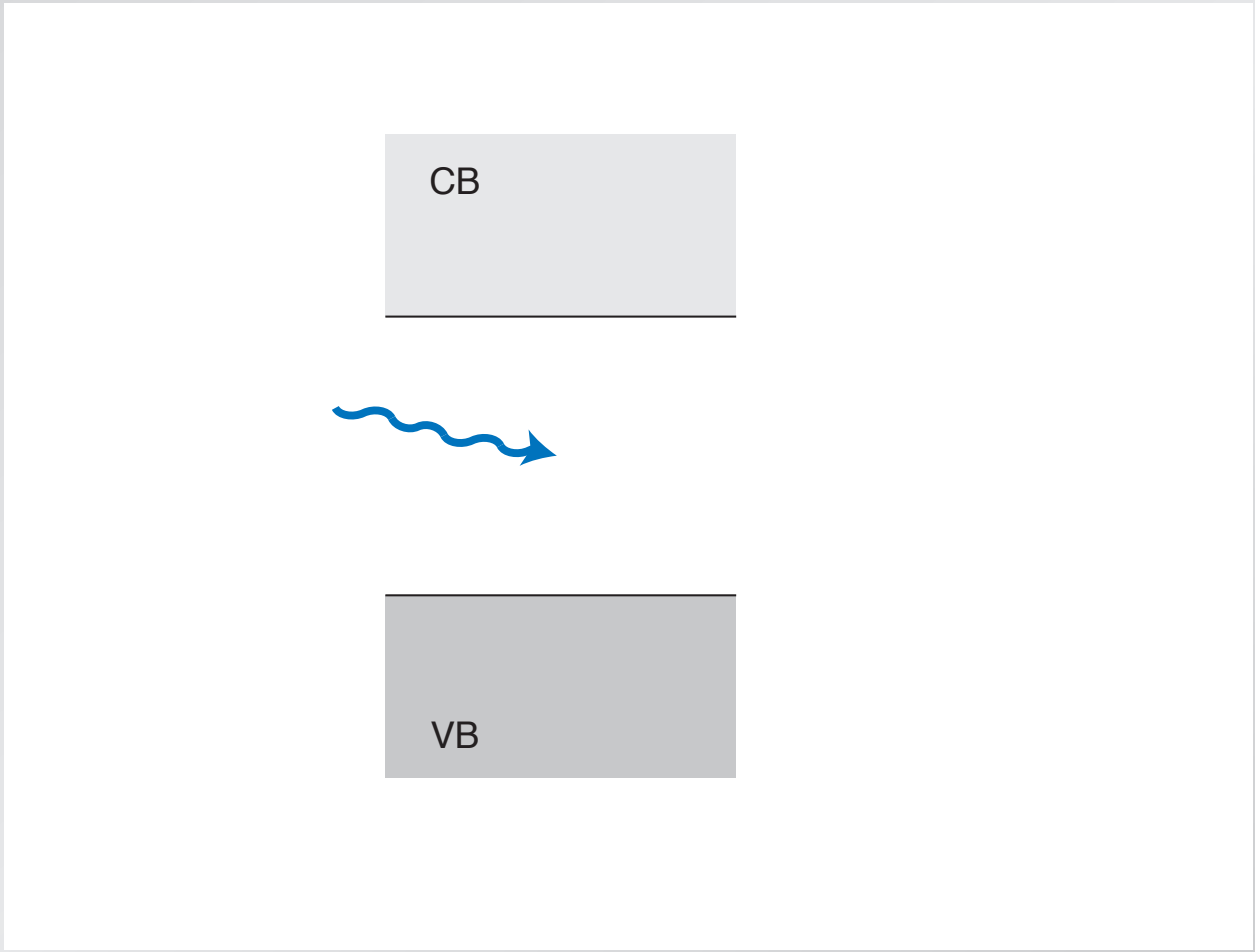

photon creates electron-hole pair…

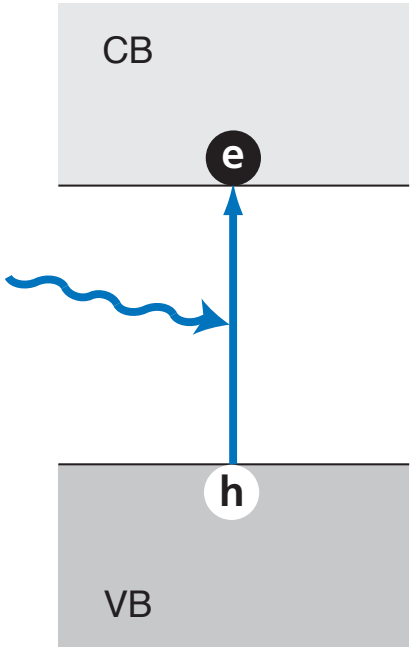

…whose energy can be extracted

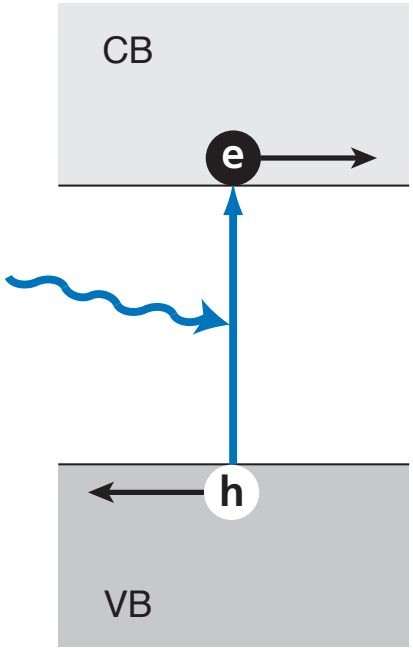

photons with energy smaller than gap…

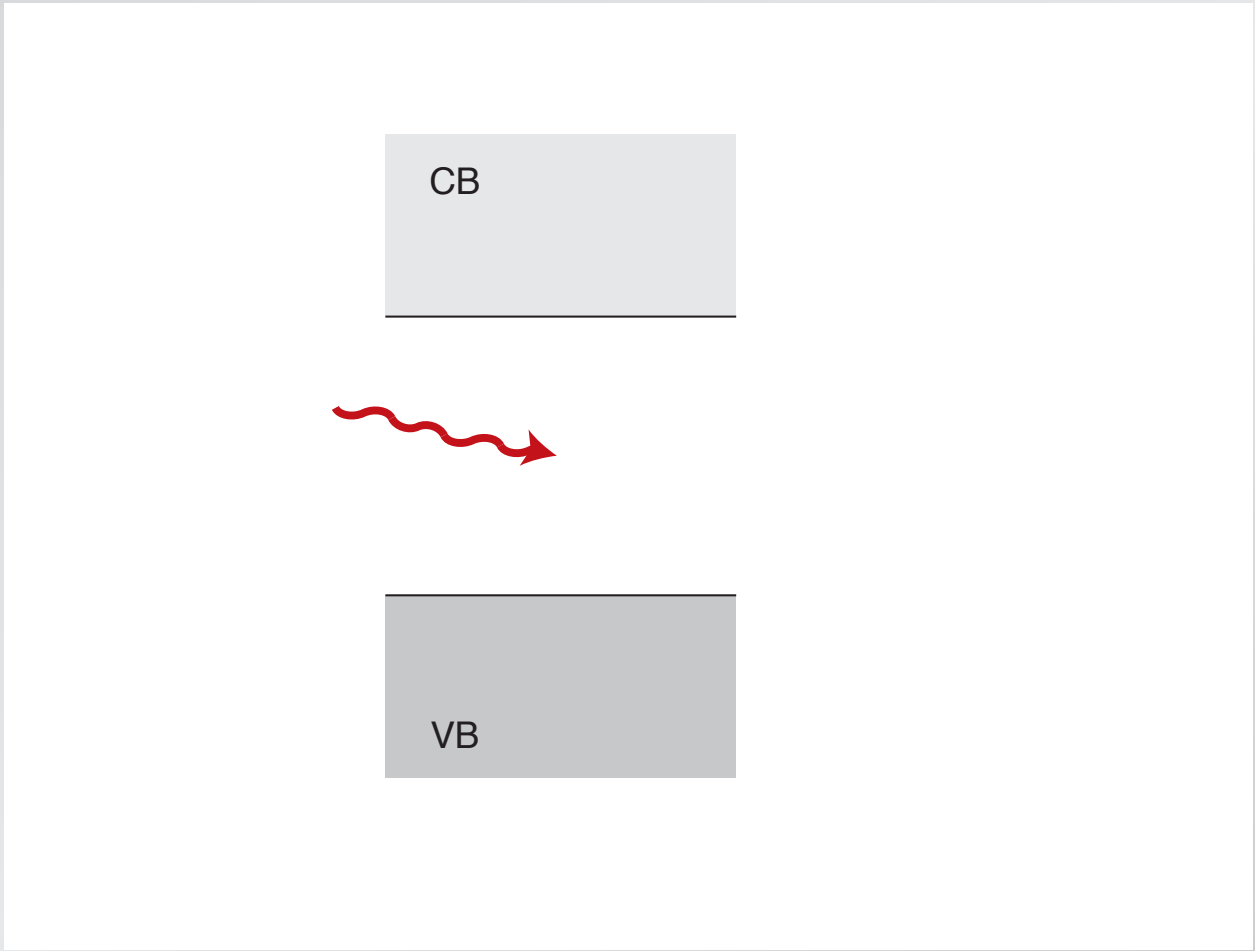

…do not get absorbed

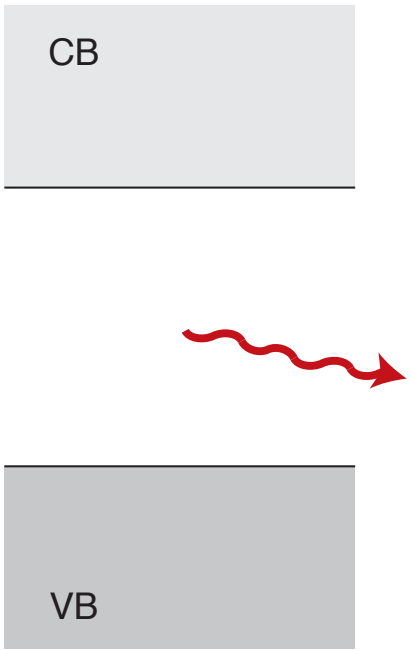

photons with energy larger than the gap…

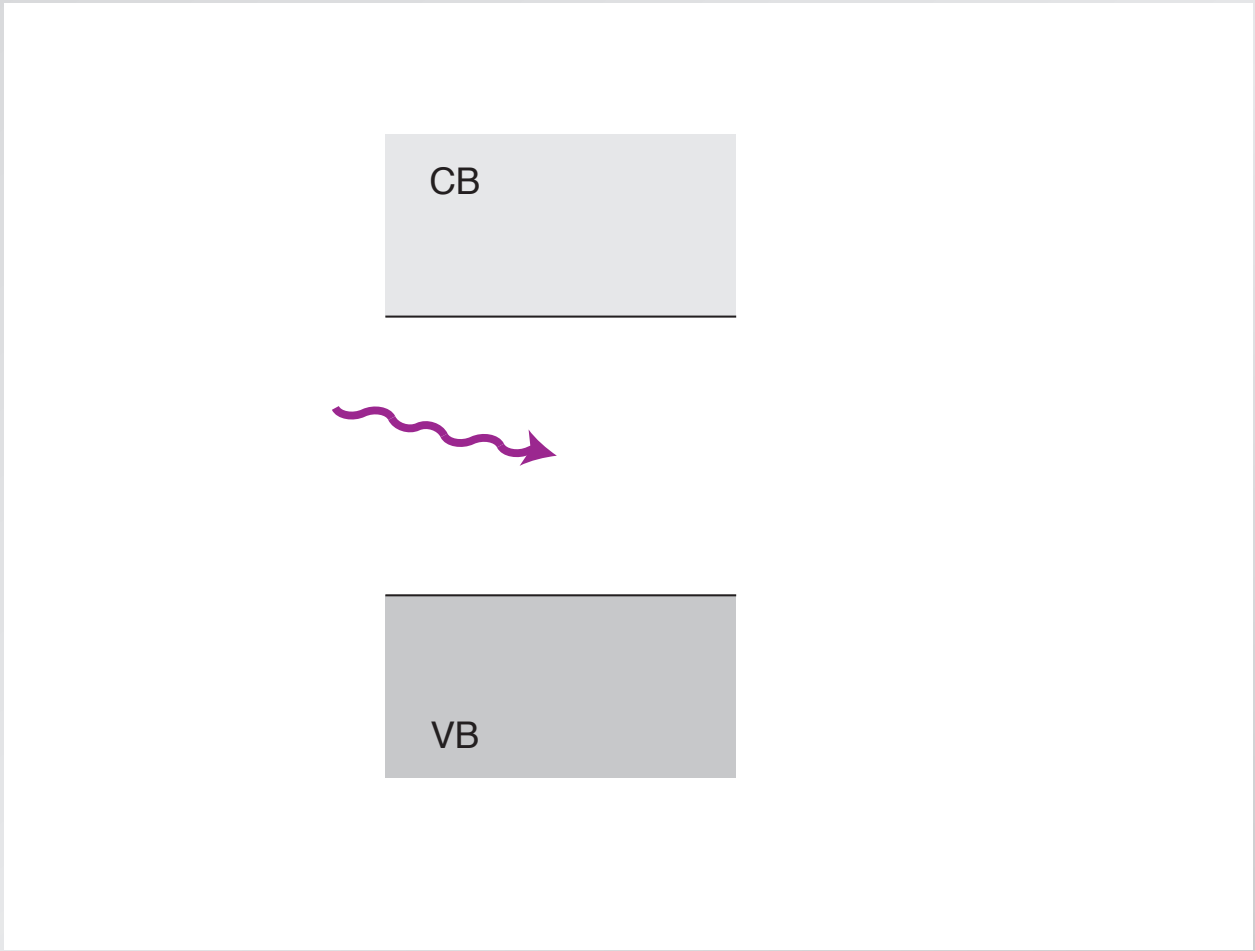

…create electron-hole pairs with excess energy…

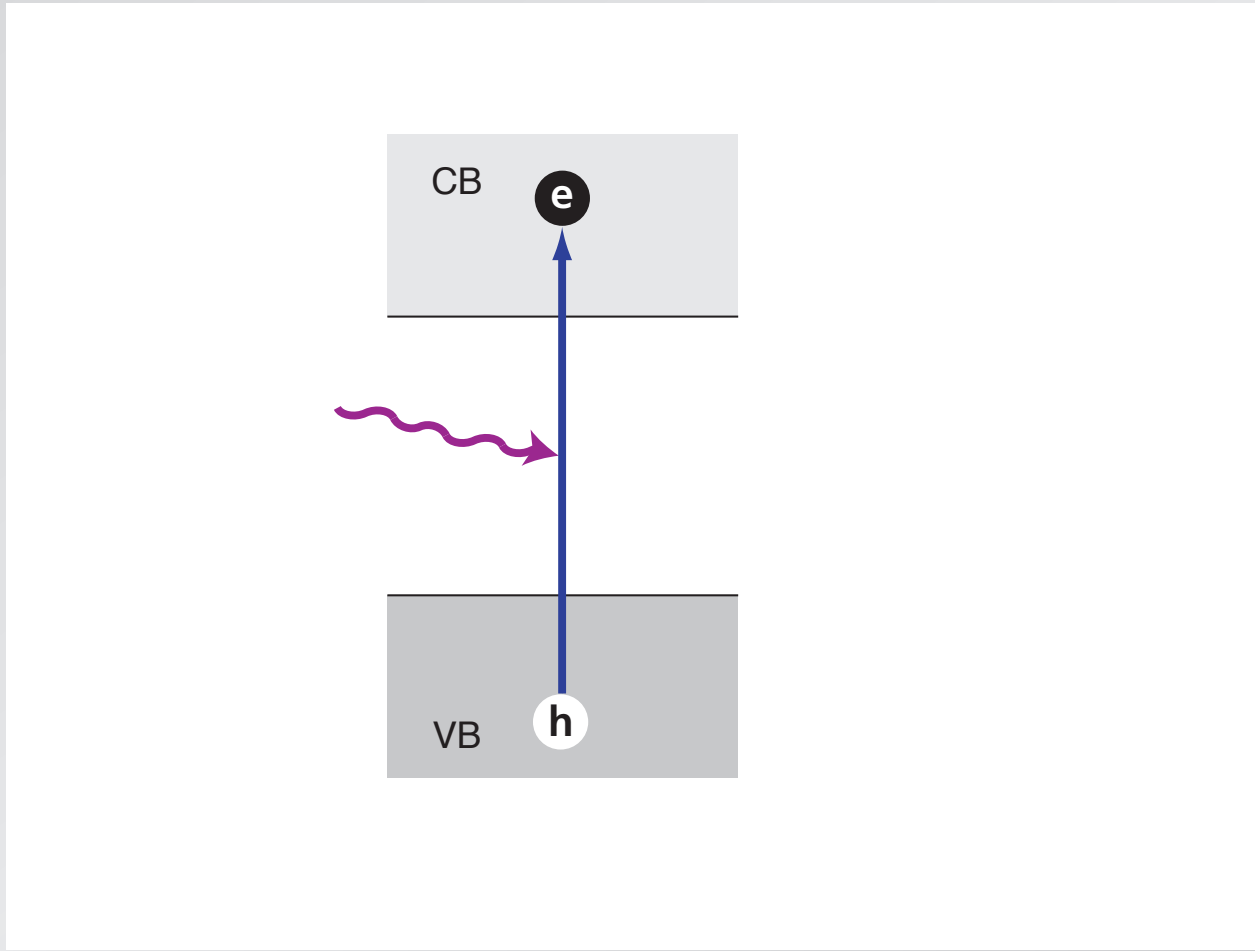

…which is lost rapidly

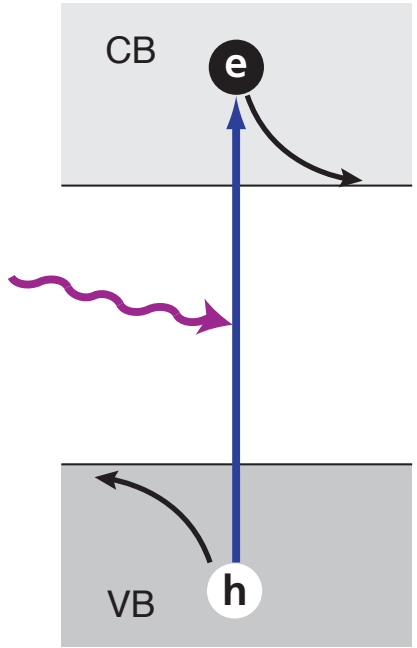

black silicon has an intermediate band

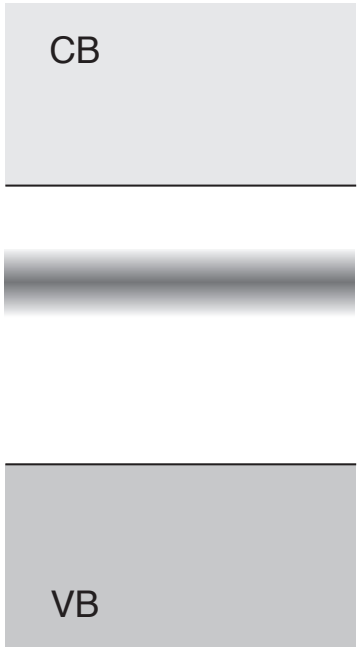

absorbs same photons as ordinary silicon…

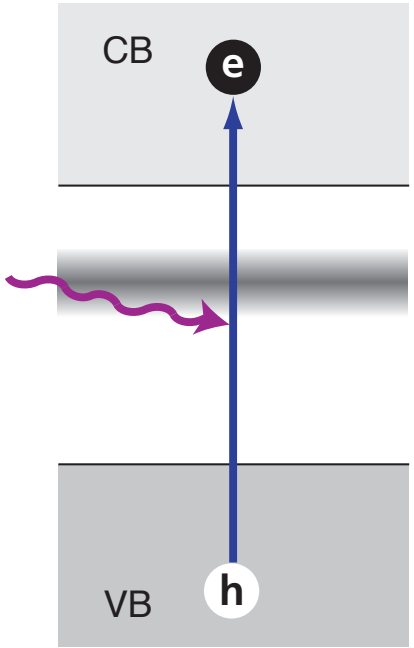

…but extends absorption to longer wavelengths

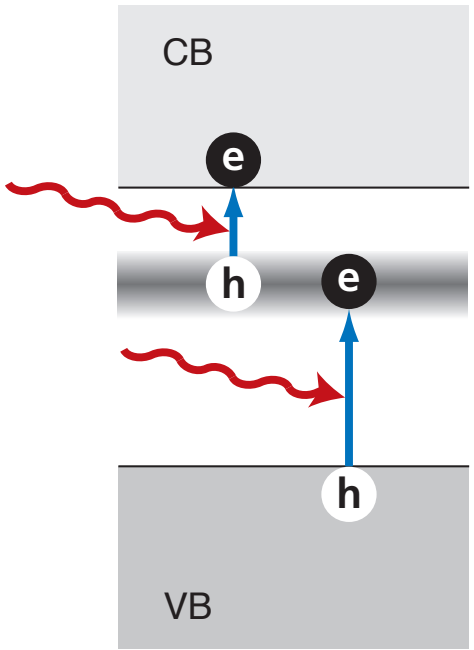

could theoretically get efficiencies over 50%

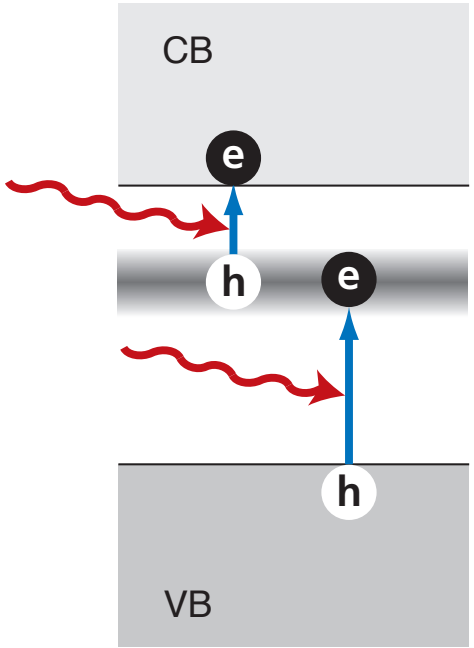

water splitting

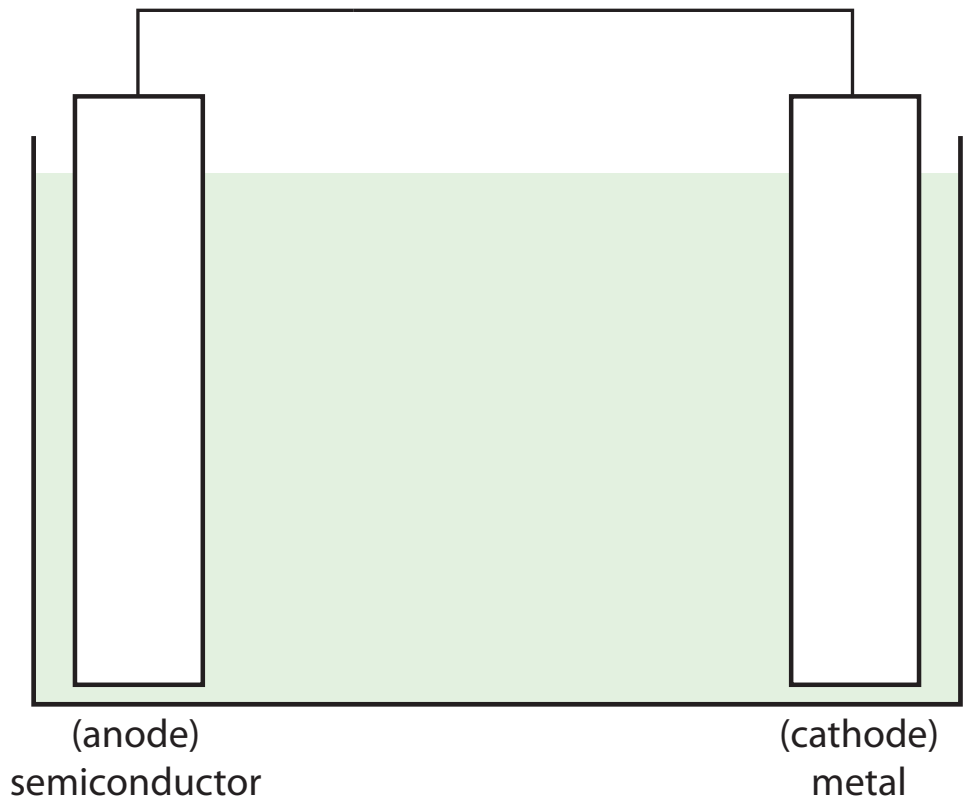

water splitting

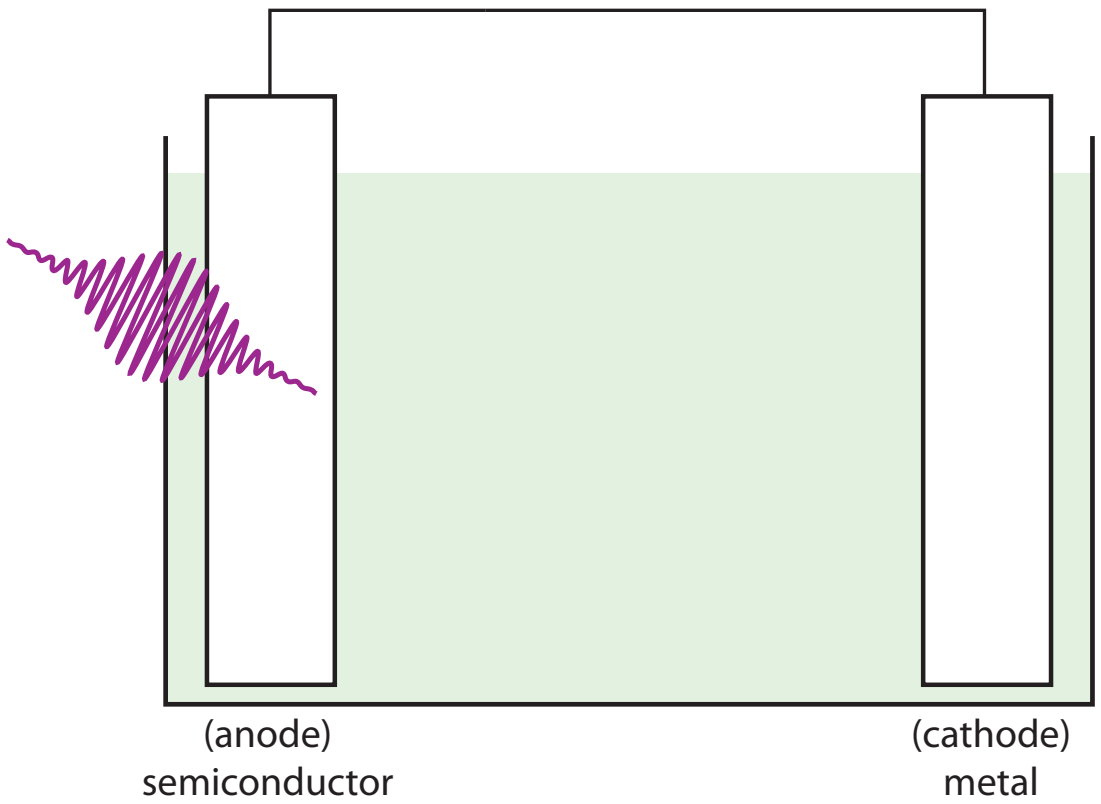

water splitting

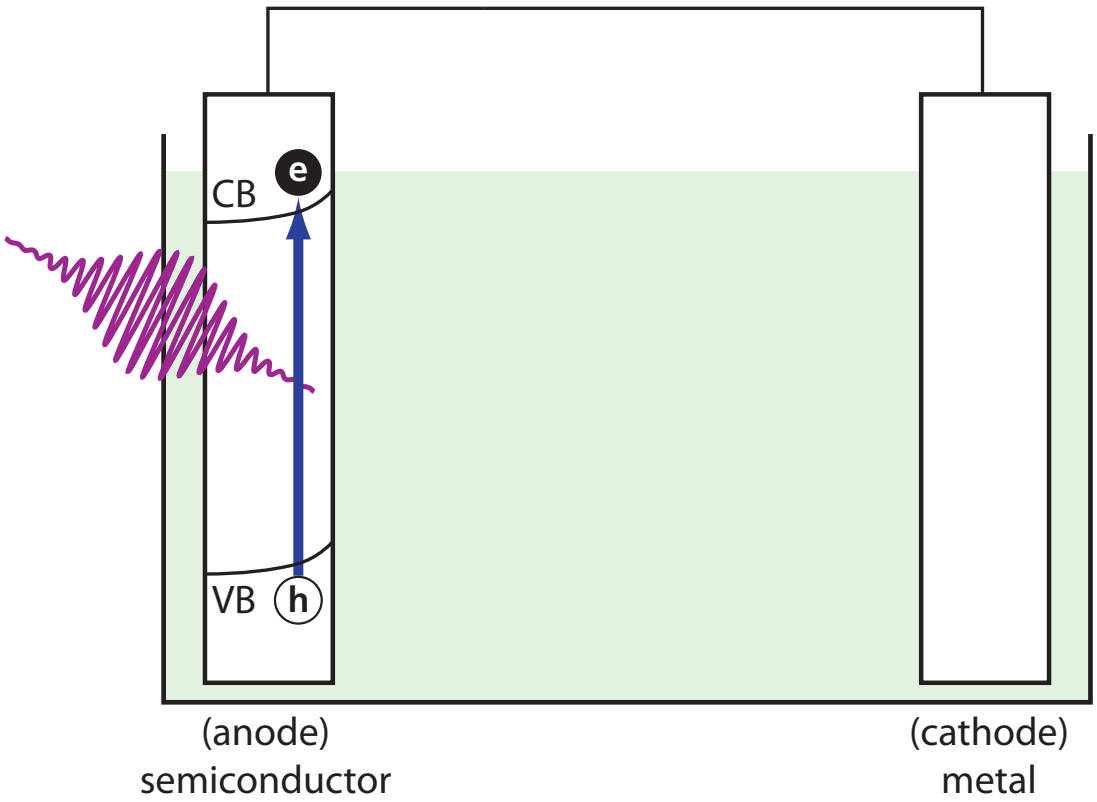

water splitting

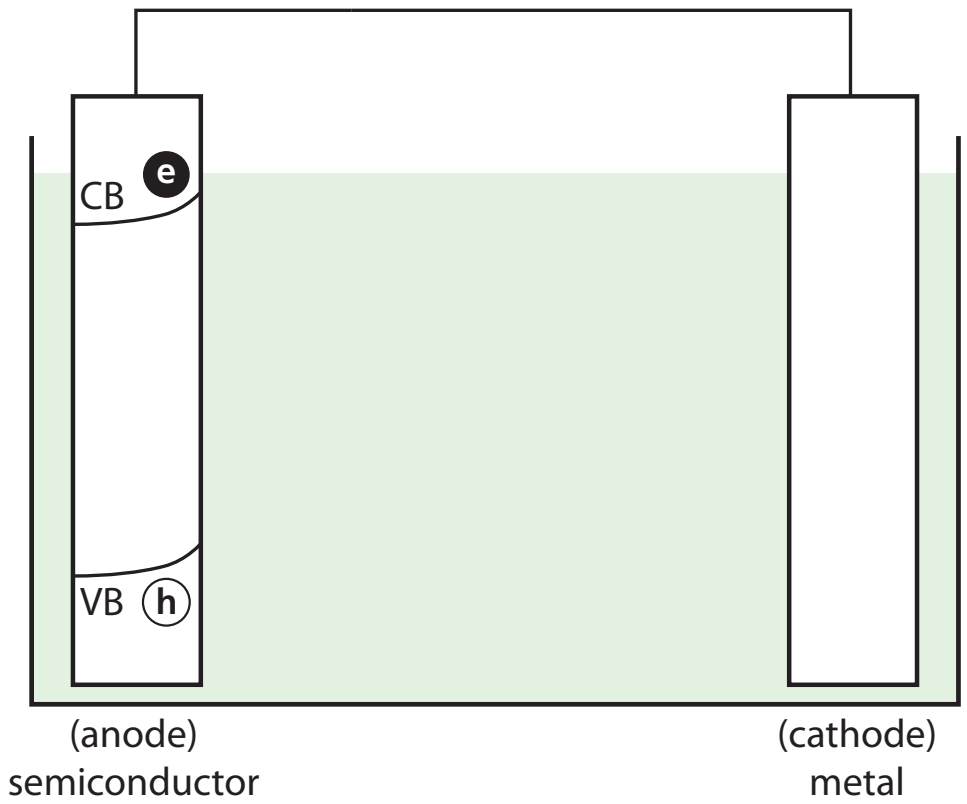

1 properties 2 intermediate band 3 devices

water splitting

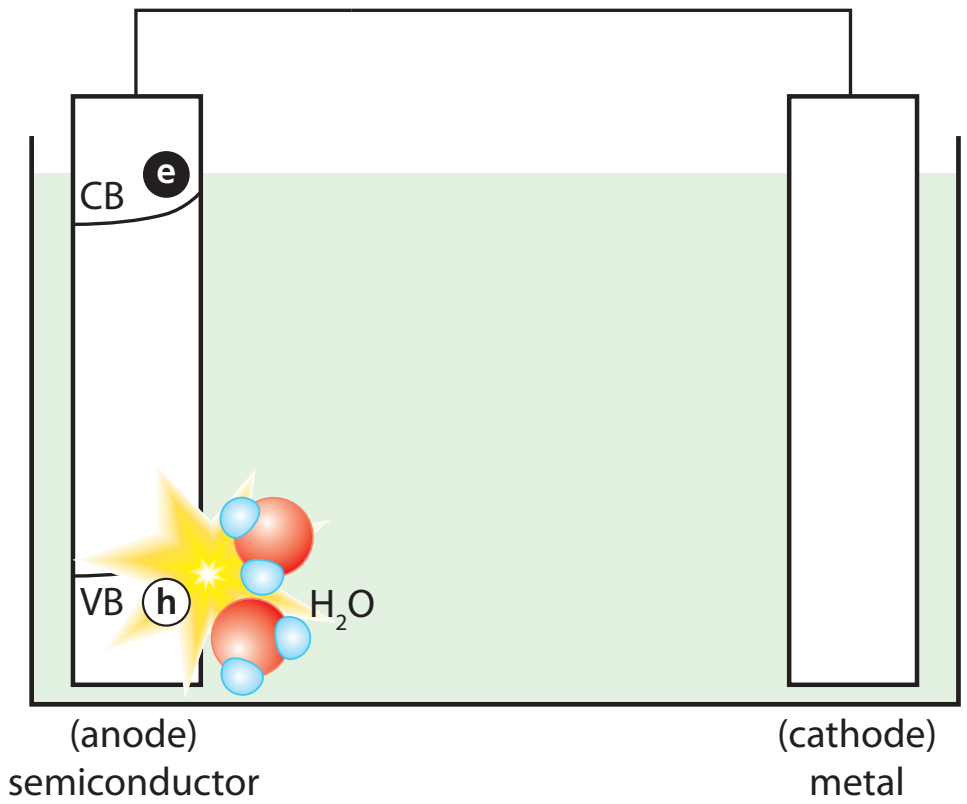

1 properties 2 intermediate band 3 devices

water splitting

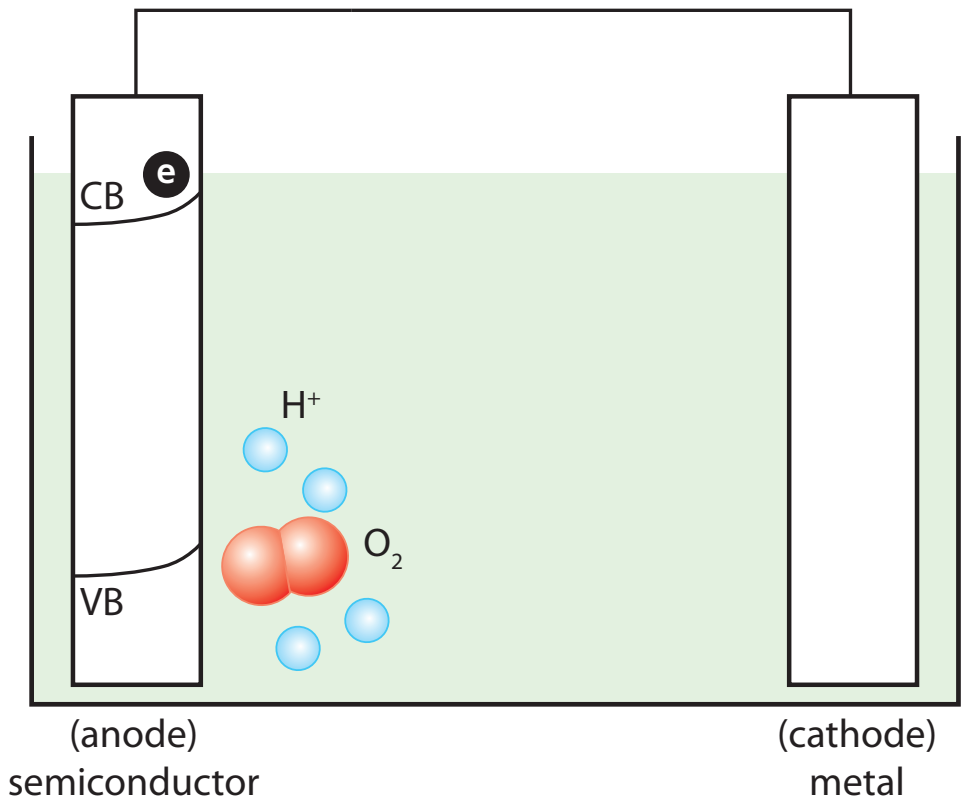

1 properties 2 intermediate band 3 devices

water splitting

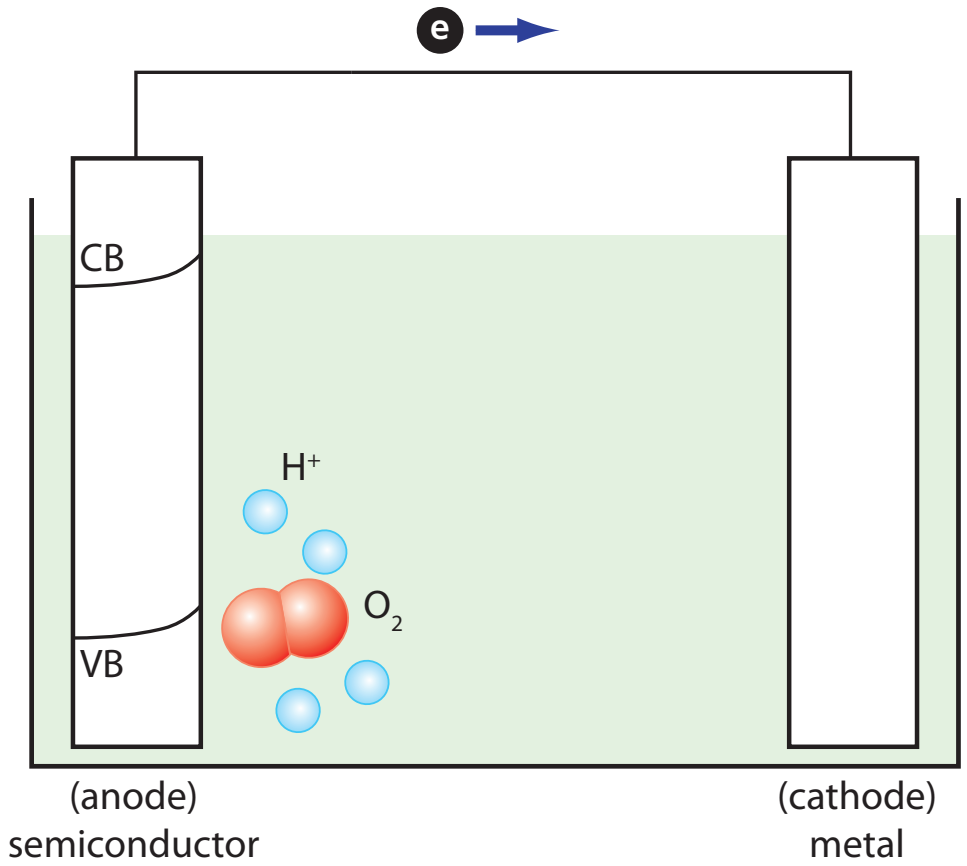

1 properties 2 intermediate band 3 devices

water splitting

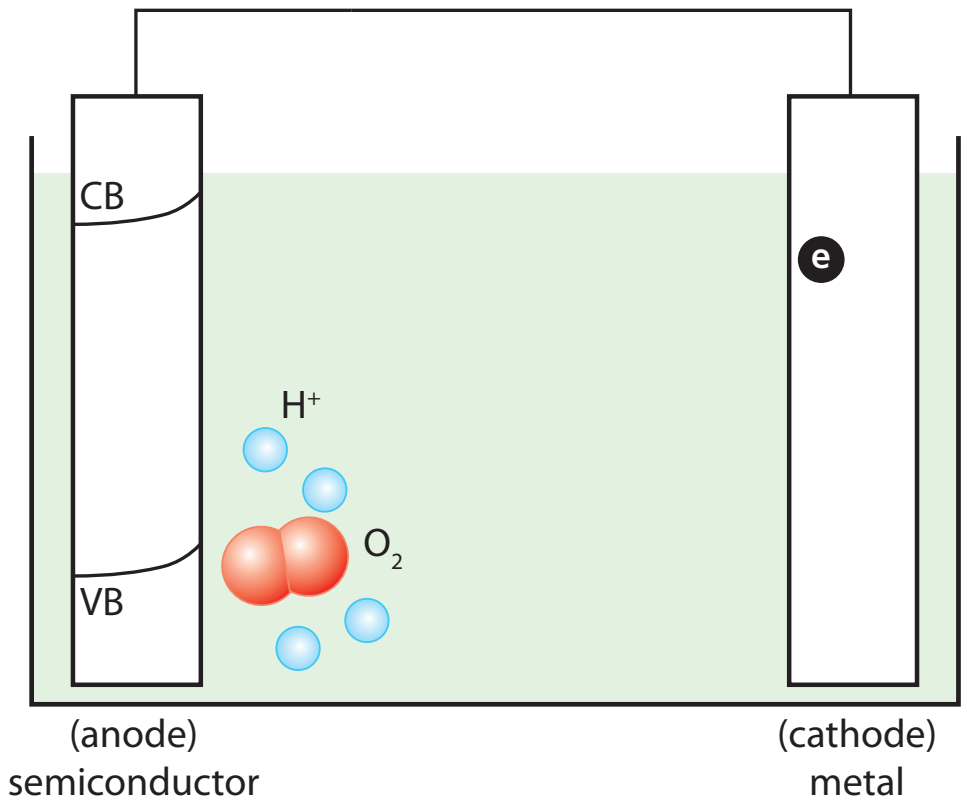

1 properties 2 intermediate band 3 devices

water splitting

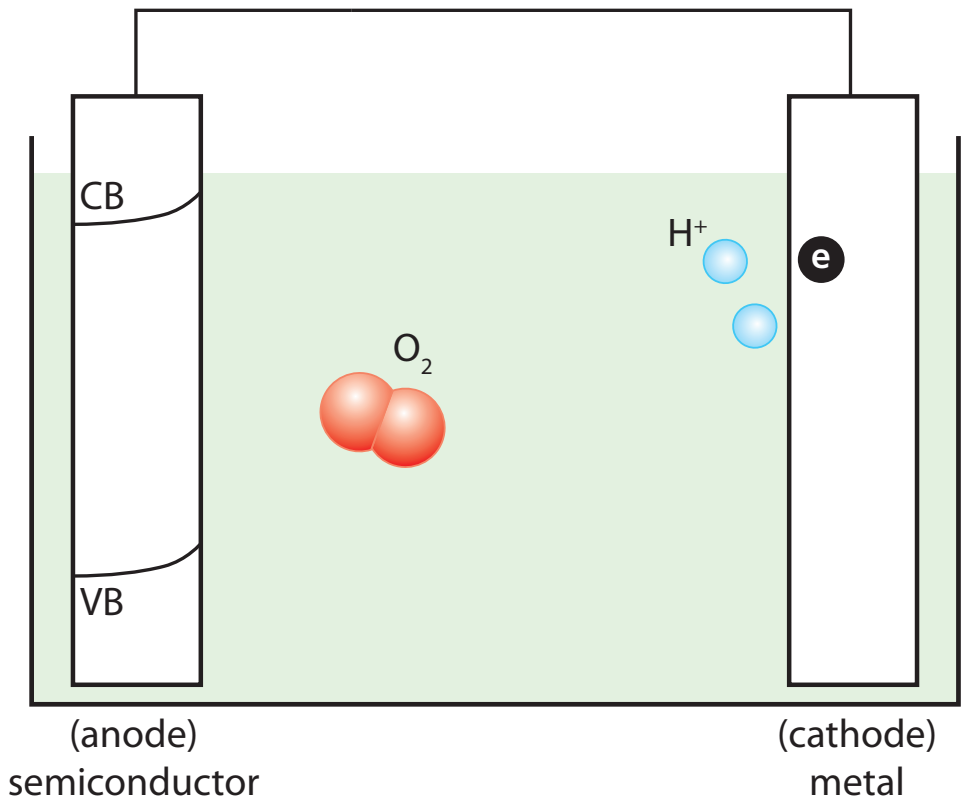

1 properties 2 intermediate band 3 devices

water splitting

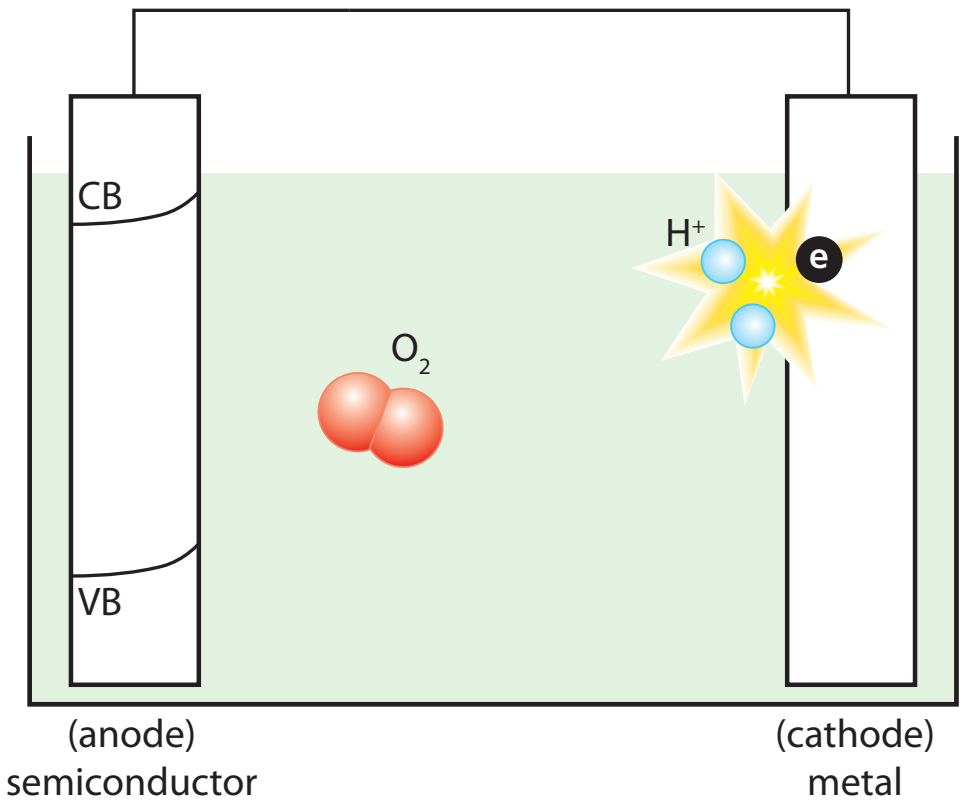

water splitting

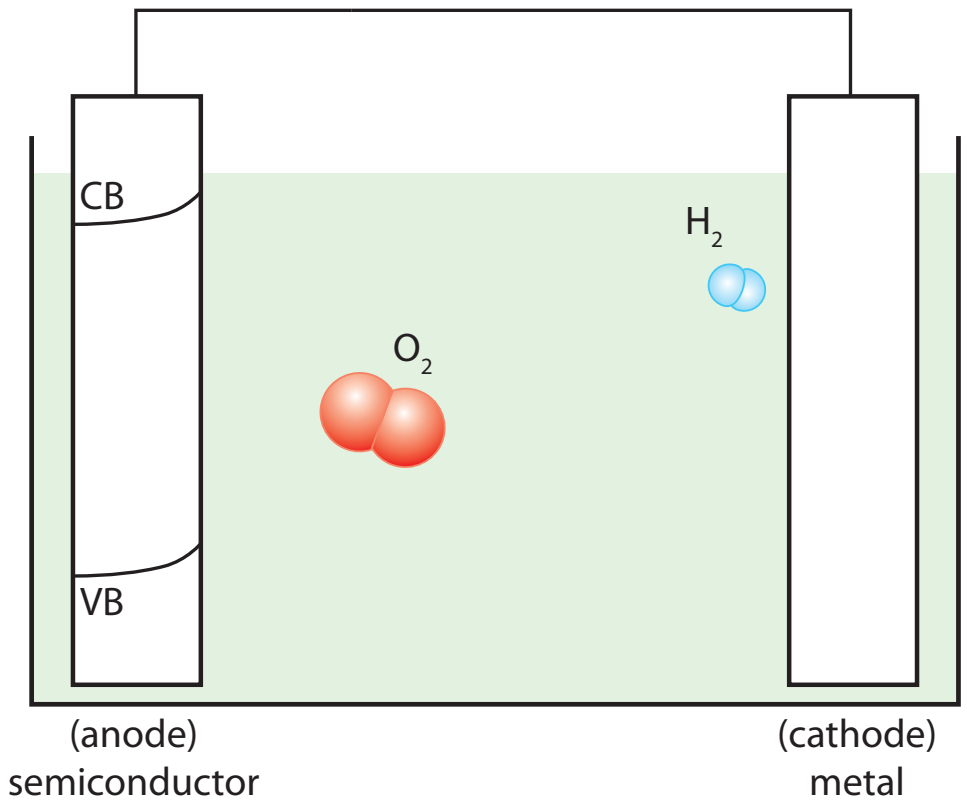

1 properties 2 intermediate band 3 devices

solar radiation spectrum

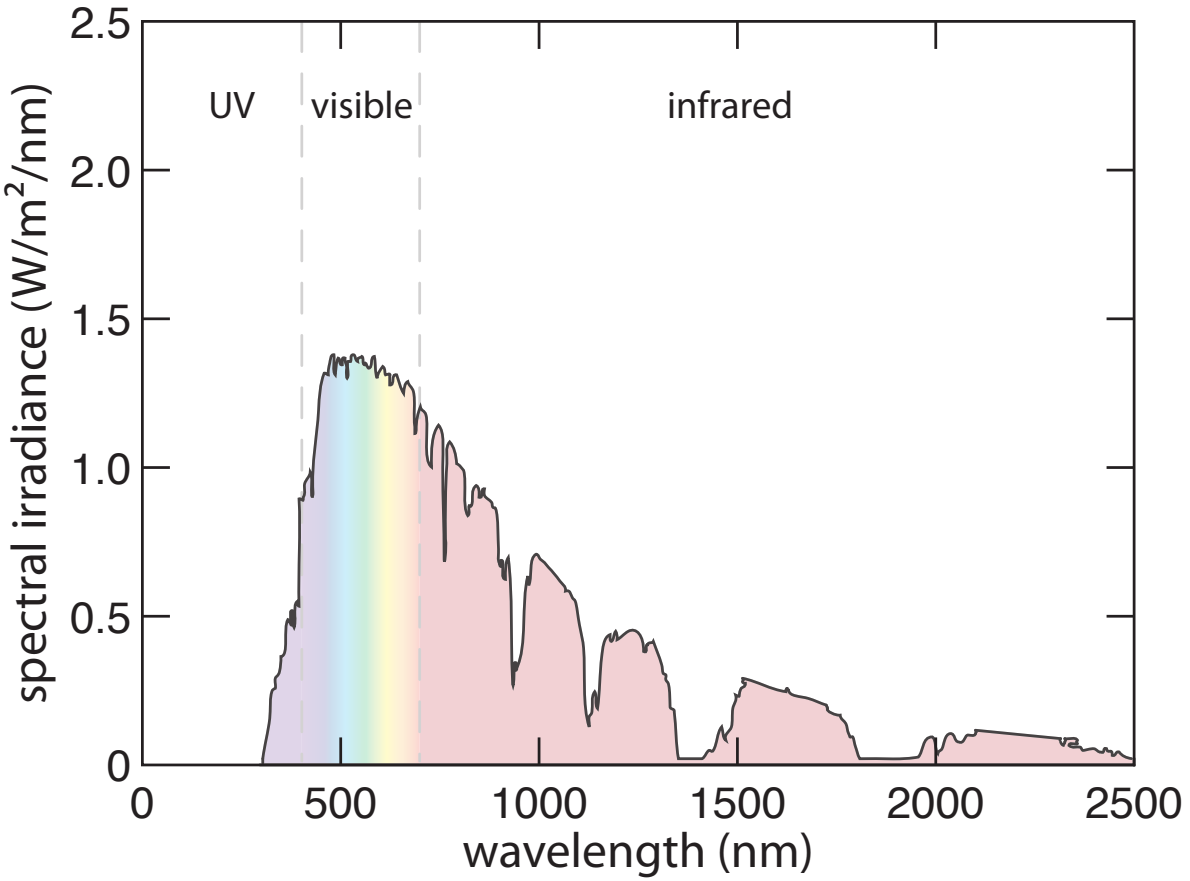

solar radiation spectrum

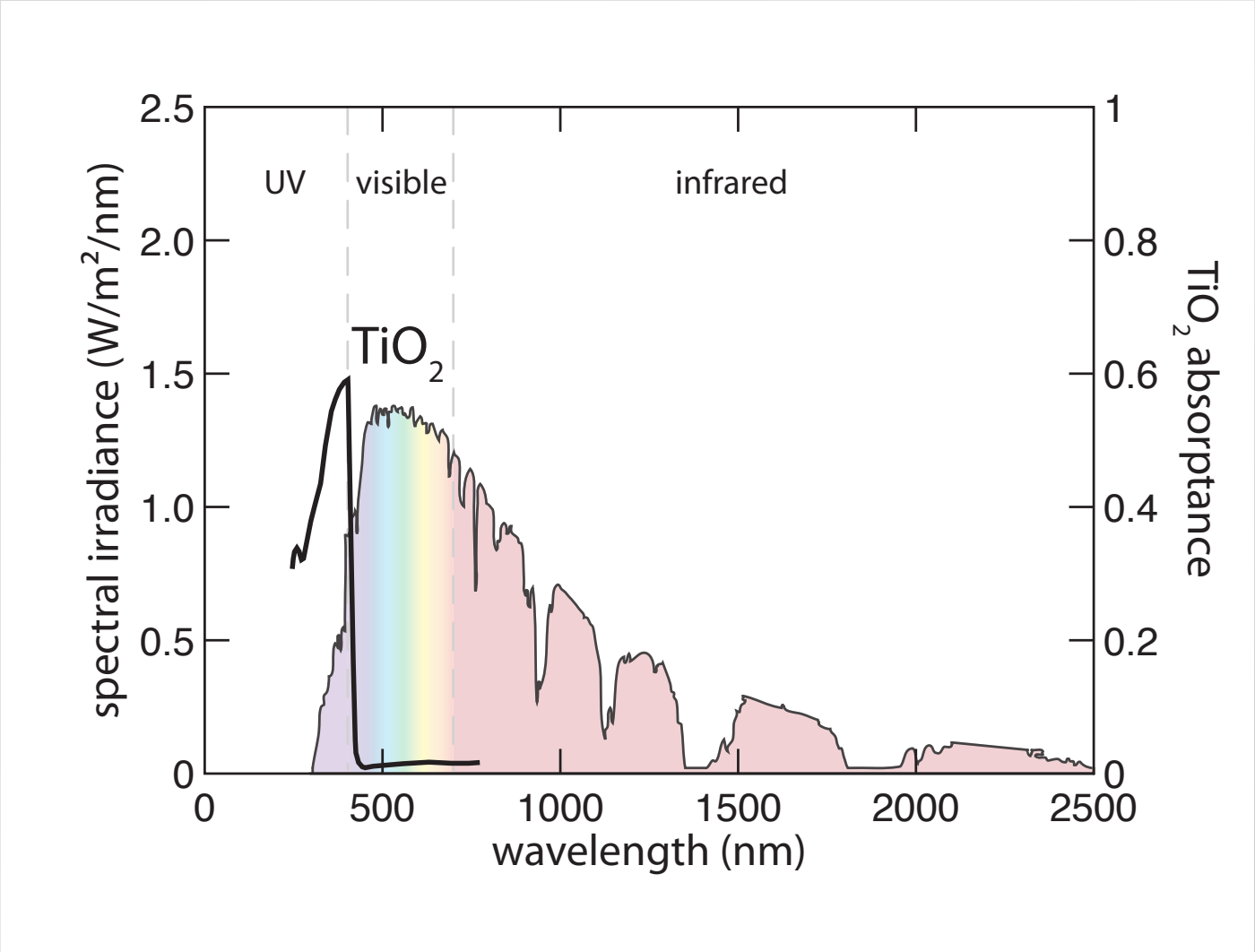

solar radiation spectrum

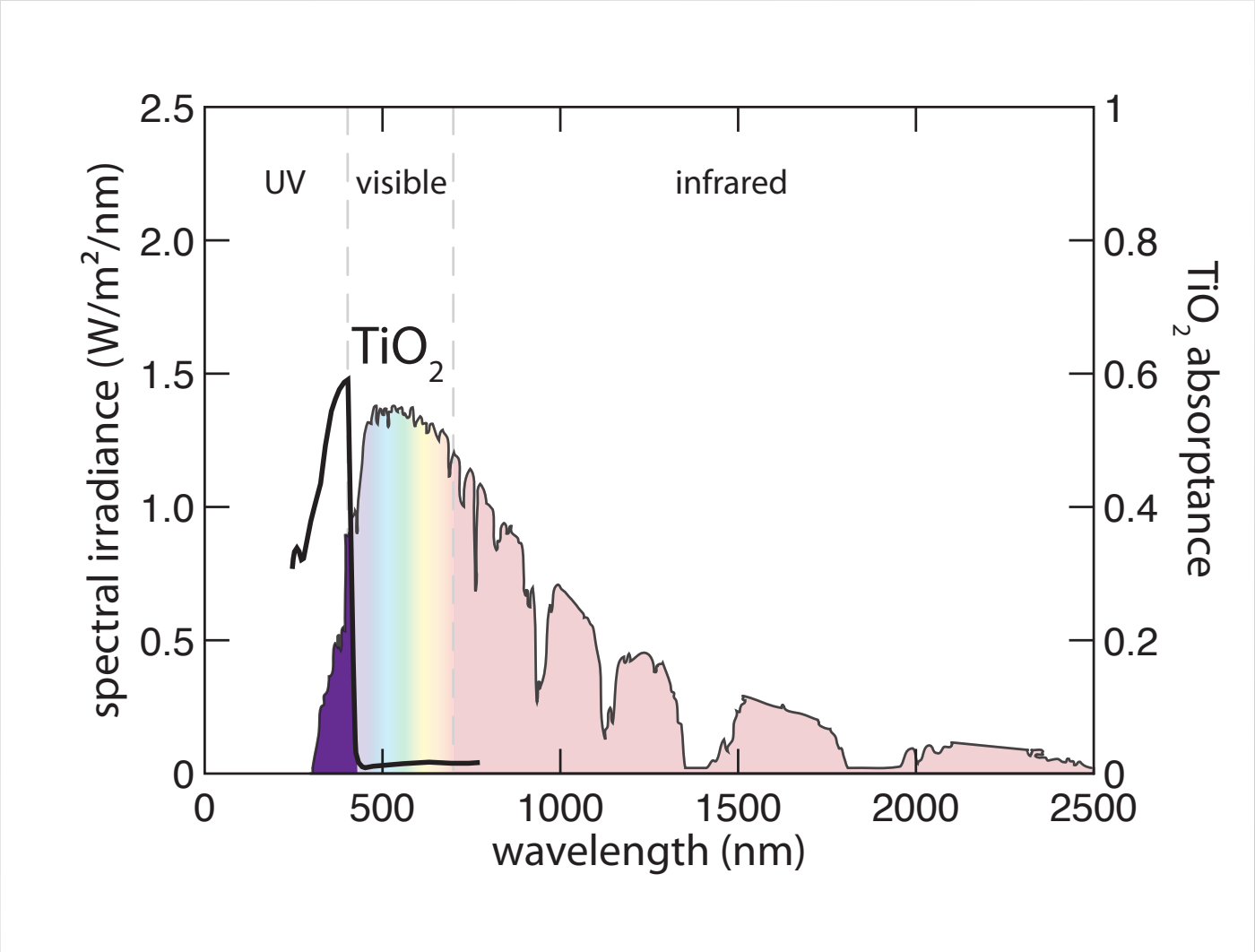

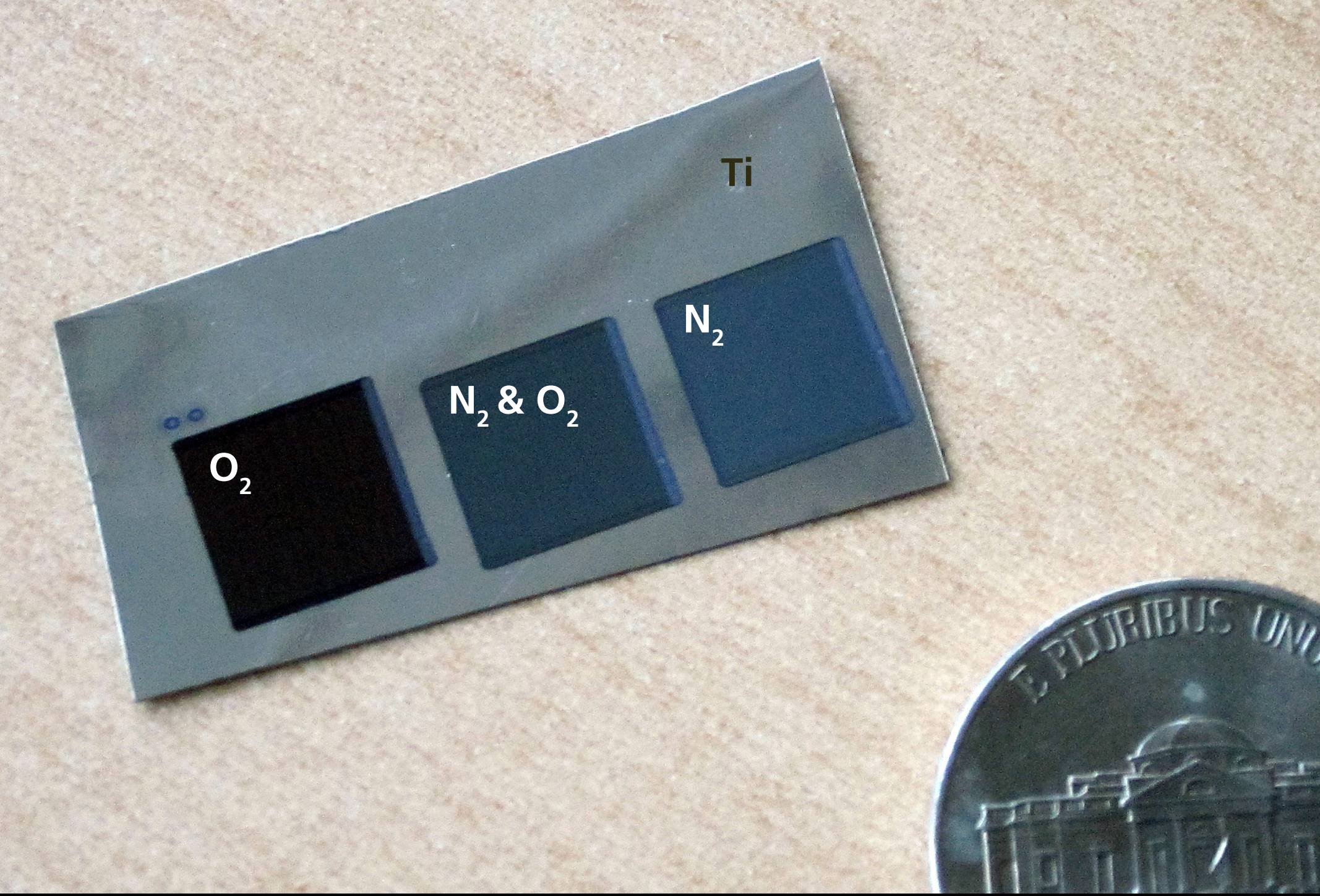

1 properties 2 intermediate band 3 devices

Things to keep in mind

- can turn b:Si absorption into carrier generation

Things to keep in mind

- can turn b:Si absorption into carrier generation
- very high responsivity in VIS and NIR

Things to keep in mind

- can turn b:Si absorption into carrier generation
- very high responsivity in VIS and NIR
- disruptive improvement in Si imaging

Things to keep in mind

- can turn b:Si absorption into carrier generation
- very high responsivity in VIS and NIR
- disruptive improvement in Si imaging
- potential benefits in solar energy harvesting

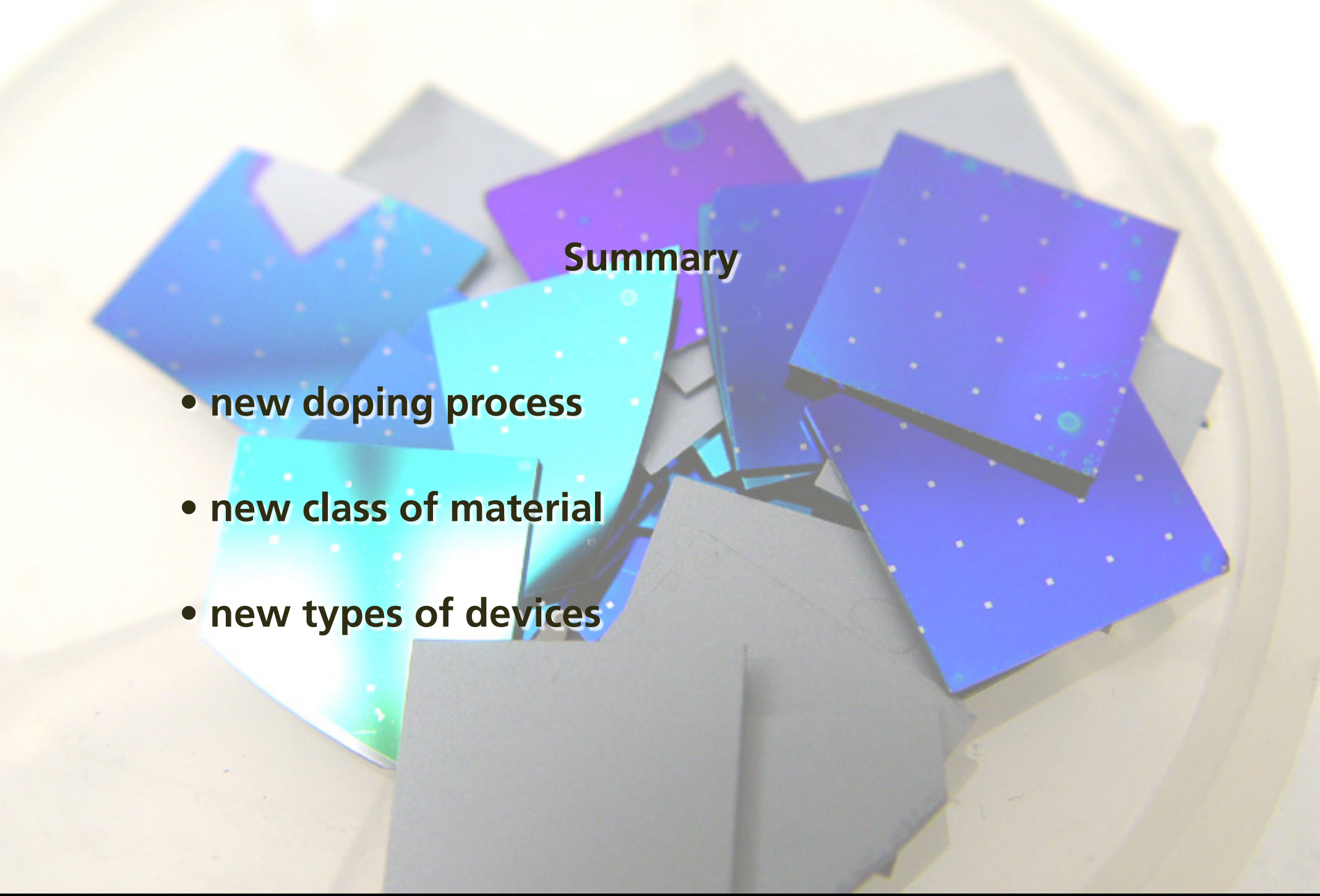

Summary

- new doping process
- new class of material
- new types of devices

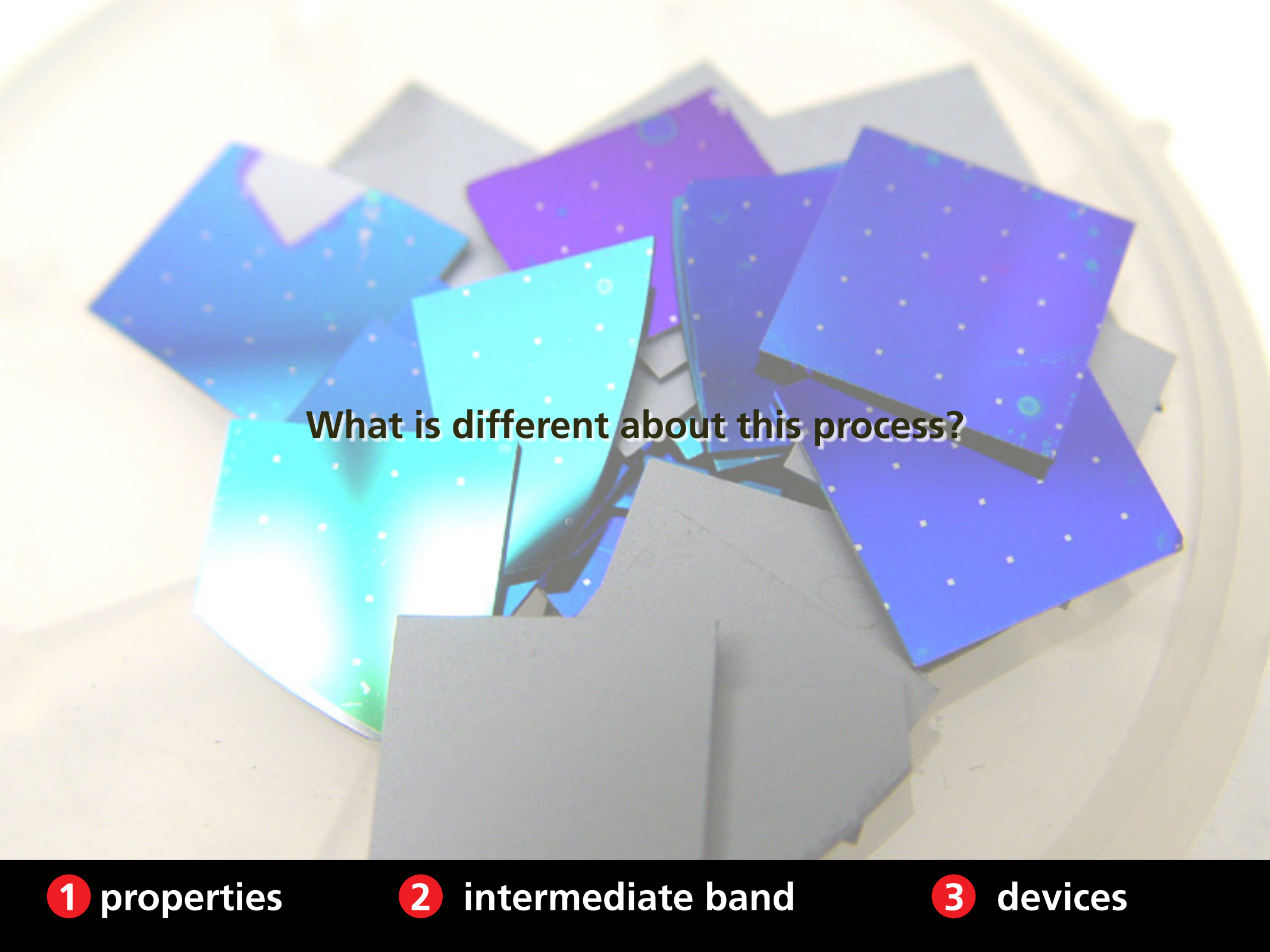
What is different about this process?
1 properties
2 intermediate band
3 devices

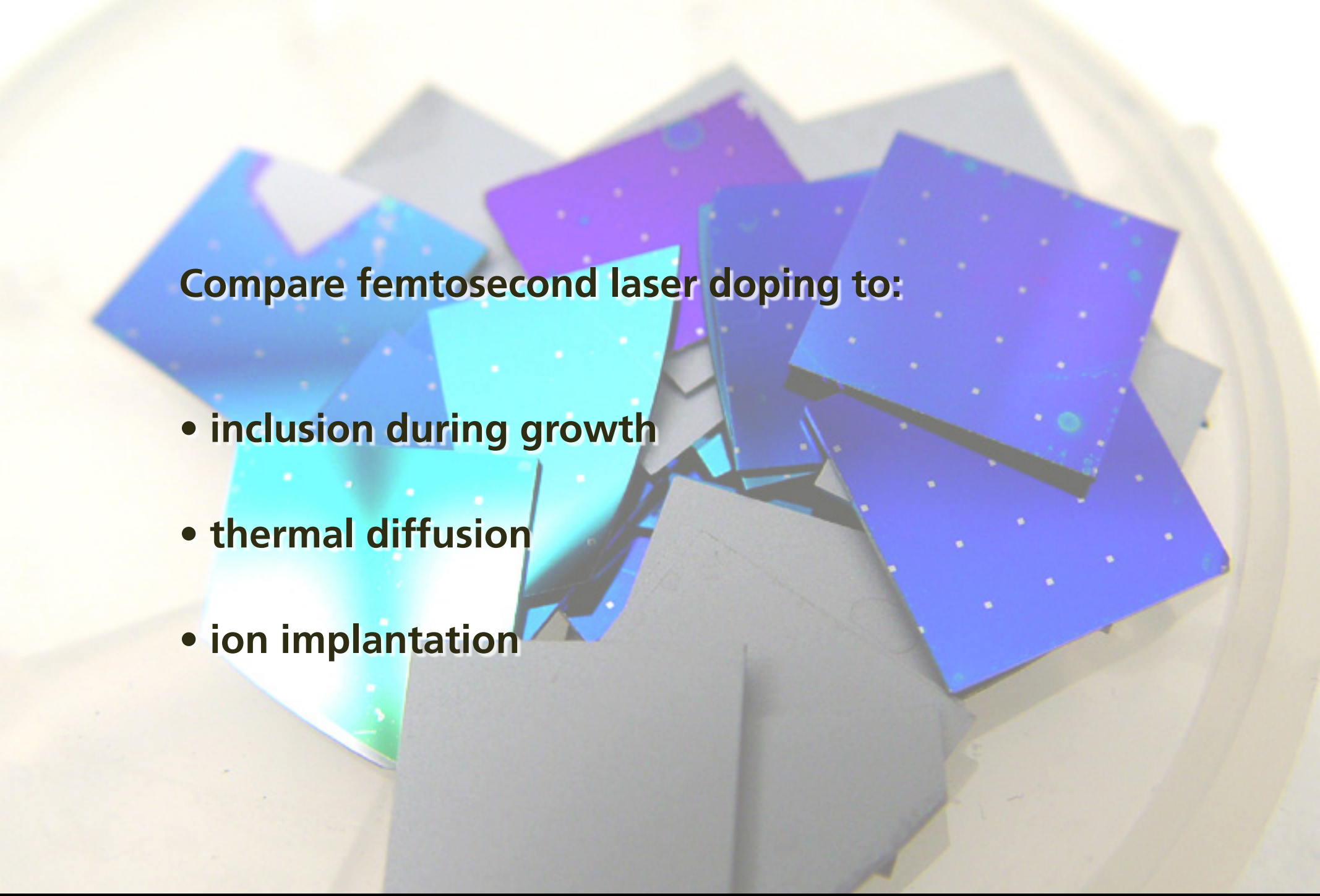

Compare femtosecond laser doping to:

- inclusion during growth
- thermal diffusion
- ion implantation

Funding:

Army Research Office
DARPA
Department of Energy
NDSEG
National Science Foundation

for more information and a copy of this presentation:

mazur.harvard.edu

Follow me!  **eric_mazur**

sionyx.com

SiOnyx